Reverse genetics analysis of biological functions of zinc transporters Znt1 (Slc30a1) & Zip10 (Slc39a10) in zebrafish

Muraina, Issa

Awarding institution:
King's College London

Title: Reverse genetics analysis of biological functions of zinc transporters Znt1 (Slc30a1) & Zip10 (Slc39a10) in zebrafish

Author: Issa Muraina

Reverse genetics analysis of biological functions of zinc transporters Znt1 (Slc30a1) & Zip10 (Slc39a10) in zebrafish

Issa Atanda Muraina

Thesis submitted to the University of London in fulfilment of the requirements for the degree of Doctor of Philosophy (Ph.D).

School of Medicine

Diabetes and Nutritional Sciences Division

Metal Metabolism Research Group

King's College London

University of London

2013

ABSTRACT

Zinc is an essential micronutrient indispensable for all forms of life, and disturbances in its homeostasis predispose the body to zinc imbalance-related diseases in man and animals. Mechanisms exist that enable organisms to regulate this metal element, which include proteins that control zinc entry into the cell, chelation whilst in the cell, and also extrusion out of the cell. ZnT1 (SLC30A1) is a zinc exporter originally cloned in mammalian cells but its homologue has also been identified in piscine species. In the present study, we have used genetics and molecular approaches in a model vertebrate system (the zebrafish *Danio rerio*) to elucidate the nutritional and functional importance of zinc and its transporters in the regulation of some crucial biological processes in the body. The Znt1 mutant of zebrafish strain sa0014 was created by the Sanger Centre using TILLING technology. The mutant fish carries a premature stop codon in the z*nt1* (*slc30a1*) gene resulting in a protein that is forty (40) amino acids shorter than the wild-type. A colony of this strain was generated and the mutation studied for its effects on ability of embryos to regulate Zn^{2+} ions needed for biological processes, such as growth and development, gene expression, zinc acquisition and extrusion, and also its effects on extracellular-regulated kinases (ERK1/2). Investigations were also conducted on embryos with *znt1* gene knockdown, through deployment of antisense morpholino-modified oligonucleotides (MO) in embryos of wild-type background, and in all of the studies it was shown that zebrafish embryos with Znt1 deficiencies display subtle but interesting phenotype, often having disturbances in zinc regulation and cell signalling when compared to their wild-type counterparts. Functional studies in adult fish revealed that *znt1* mutation affects zinc absorption and transporter regulation as well as diurnal breeding pattern, which was plausibly linked to dysregulation of circadian rhythm-controlled genes and ERK signalling. In addition, investigation was also conducted on

the function of Zip10 in embryos and it was found that the *zip10* gene is essential in early development through its involvement in epithelial-mesenchymal transition (EMT) and cell migration. This gene was also shown to be important in hatching of zebrafish embryos through its involvement in the proper development and functioning of hatching gland tissue. Interestingly, knockdown of the *zip10* gene by MO reduced the expression of hatching gland markers as well as the abundance of Zn^{2+} ions in the hatching gland cells (HGC) resulting in delayed hatching whereas *znt1* knockdown produced the opposite effects. The relevance of all these studies in health and diseases of man and animals are discussed.

ACKNOWLEDGEMENT

I will like to begin my gratitude to God almighty who has granted me the wherewithal to start and get to the end of my PhD degree in peace. My profound appreciation then goes to my first supervisor who I always refer to as my father, Prof. Hogstrand Christer, for his relentless efforts on me right from while I was in my country Nigeria to the time I commenced and finished my PhD degree under him. Indeed you are one in a million! Your excellent research supervision and advice (both formal and informal) have grounded me thoroughly in the area of scientific research and in no doubt building me to become an astounding researcher.

Equally worth appreciating is my second supervisor, Dr. Nic Bury for his invaluable advice and mentoring during the course of this project. I say a big thank you. I will not forget to thank other distinguished scholars who have contributed in one way or the other to the success of this project, notably among them is Prof. Anthony Graham of the Neurodevelopmental Biology Department of Medical Research Council (MRC) at Guy's campus, Kings College London who provided invaluable advice and first allowed me into his lab to learn the basic molecular biology techniques use for zebrafish development. Others are Dr. Imre Lyngyel of University College London, Dr. Kathy Taylor of School of Pharmacy & Pharmaceutical Sciences, Cardiff University, Dr. Peter Kille of School of Biosciences, Cardiff University, Drs. Yi Li, Colin Dolphin, Yemisi Latunde-Dada and most importantly, Dr. Maret Wolfgang, all of the school of Medicine, Kings College London for their invaluable scientific contribution towards actualization of this work.

I will like to remember my fellow colleagues in the lab both the present and the past, among which are Matthew Arno, Estibaliz Aldecoa-Otalora (Esti) and Fei Wong of Genomic centre, I will not forget your immediate assistance anytime I called upon you

regarding the GENOME issues! Others are my fellow PhD and the post-doctoral students; Annabelle Scott, Jo Richardson, Fawaz Alzaid, Natasha Polak, Soudabeh Imanikia (Soudi), Neeta Patel, Nisha Hirani, Hoi Man Cheung (Stephenine), Cathriona Loonam, Krishna Sharma, Song Yong, Sabine Schnell, Matteo Mingheti, Irina Komjarova, Nnamdi Amaeze, Lucy Stott, Vallentina Riffato,Tom Caroll and Joseph Rasinger. I say thank you all for making my periods at KCL very exciting.

This acknowledgement will not be completed if I did not mention my wonderful family members that are together with me in London during the course of my study. Notably is my heartthrob, Olatokunbo Amudalat who painstakingly stayed by me during the thick and thin periods. And also my beautiful children; Khairat Ebunlomo (aka NEF), Farida Ayomide (aka MSc) and the last one who arrived at the time of completion of my PhD programme, Abdul-Ahad Danjuma (aka PhD). My mum, Mrs Fatimoh Muraina you are duly acknowledged as well because your vist to us in London was so timely and very important. I valued your words of encouragement which always inspire me especially at the last part of my studies. I say a very big thank you all.

I will also like to appreciate my employer and the entire staff of National Veterinary Research Institute, Vom Nigeria for their supports and words of encouragement during the course of my study.

My final word of appreciation will go to bodies or people that have granted me scholarships for my PhD course. Notably is the King's College Graduate School London who gave me two awards (Kings International Graduate Scholarship and Kings Oversea Research Scholarship) and the University of London who awarded me with the Central Research Funds and lastly my supervisor who took the bills for my bench fees and also provided funds for my research in his lab. I SAY THANK YOU ALL.

DECLARATION

I declare that the work in the thesis entitled **''Reverse genetics analysis of the biological functions of Znt1 (slc30a1) and Zip10 (slc39a10) in zebrafish''** has been performed by me in the Division of Diabetes and Nutritional Sciences of the School of Medicine under the supervision of Prof. Christer Hogstrand and Dr. Nic Bury.

Information derived from other literatures has been duly acknowledged in the text and a list of references provided. No part of this thesis was previously presented for another degree or diploma at any university.

TABLE OF CONTENTS Page No

List of tables

List of figures

Abbreviations

AKT	Protein Kinase B (from Akt mouse strain)
APP	β-Amyloid Precursor Protein
APS	Ammonium per sulphate
Arntl (Bmal1)	Aryl hydrocarbon receptor nuclear translocator-like
Aβ	Amyloid beta
BMP	Bone Morphogenic Protein
Bmal1	Brain and Muscle Arnt-Like1
CatL 1	Cathepsin L
Cdna	Complementary Deoxyribonucleic acids
Cel1	Celery 1
Cry2a	Cryptochrome
CNS	Central Nervous System
Cx43	Connexin-43
DHPLC	Denaturing High-Performance Liquid Chromatography
DLP	Dual labelled Probe
DMSO	Dimethyl sulfoxide
DNAs	Deoxyribonucleic acids
EGFR	Extracellular Growth Factor Receptor
EMS	Ethylmethyl sulfonate
EMT	Epithelia-Mesenchyma Transition
ENU	Ethylnitrosurea
ER	Endoplasmic Reticulum
GSK-3α	Glycogen Synthase-Kinase-3α

HCE	High Choryolytic enzyme
HE	Hatching Enzymes
HGC	Hatching Gland Cells
HGR	Hatching Gland Remnants
HNK-1	Human Natural Killer cell-1
ICP-MS	Inductively Couple Plasma- Mass Spectrometry
IGF1	Insulin Growth Factor 1
KCL	King's College London
KLF4	Krupel-Like Factor 4
LB	Luria Bertani
LCE	Low Choryolytic enzyme
LDLR	Low Density Lipoprotein Receptor
MCA	7-Amino-4-MethylCoumarin
MO	Morpholino oligonucleotide
MTs	Metallothioneins
MTF-1	Metal regulatory Transcription Factor-1
NCBI	National Centre for Biotechnology Information
NEB	New England Biolab
NF-kB	Nuclear Factor kappa B
NIFES	National Institute for Food and Seafood Research
PBS	Phosphate Buffer Saline
PBST	PBS+Tween 20
qPCR	Quantitative Polymerase Chain reactions
RNAi	Ribonucleic Acid interference
RNAs	Ribonucleic Acids

ROS	Reactive Oxygen Species
rpm	rotation per minute
SDSC	San Diego Supercomputer Centre
SLP	Single Labelled Probe
SMA	Smooth Muscle Actin
SNP	Single Nucleotide Polymorphism
SOD	Superoxide Dismutase
STAT3	Signal Transducer and Activator of Transcription 3
TBST	Tris Buffer Saline + Tween 20
TGF- α	Transforming Growth Factor- α
TILLING	Targeting Induced Leison IN Genome
TPEN	N,N,N,N,-Tetrakis(pyridymethyl) ethylene-diamine
TMDs	Transmembrane Domain
5'UTR	5 prime Un-Translated Region
YSL	Yolk Syncyctial Layer
ZIP (SLC39)	Zinc Import Protein (Solute Carrier of family 39 member)
Zip10 MO	Zip10 Morpholino
$Zip10^{MO}$	Zip10 Morphant
ZnT (SLC30)	Zinc Export Protein (Solute Carrier of family member 30)
Znt1 MO	Znt1 Morpholino
$Znt1^{MO}$	Znt1 Morphant
ZP	Zona Pellucida.

CHAPTER ONE

GENERAL INTRODUCTION

1 General introduction

1.1 Zinc in biology

The essentiality of zinc in humans was recognised about half a century ago (Prasad *et al.*, 1961; Prasad, 2009) following its discovery in biology more than one and half centuries ago by Jules Raulin (a French botanist and chemist) who first demonstrated its importance in the growth of the mold, *Aspergillus niger* in 1869 (Vallee 1986). Zinc is ubiquitous and essential trace element indispensable for life because of its presence in many tissues of a wide range of organisms where it participates in multiple biological processes including embryonic development (Keen and Hurley, 1989). It is the second most widely used transition metal in humans, after iron, with an estimated total amount of about 2g in the body (approximately 20-30 µg/g tissue) (Strauss, 2005; Aggett and Comerford, 1995). Nutritionally, zinc in the diet is absorbed by the enterocytes in the proximal small intestine, and it is excreted predominantly through the gastrointestinal system, with minor amounts being lost through the skin and urinary system (Groff and Gropper, 2000). However, ejaculation in men or menstrual flow in women can also contribute significantly to zinc loss (Hunt *et al.*, 1992). In the plasma, zinc is bound primarily to albumen (~ 83.7%) and α2-macroglobulin (16.3%) with a small percentage bound to low molecular weight substances such as histidine and cysteine (Foote and Delves, 1984; Bettger and O'Dell, 1993). Zinc is known to serve as an essential cofactor in many biochemical processes, thus having important roles in primary metabolism such as carbohydrate and lipid metabolisms, protein and nucleic acid synthesis as well as in coordination of many other biological processes including gene transcription and expression, protein-protein interaction and protein-oligonucleotide reactions (Vallee and Auld, 1990; Vallee and Falchuk, 1993; Hirano *et al.*, 2008). In addition, it also acts as a

neuromodulator (Colvin *et al.*, 2003) as well as a novel intracellular second messenger capable of transducing extracellular stimuli into intracellular signalling events (Yamasaki, *et al.*, 2007). Zinc is also an integral component of many enzymes (such as alcohol dehydrogenase, glutamic dehydrogenase, carbonic anhydrase and other enzymes involved in electron transport and antioxidation) and transcription factors (such as zinc finger transcription factors) (Coleman, 1998; Chang *et al.*, 2005; Eide, 2011). More than 10% of the total human genomes codes for C2H2 zinc-finger, RING (Really Interesting New Gene) finger or LIM domain-containing proteins (Venter *et al.*, 2001, Andreini *et al.*, 2006). Moreover, there are likely in excess of about 1,000 metalloenzymes belonging to all major functional classes (Vallee and Auld, 1990; Maret, 2009; Andreini and Bertini, 2011). Zinc unlike copper or iron is redox inactive (redox stable) and this may account for its widespread occurrence in many biological systems without causing the risk of oxidant damage. Although zinc is not redox active under physiological conditions, it can have antioxidant properties as a result of indirect mechanisms of action to reduce or block the generation of reactive oxygen species (ROS) either through the induction of antioxidant enzymes such as superoxide dismustase (SOD) or metallothionein antioxidant function (Eide, 2011), or through other mechanisms.

Zinc deficiency is a worldwide health problem and may lead to a wide range of physiological and pathological defects in man and animals, such as impairment of growth and development, reproductive disorders, immune and neural dysfunctions (Prasad, 2001 & 2004; Overbeck *et al.*, 2008) as well as skin leisons, ocular derangements, general debility, lethargy and increased susceptibility to infection (Prasad, 2008; Simonehauser and Baumgartner, 2005). However, excessive zinc accumulation is also harmful and has been associated with increased risk of prostate

cancer (Leitzmann *et al.*, 2003), and impaired neural and immune functions, which ultimately can lead to haemolytic anaemia (Fosmire, 1990).

1.2 Cellular functions of zinc

Zinc is a basic requisite for about 3000 zinc-containing proteins that are involved in many cellular processes such as cell growth and differentiation, proliferation and migration, apoptosis, transcriptional regulation, nucleic acid and protein synthesis, protein trafficking, intracellular signalling, reproduction, immunity and neuromodulation (Passerini *et al.*, 2007; Hirano *et al.*, 2008). Zinc can potentially modulate signal recognition, second messenger metabolism and the function of protein kinases and protein phosphatases (Bayersmann and Haase, 2001, Yamasaki *et al.*, 2007, Hogstrand, 2009). It is clear that zinc plays an essential role in cellular metabolism, however little is known about how it is regulated or incorporated as a cofactor. Due to diverse functions of zinc in cellular metabolism, dysregulation of cellular zinc has been linked to a range of disorders in human such as Alzheimer's disease (Religa *et al.*, 2006), diabetes (Mocchegiani *et al.*, 2008), acrodermatitis enteropathica (Dufner-Beattie, 2007) and cancer (Taylor *et al.*, 2007), hence, suggesting an urgent need to understand exactly how zinc is controlled in aberrant cells to correct the imbalance (Hogstrand *et al.*, 2009).

1.3 Zinc regulation

Because zinc is an essential micronutrient for all organisms where it plays a pivotal role in several biochemical processes, its concentration must be tightly regulated at cellular and organismal levels to maintain adequate concentration in order to avoid potential

detrimental effects of its deficiency or excess. This is achieved at the cellular level through the coordinated regulation of zinc intake, intracellular compartmentalization and efflux. Intracellular zinc homeostasis is thus in part maintained by two families of zinc transporters that traffic zinc across biological membranes; i.e. the ZnT (SLC30) transporter family, which functions to efflux zinc out of the cytosol, and the ZIP (SLC39) transporter family, which mobilizes zinc in the opposite direction to regulate influx of zinc into cytosol from the outside of the cells or from the lumen of intracellular compartment (Eide, 2004; Palmiter and Huang, 2004). Although the mechanisms that contribute to zinc homeostasis in mammals have not been fully explored, studies of metal acquisition and transportation, sensing, redistribution and excretion mechanisms as well as regulatory and environmental factors are all integral to building an understanding of how zinc homeostasis is achieved. An increasing body of evidence demonstrates that functional analysis of zinc transporters is very important for understanding the mechanism by which zinc homeostasis is achieved. Both membrane associated transporters and mobile ligands such as metallothioneins probably contribute to overall zinc homeostasis and protection against toxicity. However, their exact physiological roles remain to be established (Muylle *et al.*, 2006). Regulation of zinc absorption or uptake in mammals or vertebrates in general is achieved through zinc transporters in the apical membrane of intestinal epithelial cells. Zinc absorption increases under conditions of zinc deficiency and decreases when zinc is in excess. In teleosts and other aquatic invertebrates, zinc uptake can also be through the gill chloride cells. There is evidence that reduction in dietary zinc content produces a marked increase in intestinal absorption with a decrease in intestinal and urinary zinc losses (Fung *et al.*, 1997). In mammals, zinc homeostasis involves the co-ordination of zinc uptake from food sources in the intestine, distribution in the plasma and secretion of

excess zinc through the bile back into the intestinal lumen, balanced with zinc losses in the urine and from cell sloughing and sweat (Krebs and Hambidge, 2001). Although there may be no storage organ for zinc in mammals, there is evidence of functional zinc storage in oviparious animals, such as amphibians and fish, where zinc is stored in the liver bound to the protein metallothionein for subsequent transport to the ovaries and incorporation into the developing oocytes (Falchuk *et al.,* 1995; Hogstrand *et al.,* 1996). Intestinal zinc cycling coupled with low urinary zinc excretion or loss must be coordinated with a third major site of zinc exchange, which is the gill. Zinc uptake via the gill from aquatic sources is itself a complex process requiring zinc transporters that operate across a range of aquatic zinc concentrations (Glover *et al.,* 2003), presenting an exceptional physiological challenge. There is an additional level of complexity when it is considered that there is potential for the gill to excrete zinc when the fish is under an exceptional strain from zinc loading (Hardy, 1987).

1.4 Zinc deficiency and toxicity

The ubiquity and versatility of zinc in cellular metabolism suggests that its deficiency or overload may well result in a generalized impairment of many metabolic functions (Hambidge, 2000). Due to its functional importance, even moderate zinc deficiency can cause problems including anaemia, loss of appetite, impairment of growth, immune dysfunction & cognitive impairment, developmental problems and teratogenesis (MacDiarmid *et al.,* 2000). Conversely, excessive zinc accumulation can be toxic to cells and has been implicated in copper deficiency anaemia, bone marrow toxicity, pancreatic damage as well as neurodegenerative conditions (Frederickson and Bush, 2001) and risk of prostate cancer. Some of these derangements as a result of zinc deficiency or excess have been associated with dysregulation of some of the zinc

transporters (Lichten and Cousins, 2009). The total zinc content of a typical fibroblast-like cell grown in ordinary tissue culture medium is ~0.25 fmol/cell or ~200μM and cells stop growing in a zinc-deficient medium when the total cellular zinc level falls to ~0.2 fmol/cell (Palmiter and Findley, 1995). At this point all nonessential zinc has been used and it is possible that critical zinc-containing proteins can no longer be synthesized or cellular division is impaired because this process is regulated by Zn^{2+} signalling (Balesaria, 2004). On the other hand, exposure of cells to high concentrations of zinc activates several protective mechanisms that include down-regulation of zinc uptake transporters, induction of zinc efflux transporters, sequestration of zinc in intracellular compartments, and induction of metal-binding proteins such as metallothioneins (Gaither and Eide, 2001). In some mammalian cells that cannot synthesize metallothioneins (MTs), zinc becomes toxic at levels above ~0.6 fmol/cell, unless the cell can sequester the excess zinc. But if the MTs can be induced, cells can accumulate considerably more zinc (Palmiter and Findley, 1995). Although the toxic mechanism of zinc is not well defined, inhibition of key metabolic enzymes, stimulation of apoptosis, as well as interference with protein folding has been suggested (Sheline *et al.*, 2000). For instance, toxicity is probably due to binding of zinc to metalloproteins that require other metals for their biological activities (Kambe *et al.,* 2004) or it could be due to disruption of Ca^{2+} ion uptake or imbalance (Hogstrand *et al.*, 1995, 1998). Although exposure to toxic levels of zinc in mammals is rare, it can be a problem to aquatic organisms including fish as a result of environmental contamination by human activities. However, cellular zinc toxicity may occur in humans as a consequence of local zinc dysregulation during conditions such as postperfusional ischemic injury (Suh *et al.,* 2000). Zinc may be an environmental threat to aquatic organisms and is one among the elements with the highest frequency of water quality criteria violation in

Europe and U.S.A (Bodar *et al.*, 2005). In fish, the gill is the critical target organ for zinc toxicity, and toxicity to systemic overload is of primary relevance because of exposure to elevated concentrations of zinc in water through the gill epithelium. Waterborne zinc exposure in fish causes mortality, growth retardation, tissue alterations, respiratory and cardiac changes, inhibition of spawning and a multitude of additional detrimental effects (Spry and Wood, 1985). A number of factors can influence toxicity including pH, speciation, exposure time, exposure concentration, genetic make-up, developmental stage, water hardness, feeding and trophic levels. It is clear that zinc plays vital roles in many processes and this is highlighted by the multitude of defects caused by zinc deficiency and overload. Elucidating the mechanisms for zinc uptake at the molecular level may aid the understanding of how zinc is incorporated and absorbed, leading to enhanced understanding of the pathophysiology of zinc deficiency and toxicity.

1.5 Cellular zinc transporters

Intracellular zinc is strictly regulated by binding to metallothioneins and glutathione and by compartmentalization through the activities of various zinc transporters or channels (Chimienti *et al.,* 2003). The successive cloning of various zinc transporters has greatly enhanced the knowledge of the molecular mechanisms governing zinc uptake. These transporters have been identified in many organisms including bacteria, plants, yeast, teleost and man (Montanini *et al.*, 2007). Zinc transporters are transmembrane proteins, controlling the movement of zinc across cellular and intracellular membranes (Fig 1.1). Transport or movement of zinc into the cytosol and out of the intracellular organelles is mediated by members of the ZIP (SLC 39) protein family whereas members of the ZnT (SLC 30) family of zinc transporters mediate zinc efflux out of the cytosol and into the

intracellular organelles. The influence of various agents such as metals, hormones, and cytokines on the expression patterns, and the genetic diseases that have been associated with some of these zinc transporters causing aberrant expression have been elucidated (Lichten and Cousins, 2009).

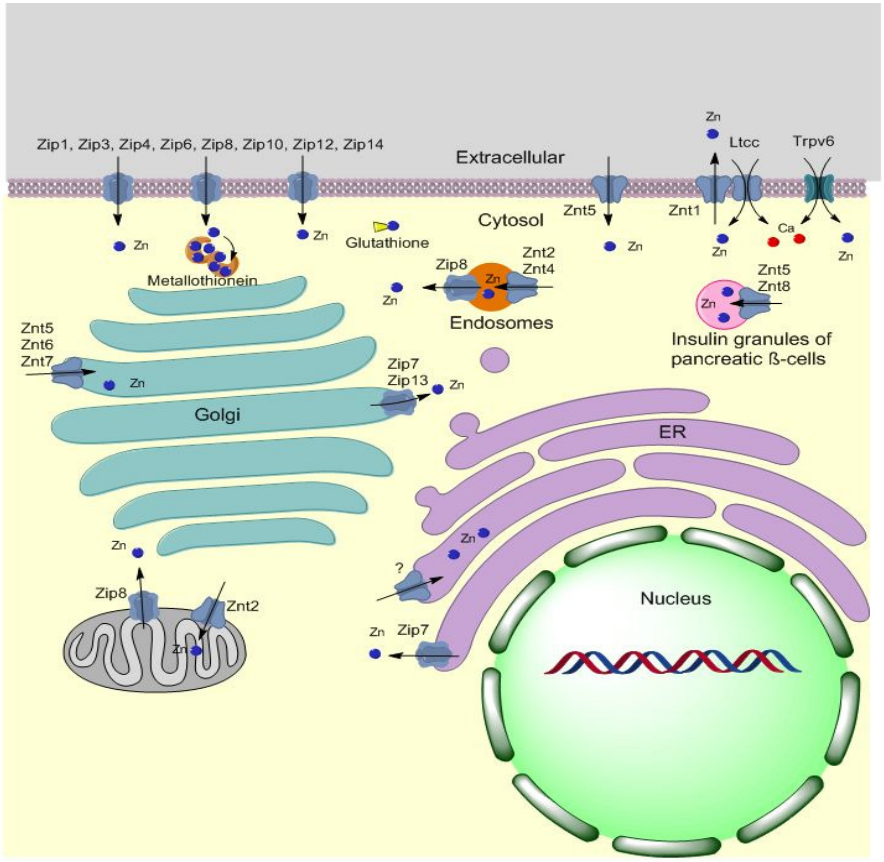

Fig. 1.1. Cellular localization of zinc regulatory proteins in a generic cell with the major intracellular and plasma membrane zinc transporters and buffers, which are found on multiple intracellular organelles and regulate cellular zinc concentrations (Adapted and modified from Hogstrand, 2011).

1.5.1 ZIP (SLC 39)

The ZIP family of zinc transporters or channels have eight transmembrane domains (TMDs) with extracellular amino and carboxy termini, a long loop region between TMDs III and IV and a very short C-terminus containing a histidine-rich domain. The ZIP family is highly heterogeneous, and based on the degree of sequence conservation, the family is broadly divided in to four subfamilies which include; **I** (ZIP 9), **II** (ZIP 1, 2 & 3), **LZT/LIV-1** (ZIP 4, 5, 6, 7/ KE4, 8, 10 & 12) and **gufA** (ZIP 11) (Gaither and Eide, 2001). With the exception of ZIP7, the LZT subfamilies of transporters contain a potential metalloprotease motif (HEXPHEXGD) in the fifth transmembrane domain (TMD V) (Taylor and Nicholson, 2003a).

The long extracellular N-terminal domains of ZIP proteins, especially the LIV-1 (LZT) subfamily, have sequences and predicted structure very similar to those of prion proteins (Ehsani *et al.*, 2011) and it has been proposed that LIV1 proteins are evolutionarily related to prion proteins (Malaga-Trillo *et al.*, 2009, Ehsani *et al.*, 2011). This prion-like motif in the N-terminus of the subfamily could mean that they can dimerise or otherwise form complexes with the prion protein.

A total of fourteen ZIP transporters have been discovered so far in mammalian cells and about ten cloned in zebrafish (Feeny *et al.*, 2005; Kambe *et al.*, 2006; Ho *et al.*, 2012). Phylogenetic comparison between the teleost and mammalian ZIP zinc channels has shown that the zebrafish ZIPs are human orthologs (Fig. 1.2) having the same number of transmembrane domains and a long intracellular loop region between TMDs III and IV with a very short C-terminus (Fig. 1.3) (Feeny *et al.*, 2005). Recent data from Ensembl zebrafish genome browser (Zv9) indicates there are twelve Zip transporters in zebrafish including Zip8 having two isoforms (Fig. 1.2). Among these transporters, the zinc transporting activity of ZIP1-8, ZIP10, ZIP13 and ZIP14 has been experimentally

verified (Cousins *et al* 2003; Zheng *et al.*, 2008; Fukada *et al.*, 2008, Lichten and Cousins, 2009). ZIP1-6 and ZIP14 have been shown to increase zinc uptake from extracellular fluid, whereas ZIP7 is believed to mediate movement of zinc from endoplasmic reticulum into the cytosol.

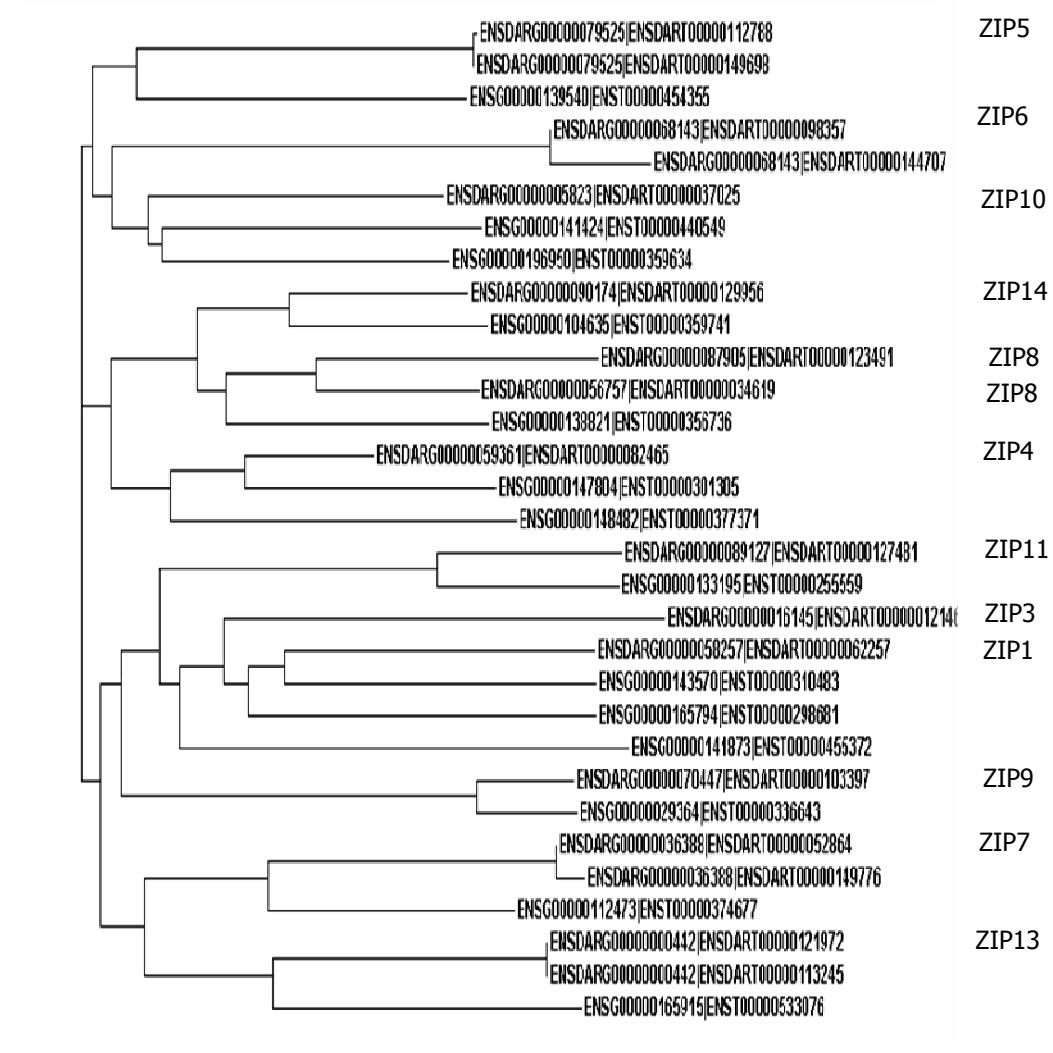

Fig 1.2: The phylogenetic tree for human and zebrafish ZIP (SLC39A) zinc transporters or channels. Apparent orthologue clusters are annotated with the human GENE name assignment from Ensembl.

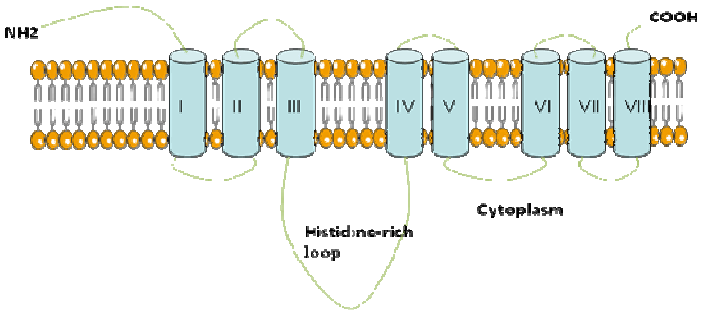

Fig: 1.3. Members of ZIP subfamilies are predicted to have eight transmembrane domains. A variable region between transmembrane domains III and IV, which is cytoplasmic and contains the His-rich motif, is thought to bind the zinc ion.

ZIP transporters or channels are involved in regulating many cellular and biochemical processes and loss of function or dysregulation of some of these proteins results in impairment of zinc homeostasis, which predisposes the body to zinc imbalance-related diseases (Lichten and Cousins, 2009). Mutation in the human *ZIP4* gene causes an inherited disorder of a mal-absorption syndrome called acrodermatitis enteropathica (Wang *et al.*, 2004; Andrews, 2008; Dufner-Beattie *et al.*, 2007). The expression of *Zip8* is regulated by the transcription factor NF-kB, which is vital in cell survival and innate immunity (Besecker *et al.*, 2008). ZIP7 is phosphorylated by casein kinase to mediate zinc release from the ER for the activation of tyrosine kinases such as Src, epidermal growth factor receptor (EGFR) and insulin-like growth factor 1 (IGF1) receptor, which promote cell proliferation (Hogstrand *et al.*, 2009; Taylor *et al.*, 2102). Furthermore, the plasma membrane zinc importers, ZIP6 and ZIP10, whose abundance is increased in breast cancers, mediate cell detachment and migration through activation of AKT (aka protein kinase B from 'Akt' mouse strain) and glycogen synthase-kinase-3α (GSK-3α) leading to decreased E-cadherin (CDH) abundance and enhanced metastasis (Lopez and Kelleher, 2010; Kagara *et al.*, 2007). Over expression of ZIP4 is

also reported in pancreatic and hepatocellualar carcinoma with increased migration (Zhang *et al.*, 2010; Weaver *et al.*, 2010). Interestingly, zebrafish *Zip6/Liv1* controls epithelial-mesenchymal transition (EMT) through its activation by STAT3 and this suggests that ZIP6/LIV-1 has a role in cell migration during development (Yamashita *et al.*, 2004). Similarly, the *Drosophila fear-of-intimacy* gene, which encodes a ZIP6-like zinc transporter, was also shown to be essential during development, where it plays a role in migration of germ cells for proper gonad development (Mathews *et al.*, 2006). Similarly, the *Drosophila catsup* (catecholamine up) gene that encodes ZIP7 is essential for regulating the circadian rhythm that controls sleep in flies (Harbison *et al.*, 2009). Zinc and abundance of ZIP1, ZIP2, and ZIP3 decline during progression of prostate cancer, leading to increased activity of NF-kB. Furthermore, ZIP1 overexpression suppressed NF-kB activity and sensitized cultured prostate cancer cells to apoptosis (Golovine *et al.*, 2008; Makhov *et al.*, 2009). ZIP13 is involved in bone morphogenetic protein (BMP) and transforming growth factor-α (TGF- α) signaling. Ablation of this gene in mice causes reduced maturation of connective tissue cells, leading to malformation of cartilage, bone, and teeth (Fukada *et al.*, 2008). In addition, mutations in this gene were found in patients with a unique variant of Ehlers-Danlos syndrome, who exhibit clinical symptoms similar to those of the knockout mice.

1.5.2 CDF/ZnT (SLC 30)

The other family of zinc transporter is known as the Cation Diffusion Facilitator (CDF) family or simply ZnT (SLC30) transporter family. The ZnT zinc transporters have been shown to efflux zinc away from the cytosol either into the organelles or out of the cell except ZnT5 (variant B) whose function is to increase zinc uptake across the plasma membrane into the cytosol (Jackson *et al.*, 2007)). Most ZnT proteins have six

transmembrane domains (except Zn T5 which has twelve) and are predicted to have similar topology containing an intracellular N-terminus and C-terminus and a histidine-rich loop, which is found between transmembrane domain IV and V, with potential for zinc binding. The amphiphatic nature of transmembrane domains I, II and V and the loss-of-function consequences of deletion of the C-terminal parts of ZnT1 indicate that it is this area of the protein that is involved in pore formation (Liuzzi and Cousins, 2004). However, recent crystallographic data of the bacterial Yiip protein, which is the ZnT analogue, suggest that the zinc transporter functions as homodimers with zinc binding activating its transport by inducing conformational change around the highly conserved salt bridges that interlock the transmembrane domains (Lu and Fu 2007; Fu, 2010). Based on sequence similarities among members of the ZnT family, they are divided into three subfamilies: **I** (ZnT 9), **II** (ZnT 1, 5, 7 & 10) and **III** (ZnT 2, 3, 4, 6 & 8) (Gaither and Eide, 2001).

Phylogenetic analysis between the teleost and mammalian ZnTs also showed that zebrafish Znts are human orthologs (Fig. 1.4) having the same number of transmembrane domains and a long intracellular loop region between TMDs IV and V (Fig. 1.5) (Feeny *et al.*, 2005). To date, there are 10 members of ZnT family identified in mammals (Lichten and Cousins, 2009) and about 7 (excluding Znt3, 6 & 10) have been cloned in zebrafish with their sequences confirmed (Feeny *et al.*, 2005). Recently, Ho *et al.*, (2012) showed the presence of Znt6 transcript by qPCR in the zebrafish embryo during development but the sequence of the PCR product was not confirmed. However, recent data from Ensembl zebrafish genome browser (Zv9) have revealed the presence of all the Znt transporters except Znt3, suggesting that only Znt3 is lacking in the zebrafish genome, thus making the total number of Znt transporters nine, including

Znt1 with two isoforms. Among these transporters, only the transporting function of ZnT1-8 has been previously confirmed (Cousins *et al.,* 2006, Lichten and Cousins, 2009), and with recent addition of ZnT10 (Bosoworth *et al.,* 2012).

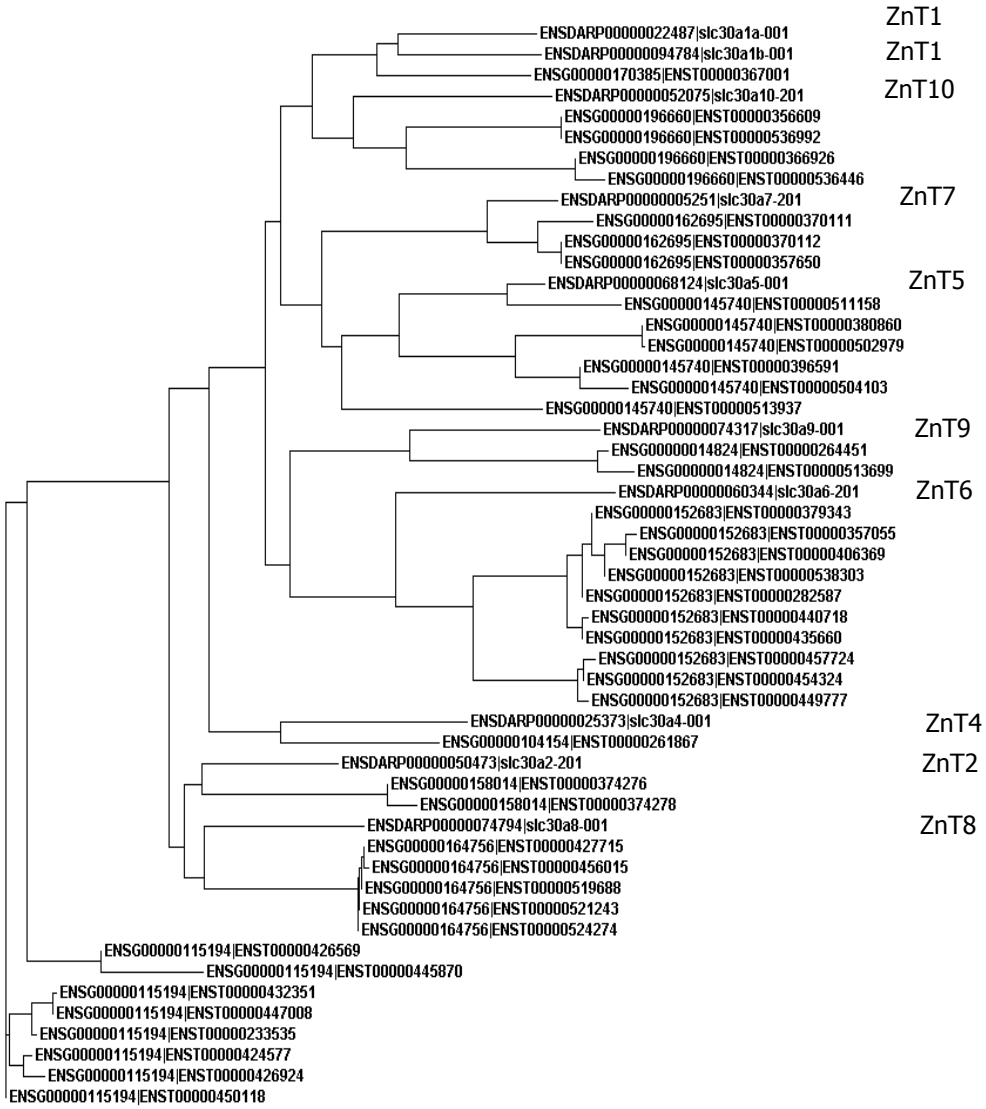

Fig 1.4. The phylogenetic tree for human and zebrafish ZnT (SLC30A) zinc transporters. Apparent orthologue clusters are annotated with the human GENE name assignment from Ensembl.

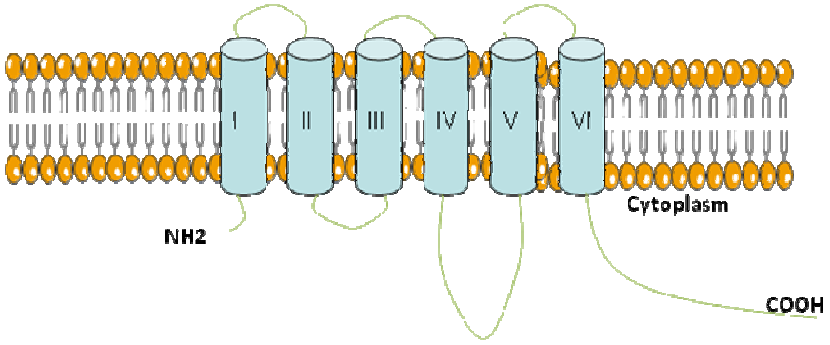

Fig: 1.5. Membrane topology of the ZnT protein family, predicted to have six transmembrane domains. A variable region between transmembrane domains 1V and V, which is cytoplasmic and contains the His-rich motif, is thought to bind the zinc ion.

The distribution and function of the ZnT proteins is regulated and changes in their distribution pattern or function have been linked to multiple diseases. Loss of zinc transporters due to gene mutations or incorrect translation of mRNA have been reported to result in various pathological conditions, which may include embryonic lethality, incorrect absorption of zinc and reduced body fat and weight in mouse (Huang *et al.,* 2007; Andrew *et al.*, 2004). Lethal milk syndrome in mouse results from a mutation in the *Slc30a4* gene encoding the ZnT4 protein (Murgia, *et al.,* 2006). Mutation in the maternal *SLC30A2* gene (which is required in human for zinc content in milk) causes transient neonatal zinc deficiency in humans (Chowanadisai *et al.*, 2006). The distribution of ZnTs is widespread, although some are more cell-specific, such as ZnT3 in neuronal synaptic vesicles (Redenti and Chappell, 2004), ZnT8 in the brain, liver and pancrease (Palmiter and Huang, 2004) and ZnT2 in mammary gland, small intestine, kidney, placenta and liver (Liuzzi and Cousins, 2004). ZnT8 is localized to insulin-containing vesicles, and a polymorphism in this gene (Arg325→Trp; R325W) has been linked to susceptibility to type 2 diabetes where the zinc transporting activity decreases (Sladek *et al.*, 2007; Nicolson *et al.*, 2009). A knockout of this gene in mice also reduces zinc transport into pancreatic β-cells, affecting insulin and glucose homeostasis

(Wijesekara *et al.*, 2010; Lemaire *et al.*, 2009). Ablation of *ZnT7* in mice caused reduced food intake and poor growth, leading to a prediabetic state (Huang *et al.*, 2007). Furthermore, *ZnT7* is also present in cells in the islets of Langerhans, where it may regulate zinc accumulation and insulin biosynthesis. However, as research in the field of zinc transporters advances, it's believed that more diseases associated with them will be discovered.

ZnT1 was the first mammalian zinc transporter to be discovered and is expressed throughout the body but notably in basolateral membranes of tissues involved in zinc acquisition or recycling like intestine, kidney and placenta (Liuzzi and Cousins, 2004; Lichten and Cousins, 2009). To date, ZnT1 and also ZnT10 are the only zinc transporters protein among mammalian ZnT members confirmed to be localized to the plasma membrane. Over-expression of the *ZnT1* gene allowed the cell to grow in the presence of a high level of extracellular zinc by promoting zinc efflux activity and could confer zinc resistance to an otherwise zinc-sensitive cell line (Palmiter and Findley, 1995). Since ZnT1 null mice showed embryonical lethality, therefore Znt1-mediated zinc transport is critical for normal development (Cousins and McMahon, 2000, Andrew *et al.*, 2004).

In most instances, the experimental evidence of cellular localisations of various zinc transporters comes from experiments with mammalian cells (Hogstrand *et al.,* 2009), with exceptions for Znt1 (Balesaria and Hogstrand, 2006), Zip1 (Qiu *et al.*, 2005), Zip3 (Qui and Hogstrand, 2005), and Zip7 (Qiu and Hogstrand, unpublished), which have been localised in cultured fish cells to the same membranes as their human orthologes. The expression and distribution of various zinc transporters in juvenile zebrafish tissues, as indicated by abundances of their respective mRNAs, is shown in Table 1.0. The expression patterns during the course of zebrafish embryonic development as reported

recently (Ho *et al.,* 2012) is illustrated in Table 1.1, whereas their tissue specific expression is shown in Table 1.2 as previously described (Thiese *et al.,* 2004).

Gene	Gill	Intestine	Kidney	Ovary	Brain	Eye	Muscle	Liver
znt1	+	+	+	++	-	-	+	+
znt2	-	-	-	-	+	+	-	-
znt4	+	+	+	++	+	+	-	+
znt5	++	++	+	++	-	+	-	+
znt7	+	+	+	++	-	-	-	-
znt8	+	-	-	-	-	+	-	-
znt9	+	-	-	+	-	+	-	-
zip1	+	+	++	++	+	++	+	++
zip3	++	++	+	+	+	+	+	+
zip4	-	++	-	+	-	+	-	-
zip6	+	-	+	++	+	+	-	-
zip7	++	++	++	++	+	++	+	++
zip8	+	+	-	-	-	-	-	-
zip10	++	++	++	++	++	+	-	++
zip13	+	+	+	++	+	+	+	+

Table 1.0. Expression of zinc transporter genes of the Znt (Slc30) and Zip (Slc39) families in tissues of juvenile zebrafish as indicated by abundances of their respective transcripts (Feeney *et al.* 2005). Relative abundance of mRNA for each transporter is shown with -, +, and ++, denoting absent or low, present, and abundant, respectively.

Gene	0 hpf	2 hpf	6 hpf	12 hpf	24 hpf	48 hpf	120 hpf
znt1	3+	3+	3+	4+	3+	4+	5+
znt2	-	-	-	-	-	1+	1+
znt4	2+	1+	1+	1+	1+	2+	2+
znt5	3+	3+	2+	3+	3+	3+	4+
znt6	1+	1+	1+	1+	1+	2+	2+
znt7	3+	3+	3+	3+	3+	3+	3+
znt8	-	-	3+	3+	3+	3+	3+
znt9	2+	2+	1+	2+	2+	3+	3+
zip1	2+	2+	2+	2+	2+	2+	3+
zip3	-	-	-	1+	1+	1+	2+
zip4	-	-	-	1+	1+	1+	2+
zip6	3+	3+	3+	3+	3+	3+	3+
zip7	2+	2+	2+	3+	3+	3+	3+
zip8	-	-	-	-	-	1+	1+
zip9	3+	2+	2+	2+	2+	3+	3+
zip10	2+	2+	2+	2+	2+	2+	2+
zip11	2+	2+	1+	2+	2+	2+	2+
zip13	3+	2+	2+	2+	2+	2+	3+

Table 1.1. Expression of zinc transporter genes of the Znt (Slc30) and Zip (Slc39) families in whole zebrafish embryos as indicated by abundances of their respective transcripts over a period of 120 hpf (Ho *et al.* 2012). Relative abundance of mRNA for each transporter is represented on a range of logarithmic scale of values as; - (0.001-0.009), 1+ (0.01-0.09), 2+ (0.1-0.9), 3+ (1.0-9.0), 4+ (10-99), 5+ (100-1000) where - denotes lack of detection.

Zinc transporter genes	Region of mRNA expression
znt1	Central nervous system (CNS), yolk syncytial layer (YSL), adaxia cells and Kupffer's vesicle
znt2	CNS
znt4	Not spatially restricted
znt5	Not spatially restricted
znt6	Not spatially restricted
znt7	CNS, blastodisc, yolk, blastoderm, notochord, prechordal plate, pronephric duct (Hsu *et al.,* 2009)
znt8	No expression data available
znt9	Not spatially restricted
zip1	YSL, neural crest
zip3	No expression data available
zip4	No expression data available
zip6	No expression data available
zip7	CNS, eye (Yan *et al.,* 2012), notochord
zip8	No expression data available
zip10	Anterior axial hypoblast, polster, hatching gland and pigment cell
zip13	No expression data available

Table 1.2. Tissue specific expression of zinc transporter genes of the Znt (Slc30) and Zip (Slc39) families in zebrafish embryonic development by ISH as described by Thiese *et al.,* 2004.

1.5.3 Metallothionein

Metallothionein (MT) and glutathione are major zinc-binding and zinc-buffering molecules in the cytosol (Colvin *et al.*, 2008; Jiang *et al.*, 1998). MT genes are induced by hormones and xenobiotics as well as heavy metals (Sazuki *et al.*, 1993) and the

protein is characterized by a very high content of cysteine residues that can bind up to seven zinc atoms, and when metallothionein is isolated from tissues it is saturated with zinc, or zinc in combination with other metals. There are two genes in zebrafish and more than ten in human. The importance of MT for zinc binding in fish cells increases in cells with high zinc load (Hogstrand and Haux, 1996; 2002; Muylle *et al.*, 2006). However, recent detailed analysis has shown that the different zinc binding sites differ by four orders of magnitude in their affinities for zinc and that unsaturated MT with up to three available zinc binding sites exists in the cell (Krezel and Maret, 2007). Studies of the promoter region of MT genes revealed that they contain metal response elements (MREs) and MTF1 was also found as the transcriptional factor that binds to the proximal MREs (Radtke *et al.*, 1993; Stuart *et al.*, 1985).

The classic general view of zinc handling by the cell has been that zinc first binds to glutathione and that an overload of the glutathione pool will activate MTF1, which will then stimulate *de novo* synthesis of ZnT1, gamma-glutamylcysteine synthetase (Gcl) and apo-metallothionein (thionein), which will then increase the capacity for zinc extrusion and sequester the zinc excess (Andrews, 2001; Hogstrand and Wood, 1996). It is now known that because MT in the cell is not normally saturated with metal, it can contribute to the initial buffering of zinc entering the cell (Colvin *et al.*, 2010). However, when experimental data of labile zinc concentrations in the cytosol of cells exposed to zinc were fitted to mathematical quantitative models, it was clear that the buffering capacity of MT and glutathione could not account for what was observed (Colvin *et al.*, 2008). Instead, the model that best fitted the data was the rapid translocation of the entering zinc to a “deep store” by a vehicle that also had buffering capacity before the zinc reappeared in the cytosol at a later stage. This vehicle was

termed a “muffler” to distinguish from a pure buffer and the “deep store” was predicted to perhaps be one or several organelles (Colvin *et al.*, 2008; Colvin *et al.*, 2010).

1.6 Zebrafish and zebrafish development

The zebrafish (*Danio rerio*) belongs to the family of freshwater fishes Cyprinidae (Nelson, 1994) and currently there are about forty four danionin species (Fang, 2001). They are naturally distributed throughout South and South-East Asia, with highest species diversity in North-East India, Bangladesh and Myanmar (Barman, 1991). Morphlogically, zebrafish are characterized by their small size, which rarely exceeds 40 mm standard length (SL) with a fusiform shaped body that is laterally compressed and a terminal oblique mouth which is directed upwards. The female is bigger than the male of the same age, which is slimmer and tapers forward compared to the female that is broader and fatter ventrally. The diagnostic features of the species are the incomplete lateral line extending to the pelvic fin base, two pairs of barbels and five to seven dark blue longitudinal stripes extending from behind the operculum into the caudal fin (Barman, 1991). The colour pattern comprises three types of pigment cell, dark blue melanophores, gold xanthophores and iridescent iridophore (Parichy, 2006a & b) (Fig. 1.6.).

Zebrafish embryo development is divided into several stages; zygote or 1-cell stage (0-0.45hr), cleavage or 2-64 cells stage (0.45-2.15 hrs), blastula or 128 cells -30% epiboly stage (2.15-5.15 hrs), gastrula or 50% epiboly-tail bud stage (5.15-10 hrs), segmentation or 1-26 somites (prim 5) stage (10-24 hrs), pharyngula or prim 5-long pec stage (24-48 hrs), hatching or long pec-protruding mouth stage (48-72 hrs), early larval stage (3-30 days), juvenile stage (1-3 months) and adult stage (3-48 months) (Kimmel *et al.*, 1995). The gastrulation stage is the critical period in development where the morphogenetic

cell movements of the involution, the convergence and extension movement occur, producing the primary germ layers and the embryonic axis (Kimmel *et al.*, 1995).

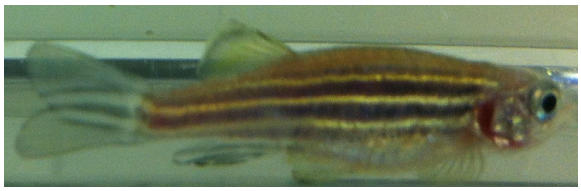

Fig 1.6. Zebrafish (*Danio rerio*)

1.7 Reverse Genetics in Zebrafish

Zebrafish is a popular model system frequently used for studies of vertebrate developmental biology, mineral uptake, toxicology and chemical/drug safety because of its numerous strengths as a molecular genetics and embryological system, in addition to its unique features such as ease of maintainance and drug administartion, short reproductive cycle, *ex utero* development and optical clarity during embryogenesis (i.e. transparency), which permits visual assessment of developing organs (Westerfield, 1993). Thus, the zebrafish is a desirable system in which to carry out classic genetic screens to identify loci required during vertebrate embryonic development and to analyze the resulting phenotypes with powerful embryological techniques (Lekven, 2000). In addition to the ability to assess gene function through overexpression from injected RNAs or DNAs in embryos, zebrafish transgenic technologies are being developed at an increasing rate.

Reverse genetics methodologies generally refer to the generation or targeted discovery of a mutation in a gene that is known by its sequence. It is a useful approach to discover gene's function by analysing the phenotypic effect of specific gene sequence, contrary

to the so-called forward or classical genetics in which the investigative process proceeds in opposite direction. That is, while forward genetics attempts to find the genetic basis of a phenotype or trait, reverse genetics aims to to find what phenotype arises as a result of particular genetic sequences. Different effective reverse genetics approaches are in existence but they tend to be organism specific. Examples include gene knockout via homologous recombination in mice (and recently in *Drosophila*), gene knock-in via insertion (transgene) in mouse and gene knockdown or silencing via antisense morpholino oligonucleotides in *Xenopus* and zebrafish oocytes or via RNA interference (RNAi) in *Ceanorhabditis elegans, Drosophila* and mouse. Other methods include transposable elements in *Drosophila* and *Ceanorhabditis elegans*, and TILLING which is a general method that is applicable to many organisms (Stemple, 2004). TILLING which stands for Targeting Induced Local Lesions in Genomes, is a reverse genetics strategy that identifies mutations in specific genes of interest in chemically mutagenized populations. TILLING was first described in 2000 for mutation detection in *Arabidopsis* but has now being extended to a wide range of plants including soyabean, rice, barley and maize as well as animal model systems, including *Drosophila, Caenorhabditis elegans*, rat, medaka and zebrafish. It has also been used for the discovery of naturally occurring polymorphisms in humans (Moens *et al*., 2008).

Mutagenized populations carry a large number of potentially deleterious recessive mutations that can be discovered based on the phenotypes of homozygous mutants (forward genetics) or by detecting them directly in the genomic DNA of heterozygous or homozygous individuals, irrespective of any phenotypes they may cause (reverse genetics). The challenge in reverse genetics is to identify rare mutations within a large population of non-mutant individuals.

Other new and very promising tools for genetic manipulation in plants and animals include zinc finger nucleases, which are artificial restriction enzymes generated by fusing a zinc finger DNA-binding domain to a DNA-cleavage domain and can be used to precisely alter the genomes of higher organisms including zebrafish (Ekker, 2008). Despite all of the strength mentioned, only one technology that is lacking in zebrafish system or indeed in any vertebrate system other than the mouse, is the ability to target mutations to specific genes through homologous recombination.

1.7.1 TILLING

The general method for TILLING in zebrafish involves screening genomic DNA from a large library of ethyl nitrosourea (ENU) or ethyl methanesulfonate (EMS)-mutagenized zebrafish for rare mutations in genes of interest using Cel1 endonuclease (from bulk celery), or denaturing high-performance liquid chromatography (DHPLC) on pools of fish to detect base-pair changes by heteroduplex analysis (McCallum *et al.,* 2000), or by direct resequencing of individual fish (Moens *et al.,* 2008). Mutations are then recovered by out-crossing the single identified carrier. In general, the key components of a successful TILLING project include, a large and well mutagenized library of fish, an efficient screening method and a near-perfect ability to recover valuable mutations once they have been found (Moens *et al.,* 2008). The method of TILLING technology for generation of a mutant carrier is briefly illustrated below in Figure 1.7.

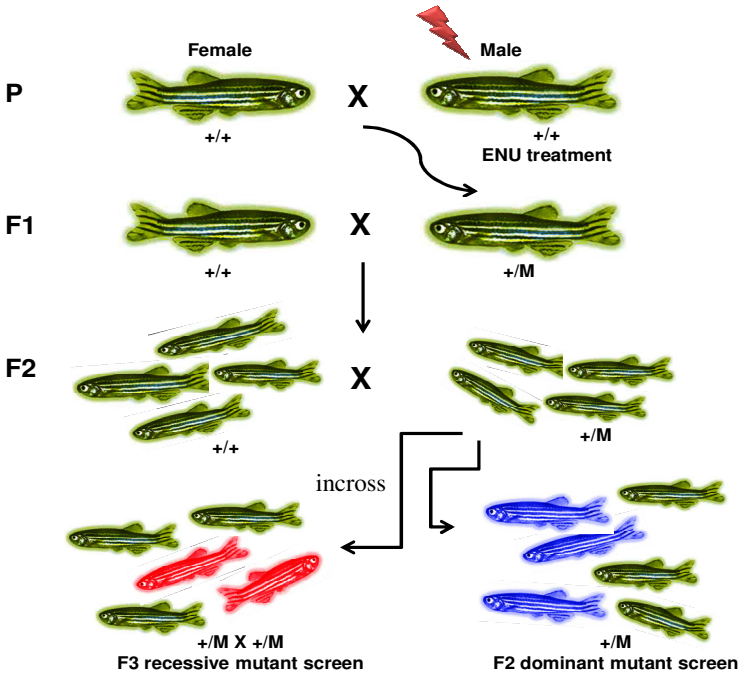

Fig 1.7: Three-generation breeding scheme for chemically-induced mutant fish. Male fish are mutagenised and then crossed to wild-type females to produce an F1 generation. An F2 generation is made by in-crossing F1 siblings. Dominant behavioural mutants can be identified in this F2 generation (blue fish). For recessive mutant carriers, a second in-cross is performed and the progeny screened for behavioural alterations (red fish) - if the inheritance in Mendelian then one quarter of the progeny should show the behavioural defect (Adapted and modified from Norton and Bally-Cuif, 2010).

1.7.2 Gene knockdown by morpholino oligonucleotides

Antisense morpholino-modified oligonucleotides (morpholinos; MOs) are the most widely used in zebrafish genetic manipulation for temporarily silencing the effect of a gene. MOs are composed of a phosphorodiamidate backbone with a morpholine ring and the same bases as DNA. MOs are designed as oligomers of 25 morpholine bases that target the RNA of interest via complementary base pairing. The presence of the neutrally charged phosphorodiamidate backbone results in molecule with high binding affinity for RNA, thereby facilitating steric hindrance of proper transcript processing or translation (Summerton, 1999). The mechanism of action of splice blocking MOs is thought to be binding and inhibiting pre-mRNA processing via inhibition of splicesome components hindering normal endogenous splicing and often leading to premature

termination and non-sense decay of the transcript (Morcos, 2007). Translational blocking MOs on the other hand bind complementary mRNA sequences within the 5' un-translated region (UTR) near the translational start site (AUG) thereby hindering ribosome assembly (Summerton, 1999). While splice-site MOs inhibit zygotic transcripts, translational MOs inhibit both maternal and zygotic transcripts (Draper *et al.*, 2001; Nasevicius and Ekker, 2000).

1.8 Zinc and hatching of teleost embryos

Vertebrate hatching is a process that involves enzymatic activity and zinc is known as an essential microelement required in minute quantities for the activation of most enzymes (Vallee, 1959) as well as inhibition (Hase and Maret, 2003; Wilson *et al.*, 2012). Waterborne zinc exposure has been shown to influence hatching of fish embryos (Somasundaram *et al.*, 1984; Dave *et al.*, 1986) and at a concentration of about 10^{-5}M under alkaline pH, zinc was shown to enhance the activity of enzymes in the hatching liquid (perivitalline fluid) at the time of hatching of sea trout towards casein or azocasein or chorion lysis (Luberda *et al.*, 1993). Among the known zinc transporters in zebrafish, only *zip10* has been shown to be expressed in the hatching gland cells (HGC) (Thiese *et al.*, 2004), suggesting that the protein encoded by this gene might participate in hatching process either through zinc traffiking to the HGC possibly for the activation of metalloprotease hatching enzyme (HE) and /or inhibition of the lysosomal cysteine protease cathepsin L (CatL 1), both of which are known as markers of the HGC and are enzymes that are involved in hatching (Sano *et al.*, 2008; Trikic *et al.*, 2011), or through direct protein-protein interaction of Zip10 with hatching proteases. Zinc may also be involved in inhibition or induction of developmental apoptosis of the hatching gland cells, which possibly may participate in the process of hatching of

zebrafish embryos because it was found that zinc at a concentration of 10-50µM prevented apoptosis whereas it resulted in cell death in human Burkitt lymphoma B cells at 50-100µM (Schrantz *et al.*, 2001).

1.8.1 Cathepsins

Cathepsins or lysosomal cysteine protease were first discovered in the first half of the 20th century with cathepsin C being the first pure enzyme that was isolated in 1940 (Gutman and Fruton, 1948). Thereafter, the discovery of other cathepsins (e.g cathepsin B, H and L) followed. The first amino acid sequences of rat (mammalian) cathepsins B and H appeared in the early 1980s, and the first crystal structure of human cathepsin B was resolved in 1990 (Barret *et al.*, 1998,Takio *et al.*, 1983 & Musil et. al., 1991). Cathepsins are optimally active in the slightly acidic, reducing milieu that is found in the lysosomes. Most of the enzymes are endopetidases except cathepsin C, but in addition cathepsin B and H also exhibit exopeptidase activity (Table 1.3). Exopetidases have restricted access to the substrate binding sites because of additional structural features such as loops or pro-peptide parts. These features may not be present in cathepsin L, which is an endopeptidase.

Name	Synonyms	Endopeptidase	Exopeptidase		Chr location
			Carboxypeptidase	Aminopeptidase	
Cathepsin L	-	+	+	+	9q21
Cathepsin V	cathepsin L2 cathepsin U	+	-	-	9q21
Cathepsin S		+	-	-	1q21
Cathepsin K	cathepsin O cathepsin O2 cathepsin X	+	-	-	1q21
Cathepsin W	lymphopain	n.d.	n.d.	n.d.	11q13
Cathepsin F	-	+	-	-	11q13
Cathepsin O	-	n.d.	n.d.	n.d.	4q31-32
Cathepsin B	cathepsin B1	+ dipeptidase	+	-	8p22-23
Cathepsin X	cathepsin Z cathepsin P cathepsin Y	- monopeptidase also dipeptidase	+	-	20q13
Cathepsin H	cathepsin I	+ monopeptidase	-	+	15q24-25
Cathepsin C	dipeptidyl peptidase I cathepsin J	- dipeptidase	-	+	11q14

Table 1.3.: Human lysosomal cysteine proteases: nomenclature and properties (Turk *et al.*, 2001). Keys: n.d., not determined, Chr; chromosome.

It is generally believed that cathepsins like other proteases are synthesized as inactive precursors (i.e. pre-pro-enzymes or zymogen) and are activated by proteolytic cleavage of the N-terminal pro-peptide, which can be facilitated either by activation by other proteases such as pepsin or cathepsin D or by autocatalytic activation at acidic pH and/or by glycosaminoglycans (Turk *et al.*, 2000). However, only the endopetidases can be autoactivated, whereas true exopeptidases, such as cathepsins C and X, require endopetidases, including cathepsins L and S, for activation (Dahl *et al.*, 2001). Cathepsins, if prematurely activated, have enormous disruptive potential, since their total concentration inside lysosomes can well exceed 1mM (Turk *et al.*, 2001). This premature activation is controlled by endogenous protein inhibitors of lysosomal cysteine proteases such as cystatins to trap accidentally escaped proteases from the lysosomes and also to help in the defence of the organism against intruders (Turk *et al.*,

1993). Zinc ions have also been shown to be involved in enzymatic inhibition of cathepsins. Recently, it was shown that there were high levels of cathepsins B, L and S in human seminal fluid compared to blood plasma (Inayat *et al.*, 2012). This implies that the presence of cathepsins in the seminal fluid could thus in theory have an effect on the function of prostate and reproduction. Cystatin C which is an endogenous inhibitor of cathepsins, was also found to be at a high level in seminal fluid with a considerable part associated with prostasomes (Carlsson *et al.*, 2011). Thus it seems likely that high concentrations of cystatin C could be counteracted by high levels of cathepsins. In a similar manner, zinc was found to be an important element occurring in millimolar concentrations in the prostatic fluid and is often used as a marker for secretory function of the prostate (Kavanagh *et al.*, 1983). Thus, high zinc content in seminal fluid indicates that a larger portion of the seminal fluid is derived from the prostate with cathepsin B content showing a positive correlation to that of zinc (Inayat *et al.*, 2012). Similarly, cathepsin L showed a positive correlation to fructose, which comes from the seminal vesicle. The presence of zinc in this fluid is essential for the optimal development and function of the male reproductive system (Nishi, 1996) either through its inhibitory effect on the growth of prostate secondary to cancer (Liang *et al.*, 1999) or its antimicrobial properties against infectious agents associated with prostate cancer development (Cho *et al.*, 2002) or its inhibitory effect on cathepsin activity for protection of the prostate. Cathepsins are found in high amounts in prostasomes which adhere to the sperm cells and can fuse with them (Wang *et al.*, 2001, Ronquist *et al.*, 2011). Thus, prostasome-bound cathepsin may bind to the sperm cells and migrate together with the sperm cell to the oocyte. Seminal cathepsins may therefore have effects not only in the male but also in the female reproductive tract. In mammal, hatching is referred to as the lysis or escape of the zona pellucida (ZP) of the blastocysts

and it was shown in female hamster that, among other factors, the embryo-derived cathepsin accelerated hatching, which enables the blastocysts to attach and invade the receptive uterine endometrium (Seshagiri *et al.*, 2009). This effect was species-specific and was inhibited by cysteine protease inhibitors (Mishra and Seshagiri, 2000). Thus Zn^{2+} in addition to cystatins may play a role in preventing the proteolytic activity of cathepsins in the prostate (thereby protecting the integrity of the prostate) before the enzyme is released, at which point it fuses with the sperm cells for migration to the oocyte for fertilization. This cathepsin in the fertilized embryo may now become activated due to release and dilution of inhibitory zinc ions thereby playing a proteolytic role in lysis of the ZP and subsequent hatching of the blastocysts required for proper implantation. It is possible this process may mirror exactly the process of lysis of the ZP of the chorion (choriolysis) in zebrafish embryo, where hatching may involve proteolytic hatching enzyme cathepsin L (Trikic *et al.*, 2011). The hatching liquid (which is composed of a mixture of perivitalline fluid and hatching enzymes) from the zebrafish embryos at the period of hatching (54-72 hpf) showed strong specificity to the artificial substrate 7-amino-4-methylcoumarin (MCA), which suggested the involvement of cathepsin L in the hatching of the zebrafish embryo (Trikic *et al.*, 2011). The importance of zinc in the inhibition of cysteine protease is also relevant to the development of Alzeimer's disease to prevent the formation of β-amyloid plaque in the brain tissue. In the brain, a subset of glutaminergic neurons co-release zinc as a neuromodulator or neurotransmitter and these neurons are called 'zinc-ergic'. Alzeimer's disease involves a lack of zinc supply by the pre-synaptic neurone (i.e. zinc-ergic neurone) into the synaptic junction leading to activation of β-secretase enzymes such as cathepsin L or B, which then causes improper or abnormal cleavage of the membrane of β-amyloid precursor protein (APP) that forms a complex with Cu^{2+} in the

synaptic junction in exchange for Zn^{2+} resulting in plaque in the neurone thereby leading to Alzeimer's disease (Tougu *et al.*, 2011). It was also shown that a range of zinc metalloproteases of the metizincin superfamily can also process APP in a ''non-amyloidogenic'' pathway by proper cleaving of APP within its β-amyloid (Aβ) region by α-secretase thus precluding the formation of intact β-amyloid peptide or degrading the preformed β-amyloid peptide by down regulating Aβ-generation and enhancing its degredation (Tougu *et al.*, 2011). Another interesting article clearly demonstrated that copper- and zinc-containing superoxide dismutase in cholesteatoma epithelium in a human patient prevents complications by suppressing or inhibiting cathepsin L activity (Kusunoki *et al.*, 2001). Synthesis and studies on the structure-activity relationship of a series of arylaminoethyl amide compounds have revealed the crystal structure of one of the synthetic compounds to be covalently bound to and inhibit the activity of cathepsin S in presence of Zn^{2+} supporting the role of zinc in inhibition of cathepsin activity (Tully *et al.*, 2006).

1.8.2 Astacins

Zebrafish hatching enzyme (*zHE1*), which is also a member of astacin group of proteases, shows a close relationship with high similarity of the conserved residues to most enzymes in the astacin family of zinc metallopeptidases such as crayfish astacin, human meprin α and ß, fresh water hydroid *MMP2*, horseshoe crab *ASTM*, nematode *NAS13*, giant squid myosinase, spider tolloid-like proteinase, human *BMP1*, sea urchin proteinase, medaka & killifish *HCE* and human embryonic ovastacin (Fig. 1.8). Zebrafish hatching enzyme 1 (zHE1) is a zinc metalloprotease with molecular weight of 21kDa (Sano *et al.*, 2008). Although the substrate specificity of zHE 1 to 7-amino-4-methylcoumarin (MCA) is broad, cleavage of chorion proteins occurs only at two sites; TVQQS ↓DYLIK (major cleavage site) and KLMLK ↓APEPF (minor cleavage site).

Both major and minor cleavage sites exist in the N-terminal regions of the chorion zonal pellucida (ZP) glycoproteins 2 and 3 respectively (Sano *et al.*, 2008). Teleostian hatching enzyme (HE) genes are divided into clade I and II. Genes that have complete or partial intron loss compared to the ancestral genes belong to clade I. On the other hand, clade II genes have a relatively stable exon-intron structure compared to the ancestral genes (Miya *et al.*, 2003; Ishiguro *et al.*, 2003; Lavoué *et al.*, 2005). The zebrafish genes belong to clade I, with partial intron loss, and comprise three genes (*zHE1a, zHE1b* and *zHE2*), which are collectively known as hatching enzymes, while the killifish and medaka hatching enzymes are examples of clade I genes with complete intron loss. There are two genes in killifish and four genes in medaka *(kHCE 1 & 2* and *mHCE 1, 2, 3 & 4*). The killifish and medaka enzymes are known as high choriolytic hatching enzymes (HCE). Clade II genes are the duplication of the genes of clade I for additional or new function, and in killifish and medeka these genes are collectively known as low choriolytic hatching enzymes (LCE). Clade II genes appear to be absent in zebrafish, suggesting that there was no gene duplication of clade I genes in the otophysans lineage (Kawaguchi, 2007). Therefore within each clade, there are 2 subclades; euteleostean (i.e. those with clade I duplication e.g. medaka, killifish) and otocephalan (i.e. those without clade I duplication e.g. zebrafish).

Purification of hatching enzymes from several fish species has been carried out and extensive studies have been conducted on medaka (*Oryzia latipes*), killifish (*Fundulus heteroclitus*) and zebrafish (*Danio rerio*) (Yasumasu *et al.*, 1989; Lee *et al.*, 1994; Sano *et al.*, 2008; Kawaguchi *et al.*, 2005).

The expression patterns and the amino acid sequence of high choriolytic enzyme genes (HCE) in killifish and medaka are similar to that of zebrafish hatching enzyme 1a & b genes (*zHE1a & b*) suggesting that they perform similar functions. It was also shown

that both *zHE1a* and *b* are similar genes (or a single gene entity) with strong expression mainly in the hatching glands and perform similar functions whereas *zHE2* is rarely expressed or has low expression in the pre-hatching embryo and thus likely has no function in egg envelope digestion (Sano *et al.*, 2008). While zHE 1 and HCE (clade I) are strongly expressed and possess similar substrate site specificity, LCE (clade II) is weakly expressed and has different substrate preference. The higher expression of clade I genes compared to clade II genes may be a result of the low or absent intron content in clade I genes thereby requiring less time to process the transcript for translation as compared to clade II genes which has huge intron size (Kawaguchi, 2010). Hatching of embryos in killifish or medaka takes place by two enzyme systems, which cooperatively digest the egg envelope by partial digestion of HCEs, causing swelling and softening of the egg envelope, which is completed by the action of LCEs to solubilize the swollen egg envelope (Kawaguchi *et al.*, 2005; Yasumasu *et al.*, 1992). LCEs hardly digest the intact egg envelope. On the other hand, zebrafish hatching is composed of a single enzyme system (zHE1), which swells and softens the chorion by cleaving chorion proteins as in HCE in euteleostei (with similar substrate specificity), and the contractile movement of the embryos ruptures the chorion (Kawaguchi *et al.*, 2007). The amino acid sequences deduced from the cDNAs of HCE and LCE indicate that they are synthesised as proenzymes, like cysteine peptidase, and stored in zymogen granules (Yasumau *et al.*, 1992). In many families of metzincin metallopeptidases, a ‘‘cysteine switch’’ mechanism is used to maintain the enzyme in its inactive (latent) or zymogen (proenzyme) state through a mechanism involving a conserved prosegment motif with a cysteine residue that coordinates the catalytic zinc ion. However, astacin from Astacus (crayfish) is another family of metzincin that does not possess a cysteine switch, so latency or state of inactivity or inhibition is maintained through other means (Guevara *et*

al., 2010). The prototypical crayfish astacin is synthesized as a preproenzyme in the midgut gland (Stöcker and Yiallouros, 2004). There is species-dependent migration of fish hatching gland cells that commonly express astacin-like proteases in common, i.e. the final location of the hatching gland cells were found in the epithelium of the pharyngeal cavity of medaka, in addition to lateral epidermis of the head in masu and salmon, while in zebrafish it was located in the epidermis of the yolk sac (Inohaya *et al.*, 1997). The difference in the final localization of hatching gland cells in different species of fish may have resulted from the difference in the migratory route of the hatching gland cells from the polster region from where most of them originate (Inohaya *et al.*, 1997).

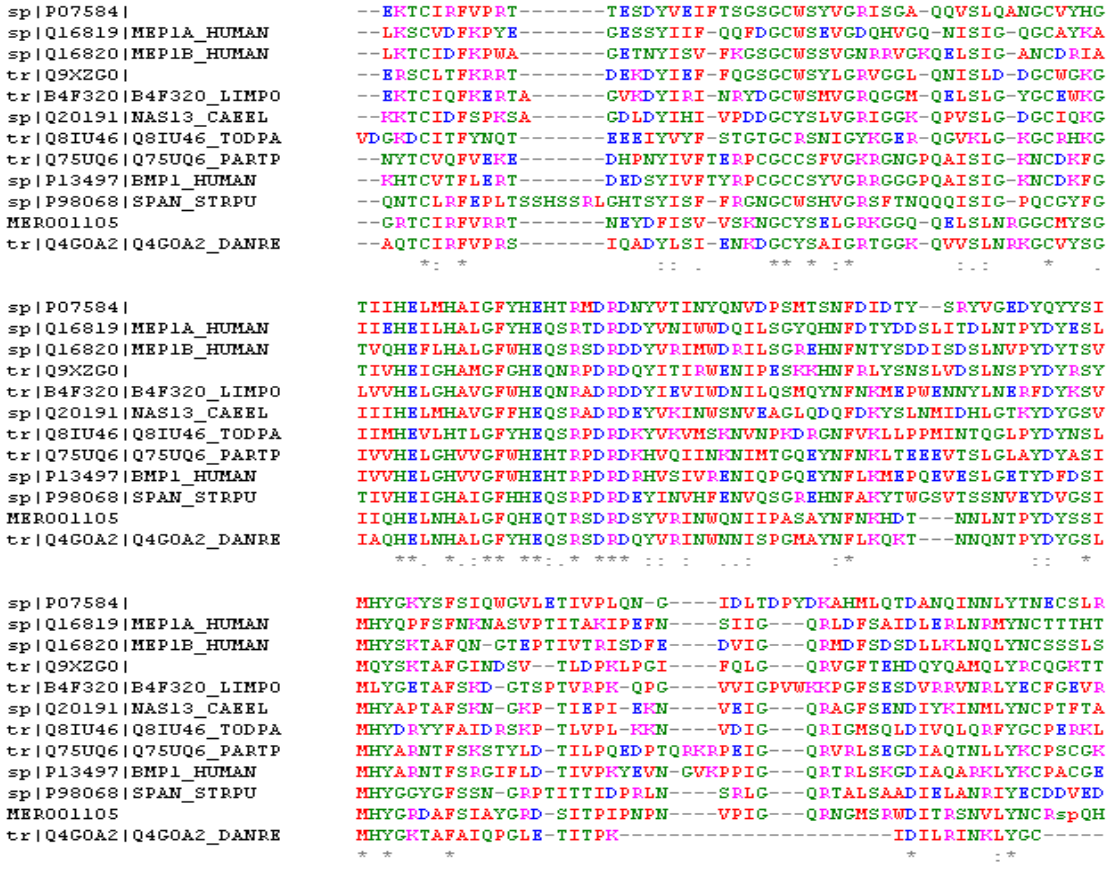

Fig 1.8. **Sequence alignment of the astacin family.** ClustalW alignment of the prosegments and catalytic domains of representative astacin family members : *AAS_ASTA*, astacin from the crayfish *A. astacus* (UniProt P07584); *HSA_MEP_*, human meprin _ (Q16819); *HSA_MEP_*, human meprin _ (Q16820); *HVU_HMP2* from the freshwater hydroid *Hydra vulgaris* (Q9XZG0); *LPO_ASTM* from the horseshoe crab *Limulus polyphemus* (B4F320); *CEL_NAS13* from the nematode *Caenorhabditis elegans* (Q20191); *TPA_MYO1* myosinase from the giant squid *Todarodes pacificus* (Q8IU46); *ATE_TLL*, tolloid-like proteinase from the spider *Achaearanea tepidariorum* (Q75UQ6), *HSA_BMP1*, human bone morphogenetic protein 1 (P13497); *SPU_SPAN*, proteinase from the sea urchin *Strongylocentrotus purpuratus* (P98068); *OLA_HCE1*, high choriolytic enzyme from the medaka fish *Oryzias latipes* (MEROPS data base access code MER001105); *HSA_OVAST*, human embryonic ovastacin (Q6HA08) and Q4G0A2_DANRE (Q4G0A2) from the zebrafish *Danio rerio*. Note the highly conserved astacin hallmark glutamate, the Met-turn region and the cysteine residues.

1.8.3 Apoptosis in HGC

The relationship between apoptosis and hatching was described by Schoots *et al.*, (1983) in pike embryo during the posthatching stage where hatching gland cells degenerate by apoptosis (unlike true holocrine cells). Apoptotic cells are seen as hatching gland remnants (HGRs) in the cellular covering of posthatching pike larvae (Schoots *et al.*, 1982). The transition of HGCs to HGRs takes place in the nucleus and begins before HE secretion (Schoots *et al.*, 1983). In subsequent larval stage all vestiges of the original hatching glands disappear (Schoots *et al.*, 1983). These early HGRs showed a positive reaction in the cytoplasm to HE detected by the PAP (peroxidase-anti-peroxidase) method, but this was not considered as a reliable evidence of the presence of HE in these HGRs, since a granular deposit was not observed. However, the reaction is useful to follow the rapid changes in the HGC during the early posthatching stages because HGRs appear as electron-dense bodies amidst electrolucent surrounding tissue. Even though only a single discharge takes place, the mode of HE secretion in fish is clearly different from holocrine secretion, since the release of the secretory product is neither accompanied by a rupture of the plasma membrane nor mixing of cytoplasmic contents (other than the granule contents) with the secretory substance. Therefore the previously suggested 'holocrine nature' of the HGC (Schoots *et al.*, 1982) is inappropriate in this respect. Indeed, because HE is stored in granules that liberate their product by exocytosis, in a strictly morphological sense the HGC should be referred to as a merocrine gland (Rhodin 1974). Merocrine glands are glands that secrete their products via exocytosis with no parts of the gland cell being lost or damaged, distinguishing them from holocrine glands where secretion causes the damage or loss of the whole gland cell, and also from apocrine glands, where part of the cell is lost during secretion. In medaka, there are posthatching or persisting HGCs that are

devoid of secretory granules and have electron dense and irregularly shaped nuclei, which could be indicative of apoptotic cell death of HGCs in this species as well (Yamamoto *et al.*, 1979). In raibow trout, HGCs are detached from the epithelium three days after releasing their granules, possibly indicating the rarely observed alternative to phagocytosis by adjacent cells or macrophages (as may be observed in zebrafish) i.e. extrusion into the lumen with closing ranks of remaining viable cells (Wyllie *et al.*, 1980). Posthatching morphological changes in the HGCs of the grass frog could represent some sort of autophagic remodelling of the cells (Yoshizaki and Katagiri 1975). In zebrafish, the homogenous prehatching granules in the HGC transform into heterogenous granules showing similarities with the secretory vacuole, although they are randomly dispersed throughout the HGC (Willemse and Denuce 1973). It was shown that agents that increase free intracellular calcium content also induce HE secretion, indicating also Ca^{2+} ions signalling in this process (Schoots *et al.*, 1981).

In zebrafish, the apoptotic process is similar to that in mammals. Caspase peptide inhibitors, functional for both invertebrate and vertebrate homologues of caspase-1,-4, and-5 or caspase-2, -3, and -7, have been shown to inhibit zebrafish DNA fragmentation *in vitro* (Rappela *et al.*, 2002). In addition, caspase inhibitors prevent nocodazole-induced apoptosis in early zebrafish development (Chan and Yager, 1998). The likelihood that the apoptosis machinery is conserved in zebrafish is supported by the identification of many apoptosis genes. Homologues of most of the apoptosis genes have been identified in zebrafish, including nine Bcl-2 family members (Mcl-1a, Mcl-1b, BLP1, Bcl-xL, Bax, Bad, Nip3, Nip3L, NR13), seven caspases (caspase-2, -3, -4, -6, -8, -9, -13), two Ced-4-like molecules (Apaf-1 and Nod1), four IAP (inhibitor of apoptosis) genes (IAP1, XIAP, survivin1, survivin 2), four death receptors (NGFR1, TNFR, DR6, ZH-DR), the death ligand TRAIL, 10 apoptosis-related kinases (Ask1a,

1b, Akt1, Akt2, DAP kinase, KRAK1, 2, RICK, RIP3, ZIPK), transcriptional factors (PML1, p53, c-Myc, *etc*.), and many other death-related molecules (Parng *et al.*, 2002). Consistent patterns of apoptosis in live zebrafish embryo using acridine orange staining can be clearly observed in the dorsal neural tube (16-30hpf), hatching glands (24-60 hpf), retina, lens, cornea (after 25 hpf), inner ear (after 48 hpf), olfactory organs (after 48 hpf), Rohon-Beard neurons and lateral-line neuromasts (after 72 hpf) (Parng *et al.*, 2002). Apoptosis has also been described in other non-neuronal structures, including the somites, muscle, tailbud, and fins (Cole and Ross, 2001; Yabu *et al.*, 2001). These organs and tissues undergo rapid development during early embryogenesis and thus exhibit complex mechanisms for cell differentiation, proliferation and apoptosis. Parng and his colleague (2002) also demonstrated that the developmental apoptosis of the hatching gland was inhibited using 2mM of caspase inhibitors III and V (calbiochem, La Jolla, CA) at 12 hpf for 24 h.

1.9 Aims and objectives of the project

Several studies have indicated that zinc and zinc transporters are of importance in embryonic development as well as performing other functions in the body. Knowledge of metal uptake and metabolism is still not fully understood at organismal level. The zebrafish is an attractive model for studies of development and other cellular processes. Therefore, it is hoped that study of these processes in zebrafish will aid in unravelling the mechanism of metal uptake, toxicity and homeostasis. The aim of the present study was to use zebrafish models with deficiencies in *znt1* or *zip10* genes to study the role of zinc and/or Znt1 and Zip10 transporters in embryonic development and to investigate the biological functions of zinc transporter (s) in adult fish with defective *znt1* gene. This aim was addressed under the following objectives:

1. To study the effects of the Znt1 transporter in embryonic development by utilizing mutant zebrafish embryos (from Sanger strain sa0014) lacking the last 40 amino acids of Znt1 protein, as well as morphant zebrafish embryos with a disrupted *znt1* gene. It was hypothesized that mutant or morphant embryos with a disrupted *znt1* gene would have problems in regulating or handling Zn^{2+} ions thereby accumulating free Zn^{2+} differently from the normal embryos.

2. To explore the effect of *znt1* mutation in adult zebrafish (Sanger strain sa0014) in the regulation of dietary zinc uptake and distribution and how this affects the expression of other zinc transporters and zinc-dependent signalling processes and pathways such as master circadian regulation and Ras-Raf-MEK-ERK (i.e. MAPK) signalling pathways. Here we hypothesized that the expression of some of these zinc-controlling genes would be different in mutant fish compared to their wild-type counterparts.

3. To study the effect of zinc and zinc transporters (Zip10 and Znt1) in the process of hatching of zebrafish embryos. It was hypothesized that the level of Zn^{2+} ions in the HGC and/or the level of expression of either of the transporters would be affected by deficiency or knockdown of either of the genes and thus would influence the expression of hatching gland markers and subsequent hatching of the zebrafish embryo.

4. To investigate the role of *zip10* in zebrafish embryonic development and its involvement in epithelial-mesenchymal transition (EMT) formation during development. This was achieved through the use of antisense morpholino oligonucleotides (MO) to knockdown Zip10 expression. The hypothesis was that *zip10* would be required for gastrular cell movement during embryonic development in zebrafish through the expression of E-cadherin (a marker of EMT).

Being an in-vivo experiment in a vertebrate model system, this whole work was aimed to give a better understanding of the biological function (s) of Znt1 and Zip10 in regulating zinc homeostasis for important biological events in the body and to also give more insights into the mechanism of development of some diseases in humans that are related to zinc-imbalance conditions such as Alzeimer's diseases, cancer, reproductive disorders and diabetes. The study would also increase knowledge of zinc uptake and distribution in piscine species and thus be of great value in the field of aquaculture and farmed fish (agriculture) because the precise mechanisms of zinc metabolism that would avoid the problem of deficiency or excess in order to promote fish growth and health would be elucidated.

CHAPTER TWO

GENERAL MATERIALS AND METHODS

2 General materials and methods

2.1 List of materials

The following sections list the general reagents, equipments, softwares and suppliers used in this project. The zebrafish strains sa0014 used in this project were obtained from Sanger Centre Zebrafish Mutation Resources.

(http://www.sanger.ac.uk/Projects/D_rerio/zmp/),

(http://www.sanger.ac.uk/cgi-bin/Projects/D_rerio/zmp/search.pl?q=slc30a1).

Equipment /Consumables	Supplier
Zebrafish stand alone aquatic housing system (version 4.0)	AQUANEERING Inc. San Diego, USA
Reverse osmosis water	ELGA process water, Derbyshire, UK (PureLab Prima®)
Sea salt	Tropical Marine Centre, Hertfordshire, UK
Calcium chloride	Sigma, Dorset, UK
Breeding tanks	ZM Ltd, Winchester, UK;
Inverted light microscope	Kyowa Tokyo

Table 2.1.1: Equipments and consumables used for zebrafish husbandary and breeding

Reagents/Consumables	Supplier
Benzocaine (ethyl-4-aminobenzoate)	Sigma, Dorset, UK
96-well block	Star Lab, UK.
Proteinase K	Applied Biosystem (Ambion®)
Tris-Hcl	Meck Chemical Ltd, Nottingham UK
NaCl	Meck Chemical Ltd, Germany
EDTA	BDH Analar
SDS	Fisher Scientific, Leicestershire, UK
Nuclease-free tubes	Star Lab
Waterbath	W14, Grant, Cambridgeshire, UK
Centrifuge	Eppendorf, Cambridge, UK.
Ethanol	Sigma, Dorset, UK.
TE buffer	Applied Biosystem (Ambion®)
NanoDrop 1000 spectrophotometer	Thermo Fisher Scientific, Leicestershire, UK

Table 2.1.2: Reagents, consumables and equipment used for zebrafish DNA extraction

Reagent	Supplier
Sequence specific primers	Sigma, UK
Taq buffer	Promega, UK
DNA Taq polymerase	,,
dNTPs	,,
$MgCl_2$	,,
Nuclease-free water	Applied Biosystem (Ambion®)
Thermocycler	DNA engine tetrad PTC-225, Bio-Rad, Hertfordshire, UK
Pin tool	Genetix # 5054
Shrimp alkaline phosphatase (SAP)	Fermentas®
SAP buffer	,,
Exonuclease 1	,,
Agarose gel and tanks	Invitrogen Life Technology, UK
Ethidium bromide	Fluka Biochemika
Bio-imaging system (Syngene)	Fisher Scientific

Table 2.1.3: Reagents, consumables and equipment used for PCR and sequencing for detection of fish genotypes (Sanger's method)

Consumables/Equipment	Supplier
96-well PCR plates	Applied Biosystems, Cheshire, UK.
Adhesive film applicator	Applied Biosystems, Cheshire, UK.
Optical adhesive film	Applied Biosystems, Cheshire, UK.
Optical compression pads	Applied Biosystems, Cheshire, UK.
96-well plate-adaptable centrifuge	Eppendorf, Cambridge, UK.
Thermomixer compact	Jencons-PLS
Nuclease-free, extended-length, filtered tips	Starlab UK Ltd, Milton Keynes, UK.
Nuclease-free microtubes (0.2 ml)	Starlab UK Ltd, Milton Keynes, UK.
Nuclease free tubes (1.5-2.0 ml)	Starlab UK Ltd, Milton Keynes, UK.
Sequence specific primers	IDT, Coralville, USA
Dual specific probes (FAM & HEX)	IDT, Coralville, USA
Fast Start Universal Probe Master (UPL Mastermix)	Roche® Diagnostic, Indianapolis, USA.
Sequence detection system	ABI Prism® 7700 sequence detection system, Applied Biosystems, Cheshire, UK
Thermal cycler	DNA engine tetrad PTC-225, Bio-Rad, Hertfordshire, UK

Table 2.1.4: Reagents, consumables and equipment used for qPCR for detection of fish genotypes (LNA method)

Reagents/Consumables	Supplier
$ZnSO_4.7H_2O$	Sigma, Dorset, UK
TPEN(N,N,N,N,-Tetrakis(2-pyridymethyl ethylene-diamine)	Sigma, Dorset, UK
DMSO	Sigma, USA

Table 2.1.5: Reagents, consumables and equipment used for zinc exposure/chelation of embryos

Reagents/Consumables	Supplier
ICP-MS machine	Perker Elma
65% HNO_3	Merck Chemical Ltd, Germany
30% H_2O_2	Sigma, Dorset, UK
Synthetic 'ZTRS' zinc probe	A gift from Dr. Zachao Xu
Epi-fluorescence microscope	Nickon Eclipse 400
Acridine orange	Sigma-Aldrich
Fluorospectrometer (synergy HT)	Bio-TEK, Fisher Scientific
96-well microplate	
DMSO	

Table 2.1.6. Reagents, consumables and equipment used for total/free zinc concentration & observation of apoptosis

Reagents/Consumables	Product details/Supplier
Sequence specific morpholino oligonucleotides	GENETOOLS, Philomath, USA
Phenol red	Sigma, Dorset, UK
Sterile dH_2O	
Glass capillary needle	World Precision Instrument, USA
Needle puller machine	Sutter, Germany
Femtoject microinjection apparatus	Eppendorf
Inverted microscope	Nikon
Incubator	GallenKamp

Table 2.1.7. Reagents, consumables and equipment used for morphants generation

Reagents/Consumables	Supplier
Ethanol	Sigma, Dorset, UK.
Chloroform	Sigma, Dorset, UK.
Nuclease-free water	Applied Biosystems, Cheshire, UK.
Propan-2-ol	Fisher Scientific, Leicestershire, UK.
TRIzol® reagent	Invitrogen Life Technologies, Paisley UK.
Phase lock tube	Prime 5, Hamburg, Germany
NanoDrop spectrophotometer	Thermo Fisher Scientific, Leicestershire, UK
Agarose gel	Invitrogen Life Technology, UK
Ethidium bromide	
Gel imaging	

Table 2.1.8. Reagents, consumables and equipment used for RNA isolation and quantification analysis.

Consumables/Equipment	Supplier
Temperature controlled centrifuge	Microlite RF, ThermoFisher, Hampshire, UK
Nuclease-free, extended-length, filtered tips	Starlab UK Ltd, Milton Keynes, UK.
Nuclease-free tubes (1.5-2 ml)	Starlab UK Ltd, Milton Keynes, UK.
BioAnalyzer (2100)	Agilent, Cheshire, UK
RNA 6000 Nano Kit	Agilent, Cheshire, UK

Table 2.1.9. Consumables and equipment used for RNA integrity analysis.

Reagent	Supplier
oligo dT Primer	Invitrogen
DNTPs	Promega, UK
Superscript reverse transcriptase	Invitrogen
$MgCl_2$	,,
Reaction buffer	,,
DTT	,,
RNase H	,,
Nuclease-free water	Applied Biosystems, Cheshire, UK.
Thermocycler	DNA Engine Tetrad PTC-225, Bio-Rad, Hertfordshire, UK
High capacity reverse transcription kit	Applied Biosystems, Cheshire, UK.

Table 2.1.10. Reagents used for reverse transcription reaction

Reagent	Supplier
Paraformaldehyde powder	Sigma-Aldrich
H_2O_2	Sigma, Dorset UK
KOH	BDH Analar
Inverted microscope	Nikon
Pronase	Sigma P6911-100MG
Forceps (#5 durmont)	WPI, USA
Methanol	Sigma, UK.
Tween 20	Sigma-Aldich
PBS	Applied Biosystems, Cheshire, UK
Proteinase K	Invitrogen Life Technology, UK
Formamide	Sigma
NaCl	Merck Chemical Ltd, UK
Na-citrate	BDH Analar
citric acid	Sigma- Aldrich
Heparin	Sigma, UK
torula yeast RNA	Sigma, UK
antisense DIG-labelled RNA probe	Prepared in the lab
SSC	Applied Biosystems, Cheshire, UK
BSA	Sigma
lamb serum	Invitrogen Life Technology
Orbital shaker	
anti-DIG-antibody	Roche Diagnostic, USA

Tris HCl	Merck Chemical Ltd, UK
$MgCl_2$	Sigma, UK
12 well microplates	
NBT/BCIP	Roche Diagnostic USA
Glycerol	Sigma

Table 2.1.11 Reagents used in ISH gene expression

Reagent	**Supplier**
High capacity RNA-to cDNA kit.	Applied Biosystems
8-strips 0.2ml PCR tubes	,,
Nuclease-free water	,,
ABI 7000 Prism thermocycler	
qPCR microplate	,,
UPL probe and mastermix	Roche Diagnostic USA
Sequence-specific primers	Sigma

Table 2.1.12 Reagents used in qPCR gene expression

Reagent	**Supplier**
Acrylamide	Sigma, Dorset, UK.
Ammonium per Sulphate (APS)	Sigma, Dorset, UK.
Bromophenol blue	Sigma, Dorset, UK.
Chemiluminescence agent (Novex®)	Invitrogen Life Technologies, Paisley, UK.
Developer	Sigma, Dorset, UK.
Fixer	Sigma, Dorset, UK.
Kodak light film	Sigma, Dorset, UK.
Glycerol	Sigma, Dorset, UK.
Glycine	Sigma, Dorset, UK.
Non-fat powdered milk	Premier Foods, Windsor, UK
PBS	Oxoid, Hants, UK.
Protease inhibitor	Sigma, Dorset, UK.
Protein weight marker (rainbow marker)	GE Healthcare Ltd, UK.
SDS	Fisher Scientific, Leicestershire, UK.
TEMED	Sigma, Dorset, UK.
Tris-base	Merck chemicals Ltd. Nottingham, UK.
Tween 20	Sigma, Dorset, UK.
β-mercaptoethanol	VWR international Ltd. Leicestershire, UK.
Pierce® 660nm protein assay	Thermoscientific.
Pre-diluted BSA sets	Thermoscientific

Table 2.1.13. Reagents used for zebrafish protein isolation and quantification/detection
Keys; PBS: phosphate buffered saline; SDS: sodium dodecyl sulphate; APS: ammonium persulphate; TEMED: tetramethylethylenediamine.

Consumables/Equipment	Supplier
Disposable gel cassettes	Invitrogen Life Technologies, Paisley, UK.
Exposure cassette	Molecular Dynamics, Fisher Scientific, Leicestershire, UK
Automatic film processor	(Konica Minolta SRX-101A)
Falcon tubes (50ml)	Grenier Bio One, Gloucestershire, UK.
Homogeniser	Ultra Turrax T8, Sartorius Mechatronics Ltd., Epsom, UK
Plastic pestle homogenizer	
Light film	Sigma, Dorset, UK.
Amersham hyperfilm™ ECL	GE Healthcare Ltd, UK
Needles	BD, NJ, USA.
Platform shaker	VWR, PA, USA.
Powerpack	Labosi Power 300, Fisher Scientific, Leicestershire, UK
Roller-mixer	Mixer SRT2, MIX1990, SLS, Nottingham, UK
Calibrated densitometer	BioRad Laboratories, Hertfordshire, UK.
Semi-dry transfer blotter	GE Healthcare, Buckinghamshire, UK.
Wet transfer tank	Bio-Rad, UK
Syringes (1 ml)	BD, NJ, USA.
Well-combs	Invitrogen Life Technologies, Paisley, UK.
Microplate reader	Synergy HT, PJB-290-040A, Fisher Scientific, Leicestershire, UK
Safelight	Photax A safelight, Paterson photographic limited, West Midlands, UK
Electrophoresis tank	XCell Surelock™ Mini-cell, Invitrogen Life Technologies, Paisley, UK
Membrane-filter paper sandwiches	Invitrogen Life Technologies, Paisley, UK.
E-cadherin pry antibodies	Abcam, UK

ERK & p-ERK pry Ab	Santacruz
Alexafluor 488 sec Ab	Abcam
HRP sec Ab	Sigma, UK
Hoesch/DAPI	Sigma, UK
Propidium iodide	Sigma, UK
BSA	Sigma, UK
Confocal/2-photon lasser scanning microscope	Nikon
Epi-fluorescent microscope	Nikon

Table 2.1.14. Consumables and equipment used for protein isolation and quantification.

Software	**Application/s**	**Source/references**
GraphPad Prism® 5	Data analysis and figures	GraphPad software, CA, USA
Primer3	Primer design	Rozen and Skaletsky, 2000
QuantityOne®	Densitometry	BioRad Laboratories, Hertfordshire, UK
Image J	Densitometry	
SDS software	Gene expression analysis	Applied Biosystems, Cheshire, UK
REST software		
Microsoft office package	Word processing, data analysis and formatting	Microsoft corporation, WA, USA

2.1.15. List of software used in this project

2.2 Methodologies

The following sections describe the general methodologies used in this project.

2.2.1 Generation of mutant and morphant zebrafish by reverse genetics

2.2.1.1 Mutant fish by TILLING technology

The zebrafish strains (sa0014) used in this project were obtained from Sanger Centre Zebrafish Mutation Resources (http://www.sanger.ac.uk/Projects/D_rerio/zmp/) (http://www.sanger.ac.uk/cgi-bin/Projects/D_rerio/zmp/search.pl?q=slc30a1).

Adult male carrier with a point mutation for *slc30a1* (*znt1)* zinc transporter gene (caused by chemical mutagenesis) was identified by Sanger Centre using TILLING technology. The point mutation occurred due to transition of Adenosine to Thiamine at nucleotide 355 in the coding sequence (A 355 T) leading to a premature termination or stop codon which results in deletion of the last 40 amino acids from the protein sequence (Fig. 2.1). The identified adult heterozygote mutant male was then out-crossed with adult wild-type female and the resultant embryos (about 200 in number at 3dpf) were collected from Sanger Centre and raised to adulthood at King's College BSU fish facility for this project.

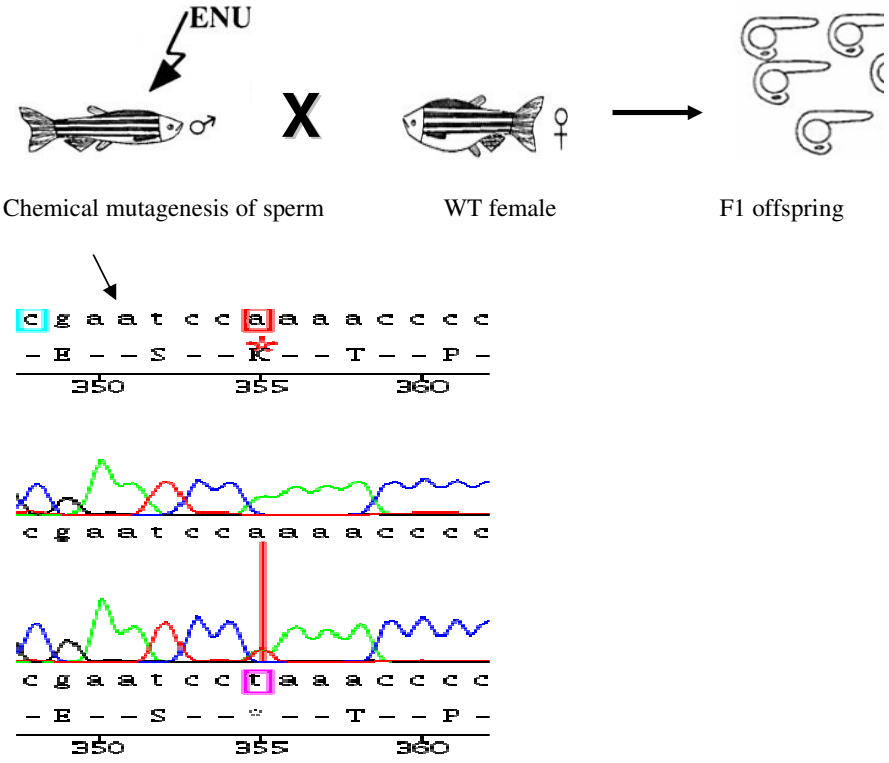

Fig 2.1. An illustration of chemical mutagenesis in zebrafish and a chromatogram showing site of point mutation (A355T) which caused deletion of the last 40 amino acid from the Znt1 protein.

2.2.1.2 Morphant fish by morpholino-modified oligonucleotides

Antisense morpholino-modified oligonucleotides (morpholinos; MOs) were injected into wild-type embryos to generate morphant embryos used in this project. The morpholinos against zinc transporter genes of interest (*slc30a1* & *slc39a10* i.e. *znt1* & *zip10*) studied in this project were designed and synthesised from GENE TOOLS Inc; USA. For translational blocking MO, only sequences upstream of the 25th base of coding sequence (ATG) from 5' UTR sequence was provided for the design. For splice blocking (exon skipping) MO, sequences of 50 bases of exon-intron or intron-exon boundary was provided for the design. The sequences of morpholinos (for both translational blocker and splice blocker or exon skipper) are shown in Table 2.2.2.

MO type	Sequences (5′-3′)
zip10 TB	TGGTATGTGTGTGAACTCTCATCAT
zip10 SB	ATCACAGCACTGAGACTCACCTCTT
znt1 TB	GCGGAGCACAGACAGAAACAAAAGCT
znt1 SB	AGAAAACAAACCCCATTTACCGGCA
p53 TB	GCGCCATTGCTTTGCAAGAATTG
Random-control-MASO	5′A 3′

Table 2.2.2. Sequences of MOs used for gene knockdown experiment. TB= translation blocker, SB= Splice junction blocker.

The lyophilized mopholinos were reconstituted with sterile dH_2O at stock concentration of 20ng/nl and a working concentration for different mopholinos were made by either 1:5 or 1:10 dilution (as the case may be) and approximately 1-2nl was injected per embryo using femtoject microinjection facility (Eppendorf®) coupled to a microscope (Nikon) and a monitor screen (Fig. 9.4) . The embryos were rapidly injected at 1-4 cell division stage through the yolk with MO of interest which is deposited close to the base of the dividing cells (i.e. animal pole) using a glass capillary needle. The glass needle was pulled by needle puller machine (Sutter®) set with the following parameters; heat (515), pull (150), vel (100) and del (150). The MO working solution was mixed with phenol red (1:10) for assessment of successful injection. Injected embryos were collected in standard fish tank water (Appendix 9.1) and incubated at 28.5^{o}C for different studies carried out in this project.

2.2.2 Zebrafish husbandary and breeding

The fish embryos (fry) and adults were initially maintained in a static tank system (40L capacity fitted with heaters and biological filters for individual tanks) and used for experiments in section 3.3.2 to 3.3.3.2, but were later reared and bred in a stand-alone zebrafish rack tank system (AQUANEERING INC) which was used for the rest of the project. The system water was constituted by reverse osmosis deionized water which was supplemented with 60 mg/L of sea salt (Tropical Marine®) and 200µM $CaCl_2$ (VWR), resulting in a conductivity of 250-350µS. The fish were reared at a temperature of 28.5 ± 0.5°C under a photoperiod regime of 14 h of light and 10 h of darkness until adulthood (i.e. 3 months and above). The system water (inside each of the tank system) was renewed or replenished by 20L of the fresh system water every other days to maintain the concentrations of nitrogenous wastes to a minimal level (ammonia; <0.02mg/L, nitrite; <1mg/L, nitrate <50mg/L). Fish were fed 3 times a day during the fry-juvenile stage with combination of liquid/powder infusoria fry feed (liquifry/ZM 000) & brine shrimp larva (ZM Ltd, UK), and 2 times a day during the adult stage with fish flake food (Aquarian® Tropical Flake Food). Water NH_3, pH and conductivity were monitored daily using appropriate kits.

Matured adult fish were bred either by pair-wise method using a small breeding tank containing a male and a female or by colony breeding method using a marble box inside a tank containing many fish. Fish were fed either live nauplii brine shrimp larvae (artemia) or frozen brine shrimp the evening before breeding. The tanks were cleaned of any un-eaten or left-over food before the marble is placed for colony breeding or before pair of mature male and female fish were transferred into a small breeding tank for pair-wise breeding. The marble or breeding tank was inspected the following morning 30min-1h after light was switched on, for embryo collection used for either

morphological observation, microinjection or for rearing to adulthood. Fish of all ages (i.e. from embryo to adult) were always maintained in fish tank water at 28.5 ± 0.5^{o}C.

2.2.2.1 Brine shrimp (artemia) culture

Artemia culture was prepared by adding 1 litre of brine solution (30g NaCl per litre of deionized dH_2O) to 1g of artemia cysts in a beaker. Continous aeration was provided using an airstone filter and the whole setup was placed near a light source for the cysts to hatch. Nauplii brine shrimp (artemia) was used for fry feeding after hatching (i.e. 2 days of culture) and was fed to fry for only 3 days after hatching before discarding and a fresh one setup thereafter.

2.2.2.2 Bleeching of zebrafish embryos

Embryos that are meant for rearing to adult were bleached at 24hpf in order to prevent contamination or transmission of infection. Briefly, the embryos were placed in a bleach solution (0.1ml of 5% sodium hypochlorite in 170ml system water) for 5 min. The solution was then poured off and the embryos were rinsed and placed in system water for another 5 min. The process was repeated twice.

2.2.3 Morphological study of embryos

Zebrafish embryos were collected (as in section 2.2.2) in a Petri dish containing fish tank water and 0.01% methylene blue. They were staged using an inverted light microscope and development was observed from zygote (0hpf) to hatching (3hpf) (Kimmel *et al.,* 1995).

2.2.4 Genotyping of mutant fish (whole embryo or adult tissue)

DNA sequencing through the Sanger method was initially used for genotyping of the Sa00014 strain. But because of cost involved in sequencing of large number of samples and also because of time taken to obtain the result, a high through-put qPCR (LNA) method for alleleic discrimination was adapted for genotyping to identify the Znt1 mutants.

2.2.4.1 Sanger's DNA sequencing method

2.2.4.1.1 Fish aneasthesia, fin clipping and genomic DNA isolation

For embryos, the whole fish was used for genomic DNA isolation and for live adult fish, a small biopsy of the tail fin was used to isolate DNA. Live adult fish were lightly aneasthesized for about 30 seconds in 50 mg/ml of benzocaine (ethyl-4-aminobenzoate) one at a time and about 3-4 mm of the tail fin was cut off using sharp scapel blade. The fin sample was immediately transferred into a 96-well block containing lysis buffer-proteinase K mixture (Appendix 9.2) and labelled, and the respective (individual) fish was identified and returned into an appropriately labelled isolation tank until individual genotype was ascertained.

N.B. Individual fish isolation was initially maintained in a labelled Duran bottle before the installation of the stand-alone zebrafish unit. This was achieved by using a 200ml Duran bottle for individual fish where the cover of the bottle was replaced with mesh/net and gently immersed horizontally in a tank of water (fitted with heater and filter pump), making sure air space is created on the surface of the bottle to allow sufficient aeration of the water inside the bottle. Alternatively and more conveniently, fish were isolated singly per tank in the zebrafish rack with appropriate label.

2.2.4.1.2 Genomic DNA extraction

As stated above, the clipped fin was immersed in 96-well blocks (Costar 2 ml assay blocks # 3960) containing 400 µl lysis buffer-proteinase K mixture (Appendix 9.2). The well block was sealed with plate sealer and incubated for 3 hours (or overnight) in water bath at 55^{o}C. The block was agitated on a vortex shaker for 2 min at 1000 rpm after few hours of incubation to properly dissolve the fin and then re-sealed with new plate sealer. The block was incubated for 30 minutes at 80^{o}C and vortex well to inactivate proteinase K and then cooled down to 4^{o}C. Isopropanol (500 µl) was added to each well and mixed by inverting ten times without vortexing. The block was centrifuged at 4,000 rpm for 40 minutes and the supernatant discarded by carefully inverting the block and blotting it on paper towels. Thereafter, 250 µl of 70% ethanol was added to the pellet in each well and the block was centrifuged at 4,000 rpm for 20 minutes. The supernatant was discarded as described above and another 250 µl of 70% ethanol was added followed by centrifugation of the block at 4,100 rpm for 15 minutes for additional washing. The supernatant was again discarded as described above and the pellet dried at 37^{o}C for 15 minutes until all ethanol was evaporated. Care was taken not to over-dry the pellet. The DNA pellet was dissolved in 500 µl of low TE buffer and the DNA concentration estimated using a NanoDrop spectrophotometer.

Alternatively, an eppendof tube was used in place of costar block for DNA isolation especially when few samples were to be processed.

2.2.4.1.3 Nested Polymerase Chain Reaction

Sequences of the primers for nested PCR used for the amplification and identification of point mutation (created in the zebrafish *znt1* gene) were designed by Sanger Centre's Zebrafish Mutation Resources (Table 2.2.3 & 2.2.4) and were synthesized by Sigma. The internal forward and reverse primers (P2 & P3) were further re-designed with M13 forward and reverse tail primers (lower case sequences) for conveniency in the bi-directional sequencing of PCR products.

Primer	Sequences (5'-3')	Tm^o	Size (pb)
Forward primer (P1)	TGCATCCTTCTCTACACCAC	60.3	726
Reverse primer (P4)	GACGTGGTAAACACACATGC	61.1	

Table 2.2.3. Sequences of outside primers for PCR1

Primer	Sequences (5'-3')	Tm^o	size
Forward primer (P2)	tgtaaaacgacggccagtCTCTTATCCTGCTCCAAACC	81.0	585
Reverse primer (P3)	CAGGAAACAGCTATGACCGGgctcagttcttctcacag	81.1	

Table 2.2.4: Sequences of internal primers re-designed with M13 tailed primers (lower case) for PCR2

Primers for PCR1 (outside primers) were first tested for optimal annealing temperature by adding 5 µl (10ng/µl) of genomic DNA template with PCR mixture composed of 1 µl of 10X Taq buffer containing 25mM $MgCl_2$, 0.2 µl (10 µM or pmol/µl) each of primer P1 & P4, 0.2 µl (10mM) dNTPs mix (comprising of dATP, dGTP, dCTP & dTTP) and 0.2 µl (0.25 U/µl) of DNA Taq polymerase (TakaRa). The reaction was made up to 10 µl with nuclease-free water and run for 35 cycles in a thermal cycler with general cycling parameters; 94^{o}C for 3 minutes enzyme activation, 94^{o}C for 20 seconds

denaturation, 55-66^{o}C for 30 seconds gradient annealing temperature and 72^{o}C for 1 minute extension. The final extension was 72^{o}C for 10 minutes. The product was electrophoresed on 1% agarose gel and the optimal annealing temperature for the primer was determined. Thereafter, PCR1 was run with the outside primers in a 10 µl reaction containing 1 µl of genomic DNA of each fish, 0.2 µl (10 µM) each of the primers, 2 µl of 5X Taq buffer, 0.4 µl (25mM) $MgCl_2$, 0.05 µl each of dNTPs (10mM each of dATP, dCTP, dGTP & dTTP) and 0.05 µl (5U/µl) of DNA Taq polymerase (Promega). The reaction was made up to 10 ul with nuclease-free water and the machine programmed to run as follow: 94^{o}C for 3 minutes, 94^{o}C for 30 seconds, 65^{o}C for 30 seconds and 72^{o}C for 1 minute and run for 18 cycles with a temperature drop of 0.5 per cycle (touch down PCR for specificity), then 94^{o}C for 20 seconds, 56^{o}C for 30 seconds and 72^{o}C for 1 minute at 20 cycles and final extension of 72^{o}C for 3 minutes.

The product from PCR1 was now transferred as a template by "hedging" (transfer 2x with a plastic multi-pin tool; Genetix # 5054) into a fresh plate containing PCR2 mix. The reaction consist of 0.2 µl (10µM) each of internal primers (P2 & P3), 1 µl of 5X Taq buffer, 0.2 µl (25mM) $MgCl_2$, 0.025 µl each of dNTPs (10mM each of dATP, dCTP, dGTP & dTTP) and 0.025 µl (5 U/µl) of DNA Taq polymerase (Promega). The reaction was made up to 5 µl volumes with nuclease-free water and the machine was programmed to run as follow: 94^{o}C for 3 minutes, 94^{o}C for 30 seconds, 56 ^{o}C for 30 seconds and 72^{o}C for 1 minute and run for 35 cycles before the final extension of 72^{o}C for 3 minutes. After the cycle, the product was cleaned-up (purified) of unincorporated nucleotides by treatment with ExoSap (Fermentas) involving incubation in PCR machine at 37^{o}C for 1 hour and at 80^{o}C for 20 minutes with 1 µl of 10X SAP buffer, 0.25 µl (1U/µl) Shrimp alkaline phosphatase (SAP), 0.025 µl (20U/µl) of Exonuclease 1

(Exo1) and 3.725 µl of nuclease-free water. 1 µl of purified product was electrophoresed on 1% agarose gel for confirmation of amplification and product size.

2.2.4.1.4 Sequencing and isolation of mutants and wild-types

1 µl of purified PCR2 product from each fish was diluted 1:10 with ddH_20 and DNA concentration was estimated. Thereafter, 5 µl (1ng/µl per 100bp) of the diluted sample was sent for sequencing at a commercial outfit. From the sequencing result, individual zebrafish genotypes were identified and isolated. Figure below show example of ABI chromatogram for identification of different genotype.

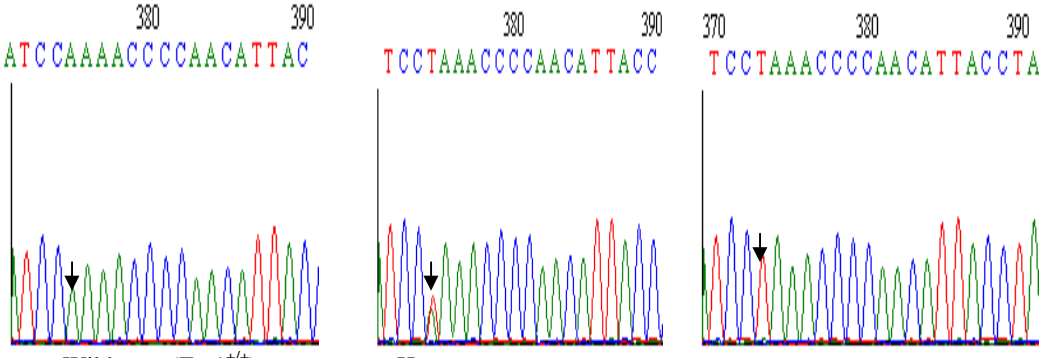

Wild-type ($Znt1^{+/+}$)

Heterozygote mutant ($Znt1^{\Delta 40/+}$)

Homozygote mutant ($Znt1^{\Delta 40/\Delta 40}$)

2.2.4.2 Locked Nucleic Acid (LNA) method

This method adapted for genotype detection involves the use of locked nucleic acid (LNA) fluorescence probes for alleleic discrimination between different genotypes by real-time PCR. The primers and probe sequence set for discrimination between the allele **A** and **T** in wild-type ($Znt1^{+/+}$) and Znt1 mutants ($Znt1^{\Delta 40/\Delta 40}$ & $Znt1^{\Delta 40/+}$) by real-time PCR was designed by IDT[1] technology and are shown below in Table 2.2.5.

[1]Designing fluorescent qPCR based assay that will discriminate between two sequences that vary by a single nucleotide can be very challenging due to many factors, but the challenge has been overcome by Integrated DNA Technology (IDT).

Primer/Probe	Sequences (5'-3')	T_m °C
Forward primer	GGG CTG TTG ATA CCG CAAA	55.8
Reverse primer	GTC ACA GAA GCG CTA GGT AAT G	55.5
Allele **A** probe	5' 6-FAM/CGA ATC +C+A+A AAC CCC AA/3' IABkFQ	49.9
Allele **T** probe	5' HEX/CGA ATC +C+T+A AAC CCC AA/3' IABkFQ	49.3

Table 2.2.5. Primer and probe sequences for LNA qPCR genotyping assay. Primers and probe sequences designed from slc30a1 mRNA with accession number NM_200879. Allele A and T were labelled with FAM and HEX florescence probes respectively as reporters at their 5' and both were also labelled with Iowa Black florescence probe as quenchers at their 3'. The + sequences are the LNA bases from the DNA bases for discrimination between the 2 alleles.

This is an example of dual labelled florescence probe qPCR assay. The principle is that of TaqMan qPCR assay which simply involves the accumulation and signal detection by the colour of the specific labelled fluorophore for the allele that is present and amplified in individual fish samples, and where the 2 florophores are detected, the sample is assumed to contain both alleles (i.e. heterozygote). Since the LNA bases significantly increase the melting temperature (T_m°C), LNA dual-labeled probes (DLP) are shorter than standard DNA DLP. Shorter probes therefore have better quenching, a higher signal-to-noise ratio and more sensitive. More importantly, the LNA DLP offers an improved ability to distinguish mutations or single nucleotide polymorphism (SNP).

2.2.4.2.1 Real Time- PCR

Genomic DNA (24 - 200 ng; dissolved in TE buffer or nuclease-free water) was mixed in 96-well qPCR plate with PCR mastermix (Roche UPL mastermix), primers and probes set making a total of 25µl reaction as follow; 12.5 µl of UPL mastermix (X2), 0.5 µl (10µM) each of forward and reverse primers, 0.25 µl (10µM) each of probe **A** and **T**, 2.5 µl of DNA template and 8.5 µl of DNase-free water. A no-template negative

control and standard positive controls for wild-type, homozygote and heterozygote were run on every plate along with the unknown samples. The cycling was run on ABI 7000 Prism thermocycler at normal default qPCR settings (Table 2.32).

Zebrafish genotypes were identified by the sigmoidal curve of the fluorophore that amplified as shown below.

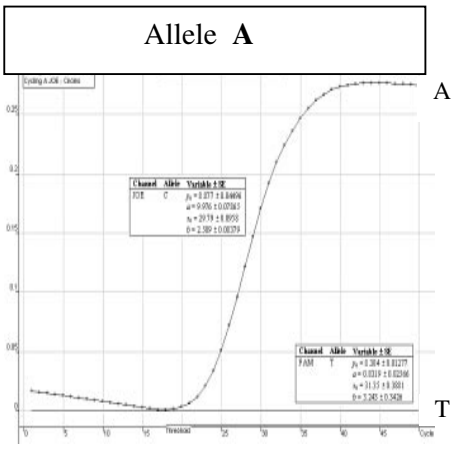

Wild-type ($Znt1^{+/+}$)

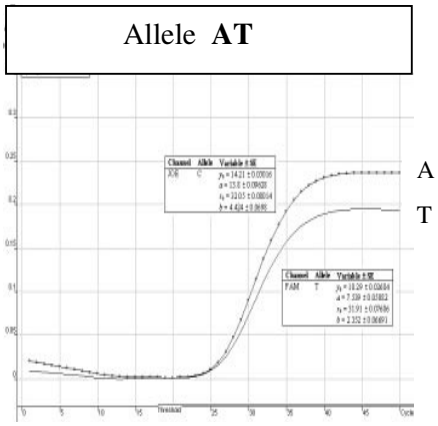

Heterozygote mutant ($Znt1^{\Delta 40/+}$)

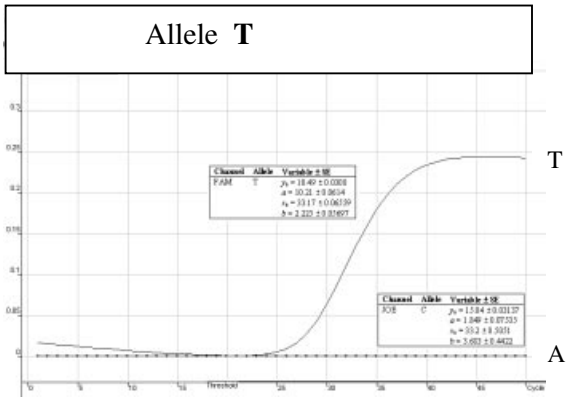

Homozygote mutant ($Znt1^{\Delta 40/\Delta 40}$)

2.2.5 Metal Analysis

2.2.5.1 Total zinc concentration of embryos

2.2.5.1.1 Acid digestion and sample preparation

A sample of each genotype (24hpf of dechorionated and/or undechorionated embryo) was rinsed with deionised dH_2O and dried in an Eppendorf tube. Each sample was digested in 100µl of 65% HNO_3 at 80^oC for 1 hour on a heating block. The sample was allowed to cool down and then additional 6 µl of 30% H_2O_2 was added and heated at 80^oC for another 1 hour or incubated overnight at room temperature to digest the lipid. Each sample was then made up to 2ml with 1% HNO_3 in ICP-MS tube.

2.2.5.1.2 Inductively Coupled Plasma Mass Spectrometry (ICP-MS)

ICP-MS was used to measure the concentration of trace metal elements (Zn, Fe, Cu, Mn and Se) and non-metallic elements (Mg and Ca) in the digested samples. ICP-MS is sensitive in the 0.001 ppb range. It is based on the production of ions (ionisation) by inductively coupled plasma (ICP) and the use of a quadropole mass spectrometer (MS) as a method of separating and detecting the ions. Samples were prepared as described above and analyzed on a Perkin Elmer ICP-MS machine (model ELAN 6100DRC) in the Mass Spectrometry Facilty, King's College London who also prepared the standard solutions. All standard curve r^2values were >0.9997. In another experiment, tissue samples from adult zebrafish (chapter 4) were weighed and digested in similar way as above and measured for elemental compositions at both KCL (King's College London) and NIFES (National Institute for Food and Seafood Research, Norway) ICP-MS facilities.

2.2.5.2 Free zinc ion detection in embryos

2.2.5.2.1 Synthesis of a ratiometric zinc fluorophore (''ZTRS'' probe)

A synthetic zinc-specific binding probe (termed ZTRS) used for in-vivo zinc imaging in zebrafish in this study was a kind gift from Dr. Zhaochao Xu of University of Cambridge. The synthetic probe is an amide-containing receptor for Zn^{2+} which is combined with a naphthalimide fluorophore (Xu *et al.*, 2009). It has an excellent selectivity for Zn^{2+} over most competitive heavy and transitional metal ions. Because of this stronger affinity for Zn^{2+}, the probe can ratiometrically detect Zn^{2+} in-vitro and in-vivo with a large emission wavelength shift from 446 to 514 nm via Cd^{2+} displacement approach. The probe has a chemical formula of $C_{30}H_{29}N_5O_3$, mol.wt of 507.5830 and K_d of 5.4 x 10^{-9}M.

2.2.5.2.2 Detection of free Zn^{2+} using fluorospectrometry method

The probe was reconstituted with DMSO at a 5mM stock concentration. A working concentration of 10µM was incubated for 10 min in 100µl reaction containing different concentration of $ZnSO_4.7H_20$, TPEN and zinc-TPEN mixture in 96-well microplate. The fluorescence intensity was measured at 360/530nm excitation/emission wavelength with fluorospectrophotometer (microplate reader) to assess the sensitivity of the probe to varying zinc concentrations. To estimate the zinc fluorescence intensity in different embryo types, 24hpf un-dechorionated embryos at different treatments were incubated in 100µl fish tank water containing 10µM of the zinc probe at 28.5^{o}C for 10 min. Thereafter, the fluorescence intensity was measured with microplate reader.

2.2.5.2.3 Detection of free Zn^{2+} using fluorescence microscopic (fluorometry) method

Embryos were prepared as above, rinsed 3 times with deionised water and staged on a fluorescent light microscope. Images were taken at specified excitation/emission wavelength of the probe and the fluorescence intensity for Zn^{2+} in different part of the body was observed.

2.2.6 Observation of apoptosis in embryo

The embryos were assessed for apoptosis by incubating them in 10µM solution of acridine orange (AO) for 10 min, then staged on a fluorescent microscope for signal intensity. The dye interacts with DNA and RNA by intercalation and electrostatic attraction respectively. DNA intercalated AO fluoresces green (525nm); RNA electrostatically bound AO fluoresces red (>630nm). It may distinguish between quiescent and activated, proliferating cells, and may also allow differential detection of multiple G1 compartments (Darzynkiewicz, 1990). AO may also be useful as a method for measuring apoptosis, and for detecting intracellular pH gradients and the measurement of proton-pump activity (Darzynkiewicz *et al.*, 1992).

.

2.2.7 Zinc regulated gene expression study

2.2.7.1 Whole mount InSitu Hybridization (ISH) method in embryo

2.2.7.1.1 Making of anti-sense RNA probe

2.2.7.1.1.1 RNA extraction from 24hpf zebrafish

About 25-50 zebrafish wild-type embryos (24hpf) were collected in system water, dechorionated and washed twice in PBS solution. A 500 µl of TRIzol® reagent was added to the washed dechorionated embryos in 2 ml eppendorf tube, homogenized and incubated for 10 minutes at 37°C. This was continued for additional 5 minutes at 30°C. Thereafter, 100 µl of chloroform was added and shook vigorously for 15 seconds before incubated at 30°C for 15 minutes. The mixture was centrifuged at 12,000 rpm for 15 minutes at 4°C. The clear upper layer (aqueous phase) was carefully collected in a fresh tube and RNA was precipitated by adding 250µl of isopropanol. The sample was incubated for 10 minutes at 30°C and centrifuged at 13,200 rpm for 10 minutes at 4°C. Supernatant was carefully discarded and the pellet was washed once in 500 µl of 75% ethanol. The sample was well mixed and centrifuged at 7,500 rpm for 5 minutes at 4°C. The ethanol was removed as much as possible and the pellet was air-dried at room temperature for 10 minutes. After drying, the RNA was re-dissolved in about 10-50 µl nuclease-free water by repeated pipetting and incubated for 10 minutes at 55°C.

2.2.7.1.1.2 RNA quantification and purity

Immediately following total RNA isolation, sample concentrations were quantified using the NanoDrop spectrophotometer. For this, 1.5 µl of total RNA sample was used to quantify RNA concentrations. A blank of nuclease-free water was used to optimise the instrument. Sample pedestals were first cleaned with nuclease-free water and ethanol prior to use. The quality and purity of RNA were indicated by the 260:280 and 260:230 ratios. According to the manufacturer's protocol (Invitrogen), a ratio of approximately 1.8-2.2 was considered optimal for both. Solvent or protein contaminated sample reduced the ratios below the optimal level and thus affect the quality and purity

of the RNA. RNA contaminated samples were purified (cleaned up) by ethanol precipitation method or by RNeasy MinElute® kit according to manufacturer's protocol.

2.2.7.1.1.3 Ethanol precipitation of RNA

RNA sample may be contaminated with solvent mainly phenol from TRIzol extraction or from salt. Sample can also be contaminated by inadequately removal of isopropanol or ethanol. These can affect the synthesis of cDNA and/or qRT-PCR if unpurified. Contaminated samples were purified by ethanol precipitation method. Each contaminated RNA sample was made up to 100 µl (can go up to 400 µl depending on the concentration) with nuclease-free water in an Eppendorf tube and 10 µl (0.1% volume) of 3M RNA-free sodium acetate (pH 5.2) was added and vortex mixed. Then 220 µl (2.2% volumes) of ice cold 100% ethanol was added and mixed thoroughly. The tube was placed at -80^{o}C for at least 20 min (or stored for later use). The sample was then put back on ice and thoroughly mixed. All the Sample or a desired volume was transferred into a microcentrifuge tube and spun for 10 min at 14,000xg. Supernatant was decanted and the remaining trace was removed with a pipettor. Carefully, 500 µl of ice cold 70% ethanol was added and centrifuged for 5 min at 14,000xg to wash the pellet. The ethanol was removed by decanting and the remaining traces by pipetting. The tube was inverted on a paper towel and allowed to dry. The RNA sample was then re-dissolved in about 10-30 µl of nuclease free water and concentration taken.

2.2.7.1.1.4 DNase treatment of total RNA sample

All the RNA samples were treated with DNase (Ambion® DNA-*free*™) kit to remove any genomic DNA contamination that may be present in any of the sample which may interfere with the gene expression analysis. The reaction was carried out in a 50µl reaction containing 10µg of total RNA (i.e. 1µg/5µl reaction). Briefly, 39µl of 10µg RNA was dispensed into Eppendorf tube, then 5µl of 10x DNase I buffer (0.1% vol) was added followed by 1µl of recombinant DNase I (rDNase). The reaction was mixed gently and incubated a 37^{o}C for 20-30 minutes. After, 5µl (0.1% vol) of re-suspended DNase inactivation reagent was added and mixed well. The reaction was again incubated at room temperature for 2 minutes with occasional mixing. The mixture was centrifuged at 10,000xg (rcf) for 1.5 minute and the supernatant (DNase treated RNA) was collected in a fresh Eppendorf tube and the concentration re-determined.

Alternatively, RNeasy® mini plus kit (Qiagen) can be used in one go for RNA extraction, clean up and DNase treatment. This procedure saves time and reduces loss of RNA sample that may arise from the above treatments. In some TRIzol extracted samples with very little amount of total RNA and high level of phenolic contamination, RNeasy mini plus kit was used for both clean up and genomic DNA removal according to the manufacturer's protocol in order to reduce RNA loss. Here, the first step of tissue lysis with 350 µl buffer RLT and QIA shredder column spinning was omitted. Simply, the total RNA was made up to 350 µl with nuclease-free water, then, transferred to genomic DNA eliminator spin column placed in 2 ml collection tube and spun at 8,000xg for 30 sec. The column was discarded and 350 µl of 70% ethanol added to the flow-through. The mixture was transferred to an RNeasy spin column and spun for 15 sec at 8,000xg. The flow-through was discarded and the column replaced back in the same collection tube. Then 700 µl of buffer RW1 was added to the column, which was

again spun for 15 sec at 8,000xg and the flow through again discarded. The column was replaced back in the collection tube and 500 µl of buffer RPE (containing ethanol) added to the column and spun for 2 min at 8,000xg. The flow-through was discarded and column put back in a new 2 ml collection tube and spun for 1 min at 8,000xg to remove residual ethanol. The column was placed in a new 1.5ml RNase-free tube and about 12-30 µl of nuclease-free water was added to the centre of the membrane in the column and spun for 1 min at 8,000xg and the total RNA was collected.

2.2.7.1.1.5 RNA purity and integrity

RNA quality was checked on 1% agarose gel containing ethidium bromide. Briefly, 1µg of RNA sample was loaded on the gel and run at 70 volts for about 45 minutes. A picture of the gel was acquired with a Gel imaging system and observed for presence of distinct bands of 18s and 28s rRNA signifying the quality of RNA. Alternatively or in addition, samples were further analysed for RNA integrity by microcapillary electrophoresis using the Bioanalyzer. An RNA integrity number (RIN) of isolated RNA was obtained. RIN of approximately ~10 (or 8-10) was considered optimal. The chips were run according to the manufacturer's protocol by the Genomic Centre staff.

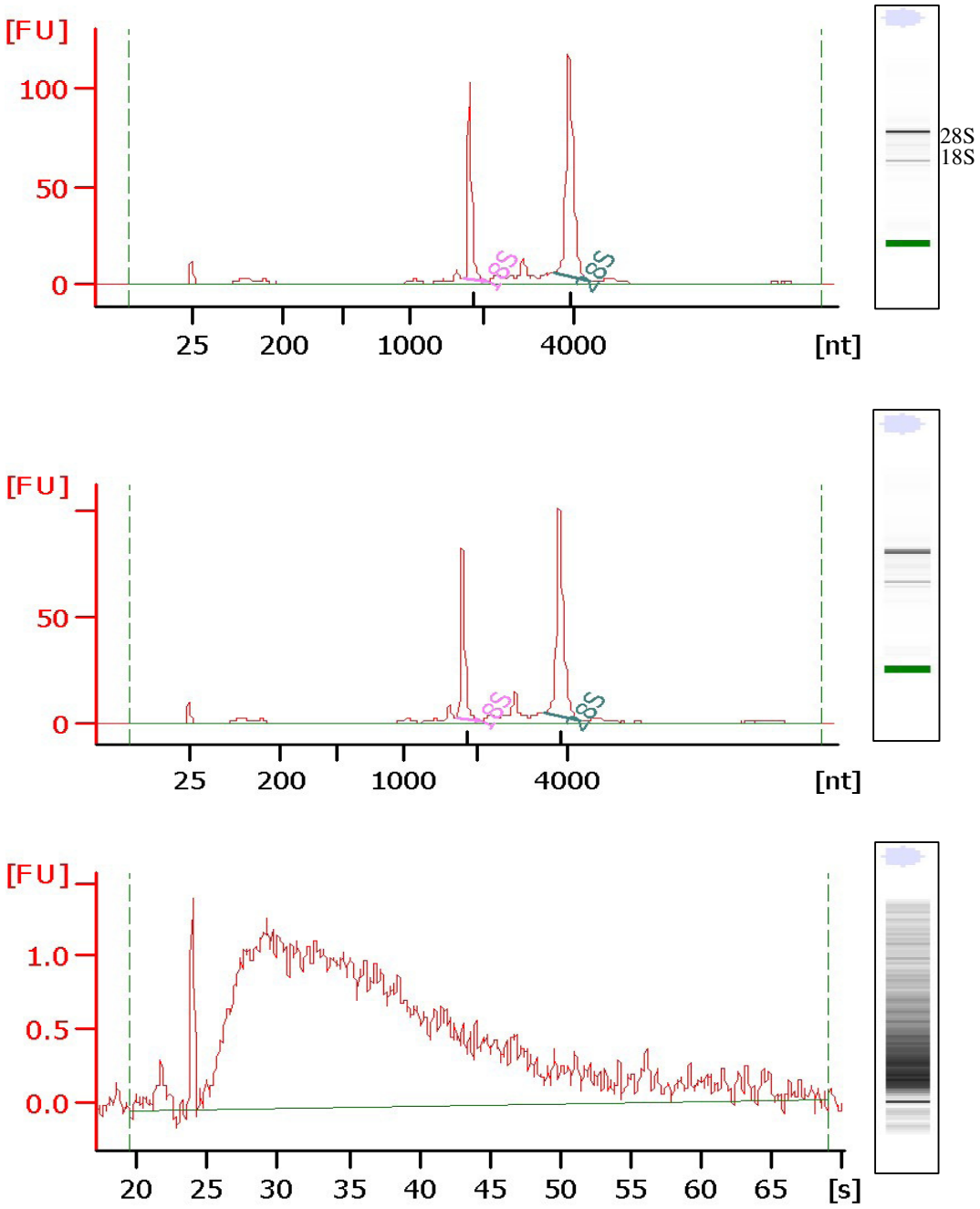

Figure 2.2. Example BioAnalyzer traces of zebrafish RNA samples. Following RNA isolation and treatment, samples were tested with the BioAnalyzer to ensure high quality sample material with clearly defined peaks of 18S and 28S RNA (trace **A** and trace **B** applicable for microarray and ISH/qRT-PCR gene expression study). Any degraded RNA samples (trace **C**) were not used in experiments. Corresponding micro-gel images were shown on the right. 18S/28S: ribosomal RNAs 18S and 28S. ISH: insitu hybridization. qRT-PCR: quantitative real-time polymerase chain reaction.

2.2.7.1.1.6 Synthesis of first strand cDNA from total RNA sample

Only mRNA from total RNA was converted to cDNA in this method. Briefly, 2 µg (7µl) of the total RNA extracted was put in a microfuge tube and 1µl (0.5 µg/µl) of oligo $dT_{(20)}$ Primer (Invitrogen) was added and the total reaction volume was adjusted to 12 µl by adding 4 µl of RNase-free water. The reaction was mixed and incubated for 10 minutes at 70^{o}C in a PCR machine (DNA engine-DYAD^{TM}). The reaction was immediately cooled on ice then the following reagents were added making up the volume to 25 µl and the reaction further incubated in PCR machine at 42^{o}C for 2 minutes; 2.5 µl of 10X reaction buffer, 3.0 µl of 25mM $MgCl_2$, 1.0 µl of 10 mM dNTPs, 2.0 µl of 0.1 mM DTT and 3.5 µl RNAase-free water (Promega). After the incubation period, 1.0 µl (200 U/µl) of Superscript reverse transcriptase (Invitrogen) was added and incubated for 1 h at 42^{o}C on a PCR machine. The incubation was continued for another 15 minutes at 70^{o}C before 1.0 µl of RNase H (2 U/µl) was added and incubated in PCR machine for 30 minutes at 37^{o}C. The first strand cDNA was obtained and stored at -20^{o}C until use.

In the alternative method, cDNA was synthesized using high capacity RNA-to cDNA kit (Applied Biosystems). Here, all total RNA (mRNA, rRNA and tRNA) were converted to cDNA in a 20 µl reaction using a convenient 8-strip (0.2ml capacity) tube . A 10 µl of 2x reverse transcriptase (RT) buffer was aliquoted into the tube and 1 µl of 20x RT enzyme mix added. Then 1-9µl of RNA sample (containing 0.2-2.0µg) was added and the reaction mixture was made up to 20µl with nuclease-free water (Applied Biosystems). The mixture was briefly centrifuged to spin down the content and to eliminate air bubbles and then incubated on a thermal cycler (PCR machine) at 37^{o} C for 60 minutes and the reaction was stopped by continuing the incubation at 95^{o} C for 5 minutes and hold at 4^{o} C (Table 2.2.6).

Step	Primer Incubation	Reverse transcription	Enzyme inactivation	End of run
Setting	HOLD	HOLD	HOLD	HOLD
Temperature (°C)	25	37	95	4
Time (min)	10	60	5	∞

Table 2.2.6 **Reverse transcription thermal cycling programme**
"∞" denotes store forever but here it means store for short-term period (up to 24 h) prior to transferring samples to -20 °C. "HOLD" denotes a setting where temperature is constant.

.

2.2.7.1.1.7 Amplification of cDNA product by Polymerase Chain Reaction (PCR)

2.2.7.1.1.7.1 Primer Design

Ensembl was used to obtain sequences of zebrafish mRNA transcript of the gene of interest (e.g. *slc30a1, slc39a10, He1a, catL1b, klf4* and *cdh1*) in zebrafish for primer design. Primer sequences for amplification of a fragment of each gene (Table 2.2.7) were designed using primer3 software (http://frodo.wi.mit.edu/primer3/), then synthesized from Sigma. The primers were reconstituted according to manufacturer's instructions.

2.2.7.1.1.7.2 Conventional PCR

A 1:10 dilution of the 1st strand cDNA product was made with milliQ or RNA-free water and the amplification reaction was set up as follows: 2 µl of diluted cDNA was added to a PCR mixture containing 4 µl of 5x reaction buffer, 0.4 µl of 10mM dNTPs mix (0.1 µl each), 0.4 µl of 10µM each of forward and reverse primers, 0.8 µl of 25mM $MgCl_2$, 0.1 µl (5U/µl) of Taq polymerase (Promega) and the reaction made up to 20 µl with RNAse-free water. The cDNA-PCR mixtures were then amplified using a thermal cycler and the general cycling parameters were employed; i.e. 94^{o}C for 3 minutes enzyme activation (1 cycle), 94^{o}C for 30 seconds denaturation, 56-65^{o}C for 30 seconds gradient annealing temperature and 72^{o}C for 1 minute extension (34 cycles), and final extension (elongation) at 72^{o}C for 3 minutes (1 cycle). The PCR product was

electrophoresed on 2% agarose gel and the correct optimal primer annealing temperature determined for each gene.

Gene	Primer sequences (5'-3')	Amplicon size (bp)
slc30a1 (*znt1*)	F: AGACCCAGTCCACCAACAAG R: AGGACATGCAGGAAAACACC	538
slc39a10 (*zip10*)	F: TCAGAAATGTCCTGCAATGG R: TGGGCTTTGACCTTAGATGG	823
he1a	F: CCCTCTCCATTCTGCTTCTG R: GCCGTTTTTCCATAGTGCAT	652
catL 1b	F: AGCCAGCATGGAAAAAGCTA R: CAGAGAAGGCTCCAGTGACC	935
klf4	F: ACCCCGGACATGAATTATCA R: TGTCCGGTGTGTTTCCTGTA	731
cdh 1	F: GGCCACAAGGTGTTTTCTGT R: CAAACCCTCTCCGTTCATGT	741

Table 2.2.7: Primer sequences used for amplification of genes for ISH probe. Genes of interest with their primer sequences, product lengths and accession numbers

2.2.7.1.1.7.3 Agarose gel electrophoresis

A 2% (w/v) agarose gel was prepared with 100ml 1X TEA buffer. The gel was melted using a microwave and when the gel cooled down to about 50^{o}C, 5 µl (0.5µg/ml) of ethidium bromide was added as a detection system. The gel was allowed to set on the gel cast and wells were created inside the gel using a gel comb. Each PCR sample was mixed with 6X blue/orange loading dye (Promega), then 10 µl of the mixture was loaded into each well and run at 80 volts for about 1 hour. The amplicon size (Table 2.2.7) and intensity of the gene fragment produced was assessed using a gel imaging system.

2.2.7.1.1.7.4 PCR products clean up (QIAquick PCR purification column)

QIAquick column (Invitrogen) is a system based on the selective binding properties of a silica membrane to purify PCR product and remove contaminants and other unincorporated reagents in the product after the cycle. The PCR product was made up to 100 µl with MilliQ (MQ) water then 500 µl of PBI buffer (5 times the product volume) was added, transferred into a QIAquick spin column in a provided 2 ml collection tube and centrifuged at 14,000 rpm for 1 minute. The flow-through was discarded and the column was replaced back into the same tube. The bound DNA on the column was washed by adding 750 µl of buffer PE and centrifuged for 1 minute at 14,000 rpm. The flow-through was discarded and the column replaced into the same collection tube and spin for 1 minute to remove the residual ethanol. The column was replaced into a clean 1.5 ml capacity micro-centrifuge tube and the DNA was eluted from the filter membrane of the column by adding 30 µl of MQ water, allowed to stand for a minute then centrifuged for 1 minute. The purified DNA was collected in the micro-centrifuge tube and stored at -20^{o}C.

2.2.7.1.1.8 Cloning of gene in plasmid vector

2.2.7.1.1.8.1 Ligation

After purification, the concentration of each gene (DNA) was measured and used to calculate the amount of DNA to be inserted in the vector (PGEM-T-Easy; Promega) according to the following formula;

$$\text{Amount of DNA (ng)} = \frac{\text{amount of vector (ng) x size of insert (kb)}}{\text{Size of vector (kb)}} \times \text{insert : vector molar ratio (3:1)}$$

where vector size = 3000kb, amt of vector recommended = 25ng, size of each gene = 0.54, 0.82, 0.65, 0.94, 0.73 and 0.74kb for *znt1*, *zip10*, *he1a*, *catL1b* and *klf4*, respectively. Concentration for each gene was 70ng/ µl, 72ng/ µl, 230ng/ µl and 151ng/ µl for *zip10*, *he1a*, *catL1b* and *klf4*, respectively.

Ligation reaction was then performed using 0.5 µl (50ng/µl) of PGEM-T-Easy vector (Promega), 5 µl of 2X rapid ligation buffer (Promega), DNA product for each gene (3.5 µl, 0.5 µl, 1.2 µl, 2.5 µl & 2.3 µl of *znt1*, *zip10*, *he1a*, *catL1b* and *klf4* respectively) and 1 µl T4 DNA ligase. Each reaction was made up to 10 µl reaction and was incubated at room temperature for 1 hour.

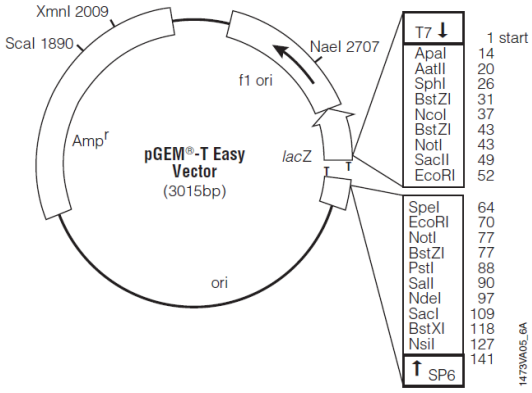

Fig 2.3. **PGEM®-T Easy vector map**

2.2.7.1.1.8.2 Transformation (Amplification of plasmid DNA in competent bacterial cells)

Promega's JM109 high efficiency (and/or DH5α) chemically competent cells (*E. coli*) were retrieved from -80^{o}C storage and immediately placed on ice until thawed. To 25 µl of the cells, 3-5 µl of the ligation product was added in a tube, mixed well with pipette tip by swirling and placed on ice for 30 minutes and subsequently heat-shocked for 1 minute in a water bath at 42^{o}C. The tube was immediately put on ice for 2 minute and 250 µl of LB broth medium was added. The tube was then incubated on a shaker (200-250rpm) at 37^{o}C for 45 minutes. The cell suspension (100 µl) was plated out onto a selection plates (LB agar incorporated with 100 µg/ml ampicillin) and incubated overnight at 37^{o}C. Individual (isolated) colonies were picked and inoculated into 3-5 ml LB broth incorporated with ampicillin and incubated overnight in a shaker (200rpm) at 37^{o}C. The bacterial culture was centrifuged, supernatant discarded and the bacterial pellets collected.

2.2.7.1.1.8.3 Plasmid DNA isolation and purification (QIAprep mini prep kit)

The plasmid DNA for each gene was extracted and isolated from bacterial cells using a Qiagen (QIAprep) mini prep kit. The pelleted bacterial cells were re-suspended in 250 µl buffer P1 and transferred into a micro-centrifuge tube. 250 µl of buffer P2 was added and mixed thoroughly by inverting the tube 6 times, then 350 µl of buffer N3 was added and immediately and gently inverted for another 6 times. The sample was centrifuged at 13,000 rpm for 10 minutes at room temperature. The supernatant was collected in a QIAprep spin column, spun for 1 minute and the flow-through discarded. The spin column was washed by adding 750 µl buffer PE, centrifuged for 1 minute and the flow-through discarded. The column was replaced into the same tube and centrifuged for

another 1 minute to remove the residual ethanol. Thereafter, the spin column was placed into a clean 1.5 ml capacity micro-centrifuge tube and the DNA was eluted from the filter membrane of the column by adding 50 µl of MQ water and allowed to stand for 1 minute, then centrifuged for 1 minute. The eluent (purified plasmid DNA) was collected inside the micro-centrifuge tube and stored at -20^{o}C until use.

2.2.7.1.1.8.4 Restriction (digestion) analysis of plasmid DNA

Restriction digestion analysis of plasmid DNA was carried out to indicate which of the isolated sample picked up the plasmid containing the insert. Restriction enzyme EcoR1 was used to excise the plasmid only at both ends enclosing the DNA (insert) to confirm the presence of the insert in the plasmid vector. The restriction analysis was performed in a 10 µl reaction containing 1 µl of 10X buffer H (Promega), 1 µl of plasmid DNA, 0.25 µl EcoR1 and 7.65 µl MQ water. The reaction was incubated for 2 hours at 37^{o}C and samples run and confirmed for proper digestion on a 1% (w/v) agarose gel.

2.2.7.1.1.8.5 Orientation of the insert in the plasmid

The orientation of the insert in the plasmid was determined to identify the correct transcription start site of the plasmid in order to make proper anti-sense RNA probe from the insert. It was carried out by restriction analysis/electrophoresis and later confirmed by sequencing of the whole plasmid DNA.

Restriction analysis reaction was carried out using a single enzyme digestion having restriction sites for both insert and plasmid (e.g. Pst1 for *znt1* and plasmid). The ideal restriction enzyme was searched from NEB (New European Biolab) website (www.tools.neb.com/NEBcutter2) and restriction analysis was performed in a 20 µl reaction containing 2 µl of 10X buffer 3, 2 µl of 10X BSA, 1 µl of Pst1, 2 µl of plasmid

DNA and 13 µl MQ water. The reaction was incubated for 2 hours at 37°C and individual samples were run and observed for proper orientation on 1% agarose gel. Alternatively, for sequence confirmation and orientation, 5 µl of purified plasmid DNA of each gene was aliquoted into Eppendorf tubes (in duplicate) and sent to a commercial sequencing outfit for sequencing using universal primers; M13 (forward) and SP6 (reverse). The sequence of each insert was checked for correctness and the orientation was confirmed using the online San Diego Science Computer (SDSC) workbench search engine for sequence comparison between the query (insert) and reference gene using BLAST (BL2SEQ).

2.2.7.1.1.8.6 Linearization of plasmid DNA

Linearization of plasmid DNA was necessary before the transcription reaction for making anti-sense RNA probe from the insert. Each plasmid DNA was linearized with appropriate enzyme from NEB catalogue (www.tools.neb.com/NEBcutter2) by mixing 10 µl of 10X buffer 3 with 2.5 µl of restriction enzyme (sal1 for *znt1* & *zip10;* and Nco1 for *he1a, catL1b* & *klf4*), 10 µl of 10X BSA (only for genes requiring sal1) and about 5-10µg of plasmid DNA. The reaction was made up to 100 µl volume with MQ water and incubated at 37°C for 2 hours. The sample was run and confirmed for proper linearization on 1% agarose gel.

2.2.7.1.1.8.7 Purification of linearized plasmid DNA

The linearized DNA was purified (cleaned-up) as described above for PCR product using QIAquick purification kit except that gel extraction kit was used. The procedure

was similar except that spin column with purple cap was used for linearized plasmid DNA instead of blue cap for PCR products.

2.2.7.1.1.8.8 *In vitro* transcription (DIG-labelled anti-sense RNA probe)

After confirming the orientation of the insert in the plasmid, it was transcribed using appropriate RNA polymerase enzyme in a 20 µl reaction consisting of 13 µl (1µg) of linearized plasmid, 2 µl of 10X transcription buffer (Roche), 2 µl NTP-DIG-RNA, 1 µl RNase inhibitor and 2 µl (20U/µl) RNA polymerase (Sp6 or T7 depending on the orientation, i.e. T7 for *znt1* & *zip10* and SP6 for others). The reaction was incubated for 2 hours at 37^{o}C before 4 µl DNase I was added and made up to 52 µl with MQ or GE probe purification buffer. This was further incubated for 45 minutes at 37^{o}C. 2 µl was taken out of the reaction and added with 1 µl RNase inhibitor which was run on 1% agarose gel for confirmation of proper transcription.

2.2.7.1.1.8.9 Anti-sense RNA (Probe) purification

The transcribed anti-sense RNA was purified using a Sephadex G50 micro column (GE healthcare). The column was placed in a 1.5 ml screw top tube provided and centrifuged at 3,000 rpm for 1 minute to empty the column. The column was replaced into a fresh 1.5ml tube and 50 µl of transcribed anti-sense RNA was transferred into the column. The column was centrifuged at 3,000rpm for 2 minutes. The anti-sense RNA was collected into the tube and made up to 100 µl with RNA grade TE buffer. This was stored at -20^{o}C until ready for use for whole mount in-situ hybridization.

2.2.7.1.1.9 Alternative and quicker method of anti-sense probe making without cloning

For *cdh1* gene, an alternative and quicker method was used to produce the probe (Thiese and Thiese, 2008). This does not require cloning of the gene in the vector (and subsequent procedures mentioned earlier) before in-vitro transcription reaction. Simply, the gene fragment was amplified with primers to which T7 promoter sequences (TAATACGACTCACTATAGGG) was added to the 5' extremity of the reverse primer for anti-sense probe making. Optionally, the sequences were also added to the 5' extremity of the forward primer for sense probe which was used as control to test the specificity of the staining of the anti-sense probe. The PCR product was purified and transcribed with T7 RNA polymerase as described above.

2.2.7.1.2 Whole-mount *in situ* hybridization technique

The high resolution whole mount *in situ* hybridization was divided into 3 days of operation and performed as follow (Thiese and Thiese, 2008; Thiese eta al, 2004).

2.2.7.1.2.1 Fixation and storage of embryo

Embryos were collected at different developmental stages (10, 24, 33, 48 and 72hpf as the case may be) for Znt1 wild-type, Znt1 homozygote mutant, Znt1 morphant and Zip10 morphant ($Znt1^{+/+}$, $Znt1^{\Delta 40/\Delta 40}$, $Znt1^{MO}$ and $Zip10^{MO}$). The embryos were dechorionated under an inverted microscope using a fine tipped forceps (#5 durmont-WPI, USA) or alternatively for large numbers of embryos, chorions were removed by pronase treatment (1/100 wt/vol). The solution was diluted with embryo water (1/4 vol/vol), warmed to 28.5 ^{o}C and poured on the embryos inside the petri dish coated with

2% agarose. The embryos were incubated for 1 minute at 28.5 ^{o}C and the solution was discarded, replaced with fresh embryo water and gently rinsed 3 times. Embryos were further incubated until all the chorions were removed. Dechorionated embryos were transferred into a new petri dish and were allowed to develop at 28.5 ^{o}C until appropriate stage for fixing.

Dechorionated embryos were then fixed overnight at 4^{o}C with 4% (wt/vol) paraformaldehyde in 1 x PBS. Older embryos with advanced melanin pigmentation (33hpf and above), were incubated in a mixture of 3% H_2O_2 and 0.5% KOH solution at room temperature for 30 min to 1 h to remove the pigmentation.

Embryos were transferred and washed in graded methanol (i.e. 25, 50, 75 & 100%) in PBST (vol/vol) in a stepwise manner for 5 minutes each and stored at -20^{o}C at least for 2 h to several months until ready for use. PBST was prepared by mixture of PBS with 0.1% Tween 20 (vol/vol).

The 3 days of *in-situ* hybridization consist of pre-hybridization and hybridization stage for first day, post-hybridization stage for second day, then washing and staining stage for third day.

2.2.7.1.2.2 Prehybridization or permeabilization (Day 1)

Fixed embryos were first rehydrated by transferring about 20 embryos of similar stage of development into Eppendorf tubes and washed in graded PBST in methanol (25, 50, 75 & 100%) in a stepwise manner on an incubator shaker at room temperature for 5 minutes each. The last washing with 100% PBST was done 4 times. After successive washing, the embryos were digested in 10µg/ml Proteinase K (Invitrogen) in PBST at room temperature for 30 sec (10hpf), 5 minutes (24hpf), 15 minutes (48hpf) and 20 minutes (72hpf) respectively. Proteinase K digestion was stopped by washing

(incubating) the embryos twice in PBST for 5 minutes at room temperature and refixed in 4% PFA in PBS (wt/vol) at room temperature for 20 minutes, then washed in 1 x PBST five times for 5 minutes each at room temperature.

2.2.7.1.2.3 Hybridization

Embryos were first pre-hybridized by adding 750µl of Hybridization Mix [5X SSC (750mM NaCl; 75mM Na-citrate; pH 7.0), 50% (v/v) formamide, 0.1% (v/v) Tween 20, 9.2mM citric acid, 50 µg/ml heparin & 500 µg/ml torula yeast RNA] and incubated for 2-5 hours at 70 ^{o}C. Then embryos were hybridized by removing the hybridization mix and replaced with 200-500 µl of hybridization mix containing about 30-50 ng of antisense DIG-labelled RNA probe (or 1:100 of antisense RNA probe with hybridization mix) and incubated overnight in water bath at 70 ^{o}C.

2.2.7.1.2.4 Post-hybridization (Day 2; washing and detection)

The probe-hybridization mixture was removed and embryos were washed in graded hybridization wash solution (hybridization mix without heparin and tRNA) in 2x SSC solution (100, 75, 50 & 25%) for 10-15 minutes each at 70^{o}C, then washed once in 2x SSC and twice in 0.2x SSC for 15 minutes and 30 minutes, respectively, at 70^{o}C. Thereafter the embryos were washed in graded PBST (25, 50, 75 & 100%) in 0.2X SSC for 10 minutes each at room temperature and in 1 ml of blocking buffer (2mg/ml BSA in PBST and 2% lamb serum in PBST) for 2 hours on a shaker at room temperature. The embryos were then replaced with 1:2000-1:10,000 dilution of anti-DIG-antibody (Roche) in blocking buffer and incubated in the dark overnight at 4^{o}C with gentle

agitation on horizontal orbital shaker (40 rpm). The hybridization wash solution was composed of hybridization mix solution without heparin and yeast RNA.

2.2.7.1.2.5 Washing and staining (Day 3)

Embryos were first washed briefly for 5 minutes in the dark at room temperature with PBST to remove the antibody solution, then washed six times for 15 minutes each in the dark at room temperature with gentle agitation. The wash solution was removed completely from the embryo and then incubated in alkaline phosphatase buffer (2M Tris HCl, 5M NaCl, 20% Tween 20 and 2M $MgCl_2$) at room temperature for 3 times at 5 min per wash. The embryos were then transferred to 12 well microplates (about 10 embryos per well) and stained with 3 µl of NBT/BCIP staining solution (Roche) in 1 ml alkaline phosphatase buffer and incubated on a shaker in the dark at room temperature. The embryos were observed under an inverted microscope every 15-30 minutes until the transcript of interest is visualised noticeably by purple colour development. After adequate staining, the reaction was stopped by simply washing the embryos in PBST three times in the dark at 4^oC, post fixed in 4% PFA for 20 minutes at room temperature, washed and stored in graded 75% glycerol. Photographs of the embryos were taken (using the Nikon microscope attached to a Nikon digital camera) before long term storage at -20^oC.

2.2.7.2 Reverse transcription-quantitative (real-time) polymerase chain reaction (RT- qPCR) method

2.2.7.2.1 RNA extraction and first strand cDNA synthesis

RNA was extracted from whole embryos (24hpf or 48hpf) and from adult intestinal and brain tissues for qPCR assay. The RNA was DNase treated and cDNA synthesised with a high capacity RNA-to cDNA kit (Applied Biosystems) as previously described. For qPCR assays, equal concentration of RNA from each embryo type or adult tissues at different treatment condition was used for cDNA synthesis and stored at -20^{o}C until analysed. In adult intestinal or brain tissue, RNA was extracted as previously described but with slight modification. Here, because of small size of the intestinal or brain tissue per fish, a phase lock 2ml tube (5 Prime®) was used for RNA extraction for clear separation of aqueous phase from organic phase in order to get enough total RNA with little or no genomic contamination. The tube was briefly centrifuged at 16,000xg for 30 seconds to spin down the gel in the tube properly. Homogenate (500µl) of the Trizol homogenised tissue was transferred into a phase lock tube and incubated at room temperature for 5 minutes. Chloroform (200µl) was added and the vial, which was then shaken (but not vortexed). The sample was further incubated at room temperature for 10 minutes. The mixture was centrifuged at 16,000xg at 4^{o}C for 10 minutes. The aqueous phase was transferred to a new RNase-free eppendorf tube and 250µl of isopropanol was added and mixed by inversion. This mixture was then incubated at room temperature for 10 minutes. Thereafter, it was centrifuged at 12,000xg at 4^{o}C for 10 minutes. The supernatant was gently decanted and the RNA pellet washed with 500µl of 75% cold ethanol by centrifuging at 12,000xg for 5 minutes at 4^{o}C. Supernatant was again decanted and the pellet air-dried for 5-10 minutes. The RNA pellet was re-dissolved in 10-15µl RNase-free water and put on ice for 10 minutes. The RNA solution

was then flicked and spun down and incubated at 60^{o}C for 5 minutes. The isolated RNA was immediately put on ice and the concentration determined with a Nanodrop spectrophotometer (Thermo Fisher Scientific, Leicestershire, UK).

2.2.7.2.2 Efficiency testing and qPCR assay

Following cDNA synthesis samples were used with transcript-specific primers to amplify regions of mRNA for quantification of gene expression. A TaqMan (hydrolysis probe) assay employing the use of a fluorophore-labelled probe to detect gene amplification in real-time was used for RT-qPCR experiments. The principle of the assay was as previously described in allelic discrimination for genotyping except that the probe contains only DNA bases and no LNA bases as the assay is not meant to discriminate between 2 nucleotide sequences. Also the probe was labeled with only one reporter dye (FAM) for each gene of interest to quantify and the reaction contained only one probe (i.e. single labeled probe; SLP) rather than a mixture of two probes (i.e. DLP) with separate fluorophores as used in allelic discrimination qPCR assay. Prior to qPCR of the target gene on the samples, the efficiency of each gene was first determined using a series of 10 fold dilution of a positive cDNA sample (i.e. 1:10, 1:100, 1:1000, 1:10,000 dilution) on a ABI 7000 Prism thermocycler at default qPCR settings (Table 2.8.2). Standards were run for every gene amplified at various dilutions from the sample concentration to quantify efficiency of amplification (Fig. 2.4.1). The efficiency expressed in percentage was calculated by plotting the cycle or quantification threshold (Ct or Qt) value in a scattered chart and the slope of the Ct values of the different dilutions of samples was included in the following equation; (E = -1/slope). The percentage efficiency was calculated from (E-1) x 100%, i.e.

Efficiency = {1- [$10_{(-1)}$]}*100 *slope.*

With this method, the expected slope for a 10-fold dilution series of the template is -3.32, when the corresponding efficiency is equal to 100%. Efficiencies between 90 to 110% were considered acceptable according to ABI (Applied Biosystems 2008) and, therefore, primers-probe sets whose efficiency were within this range were used for gene expression analysis.

The qPCR reaction was carried out in a qPCR microplate (Applied Biosystems) in a total reaction of 25 µl comprising of the following reagents:

12.5 µl of UPL mastermix (Roche), 1 µl (10µM) of forward and reverse primer each of the gene of interest, 0.25 µl of UPL probe of gene of interest (Roche), 3 µl of 1:10 cDNA template and 9.75 µl of DNase-free water. Two non-template controls not containing any sample material and standards were run on every plate. The plate was placed in a thermocycler and run for about 1hr and 50 min using a default setting. The gene amplification from each sample was normalised to that of 18s rRNA, which was used as reference or house keeping gene (hkg). The 18s rRNA has previously been determined to show little expression change in zebrafish following manipulation of zinc status (Zheng *et al.*, 2008). For amplification and detection of 18s, samples were diluted in 1:1000 due to the high abundance of the transcript.

Q-PCR expression data was analysed with the REST (relative expression software tool) software package (Pfaffl, Horgan *et al.* 2002) or by the $2^{(-\Delta\Delta Ct)}$ (*Livak*) method (Livak & Schmittgen, 2001; Schmittgen & Livak, 2008).

The REST software compares the Ct value of reference gene with target genes, and considering efficiency of primers, calculates the difference in gene expression. Statistical calculation of probability of differential expression is based on a randomization of samples using the Pair Wise Fixed Reallocation Randomisation Test

(Pfaffl, Horgan *et al.* 2002). Rest was set for a number of 1000 randomisations during this analysis.

The Livak method of relative gene expression analysis is in 3-steps, as shown in the algorithm below:

1. **Normalisation of the gene of interest per sample**

   $$\Delta C_{T\,(sample)} = C_{T\,(sample\ GOI)} - C_{T\,(sample\ HKG)}$$

2. **Normalisation per treatment group**

   $$\Delta\Delta C_T = \Delta C_{T\,(treated\ sample)} - \Delta C_{T\,(control\ sample)}$$

3. **Calculating a normalised expression ratio**

   $$2^{(-\Delta\Delta Ct)}$$

Where, C_T: threshold cycle at which amplicon fluorescence passes above background. GOI: gene of interest. HKG: housekeeping gene.

The relative quantification method above measures the fold difference in gene expression through ratio of crossing point or cycle threshold (ct) values normalized to ratio of ct values for the hkg. This method and REST were used as they do not require standards with known concentration as needed by the absolute quantification method, the accuracy of which is often disputed.

Step	**Heating**	**Enzyme activation**	**Denaturation**	**Annealing/ extension***	**Dissociation**		
Setting	HOLD		CYCLE (40-55)		HOLD		
Temp. (°C)	50	95	95	60	95	60	95
Time (min)	2:00	10:00	0:15	1:00	0:15	0.:20	0:15

Table 2.2.8. Quantitative RT-PCR thermocycling procedure.

*data is collected during the annealing/extension phase of the qRT-PCR run. "HOLD" denotes a setting where temperature is constant. "CYCLE" denotes a setting where temperature was cycled.

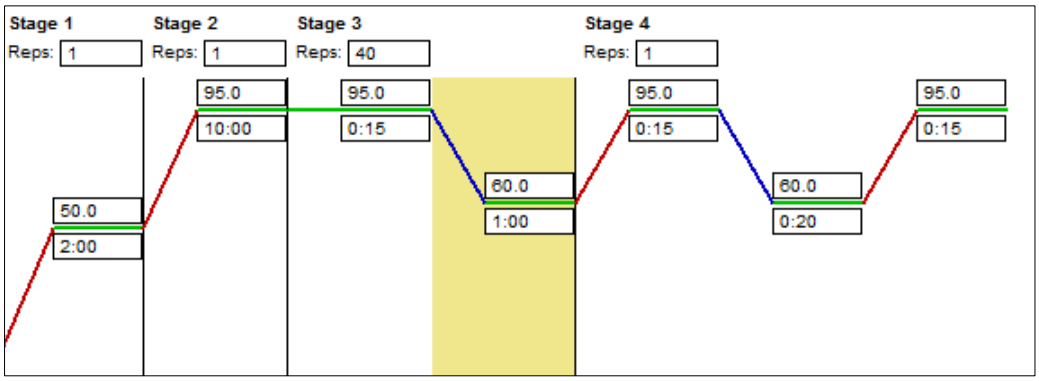

Figure 2.4. Programme setting for sequence detection software thermocycling protocol. Stage 1: heating. Stage 2: enzyme activation. Stage 3: denaturation and annealing/extension. Stage 4: Dissociation. "Reps" indicates the number of cycles the stages are repeated for. On the temperature indication line, the top box represents temperature in °C and lower box represents time in minutes. The Section highlighted in yellow is the data collection stage of the stage 3 cycle. NB: Stage 4 (dissociation stage) or melting curve is not required in probe (e.g. hydrolysis probe such as Taqman) assay but only in dye (e.g. SYBR green) assay because the probe will not bind to primer-dimers. This also increases the specificity of the assay due to specific binding of probe to amplicon.

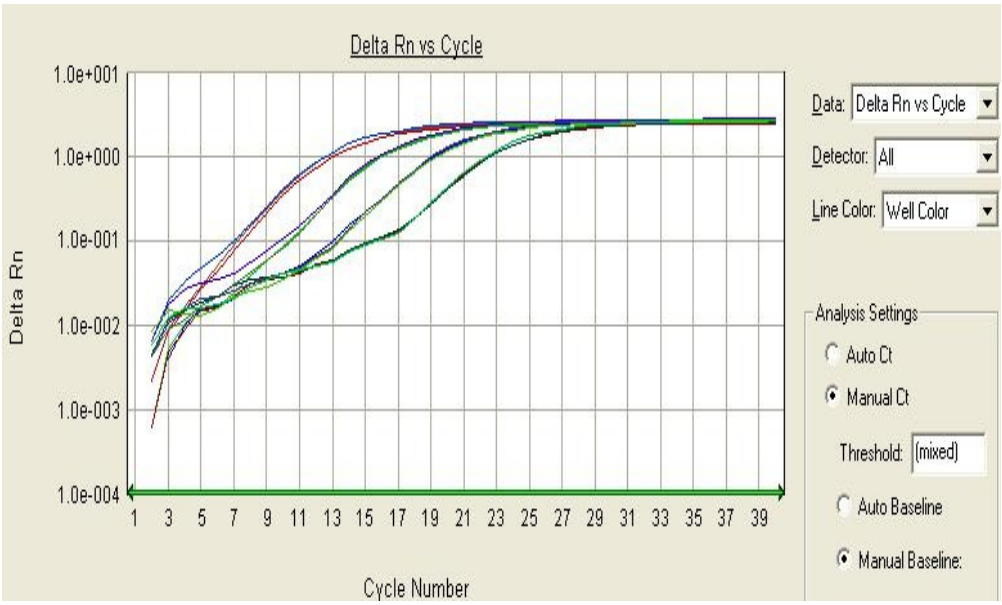

Figure 2.4.1: Example of qPCR efficiency amplification curve

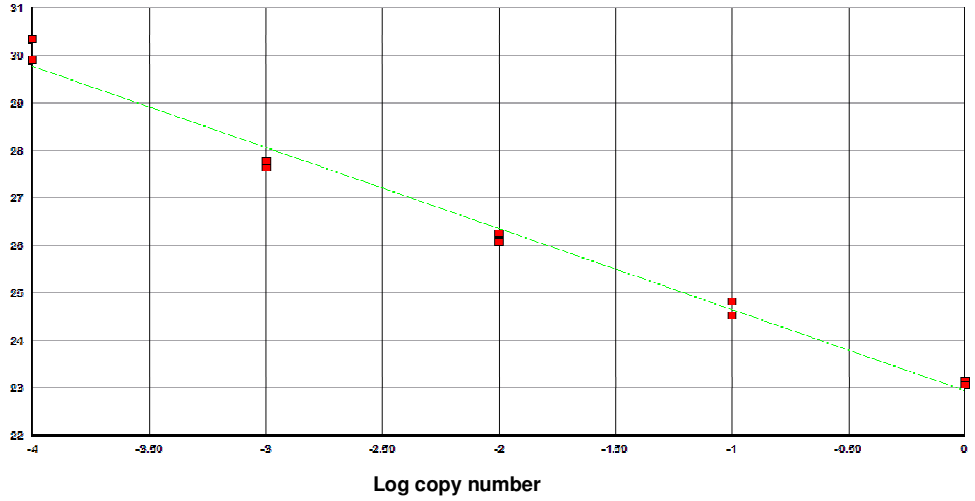

Figure 2.4.2: Example of sequence detection system generated standard curve to ensure efficiency of amplification.

2.2.8 Protein isolation and quantification

The following sections describe the process of protein isolation and quantification. Abundances of specific proteins were estimated through the use of Western blotting (WB) and/or immunohistochemistry (IHC). For buffer and gel compositions see Appendix 9.4-9.11. Total protein was isolated from embryos or adult tissue by homogenizing the tissue with lysis buffer containing of 1% SDS, 1X PBS and a cocktail of protease inhibitors (Sigma) at the ratios of 1:89:10 µl. For membrane protein isolation in embryo SDS was not used in the lysis buffer and prior to homogenization, embryos were dechorionated and deyolked for better protein resolution. Embryo dechorionation was performed manually or in large numbers with 1mg/ml pronase proteolytic enzyme solution (Sigma) in fish water at 28.5˚C for 1 minute and washed 3 times in fresh fish water. Yolk was removed from the embryos by putting them in a deyolking solution (Ringer solution + 10% EDTA (10mM) + PMSF protease inhibitor

at 0.3mM final concentrations) and triturated with the aid of small diameter glass pipette or with a 20µl capacity microtip to disburse the yolk materials. The developing embryos or embryonic cells devoid of yolk and chorion were carefully picked out of the solution and put in Eppendorf tube. As much as possible of the deyolking solution was removed from the fragmented embryonic cells and rinsed twice in cold ringer's solution. The sample was spun at 4000rpm for 5min to pellet the cells and the supernatant removed. The samples were kept at -80˚C for later analysis.

Proteins were then prepared for Western blotting as follows. About 50-100 µl or more of lysis buffer was used for homogenization depending on the amount of tissue or number of embryos for protein extraction. Embryonic tissue were lysed and homogenised in an Eppendorf tube on ice using a plastic pestle. The homogenate was repeatedly passed through a 1 ml syringe and needle to further lyse the cells. This step is (optional). Tissue lysates were then centrifuged at 1000 rpm at 4 °C for 5 min and the supernatant was transferred to a fresh tube. From the supernatant, 1µl was then taken for quantification using a spectrophotometric assay (Pierce Protein quantification kit-rapid, 51254-1KT, Sigma, Dorset, UK) based on a BSA standard curve ranging from 0 to 2000 µg/ml. Briefly, 1 µl of protein was made up to 10 µl and this was reacted with 150 µl of Pierce protein quantification reagent in a 96-well microtitre plate. The BSA protein standards of varying concentrations (10µl each) were also included in the reaction to quantify the concentration of protein of interest. Each reaction was done in duplicate and was incubated at room temperature for 5 min before taking the absorbance reading with spectrophotometer. The concentration of protein for each sample was calculated using a standard curve equation generated from BSA standards as shown; $y = mx + c$ where y is absorbance which is known, x is concentration of sample to be determined which is unknown, m and c are slope and intercept respectively which are

known. Following quantification, samples were made into aliquots of desired quantity of protein (for electrophoresis), mixed with loading buffer in the ratio of 4:1 (vol/vol) and stored at -20 °C. NB: Loading buffer is mixed with an aliquote of β-mercaptoethanol in the ratio of 19:1 before it's added to the sample for storage.

2.2.8.1 Western blotting (immunoblotting)

For the first step of Western blotting, gels were prepared for electrophoresis (see composition in Appendix 9.8) and poured inside the gel cassette. Sodium dodecyl sulphate-polyacrylamide gels electrophoresis (SDS-PAGE) consisted of 10 % (w/v) acrylamide. After setting of the gel inside the cassette, the cassette was placed inside the electrophoresis tank and then filled with SDS running buffer. Each protein sample along with protein molecular weight marker were loaded into the wells created in the gel. The electrophoresis tank was operated at a constant voltage of 130 V and a variable current from 0-5 mA. Gels were run for approximately 40 min or more.

After electrophoresis, the gel was carefully taken out of the cassette and the separated proteins in the gel were blotted onto a nitrocellulose membrane using a semi-dry transfer cell or a pre-cooled wet transfer cell (Bio-Rad). The transfer was made by creating a layered stack (i.e. sandwich) in the following order in the direction of current flow, i.e. from top to bottom for semi-dry transfer cell (filter paper – gel – nitrocellulose membrane – filter paper) or from back to front for wet transfer cell (filter pad - filter paper - gel - nitrocellulose membrane - filter paper - filter pad). It was important to ensure that the filter paper, gel and membrane were of the same size. Stacked components were soaked in transfer buffer for at least 5 min, then placed on a moistened transfer cell surface or inside the wet transfer tank, membrane-side down and gel-side up (i.e. gel placed before the membrane in the direction of current flow).

Transfer was run at 35 mA per gel-membrane for 60-90 min for semi-dry transfer or at 100 V for 60-90 min for wet transfer.

Following transfer, the membranes were washed 3 times in washing buffer then placed in blocking solution for 60 min at room temperature with constant agitation at 60 rpm. After blocking, membranes were incubated with the primary antibody diluted into 3 ml of blocking solution contained in a 50 ml Falcon tube. Primary antibody incubation was carried out overnight at 4 °C on a roller-mixer to ensure even distribution of the antibody solution over the membrane. After the primary antibody incubation, membranes were washed with washing buffer at room temperature 3 times for 10 min each. Membranes were then incubated with the appropriate secondary antibody, diluted into 3 ml of blocking solution, for 60-90 min at room temperature. After the secondary antibody incubation, membranes were washed at room temperature, 3 times for 5-10 min each, and were then ready for detection. All washes were done with constant agitation at 60 rpm, by placing membranes on a rocker.

Stripping of antibodies off the membrane for purpose of re-probing with another primary antibody was achieved using the stripping buffer (Appendix 9.11). The buffer is applied to the membrane and incubated at 50 °C for 10-20 min. The membrane was washed with washing buffer 3 times until the smell of β-mercaptoethanol was no longer perceived or was markedly reduced. The membrane was then blocked and incubated overnight with another primary antibody and the subsequent procedures continued.

2.2.8.2 Detection, densitometry and data analysis

After the incubations with primary and secondary antibodies were complete, membranes were briefly removed from the washing solution and placed on a flat surface previously cleaned and dried with ethanol, then ready for application of the detection

reagents. The electrochemoluminiscence (ECL) detection reagent components were mixed in a 1:1 ratio with a final volume of 1 ml per blotting membrane. Detection reagents were then gently and evenly pipetted onto the surface of the membranes and left for about 2-3 min before dripping off excess reagent. Membranes were then placed in a dark exposure cassette and covered with clear plastic. The photosensitive light-films were exposed to the membranes in a dark room for 5-30 min (depending on the protein for detection) then manually or automatically developed and fixed with film processing solutions.

The fixed films were manually digitised on a BioRad densitometer (or image J) using film-specific settings. QuantityOne 1-D analysis software (BioRad) allowed autocorrection of the image, lane-specific background reduction and automated band-detection. Specific band density was quantified for each of the proteins to be detected. Normalisation was to the amount of protein loaded per well and/or to the housekeeping protein β-actin or total ERK in case of pERK protein normalisation.

2.2.8.3 Immunohistochemistry

The abundance of protein expression in cells of treated embryos was assessed by immunostaining method. Briefly, embryos at a desired developmental stage were dechorionated and fixed overnight in 4% PFA at 4^{o}C. Fixed embryos were rinsed 3 times at 5 min each in ice cold 1X PBS and then permeabilized in 100% methanol at -20 ^{o}C for 10 min before washing again in PBS for 5 min. Embryos can also be preserved in graded methanol as described in section 2.2.7.1.2.1 until ready for use. Permeabilization of intracellular protein with 10 min incubation in PBS+0.25% of Triton X-100 was skipped in case of membrane bound protein. The embryos were then blocked in 1% BSA diluted in PBST for 30 min, then incubated overnight at 4^{o}C in diluted primary

antibody with 1% BSA. The antibody solution was removed and the embryos washed 3 times in PBS at 5 min each. Thereafter, the embryos were incubated in the dark for 1 hr at room temperature in diluted secondary antibody (conjugated with Alexa Fluor 488) with 1% BSA. The antibody solution was removed and the embryos rinsed 3 times in PBS for 5 min each. Embryos were counterstained for blue nuclear staining with DAPI (or Hoechst) in PBS at 0.5µg/ml for 1 min. In another experiment, propidium iodide was used for counterstaining the nucleus red especially in a situation where the fluorescence signal of DAPI seems to overlap with that of the Alexa fluor 488. The embryos were rinsed 3 times with PBS for 5 min each and visualized with epi-fluorescence (Nikon eclipse 400) or laser scanning confocal microscope (Leica DMIRE2) and multi-photon laser confocal scanning (Nikon; Eclipse Ni-EFN Upright/ A1R Si MP Confocal).

2.2.9 Statistical analysis

Each data set, for RT-qPCR and western blotting studies was normalised prior to statistical testing. Gene expression (qPCR) data were normalised to 18S rRNA as reference or housekeeping genes. Protein abundance data were normalised to both the amount of protein loaded and to the density of corresponding house keeping β-actin bands. For pERK protein assay, protein abundance was normalised with total ERK bands. All data for qPCR (ΔCt) were analysed statistically using a non-paired Student's t-test, 1-way or 2-way ANOVA with Dunnet's post-hoc test as the case may be. In all cases significance indicated at $p \leq 0.05$. Grubbs' test was used for outliers among data sets in certain cases. Other statistical tests are as indicated in the methods section of each chapter or in the legends of Figures and Tables.

CHAPTER THREE

ROLE OF ZNT1 IN EMBRYONIC DEVELOPMENT

3 Role of Znt1 in embryonic development

3.1 Introduction

In most organisms including plants and animals, two families of transmembrane proteins play critical roles in transporting zinc, the Cation Diffusion Facilitator (CDF/ZnT/SLC30) family (Palmiter and Huang 2004) and the Zinc/Iron regulated transport (Zrt-, Irt) - like protein (ZIP/SLC39) family (Eng *et al.* 1998; Guerinot 2000; Eide 2004). Members of the CDF family occurs at all phylogenetic levels from bacteria to archea and eukaryotes (Montanini *et al.*, 2007). The crystal structure of the bacterial CDF (Yiip) protein, which is also a zinc transporter, suggests that it functions as homodimer (Lu and Fu 2007, Fu, 2010) and this is consistent with the results of cell biology studies in yeast (Ellis *et al.* 2005). In mammals and other vertebrates, all characterized CDF proteins transport Zn^{2+}, hence the term ZnT for zinc transporter (Palmiter and Findley, 1995). Most vertebrates contain 10 predicted ZnT proteins (Liuzzi and Cousins 2004; Palmiter; Huang 2004; Seve *et al.* 2004; Kambe *et al.*, 2006 and Lichten & Cousins, 2009). Znt3, however, is absent in zebrafish (Ensembl release; Zv9). ZnT1 was the first mammalian zinc transporter to be discovered and it is expressed throughout the body but notable in basolateral membranes of epithelia involved in zinc acquisition or recycling like intestine, kidney and placenta (Liuzzi and Cousins, 2004; Lichten and Cousins, 2009). It is the only known zinc transporter protein among mammalian ZnTs that localises to the plasma membrane and functions to transport excess cytoplasmic zinc out of the cells (Palmiter and Findley, 1995). *ZnT1* was originally discovered as a gene coding for a transcript that conferred zinc resistance to an otherwise zinc-sensitive cell line (Palmiter and Findley, 1995). The authors further demonstrated that zinc resistance was the result of a zinc efflux activity of ZnT1.

A better understanding of how multiple zinc transporter proteins function coordinately in an animal will require a genetically tractable model system that can be used to dissect the complementary, redundant, and antagonistic activities of multiple ZnT and ZIP proteins. The zebrafish (*Danio rerio*) has become an important vertebrate model system well suited for studies in genetics, embryology, development, and cell biology because of the unique characteristics it possesses (Westerfield, 1993). In addition, there is strong conservation between zebrafish and humans for most genes, which makes zebrafish an exellent model organism for studying complex biological processes (Chen and Fishman, 1996 ; Granato and Nusslein-Volhard, 1996). In this model, tissue-specific expression of *znt1* in embryos at various developmental stages has previously been described (Thiese *et al.,* 2004) (Table 3.0).

Stages of embryo development	**Region of *znt1* gene expression**
50% epiboly to tail bud (5-10hpf)	YSL
1-4 somites to 10-13 somites	YSL, adaxia cells and Kupffer's vesicle
14-19 somites (16hpf)	CNS and YSL
20-25 somites to Prim 5 (19-24hpf)	CNS and YSL
Prim 15 to Prim 25 (30-36hpf)	CNS and YSL
High pec to Long pec (42-48hpf)	CNS and YSL

Table 3.0. Tissue specific mRNA expression of *znt1* (*slc30a1*) gene in developing zebrafish embryo by ISH as described by Thiese *et al.,* 2004.

The function of ZnT1 or its orthologues has also been previously demonstrated in many other model systems. For example, the expression in a cell culture system of a mutated mammal (rat) protein that lacks either the whole of C-termini end or the 1st to 3rd transmembrane domains (TMD) was shown to produce a zinc-sensitive toxic

phenotype, whereas a partial deletion of 72 amino acids from the C-termini end still conferred resistance to zinc toxicity same way as the wild-type cells containing full-length ZnT1 protein (Palmiter and Findley, 1995). Homozygous deletion or knockout of the whole *ZnT1* gene in mice was shown to be embryonic lethal whereas in *Caenorhabditis elegans* as well as in *Drosophila*, a loss-of-function mutation of their respective ZnT1 orthologs also result in animal with impair growth and development (Andrews *et al.*, 2004; Bruinsma *et al.*, 2002; Wang *et al.*, 2009). In addition, over expression of the gene in *Xenopus* oocyte expression system was also shown to accelerate oocyte meiotic maturation (Jirakulaporn and Muslin, 2004). In all of the invertebrate model systems, ZnT1 was demonstrated to positively regulate Ras-ERK signalling pathway by binding through its C-terminus end to Raf-1 kinase to activate it. It was further revealed that loss-of-function mutations of ZnT1 and/or an increase in the concentration of cytosolic zinc was a suppressor of Ras-ERK signalling, which has been implicated in impaired growth and development of the embryo as well as in myocardial injury (Jirakulaporn and Muslin, 2004, Lazarczyk *et al.*, 2008, Bruinsma *et al.*, 2002; Beharier *et al.*, 2012). However, there is a conundrum in this regard whereby several other studies have reported increased cytosolic zinc as an inhibitor of protein tyrosine phosphatase (PTP) activity (Haase and Maret, 2003; Hansson, 1996) resulting in the activation of mitogen-activated protein kinases (MAPKs) such as extracellular-signal-regulated kinases 1 and 2 (ERK1/2), c-Jun N-terminal kinase (JNK) and p38 as well as the tyrosine kinases Src and epidermal growth factor receptor (EGFR), which are inactivated by phosphatases through a dephosphorylation processes (Sato *et al.*, 1995; Wu *et al.*, 1999). Similarly, Ho *et al.*, (2008) also showed the effect of elevated intracellular zinc (as a result of depleted glutathione-induced oxidative stress) on activation of phosphorylated ERK1/2 through selective inhibition of ERK1/2

phosphatase in a mouse neuroblastoma cell line or rat cortical neuronal cells triggering a robust positive feedback loop operating through activated ERK1/2 that rapidly sets into motion a zinc-dependent pathway of cell death. This opposing effect of zinc in ERK signalling as shown by different studies is unclear but might be explained partly by whether different pathways are used by zinc in ERK activation, especially when the function of a zinc regulatory protein such as ZnT1 is altered. It is possible that a physiological increase in intracellular zinc concentration leads to over-expression of the endogenous ZnT1 facilitating its binding to Raf-1 kinase (and/or through the action of zinc on phosphatase inhibition) leading to enhanced activation of ERK through its phosphorylation. Consisited with this suggestion, it was shown that only the C-termini part of ZnT1 is involved in Raf-1 activation and subsequent ERK signalling, and over expression of this region alone could not regulate intracellular zinc and cannot protect cell against zinc toxicity (Beharier *et al.*, 2012). However, the rapid effect of zinc on ERK activation, reported in some studies to oocur in minutes, is inconsistent with such a mechanism.

Because ZnT1 is an activator of Raf-1, a low expression level of ZnT1 at basal level may be important for maintaining an inactive state of the Ras-Raf mediated pathway necessary for growth and development (Beharier *et al.*, 2012). Similarly, the possible cross-talk between ZnT1 and the Ras-ERK pathway might also be indicated in experiments with zebrafish embryos (Krens *et al.*, 2008) or mouse embryos (Saba-El-Leil *et al.*, 2003) where knockdown of extracellular-regulated kinase 2 gene (*erk2*) resulted in developmental defects similar to that reported for *Znt1* disruption in other animal models (Lazarczyk *et al.*, 2008, Bruinsma *et al.*, 2002; Andrew *et al.*, 2004). This observation further supports the idea of functional interaction between ZnT1 and MAPK pathway activation necessary for diverse cellular process including cell growth,

proliferation, differentiation, survival and vertebrate development (Ballif and Blenis, 2001). Recently, ZnT1 protein has also been shown to be involved in cross-talk with both L and T-type calcium channels regulating calcium homeostasis (Levy *et al.*, 2009, Beharier *et al.*, 2012, Mor *et al.*, 2012). Moreover, an interaction between ZnT1 and 14.3.3 membrane protein was also demonstrated (Jirakulaporn and Muslin, 2004). 14.3.3 protein is involved in subcellular sorting and localization of classes of client membrane proteins (Andrew *et al.*, 2011). Interestingly, ZnT1 is also a membrane protein and might require interaction with 14.3.3 protein for its correct sorting and membrane localization.

Although previous studies in our laboratory have characterized the molecular functions of Znt1 and other zinc transporters in wild-type zebrafish, this is the first *in-vivo* experiment (to the best of our knowledge) trying to demonstrate the possible biological effect(s) in zebrafish with a disrupted or mutated *znt1* gene. *Znt1* gene disruption was generated in live zebrafish by the Sanger Centre using chemical mutagenesis, which resulted in a truncation due to deletion of the last forty amino acids from the C-terminus of the protein sequence (see section 2.2.1.1). Although previous *in-vitro* studies using rat ZnT1 with a deletion of the last seventy two (72) amino acids from the C-terminus did not show defect in zinc extrusion in cultured cells (Palmiter and Findley, 1995), other recent studies have demonstrated the interaction of this part of the cytosolic C-terminal domain of ZnT1 with many other intracellular proteins, which thus influence cell signalling pathways, in particular those that affect growth and development (Beharier *et al.*, 2012, Jirakulaporn and Muslin, 2004).

3.2 Study objective

The objective of this chapter is to explore if zebrafish embryos with a *znt1* gene disruption either permanent (by chemical mutagenesis i.e.TILLING) or temporary (by MO knockdown) have characteristic phenotypic features different from their wild-type counterparts during the course of development.

3.3 Materials & methods

3.3.1 Bioinformatics analysis of the Znt1 mutation

Preliminary bioinformatics analysis of the region of Znt1 mutation to identify the putative functional motifs involved searching using the Eukaryotic Linear Motif (ELM) (http://www.elm.eu.org/cgimodel.py). We also performed sequence alignment of zebrafish Znt1 with that of other higher vertebrates using ClustalW (http://www.ebi.ac.uk/clustalw) and available literature (Palmiter and Findley, 1995) to determine the motifs that are highly conserved. Structural homology modelling of the fish Znt1 was also achieved by alignment with the human ZnT1 sequence and comparison with the bacterial Yiip (3h90) zinc transporter, which is a reference structure in the protein database (PDB) as published by Lu and Fu (2007).

3.3.2 Genotyping and isolation of adult heterozygote mutant fish

Zebrafish (Sanger strain sa0014) were raised in a static tank system until mature adult (~ 4 months) and twenty fish were genotyped with the Sanger's DNA sequencing method as described in section 2.2.4.1.

3.3.2.1 Developmental study of embryos obtained from heterozygote adults

NB: Unless otherwise stated, wild-type, heterozygote and homozygote fish of the sa0014 strain are denoted as $Znt1^{+/+}$, $Znt1^{\Delta 40/+}$ and $Znt1^{\Delta 40/\Delta 40}$ respectively.

Adult male and female heterozygote mutants ($Znt1^{\Delta 40/+}$), isolated as in section 3.3.2, were periodically bred in pairs and the eggs were collected in a Petri-dish containing clean embryo water or standard fish tank water (see composition in Appendix 9.1) as described in section 2.2.2. The fertilized embryos were carefully sorted and incubated at 28.5^{o}C for either morphological developmental study pre- & post- hatching or for development until adulthood for further study or use as brood stock. From a batch or clutch of spawn, all embryos that died during the gastrulation stage and some of the surviving larva, which were randomly selected, were genotyped by Sanger's method in order to isolate and ascertain the viability of homozygote embryo-larva.

3.3.2.2 Water-borne zinc exposure and depletion of embryos (mixed genotypes)

Batches of fertilized embryos were collected from either pair-wise breeding (in a small breeding tank) or colony breeding (inside the marble box) of heterozygote males and females. Embryos were divided into three groups containing about 90 embryos per group and each group incubated for 5dpf in standard embryo water (as control group) or embryo water supplemented with 100µM of $ZnSO_4$ or supplemented with 5µM TPEN (both as treatment groups). The development of embryos in each treatment and control group were monitored from pre to post hatching with the aid of inverted microscope (Nikon®) for any sign of abnormality. Embryo-larvae that displayed morphological abnormality to either of the treatments were genotyped by LNA method to ascertain their genotypes.

3.3.3 Genotyping and isolation of adult homozygote mutant fish

Several embryos that were collected from adult heterozygous breeding for further study were reared in a static tank system until they developed to mature adulthood. Fish were then genotyped following the LNA genotyping method and fish of the same genotype were pooled and reared together. Similarly, the total number of embryos that survived passed the critical stage of development (i.e. 1 month and beyond) were recorded and the frequency of representation of each genotype was determined and the survival ratio was compared to Mendelian frequency of inheritance.

3.3.3.1 Developmental study of embryos obtained from homozygote adults

Adult mature male and female homozygotes ($Znt1^{\Delta 40/\Delta 40}$) were periodically bred in pairs and the eggs were collected in a Petri-dish containing clean embryo or fish water as described. The fertilized embryos were carefully sorted out, incubated at 28.5^{o}C and compared with wild-type embryos ($Znt1^{+/+}$) of the same age until hatching.

3.3.3.2 Water-borne zinc exposure and depletion of homozygote embryos

Pooled fertilized embryos from colony breeding of female and male homozygotes were collected and divided into three groups containing about 100 embryos per group with each group treated as in section 3.3.2.2. Embryonic development was observed at 33hpf before hatching. Similar experiments were also set up for wild-type embryos to provide controls.

3.3.4 Spawning behaviour of adults of different genotypes

Adult fish of each genotype were bred in pairs and the time of spawning was noted. The experiment was performed 3 times, each comprising 2 sets of pairs (male and female) for each genotype.

3.3.5 Znt1 morphant fish embryo production and study of development

Translational blocking morpholino oligonucleotides (MO) against zebrafish *znt1* (*slc30a1*) were injected into 1-4 cell stage wild-type embryos at 2-4ng per embryo (see section 2.2.1.2). Embryos were incubated at 28.5^{o}C and monitored through developmental stages until hatching. A scramble or mismatch MO was injected in a similar way as control. Because of the off-target effect of some MOs (Robu *et al.*, 2007), a splice blocking MO to *znt1* was also injected and the stage of embryogenesis was compared with that of translation blocker MO injected embryos. Also, because of the fact that most of the off-target effect of MOs is due to *p53* gene activation (by some MO sequences) causing non-specific neuronal cell death (Ekker and Larson, 2001; Pickart *et al.,* 2005), a *p53* translation blocking MO was co-injected with each of the 2 types of the *znt1* MOs in some experiments in the ratio of 1.0:1.5 respectively and the result of the embryonic development was compared to that resulting from injecting *znt1* morpholinos alone.

3.3.5.1 Water-borne zinc exposure and depletion of morphant embryos

Injected Znt1 morphant embryos (Znt1^{MO}) were collected and divided into three groups (comprising of about 50 embryos per group in 3 independent experiments) with each treated as in section 3.3.2.2 above, and embryonic development was observed at 33hpf

before hatching. Similar experiments were also set up for wild-type embryos as controls. Comparisons were made with mutant embryos ($Znt1^{\Delta 40/\Delta 40}$), generated as in section 3.3.3.2 above.

3.3.6 Gene expression study of Znt1 mutant and morphant embryos

3.3.6.1 *In situ* Hybridization method (ISH)

DIG-labelled antisense RNA probe for the *znt1* gene was prepared as described in sections 2.2.7.1.1 to 2.2.7.1.1.8.8, and ISH was performed on 24hpf Znt1 homozygote, Znt1 morphant and wild-type embryos as described in section 2.2.7.1.2.

3.3.6.2 Quantitative RT-PCR (qPCR)

Total RNA was isolated from 24hpf embryos of mutants, morphants and wild-types respectively using TRIzol® (Invitrogen™) according to the manufacturer's protocol. Following first strand cDNA synthesis using the High Capacity Reverse Transcription kit (Applied Biosystems™), gene expression levels were analysed by RT-qPCR using an ABI Prism 7700HT Sequence Detection System as described in 2.2.7.2. The probe and primer sets were designed by Roche universal probe library software (www.universalprobelibrary.com) and the sequences are shown in Table 3.1 below. Quantitative measurement of gene expression was derived using the $2^{(-\Delta\Delta Ct)}$ *method*, also known as the *Livak method* (Livak & Schmittgen, 2001; Schmittgen & Livak, 2008) or using the REST software package (Pfaffl *et al.,* 2002). Data were expressed as ratios to the control and normalised to the reference or housekeeping gene, 18s rRNA.

Gene	qPCR primer/probe sequences (5'-3')	Tm	Probe#	Amplicon size (bp)
znt1 (*slc30a1*)	F: gttaatgcggagcggaag R: atatggagcactgccattaatct Probe: cagcccgg	59 59	64	78

Table 3.1: *Znt1* gene with qPCR primer sequences, UPL probe number and product lengths

3.3.7 Metal analysis

3.3.7.1 Total zinc concentration in Znt1 mutant, morphant and wild-type embryos

Embryos at 24hpf (dechorionated & chorionated) from *znt1* homozygote, heterozygote, wild-type and morphant respectively were acid digested, prepared for ICP-MS and measured, as described in 2.2.5.1. Data are expressed as means $\pm$ SEM of 10 observations per group. Statistical analysis was carried out using GraphPad Prism 5 (San Diego, CA, USA). A one-way ANOVA followed by Dunnet's post hoc test was used to compare means of zinc concentration between the groups while Student's unpaired t-test was used for other metal elements between control wild-type and homozygote mutant in dechorionated embryos. Significance was indicated when $p \leq 0.05$.

3.3.7.2 Free Zn^{2+} imaging in Znt1 mutant, morphant and wild-type embryos

A synthetic ratio-metric zinc-specific probe (ZTRS) for in-vivo zinc imaging in zebrafish (see section 2.2.5.2.1) was a kind gift from Dr. Zhaochao Xu of University of Cambridge (Xu *et al.*, 2009). The affinity of the probe to zinc ions was first determined by incubating 10µM probe in deionized water and in deionised water containing 100µM $ZnSO_4$, 10µM TPEN and zinc-TPEN combination respectively. Similarly, wild-type

embryos were incubated for 1 h at the blastula stage in either standard fish tank water or fish tank water containing 100µM $ZnSO_4$ or fish tank water containing 10µM TPEN. Embryos were then rinsed in deionized water and further incubated for 10 min in 10µM of the ZTRS probe and the fluorescence intensity was assessed by both fluorospectrometric and fluorescence microscopic methods as described in section 2.2.5.2. Thereafter, 24hpf embryos of *znt1* homozygotes, morphants and wild-types were incubated as above and the fluorescence intensity was assessed fluorospectrometrically (in chorionated embryos) and by fluorescence microscope (in chorionated and dechorionated embryos). Dechorionated embryos were also co-stained with rhodamine dye along with ZTRS for fluoro-microscopic (co-localization) analysis. Data are expressed as means $\pm$ SEM of 6 observations per group. Statistical analysis was carried out using GraphPad Prism 5 (San Diego, CA, USA), a Student's unpaired t-test or a one-way ANOVA followed by Dunnet's post hoc test as the case may be was used to compare means; significance was indicated when $p \leq 0.05$.

3.3.8 Extracellular-regulated kinase (ERK) signalling in Znt1 homozygote mutant, Znt1 morphant and wild-type embryos

Embryos at early to mid gastrulation stages (5-8hpf) were used for phospho-ERK immuno-staining technique. A primary antibody to phospho-ERK1/2 (rabbit polyclonal; Santacruz®) was used at 1:100 dilutions and a secondary antibody (goat anti-rabbit conjugated to Alexa Fluor 488; Abcam®) was used at 1:200 dilutions as described in section 2.2.8.3. Expression of p-Erk1/2 proteins in stained embryos were observed under epi-fluorescence microscope. In a related experiment, about 10µg of protein was extracted from 24 hpf embryos of wild-types and homozygotes respectively and analysed for phospho-ERK by Western blotting as described in sections 2.2.8 to 2.2.8.2,

using rabbit polyclonal p-ERK1/2 as the primary antibody (at 1:2,000) and goat anti-rabbit conjugated to horse radish peroxidase as the secondary antibodies (at 1:5,000). Antibodies to total ERK 1/2 were used as normaliser or reference protein (at 1:1000) along with the secondary antibody (at 1:2,000). Films (blots) were processed and developed by automatic processor (Konica Minolta SRX-101A) and the bands were quantified by image J.

3.4 Results

3.4.1 Bioinformtic analysis

The multiple sequence alignment for mouse, rat, human, zebrafish and fugu ZnT1 protein showing the six trans-membrane domains and the C-terminal end is shown in Figure 3.1. There are evolutionarily conserved residues between human/mouse ZnT1 and zebrafish Znt1 including in the C-termini, which is truncated in the zebrafish Znt1 mutant. Most of these conserved residues or motifs in zebrafish are also conserved in fugu Znt1, which has previously been functionally verified (Balesaria and Hogstrand, 2006). This suggests that truncation of the C-terminus in zebrafish Znt1 might affect the function of the protein.

The result of ELM search (Appendix 9.20) for functional motifs identified a PDZ motif, which is a short sequence at the carboxyl terminus of the target protein that is recognised as a consensus motif for binding of proteins with a PDZ domain. The motif 'ESSL' is conserved in most organisms, including human, as shown in the ClustalW alignment (Fig. 3.1). There was also a binding site for 14-3-3 protein, 2 putative casein kinase (CK) sites and a putative mitogen activated protein kinase (MAPK) site as well as a GSK3β phosphorylation site in the truncated portion of the zebrafish gene as depicted in Figure 3.1.1 and 3.1.2. Thus, although it has been suggested that the mouse

ZnT1 can export zinc without part of its C-terminal end in cultured cells, the presence of phosphorylation sites and other protein-protein interaction motifs suggest that this region might be involved in regulation of the Znt1 protein or in Znt1 regulating other proteins in zebrafish *in vivo*.

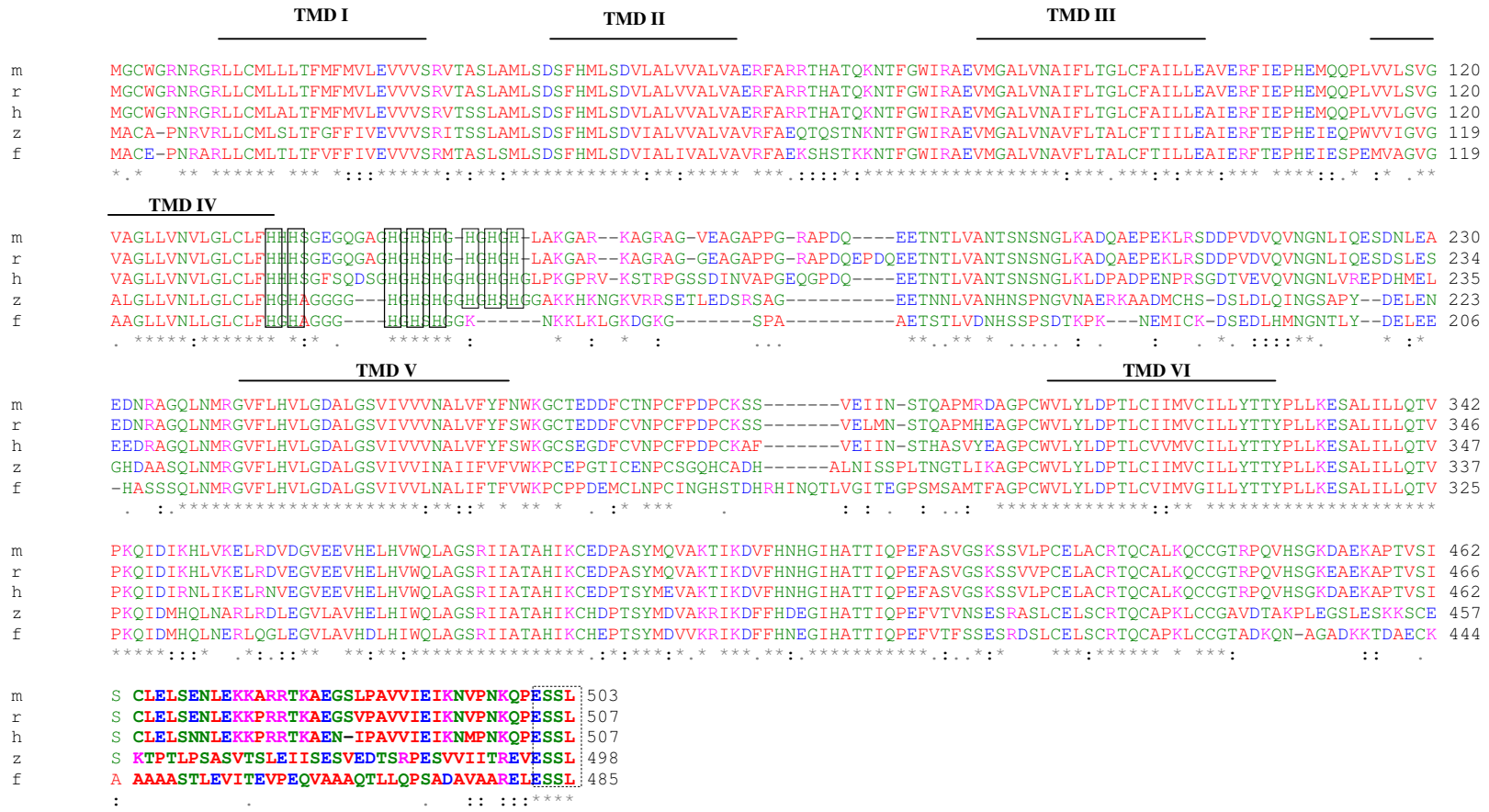

Figure 3.1: ClustalW multiple sequence alignment of ZnT1 for mouse (m), rat (r), human (h), zebrafish (z) and fugu (f), showing the six presumptive membrane-spanning domains (I-VI). Fully conserved residues shown by identical amino acids with same colour are indicated by (*) while conservative changes with either similar or different colours are indicated by (:) or (.) for strong or weak conservation groups respectively. The **boldface** sequences are the missing (truncated) amino acids at the C-terminus of the mutated Znt1 protein in zebrafish. Conserved histidine residues between TMD IV and V are highlighted by the solid rectanglar box while the conserved motifs in the truncated C-termini region are highlighted with dotted rectangular box. Keys: m-mouse, r-rat, h-human, z-zebrafish, f-fugu

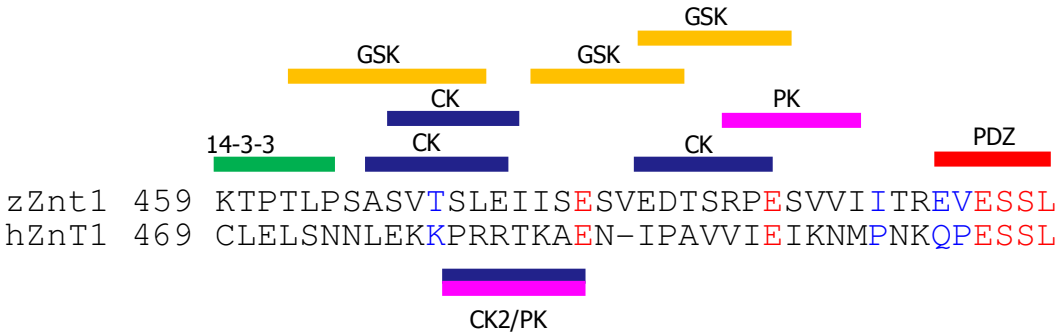

Fig 3.1.1: Sequence alignment and predicted functional motifs of part of the carboxyl termini of zebrafish Znt1 and human ZnT1 showing the potential phosphorylation sites or signal peptides. The zebrafish Znt1 was predicted to contain some signal peptides that are not all evolutionarily conserved at that portion of the C-terminus in human (except the PDZ & CK2/PK) but are found further upstream in the human sequence, suggesting that the kinases might be important in fish as predicted and verified in human, especially the 14-3-3 binding site which was found to bind 14-3-3 in the human ZnT1. Note the evolutionarily conserved residues between zebrafish and human highlighted in 'red' colour letters and the conservative changes in 'blue' colour.

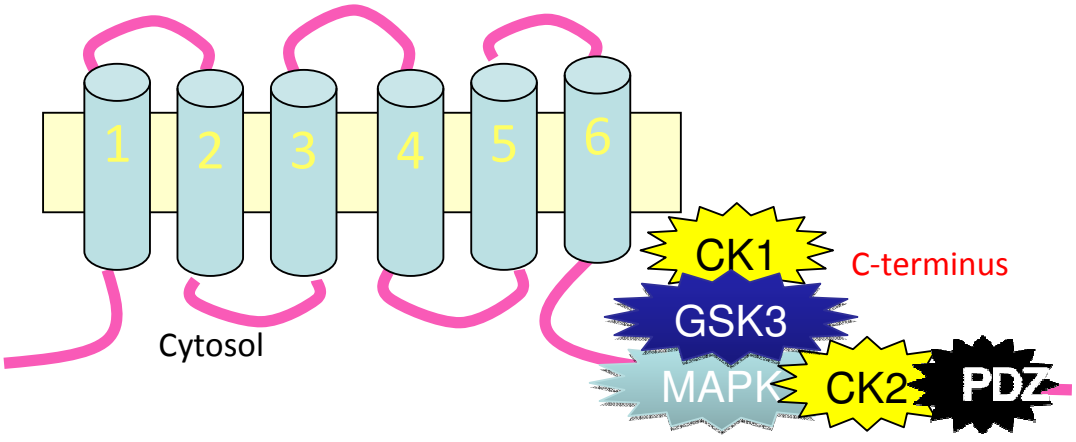

Fig 3.1.2: Diagram depicting the potential phosphorylation sites at the C-terminal end of zebrafish Znt1 protein that is predicted to be affected in the truncated Znt1 protein of the mutant fish. The barrels with numbers represent the six transmembrane domains.

3.4.2 Isolation of heterozygous mutant

The initial method of fish husbandry using the static tank system gave about 10% of total fish (n=200) surviving to mature adults comprising of fourteen (14) wild-types and six (6) heterozygotes, composed of 4 females and 2 males. Gel electrophoresis of the PCR products used for genotyping and the chromatogram of different genotype are shown in Figure 3.2 below. The optimal primer annealing temperature for amplification of the genomic DNA template is shown in Figure 3.2A, although all the eight selected gradient temperatures (i.e. 55.0, 55.3, 56.0, 56.8, 58.1, 59.6, 61.6 and 63.5°C) were appropriate for primer annealing. The product size for PCR1 was 726pb and that of PCR2 was 585bp, which was used for sequence analysis (genotyping) (Fig. 3.2B).

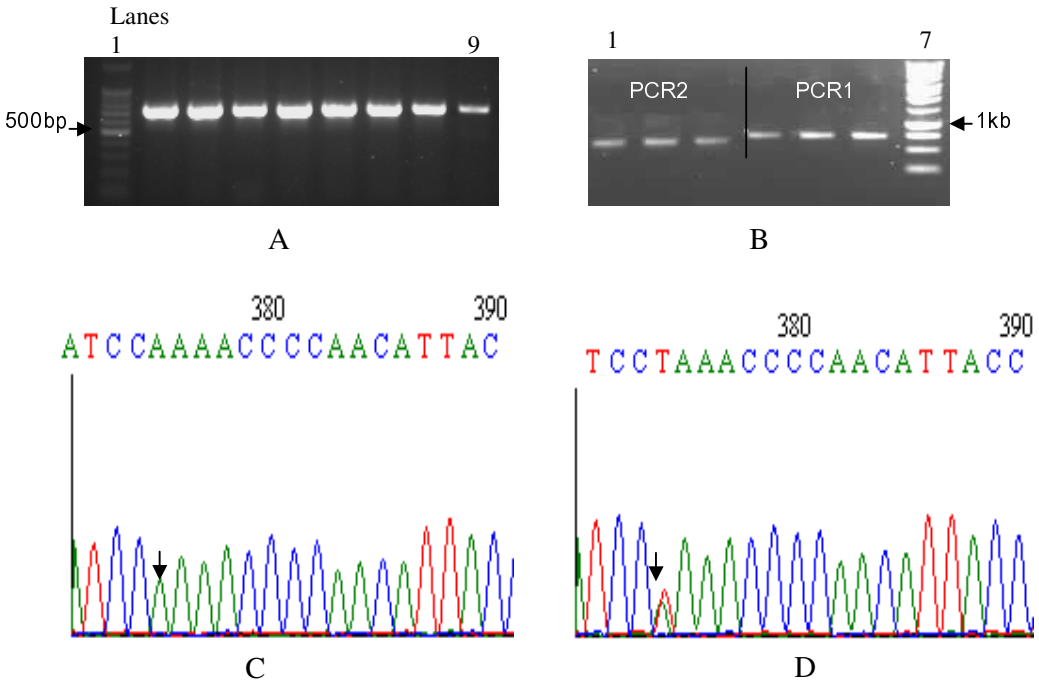

Figure 3.2: (A) Products generated using primer gradient annealing temperatures between 55°C & 63.5°C (lanes 2 to 9) for nested PCR. (B) Amplification and product size of PCR1 (726pb) and PCR2 (585bp), which was sequenced and analysed to determine the respective genotype. Lane 1 in A and lane 7 in B represent 100 bp and 1kb ladders respectively. (C & D) ABI chromatogram tracing of wild-type and heterozygote fish respectively. The arrow head show region of point mutation with one peak of nucleotide A and double peak of nucleotides A/T in wild-type and heterozygote fish respectively.

3.4.2.1 Effect of the *znt1* mutation on the development of embryos obtained from heterozygote adults

There was no obvious gross abnormality in embryonic development of the eggs collected from all the pair-wise breeding of heterozygote males and females above except some embryonic deaths after the gastrulation stage (~13%), which included the homozygote, heterozygote and wild-type. All 3 genotypes were also represented among the normal embryos (Table 3.1 and Fig. 3.3.1). This suggested that the Znt1 homozygote from heterozygote parents is embryonically viable and that mortality of some embryos after the gastrulation stage was not related to the mutation.

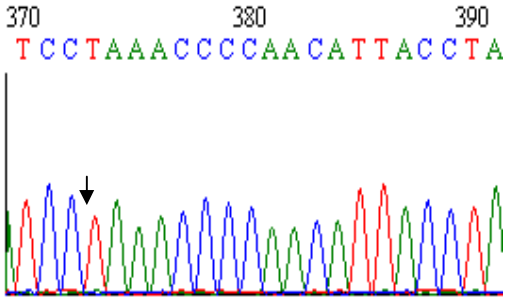

Figure 3.3.: ABI chromatogram tracing of homozygote mutant with arrow head showing region of point mutation with a single peak where nucleotide A in wild-type is mutated to T as a result of chemical mutagenesis.

Total number of eggs collected	No of dead eggs past gastrulation stage	No of surviving larvae 7dpf	Total no of dead eggs genotyped (10)			Total number of surviving larvae genotyped after 7dpf (10)		
			+/+	Δ40/+	Δ40/Δ40	+/+	Δ40/+	Δ40/Δ40
80	10	70	8	1	1	3	5	2

Table 3.2: Viability of embryos and larvae of the different genotypes

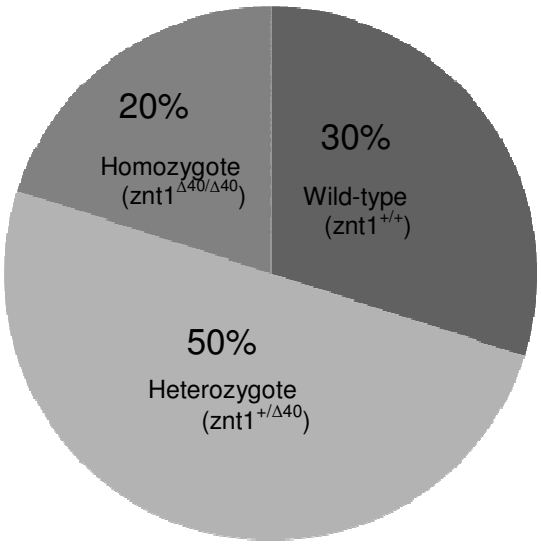

Fig 3.3.1.Pie chart representation of the viability of embryos and larvae of different genotypes at 7dpf (n=10).

3.4.2.2 Effect of water-borne zinc supplementation and depletion on embryos obtained from heterozygote adults

There was no obvious gross difference in embryonic development between the three genotypes when treated with 50µM $ZnSO_4$ (N=100). However, some of the larvae that were treated with the zinc chelator TPEN (5µM) showed abnormal spine formation (curved notochord) 1-3 days post hatching (N=90). Genotyping showed that all of the 26 (29%) larvae having spine deformities as a result of TPEN treatment carried the *znt1* mutation i.e. 21 (23%) heterozygote and 5 (6%) homozygote, suggesting a partial penetrance of abnormality (Fig. 3.4). In addition, accelerated and delayed hatching were observed in TPEN and $ZnSO_4$ treatment groups respectively irrespective of the genotype. This preliminary observation led us to full experimentation on the effect of TPEN and $ZnSO_4$ on hatching of zebrafish embryos as presented in a later chapter (chapter 5).

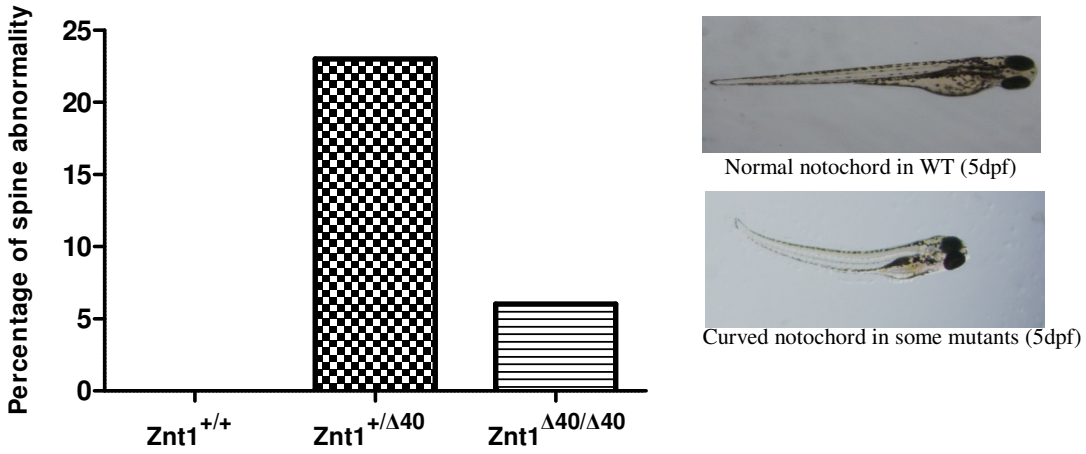

Fig 3.4: Effect of loss of the last 40 amino acids in Znt1 on spine deformities. An observational study showing the percentage of hatched embryos (collected from colony breeding of heterozygote parents in a single spawn) having abnormal or curved spine at 2dph following 5µM TPEN exposure from 10hpf until 5dpf (n=90). $Znt1^{+/+}$, $Znt1^{\Delta 40/+}$ and $Znt1^{\Delta 40/\Delta 40}$ denote wild-type, heterozygote and homozygote embryos respectively.

3.4.3 Effect of *znt1* mutation on isolation of adult homozygotes

Out of the total 215 juvenile-adult fish that were genotyped, it was observed that homozygotes also survived the critical developmental stage past 14dpf for at least 4 weeks. However, both homozygote and heterozygote Znt1 mutants were under-represented according to Mendelian ratio; more pronounced in the homozygote than the heterozygote mutant. The observed ratio was 1.0 : 1.7 : 0.4 for wild-type, heterozygote & homozygote respectively as against the expected ratio of 1.0 : 2.0 : 1.0 indicating a survival ratio of 100% : 85% : 40% for wild-type, heterozygote & homozygote respectively (Fig. 3.5). Although this result is from a preliminary observational (unplanned) study rather a controlled (planned) experiment, it was considered useful to indicate to how many fish are needed to be raised to juvenile-adult from pooled embryos of colony breeding of heterozygotes, in order to isolate certain numbers of each genotype at juvenile-adult stage for a particular or specific experiment.

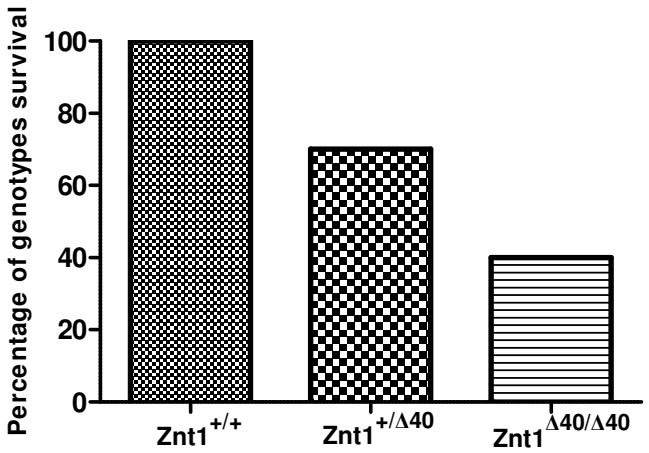

Fig 3.5: Percentage of different genotypes surviving past the critical growth stage (2wks post hatching) to juvenile/adult stage (n=215). NB: This is a preliminary observational result rather than result from planned (controlled) experiment because embryos were collected at random from many colony breedings of heterozygotes and were reared to adults and genotyped.

3.4.4 Effect of mutation on the time of spawning in adult fish

The effect of the *znt1* mutation on spawning in adult fish showed that the homozygote mutant displayed some erratic spawning behaviour whereby they sometimes layed eggs much later than the wild-type or heterozygote after exposure to light was begun (which stimulates the spawning process). While all the groups of wild-type and heterozygote fish spawned between 30 to 60 min after light was switched on, some homozygotes spawned between 3-4 hours after light was switched on. This meant that 100% (i.e. 4/4) of wild-type or heterozygote and 25% (i.e.1/4) of homozygotes spawned between 30-60min whereas 0% (0/4) of wild-type or heterozygote and 75% (3/4) of homozygote spawned between 3-4 hrs after light was switched on (Fig. 3.6). It was hypothesized that this effect might be related to disturbances in MAPK signalling in mutant fish, which can affect the master circadian gene regulation in adult. This hypothesis would be investigated and the result presented in subsequent sections; 3.4.10, 4.4.4 and 4.4.5.

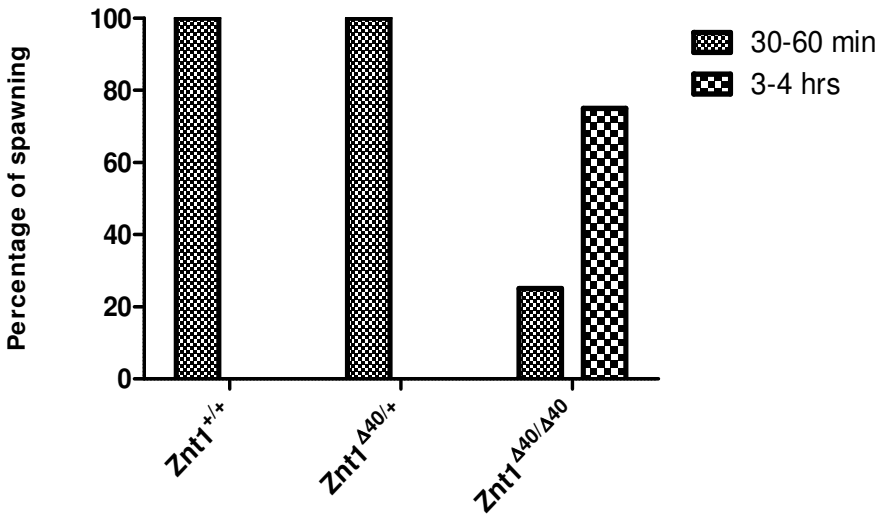

Fig 3.6: A preliminary study showing the percentage and time of spawning per pair of fish genotype after light was switched on (n=4 pairs of breeding fish per genotype)

Some other phenotypic characteristic features commonly observed in adult mutants but rarely observed or observed with less frequency in wild-type fish included split pigmentation (2% of WT, 17% of heterozygote and 26% of homozygote), kinked tail/arched spine affecting swimming or locomotory behaviour and general unfitness (0% of WT, 10% of heterozygote and 12% of homozygote), delay of puberty with early ceasation of fertility and overall shorter life span with increased mortality in aged or spent fish (Appendix 9.19; Figure 9.5).

3.4.5 Effect of the *znt1* mutation on the development of embryos obtained from homozygote adults

Although homozygote embryos were viable, they showed slight morphological differences in the stage of the development. In a preliminary experiment, 80% of homozygote embryos were seen to have delayed pigmentation and enlarged or unabsorbed yolk when compared to their wild-type counterparts at 33hpf, indicating delayed development or slower embryogenesis (Fig. 3.7). Quantification of yolk size was subsequently conducted along with morphant embryos in follow-up experiments (see Section 3.4.6; Fig. 3.9.2).

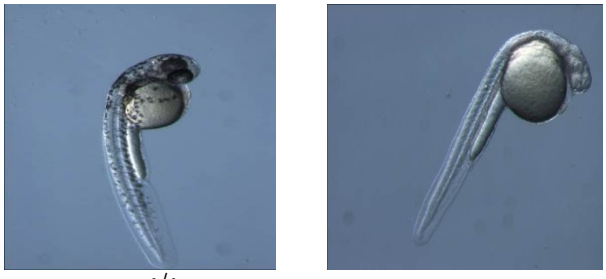

Fig 3.7: Morphological differences in the stages of development (i.e. delayed development) in homozygote mutant ($znt1^{\Delta 40/\Delta 40}$) compared to wild-type ($znt1^{+/+}$) as observed in 80% of mutant embryos of a single spawn. Mutant embryos show delayed pigmentation and enlarged or unabsorbed yolk at 33hpf. Embryos were collected from colony breeding and 100 embryos of each genotype were monitored.

3.4.5.1 Effect of water-borne zinc exposure or depletion on homozygote embryos

While TPEN was observed to accelerate the development of homozygote embryos to the same stage as that of the wild-type embyos, zinc supplementation was seen to further retard the development. Wild-type embryos showed no change in response to either treatment (Fig. 3.8 & 3.8.1).

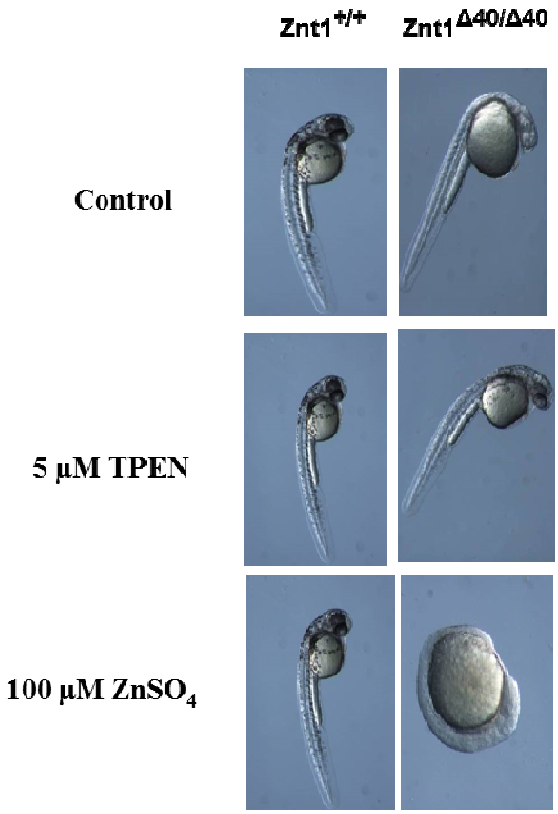

Fig 3.8: Preliminary experiment showing the effect of Zn exposure/depletion on the embryonic development of homozygote and wild-type zebrafish at 33hpf. Supplementation of zinc to the inclubation water retards embryonic development while addition of TPEN accelerates development in the homozygote mutant as shown by differences in the stages of development when compared with wild-type embryos receiving the same treatments. Embryos were collected from a single colony breeding and 100 embryos of each genotype were monitored.

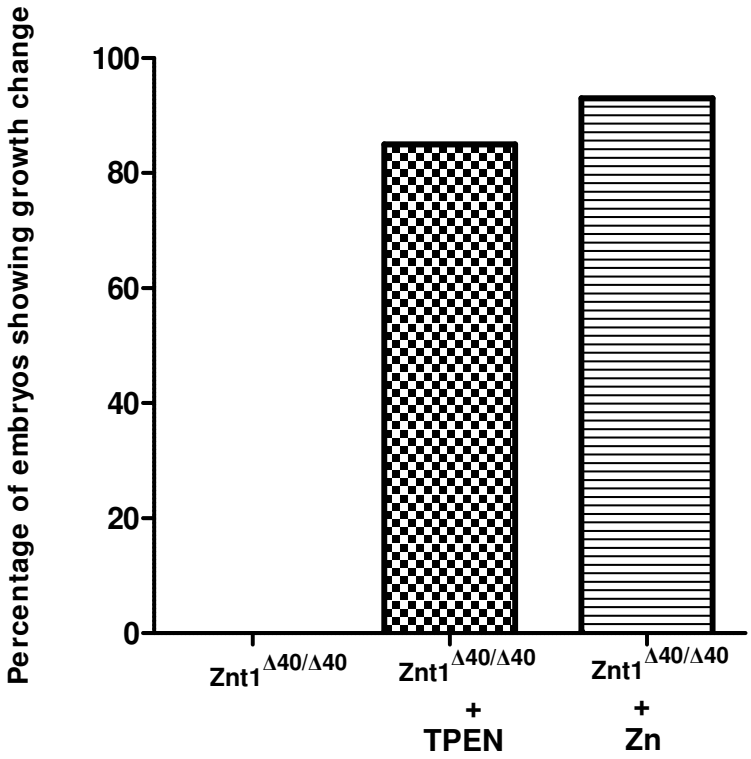

Fig 3.8.1: Percentage of homozygote embryos with development hastened by 5µM TPEN or delayed by 100µM zinc added to the incubation medium. Embryos were collected from a single colony breeding and 100 embryos of each genotype were monitored.

3.4.6 Effects of the *znt1* MO gene knock down on embryonic development

Znt1 gene knock down by MO at 2-4ng per embryos resulted in a slower embryonic development than that observed in homozygote mutant embryos and with more severe delay in development especially at 24hpf in addition to reduced pigmentation and enlarged or unabsorbed yolk at 48 and 51hpf, respectively (Fig. 3.9). There was a significant increase in the size of the yolk in the morphants and mutants compared to wild-type (3.9.2). The effect seen with the translation blocking MO (Fig. 3.9) was similar to that seen with the splice blocking (exon-skipping) MO and also with the p53 co-injected MO (Fig. 9.1) demonstrating that the effect of the MO was specific and not an off-target effect. The control mismatched (scramble) MO resulted in normal

development indistinct from the un-injected control. The effect of MO was observed to be dose-dependent and a high dose of 20ng caused death of all embryos at the early cleavage stages.

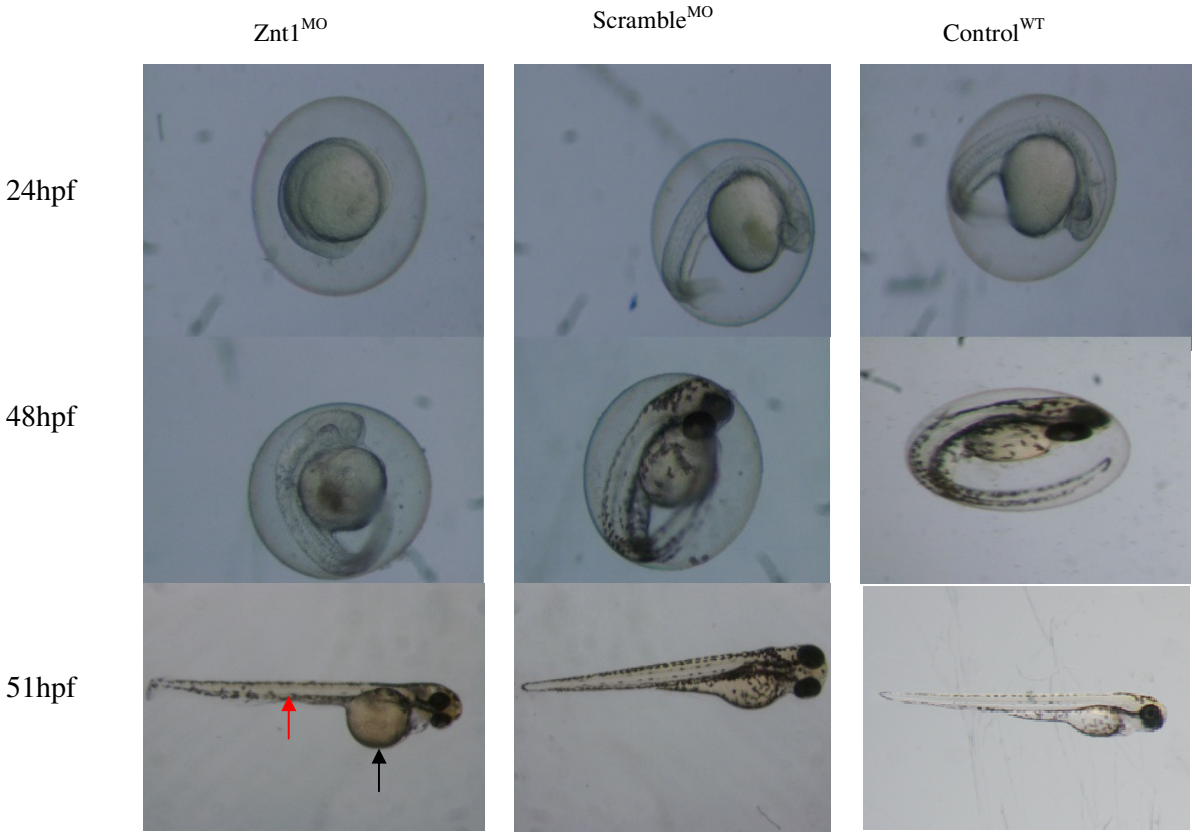

Fig 3.9: Morphological differences in the stages of development (as evidenced by delayed development, reduced pigmentation and enlarged yolk) in znt1 morphant ($Znt1^{MO}$) injected with translational blocking MO compared to embryo injected with scrambled (control) MO ($Scramble^{MO}$) and un-injected wild-type control ($Control^{WT}$). The morphants showed enlarged or unabsorbed yolk (black arrow) and slender muscle mass (red arrow) compared to control (n=100 with 3 experiment per group). There were behavioural disturbances (circling) in some morphants.

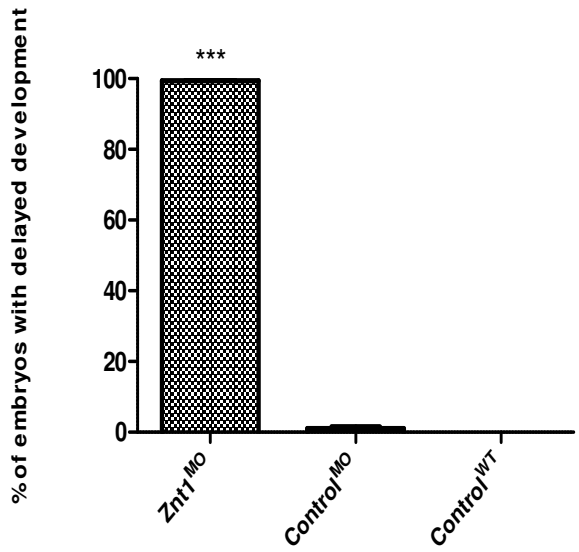

Fig 3.9.1: Percentage of embryos showing growth retardation or delayed developmental stage as evidenced by enlarged yolk size and reduced pigmentation in embryos injected at 2-4 cell stage with 2-4ng/embryo of znt1 MO (n=100 embryos with 3 experiments per group). Data are presented as the mean ± SEM (n =100) where $p \leq 0.05$ is considered significant following 1-way ANOVA. **Key:** (***); p<0.001. $Znt1^{MO}$, $Control^{MO}$ and $Control^{WT}$ denote znt1 morphant, control embryos injected with scrambled (mis-match) MO and control un-injected wild-type embryos respectively.

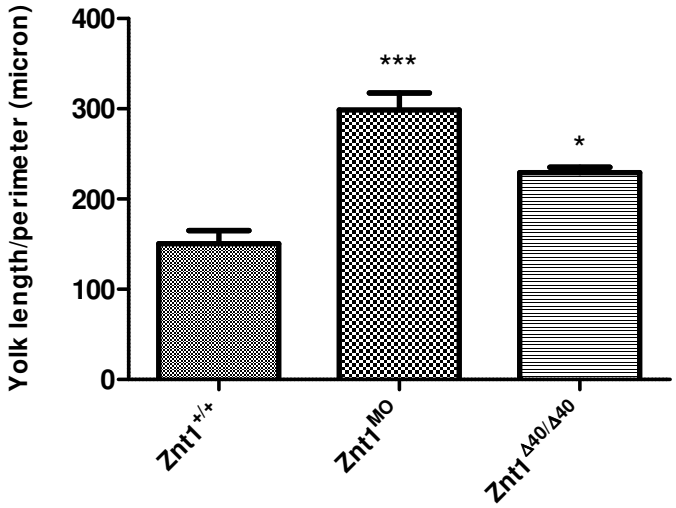

Fig 3.9.2: Effect of Znt1 deficiencies on yolk resorption at 3dpf. Embryos were monitored until 3dpf following treatment and the phtographs taken (Fig 3.9). The size of the yolk was then estimated in morphant, mutant and wild-type embryos using image J. Data are presented as the mean ± SEM (n =5) where $p \leq 0.05$ is considered significant following 1-way ANOVA. **Key:** (*); p<0.05, (***); p<0.001. $Znt1^{+/+}$, $Znt1^{MO}$ and $Znt1^{\Delta 40/\Delta 40}$ denote wild-type, znt1 morphant and znt1 homozygote mutant embryos respectively.

3.4.6.1 Effect of water-borne zinc exposure or depletion on Znt1 morphants ($Znt1^{MO}$)

Depletion of zinc by TPEN in the Znt1 morphant ($Znt1^{MO}$) accelerated development while zinc supplementation retarded the development. This same effect was observed with $Znt1^{\Delta 40/\Delta 40}$ mutants in section 3.4.5.1 above but in morphants zinc supplementation to the incubation medium caused more severe growth retardation and increased incidence of death.

3.4.7 Effect on *znt1* gene expression of morphant and homozygote mutant

The results of gel electrophoresis for generating the DIG-labelled antisense RNA (*znt1*) probe used in section 3.3.6.1. are shown in Appendix 9.15 (Fig. 9.1-9.1.2).

Znt1 mRNA levels were slightly reduced or near normal in both Znt1 homozygote mutant and Znt1 morphant embryos except in the hatching gland where it was completely abolished as shown by whole mount ISH (Fig. 3.10). Intriguingly qPCR showed slightly increased or no change in expression in homozygote mutants and a massive up-regulation in morphants (Fig. 3.10.1).

Fig 3.10: ISH expression showing reduced to near normal expression of znt1 mRNA in 24hpf znt1 homozygote mutant and morphant embryos compared to wild-type notably around the CNS & yolk syncytial layers (white and red arrows) and also in the hatching gland (black arrow) where it was completely absent in mutant and morphant.
Keys: $Znt1^{+/+}$, $Znt1^{\Delta 40/\Delta 40}$ and $Znt1^{MO}$ denote wild-type, znt1 homozygote and znt1 morphant embryos respectively.

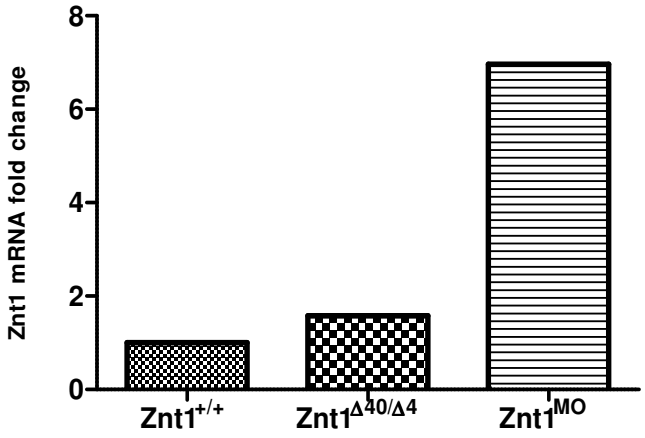

Fig 3.10.1: qPCR expression showing the znt1 mRNA fold change expression in mutant and morphant compared to wild-type. n=3 per group. Fold change expression was calculated by the Livak method (efficiency of the gene was 105%).

3.4.8 Effect of Znt1 deficiencies on total and free Zn^{2+} accumulation

There was no statistically significant difference in total zinc level in Znt1 homozygote mutant embryos, Znt1 morphant embryos and both the Znt1 heterozygote embryos (derived from crossing of homozygote male with wild-type female and vice versa) compared to the wild-type embryos at 24hpf of development. Only copper and selenium contents were significantly higher in homozygote mutants compared with wild-type embryos. However, the level of free Zn^{2+}, as measured by the ZTRS fluorescent probe, was higher in the homozygote mutant and morphant than in the wild-type embryos. Thus, disruption of Znt1 by mutation or knockdown resulted in a redistribution of zinc within the embryos.

3.4.8.1 Total zinc and other metal concentrations

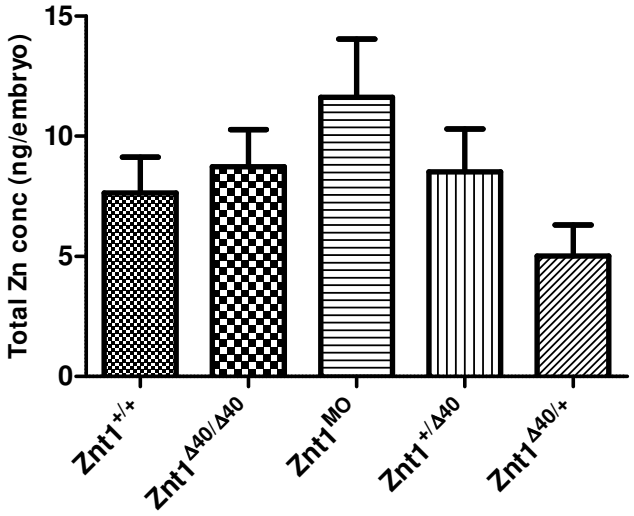

Fig 3.11.0: Effects of znt1 deficiencies on total zinc content per embryo. Total zinc concentration per embryo was measured by ICP-MS in wild-type, znt1 homozygote, znt1 morphant and znt1 heterozygotes. Data are presented as the mean ± SEM (n =10). $p \geq 0.05$ following 1-way ANOVA for multiple comparison of groups with each other where wild-type embryo is the control. Legends: $Znt1^{+/+}$; wild-type, $Znt1^{\Delta 40/\Delta 40}$; homozygote, $Znt1^{MO}$; morphant, $znt1^{+/\Delta 40}$; heterozygote (from wild-type male crossed with mutant female) and $Znt1^{\Delta 40/+}$; heterozygote (from mutant male crossed with wild-type female).

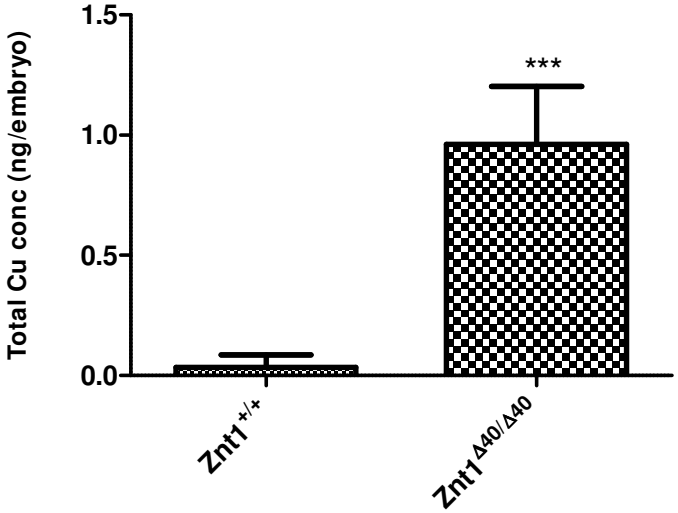

Fig 3.11.1: Effects of znt1 deficiencies on total copper content per embryo. Total copper concentration per embryo was measured by ICP-MS. Data are presented as the mean ± SEM (n =10). $p \leq 0.05$ following student's t test. Legends: (***); $p \leq 0.001$

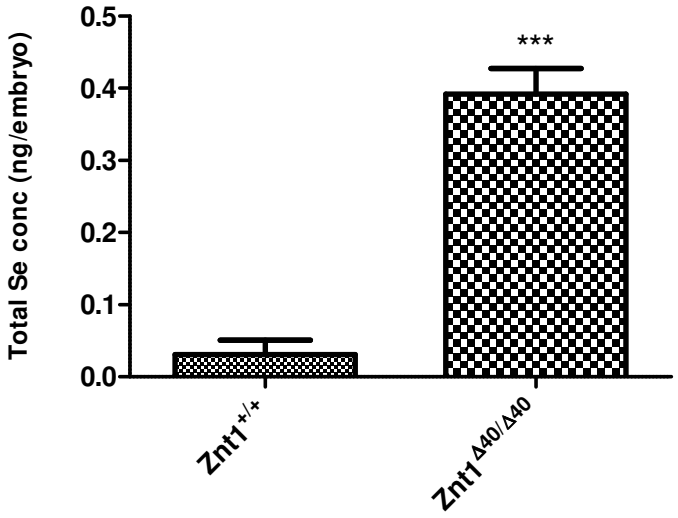

Fig 3.11.2: Effects of znt1 deficiencies on total selenium content per embryo. Total selenium concentration per embryo was measured by ICP-MS. Data are presented as the mean ± SEM (n =10). $p \leq 0.05$ following student's t test. Legends: (***); $p \leq 0.001$

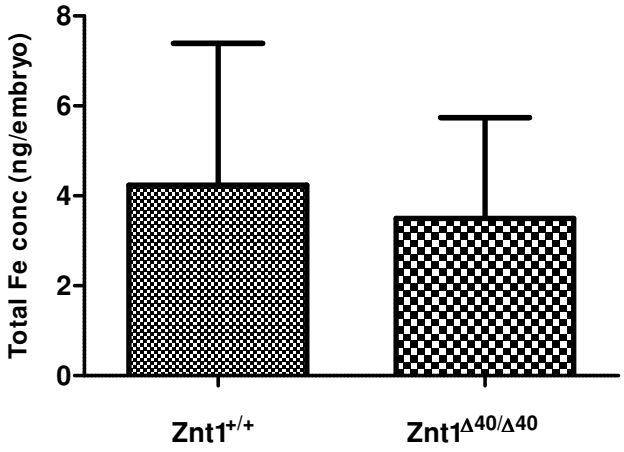

Fig 3.11.3: Effects of znt1 deficiencies on total iron content per embryo. Total iron concentration per embryo was measured by ICP-MS. Data are presented as the mean ± SEM (n =10). $p \geq 0.05$ following student's t test.

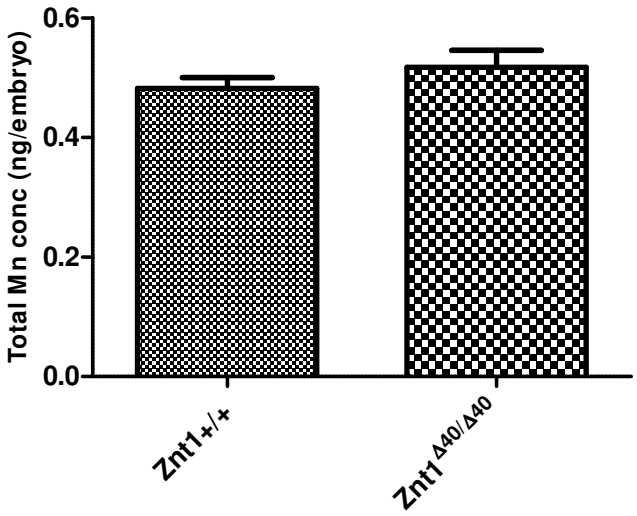

Fig 3.11.4: Effects of znt1 deficiencies on total manganese content per embryo. Total manganese concentration per embryo was measured by ICP-MS. Data are presented as the mean ± SEM (n =10). $p \geq 0.05$ following student's t test.

3.4.8.2 Free zinc (Zn^{2+}) ions

3.4.8.2.1 Fluorospectrophotometry

The ZTRS probe showed about 9-fold increased fluorescence intensity in 100µM zinc supplemented deionized water compared to non-supplemented water confirming the sensitivity of the probe to free Zn^{2+} ions (Fig. 3.12). There was higher free Zn^{2+} fluorescence intensity in homozygotes than wild-type with about a 6-fold increase in the non-zinc exposed condition (Fig. 3.12.1A). Interestingly, the morphant also showed about a 7-fold increase in intensity compared with wild-type (Fig. 3.12.1B). There was also a significant increase in homozygotes compared with wild-types in zinc exposed or depleted conditions (Fig. 3.12.2A, B & C).

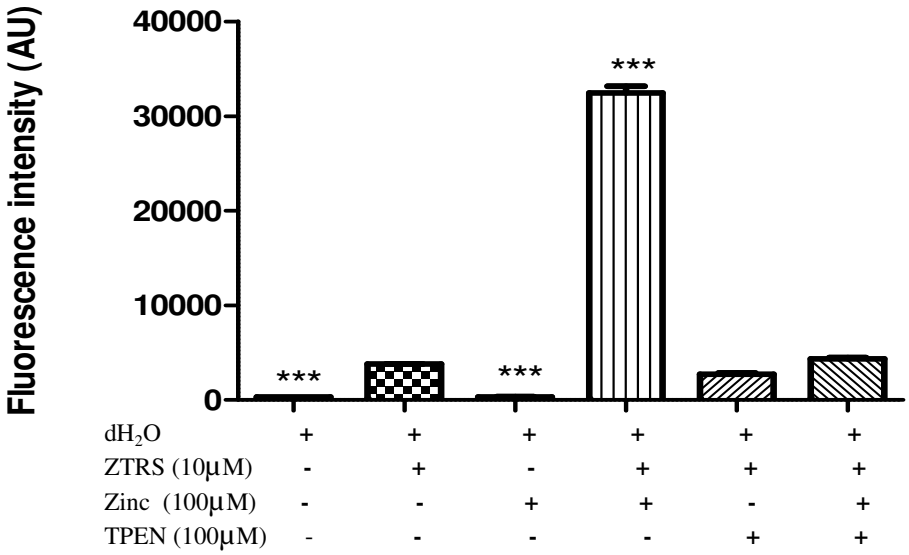

Fig 3.12: ZTRS zinc probe sensitivity and specificity to zinc supplementation. Zn^{2+} fluorescence signals in 100µl of medium containing 10µM of ZTRS zinc fluorophore in either dH_20, TPEN solution (100µM), Zn solution (100µM) or Zn+TPEN solution (100+100 µM each). Fluorescence intensity (arbitrary units) for each treatment was compared to background signal of dH_20 with ZTRS. No signal was observed in dH_20 alone or Zn solution alone (i.e. without the ZTRS probe). Data are presented as the mean ± SEM (n =5) at $p \leq 0.05$ following 1-way ANOVA for multiple comparison of group means with each other. Legends: (***); $p \leq 0.001$. (N= 3 separate experiments).

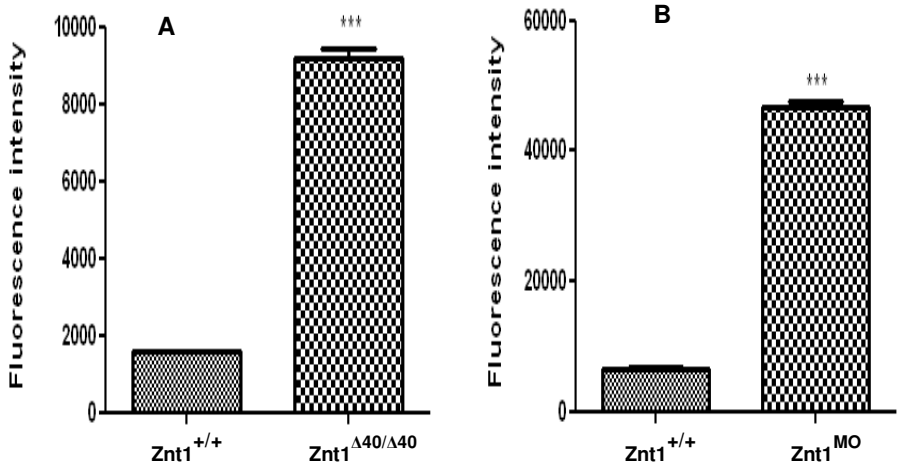

Fig 3.12.1: ZTRS fluorescence signals in (A) 24hpf WT & znt1 homozygote and (B) 24hpf WT & znt1 morphant embryos. Data are presented as the mean ± SEM (n =5) at $p \leq 0.05$ following Student's t-test. Legends: (***); $p \leq 0.001$

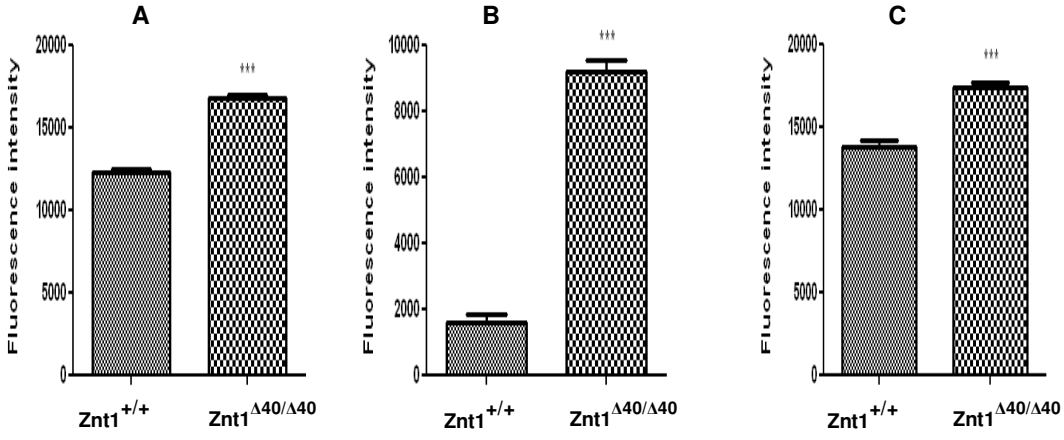

Fig 3.12.2: ZTRS fluorescence signals in 24hpf WT & znt1 homozygote embryos incubated overnight in (A) Zn (100 uM), (B) TPEN (10 uM), (C) Zn+TPEN (100 +10uM). All groups were rinsed thoroughly and fluorescence measured after incubation for 10 min in 100ul of 100 uM 'ZTRS' fluorophore. Data are presented as the mean ± SEM (n =5) at $p \leq 0.05$ following Student's t-test.
Legends: (***); $p \leq 0.001$

3.4.8.2.2 Fluorescence microscopy (fluorometry)

Chorionated (un-hatched) embryo

At 4hpf (blastula stage), zinc exposed wild-type embryos showed increased fluorescence in the chorion thereby obliterating or blocking the fluorescence signal in the developing embryo, whereas control embryos and zinc depleted embryos showed fluorescence in the developing embryo but not the chorion (Fig. 3.13). This suggests that zinc supplementation caused increased zinc accumulation in the chorion and/or the perivitalline fluid, which over saturated the fluorophore thereby making it unavailable for imaging the developing embryo.

At 24hpf, Znt1 homozygote mutants and Znt1 morphants showed increased fluorescence intensity representing free Zn^{2+} ions in the chorion and/or perivitalline fluid compared with wild-type thereby causing diminished fluorescence attributable to free Zn^{2+} ions in the HGC of mutants and morphants (3.13.1A). Exposure of embryos to

100µM zinc further increased the fluorescence intensity in the chorion of mutants and morphants compared with wild-types. The chorion and /or perivitelline fluid begin to show zinc accumulation resulting in reduced HGC intensity compared to un-exposed wild-type embryos (3.13.1B). Interestingly, the chorion of the homozygote mutants also showed increased fluorescence intensity compared with the wild-type counterpart after removal (3.13.1C).

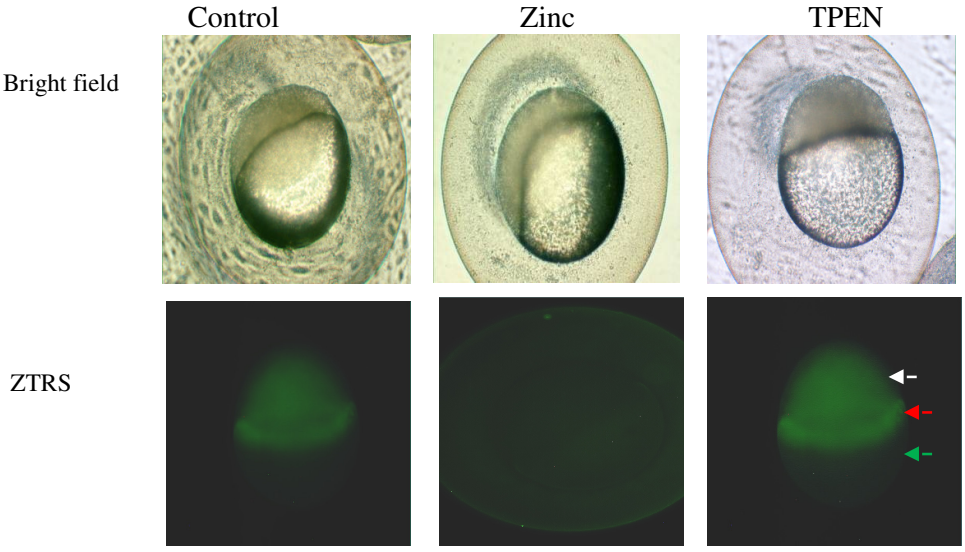

Fig 3.13: Zinc supplementation reduced or blocked signal intensity (imaging) of developing embryo inside the chorion but increased signal intensity of the chorion/perivitaline fluid. There was increased intensity of developing embryos in TPEN treated embryos compared with control. Note the higher level of Zn^{2+} ion in the migrating (gastrular) cells of the embryo (red arrow) compared to the blastoderm (white arrow) or yolk cells (green arrow), which showed the lowest Zn^{2+} ions at that stage of development . Experiment repeated 4-5 times (n=5) with consistent observation (i.e. 90-100% of embryo observed for each phenotype).

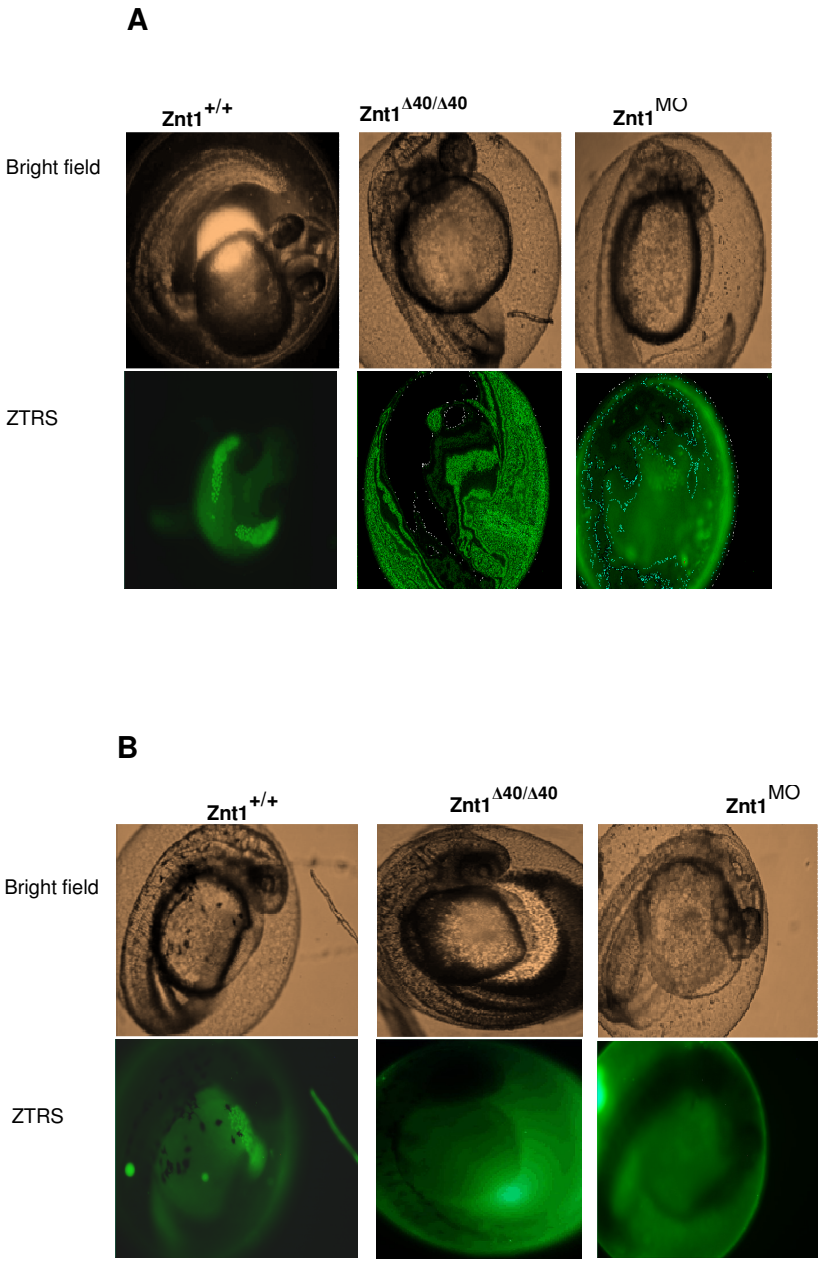
A
Znt1+/+
Znt1Δ40/Δ40
Znt1MO
Bright field
ZTRS
B
Znt1+/+
Znt1Δ40/Δ40
Znt1MO
Bright field
ZTRS

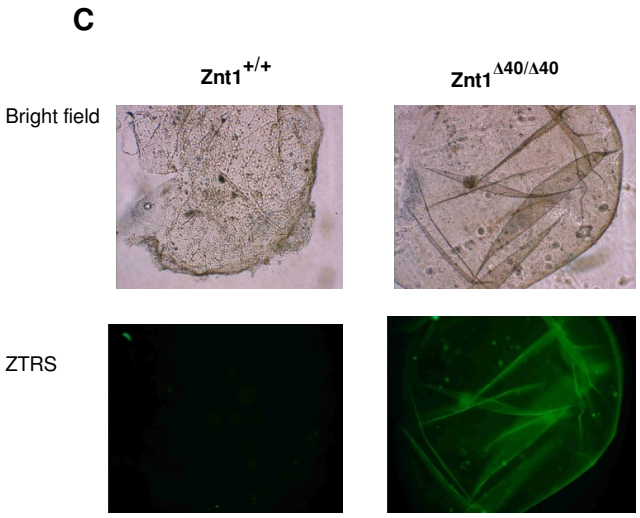

Fig 3.13.1: A-C showed the ZTRS fluorescence intensity for Zn^{2+} around the developing embryos which is more pronounced in the chorion/perivitalline fluid of homozygotes and morphants. Note the signal intensity of the chorion in homozygotes and morphants with reduced visibility of the developing embryos (24hpf) in normal and zinc excess condition compared with wild-types. Homozygotes and morphants give more signal in the chorion compared with WT. Experiment repeated 4-5 times (n=5) with consistent observation (i.e. 90-100% of embryo observed for each phenotype).

Dechorionated (hatched) embryos

Hatched or dechorionated embryos showed punctate (localized) staining with higher fluorescence intensity in the body of homozygotes compared with wild-types (Fig. 3.13.2A). Exposure of embryos to 100µM of zinc increased the intensity of the punctate staining in Znt1 deficient embryos compared with wild-type embryos (Fig. 3.13.2B). Interestingly, treatment of zinc exposed embryos with 10µM TPEN quenched the fluorescence of the punctate staining (Fig. 3.13.2C).

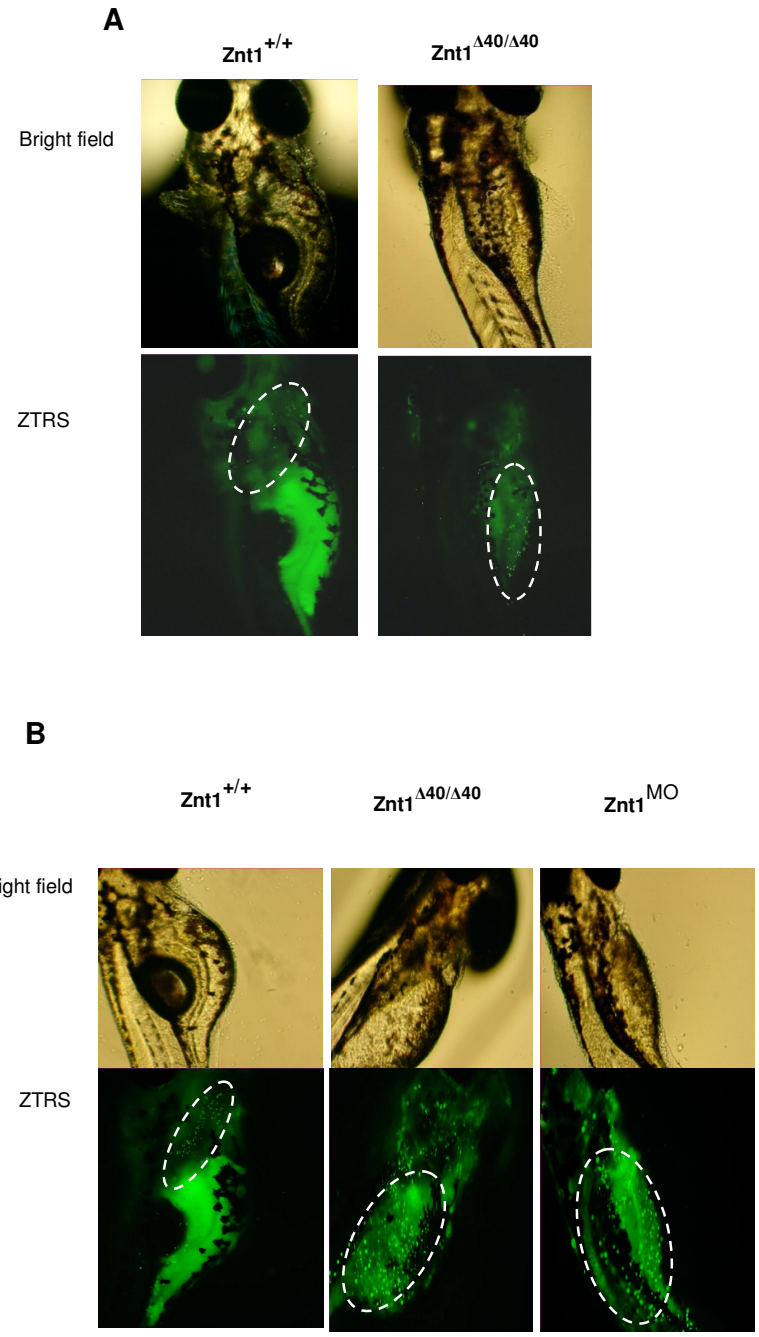
A
Znt1+/+
Znt1Δ40/Δ40
Bright field
ZTRS
B
Znt1+/+
Znt1Δ40/Δ40
Znt1MO
Bright field
ZTRS

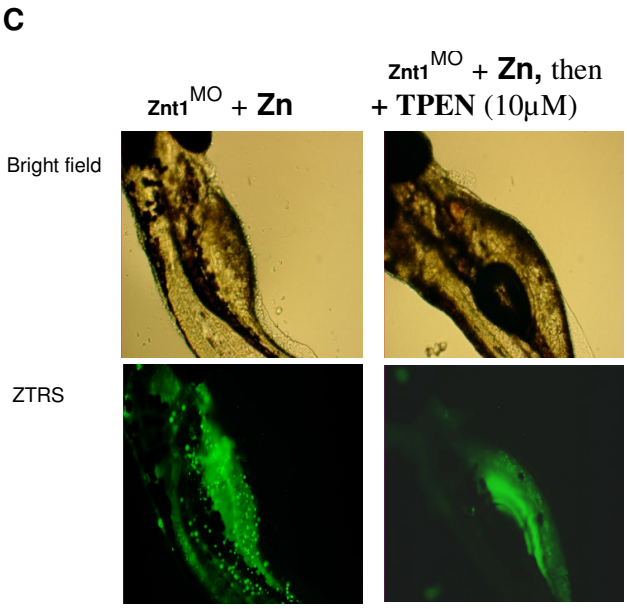

Fig 3.13.2: A-C show the intensity of free Zn^{2+} apparently trapped in the body (skin) of the hatched embryos, which is more pronounced in homozygotes and morphants compared with WT in either zinc normal (A) or zinc supplemented (B) conditions (white highlights). Note the effect of depletion of trapped zinc by TPEN in C. Experiment repeated 4-5 times (n=5) with consistent observation (i.e. 90-100% of embryo observed for each phenotype).

3.4.9 Rhodamine staining of mitochondria-rich cells

It was observed that most of the cells stained by the ZTRS zinc probe (except hatching gland cells) on the body of the fish were equally stained by rhodamine (Fig. 3.14), suggesting some of the ZTRS stained cells to be ion-transporting cells (ionocytes), which are rich in mitochondria. More of these stained cells were observed in mutant than wild-type zebrafish (with or without zinc supplementation) suggesting either more free zinc accumulation or altered distribution in mutants compared to wild-type, probably as a result of disrupted zinc extrusion from the chloride cells in the mutants. Staining was commonly observed in olfactory cells, superficial epithelial cells (especially of the skin) of living fish and dead tissues. No staining of rhodamine was observed in the hatching gland cells (even though ZTRS staining was present with high

intensity; red arrow) confirming the specificity of staining of mitochondria-rich ionocytes by rhodamine.

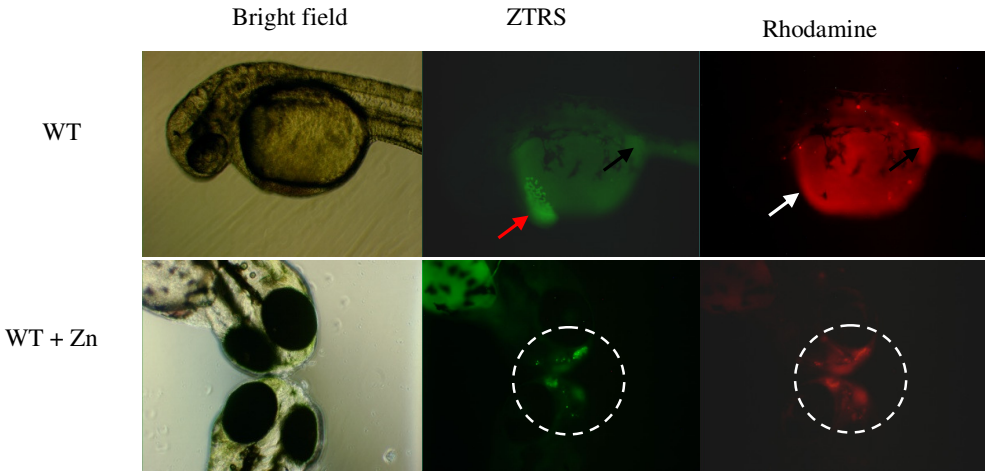

Fig 3.14: Staining of the mitochondria-rich cells with rhodomine. Wild-type (WT) embryo (with or without zinc exposure) was stained with both ZTRS and rhodamine (10µM each). Note the presence of ZTRS (red arrow) but absence of rhodamine signal (white arrow) in the HGC and limited colocalised staining of both fluorophores on the body of the fish (black arrows) (upper panel). The lower panel shows the presence of mitochondria-rich cells in the olfactory cells of the fish following zinc exposure, which were co-stained by ZTRS and rhodamine (broken white circles). Experiment repeated 4-5 times (n=5) with consistent observation (i.e. 90-100% of embryo observed for each phenotype).

3.4.10 Effect of Znt1 deficiencies on ERK 1/2 signalling

There was increased activation and signalling of phospho-ERK1/2 showing more extensive migration of pERK positive cells with epiboly movement in wild-type compared with homozygote mutants or morphants at 5hpf. There was reduced staining or activation in the leading edges of the epiboly in the mutants and morphants, indicating that pERK1/2 activity or movement was delayed or reduced in Znt1 deficient embryos (Fig. 3.15A). This defect in signalling is thought to be responsible for hindering the the epiboly migration thereby slowing down the development. Intriguinly, pERK protein was barely detected in 24hpf embryos of both genotypes indicating that

immunohistostaining is probably more sensitive than Western blotting in detecting pERK in embryos (Fig. 3.15B).

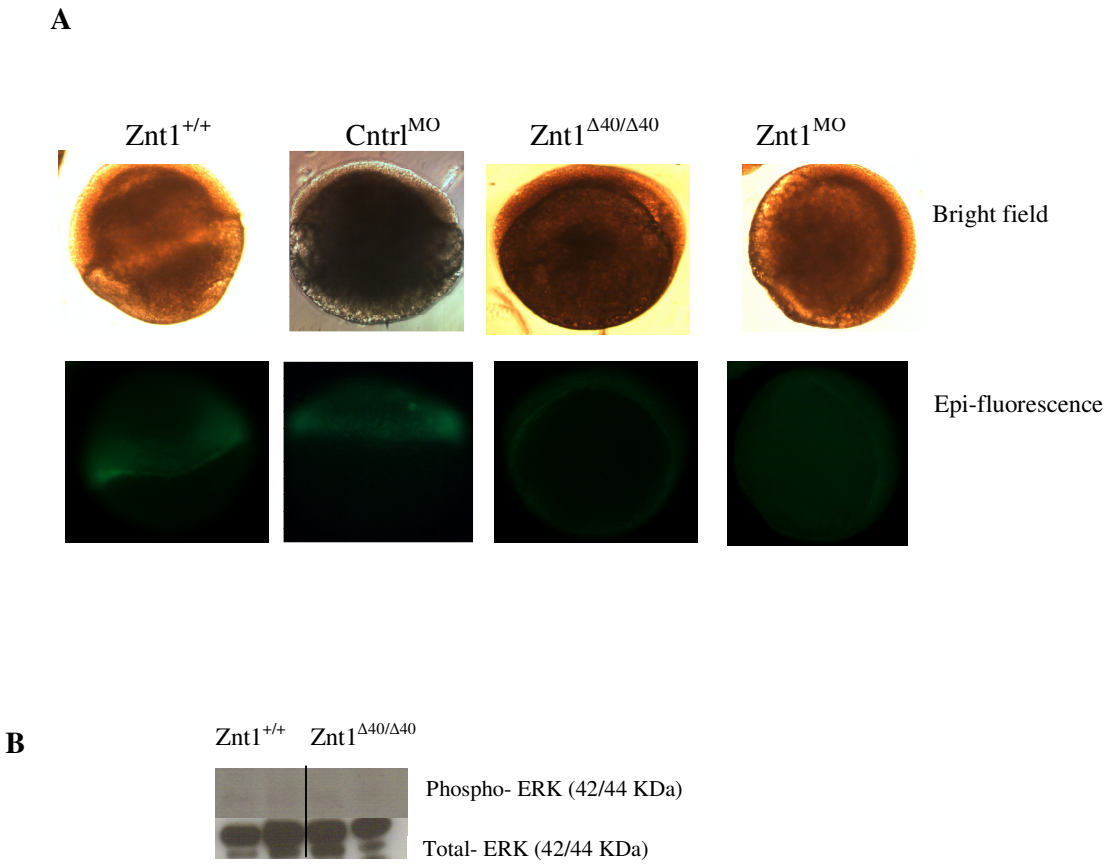

Fig 3.15: Effect of *znt1* mutation on phospho-ERK signalling in zebrafish embryos. Panel A shows increased activation and migration of phospho-ERK 1/2 positive cells in 5hpf (50% epiboly) wild-type and control MO injected embryos but decreased activation in Znt1 mutant and morphant embryos of similar developmental stage. Expression of Phospho-ERK protein was measured by Western blotting technique in 24hpf wild-type and Znt1 mutant embryos but was barely detected in embryos of both genotypes (panel B). Experiments were repeated 3 times (n=20 for each embryo type) with consistent observation (i.e. up to 90-100% of embryos showed consistent phenotype for each genotype).

3.5 Discussion

3.5.1 Bioinformatics

The results of the bioinformatics analysis suggest that there was high degree of homology between zebrafish Znt1 and mammalian ZnT1 including that from human (i.e. 96% similarity and 56% identity with human), indicating that this protein perform similar function in all the species. The truncated part of the C-terminus of this protein in zebrafish may also perform important functions in the regulation of the protein in zebrafish because this region also has some degree of homology with the human protein, and contains conserved residues (Fig. 3.1.1). It also contains the evolutionarily conserved PDZ domain and potential binding sites for 14-3-3, MAPK, CK2 and GSK3, which are predicted to interact with ZnT1 for diverse cellular processes including growth and differentiation, signal transduction, migration and invasion. Most of the predicted signal peptides (i.e. the binding sites) found in truncated region of zebrafish C-terminus have also been found upstream of this region in human, indicating that they might be functionally important in fish and in human. For example, 14-3-3 has been experimentally verified to interact with a certain region of the C-terminus of mammalian ZnT1 (Jirakulaporn and Muslin, 2004). Interestingly, the highly conserved PDZ binding domain in most of the organisms was also experimentally found to be phosphorylated in human at S506 (Zahedi *et al.*, 2008). Another zinc protein family known as the PDLIM include proteins that have the PDZ domain and LIM domain for binding where the PDZ domain is found to interact with the C-terminal domain (presumably the PDZ motifs) of the partner proteins (Jalen *et al.*, 2003). It remains to be determined if PDLIM proteins or any other PDZ domain proteins interact with this motif in Znt1.

3.5.2 Effect of *znt1* mutation on embryonic development

3.5.2.1 Embryos from heterozygote parents

The result of the growth and development of embryos derived from heterozygote parents suggested that the Znt1 homozygote embryo was viable at least up to 7dpf of observation contrary to the effect seen in mouse embryo where the ZnT1 null mutation was embryonic lethal at 9th day of gestation (Andrew *et al.*, 2004). This may be as a result of partial loss-of-function or altered function in the zebrafish mutation compared to the complete loss-of-function in the ZnT1 knockout mouse. It is also possible that the other Znt1 allele might have a positive influence, in which case the parent's genotype might be responsible for the apparent viability with normal embryogenesis of the homozygous embryo because a mother that is heterozygous for the mutation may still be capable of loading or regulating zinc in the egg environment for the initial survival of the embryo. A similar observation of no apparent phenotype in homozygous mutant embryos was previously shown in mouse embryos homozygous for Zip1 at normal dietary zinc intake by the parents but when intake was low, embryo survival was affected (Dufner-Beattie *et al.*, 2006) explaining that not in all cases of homozygous gene disruption do we have lethality but manipulating dietary zinc intake can produce an effect in the offspring. This suggests that manipulating the zinc in zebrafish homozygote embryos obtained from heterozygote parents may have adverse effect on the survival of the embryo. In line with this assertion, the zebrafish Znt1 mutant embryos (both homozygote and heterozygote) were found to show only a partially penetrant phenotypic feature of juvenile spine defect or abnormally curved notochord compared with wild-type embryos with normal (straight) spine when zinc was depleted over periods of 4-5dpf. This may be linked to the involvement of zinc or zinc signalling in cartilage and bone formation as previously described in mouse, with zinc deficiency

decreasing matrix mineralization and delaying osteogenic activity (Kwun, 2010), or skeletal and connective tissue deformities in mouse with targeted knockout of either of several zinc transporter geness such as *znt1*, *znt5*, *zip4* or *zip13* (Andrew *et al.*, 2004; Dufner-Beattie *et al.*, 2007a,b; Inoue *et al.*, 2002 and Fukada *et al.*, 2008). However, in zebrafish, bone formation starts at around 7dpf, therefore it is possible that the *znt1* mutation affects the formation of connective tissues or cartilage, which occurs at an earlier developmental stage. A similar bone defect was also described in zebrafish embryos carrying a heterozygous mutation for copper transporter *atp7a* gene (*calamity* or *catastrophe* mutant), only when copper was depleted with neocuperoine but no overt phenotype was observed when copper uptake was normal (Madsen and Gitlin, 2008).

3.5.2.2 Effect of mutation on survivability of embryos to adulthood

The overall percentage survival rate indicated that the homozygote mutants are more sensitive to stressors during the critical stage of development (14-30dpf) compared with heterozygote mutants and wild-types, which lead to homozygotes being under-represented according to Mendelian ratio at adulthood. Such factors that affect survivability of mutants more than wild-types might be linked to immune system maturation which is affected by disruption in zinc homeostasis (Overbeck *et al.,* 2008; Prasad, 2008) because adaptive immunity is not fully developed until 4 weeks of age thereby possibly making mutants more susceptible or sensitive than wild-type. Other factors that could probably affect survival rate of mutants include resistance to bacterial challenge, ability to feed properly or tolerance to variation in water quality because it has been reported that these and other factors are affected by disruption in zinc homeostasis (Prasad 2008). It is also possible that fluctuations in abiotic factors, such as temperature and water chemistry, are not well tolerated or regulated by the mutants,

thereby possibly causing precocious hatching (Czerkies *et al.*, 2001), which exposes them to the stressors earlier in life than the wild-type leading to increased mortality and/or making those that ultimately reach maturity having shorter life span than the wild-type, as observed in some of the adult homozygote mutants.

3.5.2.3 Embryos from homozygote parents

Contrary to the observation of the homozygote embryos from heterozygote parents, the embryos from homozygote parents displayed a slightly delayed development (evidenced by the difference in the stages of development such as enlarged yolk and delayed pigmentation) when compared to wild-type of similar hours of development post fertilization. This indicates that loading or regulation of zinc in embryos is affected by parent homozygosity. It was interesting to note that this effect was rescued in pre-hatch embryos by zinc depletion and intriguingly zinc supplementation worsened the condition suggesting that the homozygote contains a higher concentration of free Zn^{2+} ions than the wild-type (as confirmed by fluorophore) and that excess zinc can retard embryonic development, as was equally demonstrated here in zebrafish Znt1 morphant embryos. This developmental defect was also shown in an experiment with *C. elegans* with a loss-of-function mutation of the *cdf-1* gene (which is an homologue of zebrafish *znt1*) with or without supplemental zinc exposure (Bruinsma *et al.*, 2002) and this effect may be connected to an impaired Ras-ERK (MAPK) signalling pathway in mutant worms (Bruinsma *et al.*, 2002) or in *Xenopus* oocytes, which showed a delayed meiotic maturation when ZnT1 was disrupted or under-expressed (Jirakulaporn and Muslin, 2004). It was further demonstrated that insulin can stimulate this meiotic maturation in the presence of functional *cdf-1* by signalling through the Ras/Raf/MEK/ERK pathway and that concurrent injection of Zn^{2+} (supraphysiological concentration; 2.5 mM)

caused a dose-dependent reduction in ERK phosphorylation and enzymatic activity that correlated well with delayed oocyte maturation as indicated by an attenuated germinal vesicle breakdown (Bruinsma *et al.*, 2002).

Similarly, the mechanism behind growth retardation in zinc deficient conditions has also been linked to the fact that zinc has an insulin-mimetic effect in animals and can replace insulin in cell culture as well stimulating cellular glucose uptake by causing increased phosphorylation of the insulin receptor through inhibition of PTP1B, leading to down-stream signalling pathways and recruitment of the insulin-responsive glucose transporter 4 (GLUT4) to the plasma membrane (Prasad, 2009; Haase and Maret, 2004b; Tang and Shay, 2001 and Wong *et al.*, 2006).

3.5.3 *Znt1* mutation and *znt1* gene expression

The reduced expression of the *znt1* gene in the Znt1 mutant and the Znt1 morphant embryos especially around the yolk syncytial layer and the central nervous system as observed in the present study by ISH may point towards the role of Znt1 in these regions (Thisse *et al.*, 2004). This may explain the behavioural disturbances (circling) observed in morphant or it may be due to abnormal notochord (i.e. curved spine) and/or reduced muscle mass seen in the morphants and mutants as a result of the defective gene causing reduced expression of the protein normally required to regulate zinc in those tissues and also around the YSL, which may be required for zinc uptake from the yolk to the developing embryo. This may possibly result in a mutant or morphant embryo with reduced ability to absorb zinc/nutrient from the yolk, resulting in enlarged (unabsorbed) yolk with increased zinc accumulation and thus lessening zinc available for fish development as previously demonstrated in a rodent model with defective zinc flux from placenta or yolk sac membrane to the growing embryo (Andrews *et al.*, 2004;

Liuzzi *et al.*, 2003). Intriguingly, qPCR data showed a slight increase in *znt1* expression in the mutant and a larger increase in morphant. This may be due to the fact that the qPCR technique, which is more sensitive, measured the expression in the whole animal compared to ISH that is localised but less sensitive in detecting expression. The increased expression may reflect a compensatory mechanism by the gene as driven by Mtf1 in response to defective Znt1 function to cope and flux out the excess intracellular zinc to protect cells from zinc toxicity (Fig. 3.16). In fish, disturbances in zinc homeostasis cause anorexia, poor growth, bone deformation, reduced survival and cataracts (Eid and Ghonim, 1994; Gatlin and Wilson, 1983), hence lending credence to some of the effects observed in our present study.

3.5.4 Total and free Zn^{2+} levels in mutant and morphant embryos

The level of total zinc per embryo as observed in the present study was similar to previous work by Ho *et al.,* (2010). Although the *znt1* mutation in the current study did not show change in total zinc levels between wild-type and mutants, there was increased accumulation of copper (Cu) and selenium (Se) in the homozygote mutant as was previously reported in *C. elegans* in which loss-of-function of the *cdf-1* gene resulted in increased Cu and manganese (Mn) loads (Davis *et al.*, 2009). However, there was no difference in Mn accumulation between mutant and wild-type embryos in the present studies, perhaps because of differences among species or because the *znt1* mutation in the zebrafish was not a complete loss-of-function. Contrasting with differences in zinc concentration between homozygote and wild-type embryos measured by ICP-MS at 24hpf, the increase in free Zn^{2+} level in homozygote mutant and morphant embryos at 24hpf compared with wild-type (chorionated and undechorionated) as demonstrated by extensive studies with a fluorescent zinc sensor could be due that ICP-MS measures

total embryonic zinc (bound and unbound) unlike the fluorophore that measures only the free Zn^{2+} ions. Total zinc measurement may not give much information because the pool of 'free' available or unbound Zn^{2+} which is needed for the rapidly developing embryo and other biological processes is relatively small compared to total zinc and can only be detected by fluorescent sensor to give more accurate and reliable information (Andrews *et al.*, 2004). This increase in Zn^{2+} signal intensity detected by the zinc fluorescent sensor in homozygote and morphant embryos is similar to that reported in the *Drosophila* Znt1 mutant measured by metallothionein B-enhanced yellow fluorescence protein (MtnB-EYFP) as the indicator for free zinc measurement (Wang *et al.*, 2009) suggesting high zinc accumulation in both animal models that causes toxicity and impaired embryonic development. This suggestion is also supported by the fact that the lethality of waterborne zinc to fish is caused by the free Zn^{2+} ions, and dissolved organic matter and calcium in water are the principal factors for reducing zinc toxicity (Hogstrand *et al.*, 1995; Santore *et al.*, 2002, De Schamphelaere *et al.*, 2005 and Todd *et al.*, 2009). The high zinc signal at the margin of the epibolising embryo probably reflects the increased thickness of the tissue in this region, which may contain high Zn^{2+}. The higher signal of this region in zinc depleted chorionated embryos compared to zinc supplementation could be due to over saturation of the fluorophore by excess zinc (bound to the chorion and/or perivitalline fluid) thus preventing or reducing the concentration of the fluorophore reaching the developing embryos. Thus, the increased zinc signals in the chorion of 24hpf mutants and morphants with or without zinc supplementation compared to wild-type probably prevented the visibility of their HGC due to over saturation of the fluorescent probe by zinc leading to reduced concentration of probe reaching the HGC or it could possibly be that there was a reduction in the presence of their HGC or a reduction in the concentration of Zn^{2+} ions in these cells.

This observation was further investigated in dechorionated embryos in a later chapter (chapter 5).

The punctuate staining revealed by the zinc fluorescent sensor in the body (especially the superficial epithelium of the skin) of mutant and morphant embryos post hatching with or without waterborne zinc exposure could be attributed to the fact that there was a reduced ability of mitochondria-rich cells (ionocytes) to function in basolateral transfer of zinc ions in the mutant leading to increased free Zn^{2+} ion accumulation or trapping in these cells. Alternatively, altered distribution of free Zn^{2+} ions within the cytosol and the organelles may be accountable. Moreover, ionocytes may also proliferate during zinc overload in some fish species such as dogfish where they act as a way of compensatory response to restore altered osmo-regulatory capacity in order to cope with the metal ion stress (Crespo and Sala, 1986). This was equally observed more frequently in mutant and morphant with defective Znt1 causing increased zinc load due to reduced ability for zinc extrusion via the chloride cells. This effect was also shown in normal zebrafish with increased metal load (Lin *et al.*, 2006, Wilson and Laurent, 2002).

3.5.5 Effect of Znt1 truncation on ERK 1/2 signalling in the embryo

Although the signalling or the abundance of phospho-ERK protein was similar (but below detection levels) in both genotypes at 24hpf as assayed by Western blotting, histoimmunostaining assay showed increased or enhanced ERK activation in WT compared with mutants and morphants. This indicates that the latter assay was more sensitive than the former in detecting phosphorylated Erk protein in zebrafish embryos.The reduced or delayed activation or slow migration of the phosphorylated Erk1/2 positive cells in mutants and morphants suggests that the MAPK signalling pathway may be affected, probably because of the inappropriate binding of the C-

terminal end of truncated Znt1 with the N-terminal regulatory portion of Raf-1, which is responsible for pathway activation. It could also be due to the inability of truncated Znt1 of the mutants or its lack in morphants to regulate intracellular Zn^{2+} ions, which is also a suppressor of the pathway, leading to delayed development of the embryo as also observed in *C. elegans* development or *Xenopus* oocyte meiotic maturation (Jirakulaporn and Muslin, 2004, Lazarczyk *et al.*, 2008, Bruinsma *et al.*, 2002). Alternatively, it is possible that a reduced localization of Znt1 at the plasma membrane of the mutant embryo affects MAPK signalling. Consistent with this observation of Znt1 truncation and developmental defects in zebrafish embryo were *erk2* morphant zebrafish embryos (Krens *et al.*, 2008) and *erk2* mutant mouse embryos (Saba-El-Leil *et al.*, 2003) where truncation of this gene produced similar developmental defects in both species especially in zebrafish where the gastrular cell migration processes was affected during embryogenesis. There was a reduction in activation of pErk at the margin or the leading edges of *erk*2 morphants during the gastrulation stage in zebrafish embryogenesis as observed in the present studies with Znt1 mutants and morphants suggesting that Erk2 is the active MAPK in the margin (Krens *et al.*, 2008). These observations lend further credence to support the interaction between ZnT1 and MAPK pathway activation being necessary for diverse cellular process including cell growth, proliferation, differentiation, survival and vertebrate development (Ballif and Blenis, 2001). The erratic timing of spawning which sometimes observed among adult homozygote Znt1 mutants may be connected to disturbance in MAPK signalling pathways (seen in Znt1 mutant embryos), which influence the core circadian gene through activation of cAMP response element binding (CREB) protein (Akashi and Nishida 2000; Cermakian *et al.*, 2002; Fu and Lee, 2003). The disturbance in MAPK signalling in adult mutant fish possibly affecting master circadian gene regulation was

further investigated in the next chapter (chapter 4) to address the hypothesis of delayed development in embryos and abnormal spawning behaviour in adult. These processes might be connected to disruption in zinc homeostasis due to dysregulation of Znt1 protein causing compensatory changes in expression of other zinc transporters. It is known that excess zinc or zinc toxicity in fish causes mortality, growth retardation, tissue alterations, respiratory and cardiac changes, inhibition of spawning and a multitude of additional detrimental effects (Spry and Wood, 1985) as observed in our mutant fish.

In conclusion, from some of the preliminary results observed in this chapter, especially on hatching and hatching glands, it was hypothesised that water-borne exposure of zebrafish embryos to zinc or TPEN (zinc depletion) affects hatching. More importantly, the expression of *znt1* gene and the detection of Zn^{2+} ions in the HGC of zebrafish embryo could possibly have a vital role to play in the whole process of hatching. These hypotheses are further pursued in greater detail in chapter 5 to unravel the mechanisms involved in hatching of the zebrafish embryo.

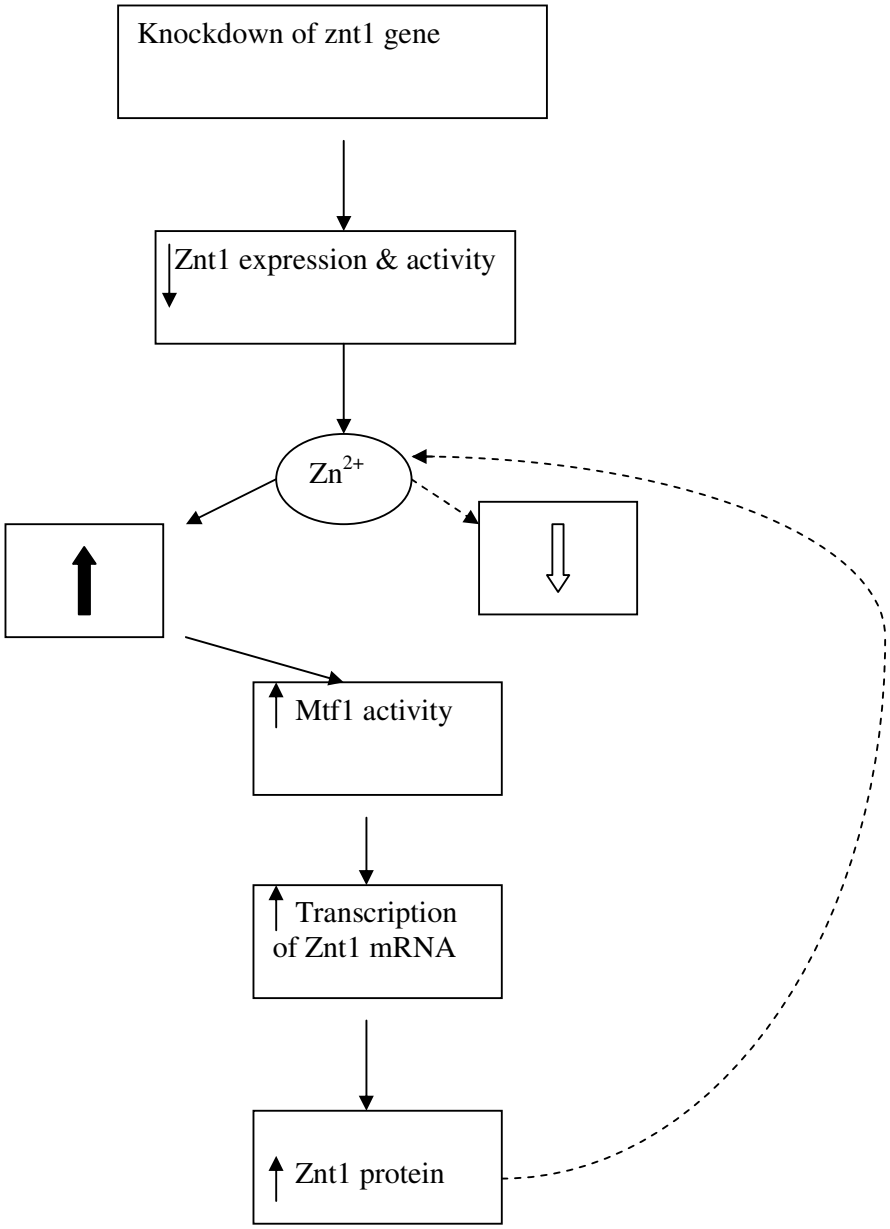

Figure 3.16. Proposed mechanism illustrating how a reduced Znt1 activity brings about a positive feedback regulation of its own expression by a way of compensatory response. Knockdown of *znt1* gene caused increased intracellular zinc accumulation which triggers more transcription of Znt1 mRNA through enhanced activity of Mtf1, thus leading to compensatory increased expression of Znt1protein to regulate the intracellular zinc level. Up and down arrows represent increase and decrease regulation while dashed arrows show the consequence of the compensatory upregulation of Znt1.

3.5.6 Summary

The zebrafish Znt1$^{\Delta 40/\Delta 40}$ embryo is homozygous viable but with slightly enlarged (unabsorbed) yolk and increased free Zn^{2+} ions accumulation compared with the wild-type embryo, causing a slower embryogenesis and reduced survivability after the critical developmental stage of 4 weeks post hatching and beyond. Zinc chelation for 1-3dph produced a phenotype with a partial penetrance of curved notochord in some mutant embryos. These effects were also observed but more pronounced in embryos with *znt1* gene knockdown by MO (i.e. the Znt1 morphant; Znt1^{MO}). There was also an impaired MAPK (p-ERK 1/2) signalling in Znt1 deficient embryos compared to normal wild-type embryos. It was observed that adult homozygote mutants showed erratic behaviour in spawning compared to wild-type fish. All these effect might be related to the defect in the *znt1* gene, leading to inability to properly handle or regulate free Zn^{2+} ions and/or causing a disturbance in MAPK signalling cascade necessary for crucial biological processes in the body.

3.5.7 Future studies

In order to consolidate on the information gathered from the experiments with the Znt1 mutant embryo, the following studies need to be conducted:

i. Experiments to further confirm the functional importance of the truncated region of Znt1 in zebrafish through a cell-based assay transfected with cloned Znt1 (cDNA) from wild-type and mutant embryos respectively. Alternatively, primary cells derived from embryos of each genotype can be used for this assay or a similar mutation can be created in a full-length Znt1 cDNA by PCR technique and this can be transfected in cell culture for functional assay compared to intact wild-type. This type of experiment will give mechanistic

information on the effect of the mutation in cellular regulation of zinc as well as its effect on interaction with other cellular protein such as Raf-1 and 14-3-3. This aspect of the study is currently on-going in our laboratory.

ii. Experiments to quantitate the actual concentration of free Zn^{2+} ions in zebrafish Znt1 mutant and wild-type embryos using a ratiometric protein-based or chemical-based zinc sensor.

iii. The study on the effect of mutation on survivability of embryo of different genotypes to juvenile-adult stage should be properly planned and carried out using a pair-wise collection of embryos from heterozygote parents. In this case the total number of embryos collected from the beginning of the experiment needs to be known so that the actual percentage of different genotypes that die or survive until juvenile-adult stage can be accurately determined.

CHAPTER FOUR

EFFECT OF DIETARY ZINC SUPPLEMENTATION IN COMBINATION WITH ZNT1 MUTATION IN JUVENILE-ADULT FISH

4 Effect of dietary zinc supplementation in combination with *znt1* mutation in juvenile-adult zebra fish

4.1 Introduction

Animals have evolved multiple trafficking pathways to regulate zinc metabolism in order to ensure a required supply and to protect against the toxic effects of zinc excess (King *et al.*, 2000; Sekler *et al.*, 2007). Intracellular zinc is strictly regulated by binding to metallothioneins (MTs) and glutathione and/or by trafficking through the activities of various zinc transporters or channels (Chimienti *et al.,* 2003). These zinc transporters are expressed in a tissue-specific manner, and respond differentially to dietary zinc level and physiological conditions. Therefore, a loss of function or dysregulation of certain zinc transporters would result in an impairment of zinc homeostasis and predispose the body to zinc imbalance-related diseases such as cancer, asthma, diabetes and Alzeimer's disease (Lichten and Cousins, 2009). Despite intensive studies of zinc transporters at the cellular level, their physiological function in the maintenance of zinc homeostasis at the organismal level is still less understood, especially the mechanism underlying dietary zinc absorption. For instance, acrodermatitis enteropathica (AE) is a rare genetic disease in humans caused by impaired intestinal zinc uptake as a result of mutation of *hZip4* gene (Wang *et al.*, 2002; Kury *et al.*, 2002; Nakano *et al.*, 2009), similar condition of which has been reported in farm animals (Simonehauser and Baumgartner, 2005; Yuzbasiyan-Gurkan and Bartlett, 2006; Siebert *et al;* 2013). The ZIP4 protein is localized at the apical membrane of the enterocytes in mouse, consistent with its role in intestinal zinc absorption (Dufner Beattie *et al.*, 2003). The zinc inside the absorptive enterocytes is pumped into the circulation for systemic supply by ZnT1, which is the only known zinc efflux protein localized at the basolateral membrane of the enterocytes

(Luizzi *et al.*, 2003; McMahon and Cousins, 1998; Yu *et al.*, 2007). In genetic studies, targeted knockout or mutation of the z*nt1* gene in mouse (Andrews *et al.*, 2004), *C. elegans* (Bruinsma *et al.*, 2002) and *Drosophila* (Wang *et al.*, 2009) has also revealed a role for this gene in dietary zinc uptake and re-distribution in the adult, as well as causing embryonic lethality or developmental defects as explained in previous chapter. This further lends credence to the critical role of ZnT1 protein in fetal development in mice by transporting maternal zinc into the embryonic environment (Andrew *et al.*, 2004). In zebrafish, tissue distribution and mRNA expression of most zinc transporters in response to dietary zinc status were first reported by Feeney *et al.,* (2005) and Zheng *et al.*, (2008).

One of the important aspects of zinc metabolism is the ability of the protein(s) involved to adjust and regulate its abundance and activity to the changing levels of dietary zinc through transcriptional, post-transcriptional, translational and post-translational regulation (Dufner Beattie *et al.*, 2003b; Mao *et al.*, 2007; Weaver *et al.*, 2007; Davis *et al.*, 2009). Zinc regulation is important in controlling many biological processes in the body and because of the important role of ZnT1 in regulating cytosolic zinc, its aberrant expression in the zebrafish model system may likely affect some of these processes including MAPK signalling as described in the previous chapter (Jirakulaporn and Muslin, 2004; Ho *et al.*, 2008) and master circadian gene regulation. Importantly, Zn^{2+} has been shown in the peripheral oscillator to influence core circadian rhythm by modulating the interaction or the binding of the *Bmal1/Clock* transcription factor with the E-box element, which is a key event in the regulation of clock and clock-controlled gene expression, and stimulates the transcription of period (*Per*) and cryptochrome (*Cry*) genes (Fig. 4.1) (Munoz *et al.*, 2006) as well as transcription of the orphan nuclear receptor gene *Rev-Erb* (Steven and David, 2002).

Mutation in any of the clock genes or other mutations that affect the expression of the genes (especially *clock* or *Bmal1*) have been shown to alter behaviour rhythmicity in rodents (King *et al.,* 1997). Interestingly, the Ras-MAPK signalling pathway was also shown to control circadian output pathways in fly and chicks (Williams *et al.*, 2001, Ko *et al.*, 2001) and it's likely that similar pathways are involved in maintaining peripheral clock control in fish and mammals. Cermakian *et al.*, (2002) established a link between light-induced transcriptional activation of clock genes and MAPK pathways in an *in vitro* study using light-responsive zebrafish cell lines (Z3) to explain light-induced signal transduction, possibly through cryptochromes that are present in zebrafish circadian system (Pando and Sassone-corsi, 2002). Similarly, it was shown that the MAPK (ERK) signalling pathway is also activated by circadian-regulated production of growth factors (Fu and Lee 2003). Thus, it is reasonable to believe that there are some forms of cross-talk between Zn^{2+} ions, ZnT1, Ras-ERK signalling and master circadian oscillation, as illustrated in Figure 4.0. Therefore, the accumulated data obtained from embryos and adult fish as previously described in Chapter 3, suggests that *znt1* mutation might be responsible for some of the effects observed in adult fish due to dysregulation of zinc leading to disturbances in zinc homeostasis, thus affecting certain biological processes in the body such as MAPK signalling cascade and master circadian regulation. The hypothesis of possible interconnectivity or cross-talk between zinc, ZnT1, MAPK signalling and master circadian oscillation in adult zebrafish mutants and wild-type is investigated in the present study.

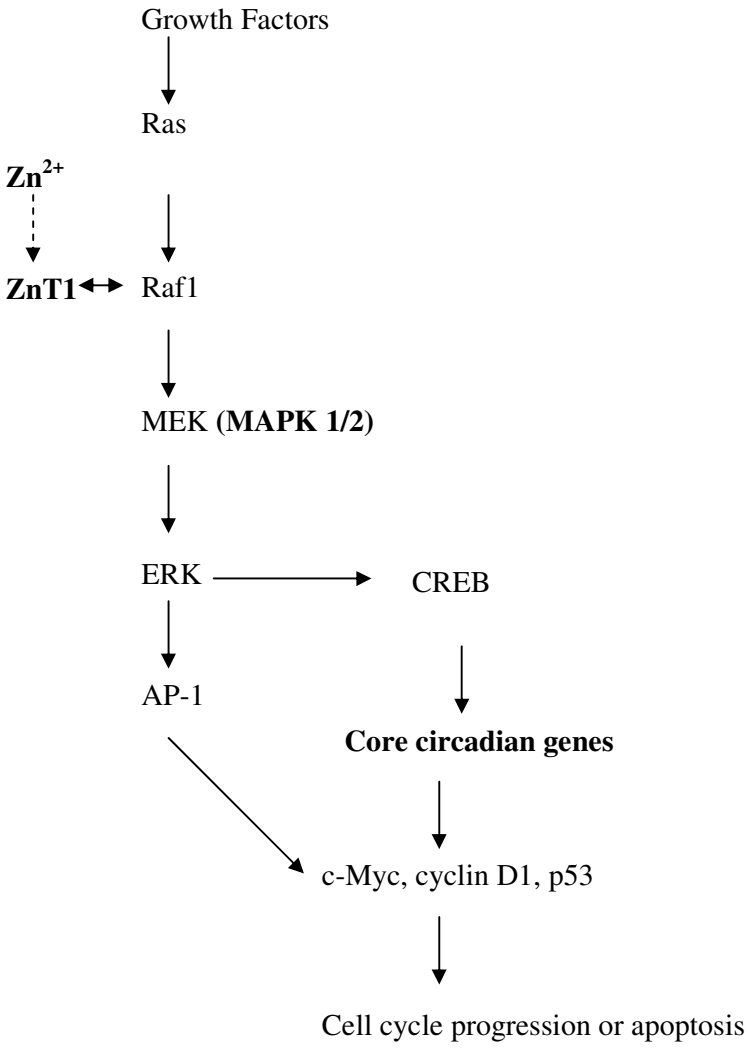

Fig 4.0. Schematic representation of signalling pathways linking the circadian clock to MAPK pathways. Circadian-regulated production of growth factors activates the mitogen activated protein kinase (MEK, MAPK1,2)/extracellular signal-regulated kinase (ERK) pathways which can result in cell-cycle progression or apoptosis in peripheral tissues. Signalling through the MEK pathways, however, leads to activation of the c-AMP response-element binding protein (CREB). CREB activates the transcription of core circadian genes in peripheral tissues. Additionally, ERK signalling activates the transcription factor AP-1, which regulates production of c-Myc, cyclin D1 and p53, and thereby mediates cell proliferation or apoptosis (Modified from Fu and Lee, 2003). Zinc (Zn^{2+}) is also known to participate indirectly in the downstream activation of the pathways either through activation of ZnT1 thereby facilitating its interaction with Raf1 kinase (Jirakularporn and Muslin, 2004) or alternatively through inhibition of phosphatase activity (Hogstrand *et al.,* 2009).

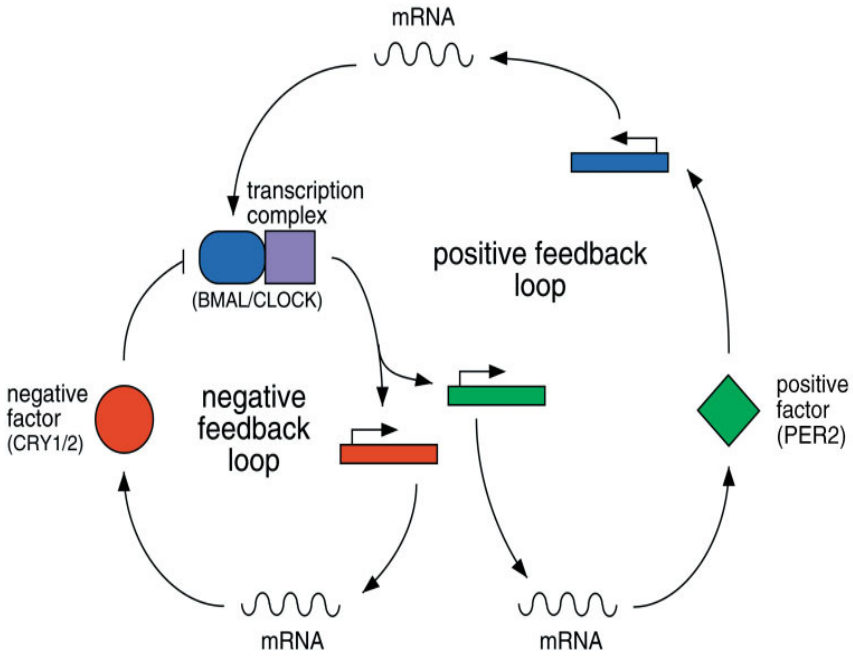

Fig 4.1: Schematic representation of interlocking positive and negative feedback loops involved in the regulation of most molecular clocks. A general feature of circadian clocks, at the molecular level, is the presence of transcriptional–translational autoregulatory loops. Positively acting clock components increase the transcription of other clock genes, which encode proteins that have positive or negative feedback effects on their own expression. Specific protein examples given in parentheses are from the mouse circadian system (Figure taken from Pando and Sassone-Corsi, 2002).

4.2 Study objective

The objective of the present study was to test, in adult fish, the hypothesis arising from some of the effects reported in the previous chapter such as delayed development and erratic spawning mediated by defect in zinc homeostasis due to dysregulation of zinc transport affecting MAPK signalling and clock gene expression. It was hypothesized that the Znt1 mutant would show decreased pERK (MAPK) activation and altered expression of clock genes, and that manipulation of dietary zinc and internal zinc load would correlate with changes in clock genes expression and pERK activation, and with compensatory changes in the expression of other zinc transporters in wild-type and

mutant fish. Therefore, we conducted an experiment where we fed Znt1$^{+/+}$, Znt1$^{+/\Delta 40}$ and Znt1 $^{\Delta 40/\Delta 40}$ zebrafish for four weeks on formulated diets containing either a concentration of zinc typical for commercial feeds (220 mg/kg dry weight) or the estimated dietary zinc requirement (20 mg/kg dry weight).

4.3 Materials & methods

4.3.1 Feed formulation and analysis

The feed used in this experiment was formulated and analysed by the National Institute for Food and Seafood Research (NIFES) in Norway, using trace element requirements for different fish species as published by the National Research Council, USA (NRC, 1993), as a guide (Table 4.1). Two diets were produced aimed at bracketing the homeostatic range of dietary zinc intake in zebrafish. The zinc requirement for zebrafish has yet to be experimentally determined, but the requirement for other cyprinid species, namely common carp, tilapia, and channel catfish, have been set and range from 20 to 30 mg/kg complete feed (dry wt) (NRC, 1993). Therefore, a zinc inclusion level of 20 mg/kg complete feed was chosen for a diet representing the lower limit of the homeostatic range in zebrafish, and termed ZnN or feed A. The maximum permissible level of zinc in commercial fish feeds in the EU has been set to 200 mg/kg complete feed (dry wt) by the Scientific Committee for Animal Nutrition (SCAN, 2003). As this level was considered tolerated by 'fish', it was adopted to represent a high-zinc diet (termed ZnH or feed B) for the present study.

Fish species	Zn mg/kg	Cu mg/kg	Cd mg/kg	Fe mg/kg	Hg mg/kg	Mn mg/kg	Pb mg/kg	Se mg/kg
i.Channel catfish	20	5	NR	30	NR	2.4	NR	0.25
ii. Rainbow trout	30	3	NR	60	NR	13	NR	0.3
iii. Pacific salmon	R	NT	NR	NT	NR	R	NR	R
iv.Common carp	30	3	NR	150	NR	13	NR	NT
v. Tilapia	20	R	NR	NT	NR	R	NR	NT
Maximum permissible Levels	200	25	0.26-1.2	750	0.5	100	0.04-0.28	0.5

Table 4.1: Trace element requirements and maximum permissible levels in feed for different fish species (http://www.nap.edu/openbook.php?record_id=2115&page=63#p200062009960063001)

Keys: R, required in diet but quantity not determined; NT, not tested; NR, no dietary requirement demonstrated under experimental conditions.

4.3.2 Animal feeding experiment

For the feeding experiment, fish were grouped into two and each group fed with each feed type (i.e. feed A and B). Briefly, pooled embryos obtained from the crossings of heterozygote parents ($Znt1^{\Delta 40/+}$ x $Znt1^{\Delta 40/+}$) were reared for 8 weeks under standard husbandry conditions and were then divided equally into two groups comprising of fifty fish each. One group was fed with feed A (which was referred to in this experiment as normal zinc diet or simply ZnN, 20 mg Zn/kg) while the other group fed with feed B (which was referred to in this experiment as high zinc diet or simply ZnH, 220 mg Zn/kg) at a total ration of 5% of the body weight per day divided in two meals (morning & evening) for a period of 4 weeks of the experiment. Blood worm meal was given to both groups once a week to supplement a potential iron shortage in the feed formulation. The composition of blood worm meal is shown in Appendix 9.12. Fish

were reared under photoperiods of 14 hours of light (9:00am-11:00pm) and 10 hours of darkness (11:00pm-9:00am).

4.3.3 Sample collection & processing

At the end of the four week feeding experiment, fish from each group were individually anaesthesized during the light phase periods (photoperiods) and different tissues were collected and immediately snap frozen in liquid nitrogen or in dry ice then stored at -80^{o}C until analysis. Tissues collected were intestine, brain, eye, a section of caudal tissue (composed of skin, muscle and bone), and caudal fin. The fin was used for genotyping of individual fish from each group to identify and classify them into wild-type, heterozygote and homozygote which are denoted as Znt1$^{+/+}$, Znt1$^{\Delta 40/+}$ and Znt1$^{\Delta 40/\Delta 40}$ respectively (section 2.2.4).

4.3.4 RNA extraction, DNAse treatment and cDNA synthesis

Individuals of each genotype from each group were identified as described in section 2.2.4 and total RNA was extracted from intestinal and brain tissues of each fish, DNAse treated and cDNA synthesized as previously described in general materials & methods (section 2.2.7.1.1.1-2.2.7.1.1.6) but with a slight modification to the extraction process. Here, because of small size of the intestinal and brain tissue samples, a phase lock 2ml tube (5 prime®) was used for RNA extraction for clear separation of the aqueous phase from the organic phase in order to get enough total RNA from the tissue containing little or no genomic contamination as described in section 2.2.7.2.1.

4.3.5 Zinc regulated gene expression study

4.3.5.1 Zinc transporters and metallothionine expressions

Zinc regulatory genes known to be differentially expressed in fish and/or mammals in response to changes in dietary zinc status in the intestine (Feeny *et al.*, 2005; Zheng *et al.*, 2008; Lichten and Cousins, 2009) were selected in zebrafish and analysed with qPCR as previously described (section 2.2.7.2) using a 1:10 dilution of the cDNA sample synthesized from 1µg of total RNA of each fish from different groups. The primer and probe sequences for each gene studied are shown in Table 4.2 below. Gene expression data were normalised to 18s rRNA expression. Average expression data per gene of all fish from each genotype per group were calculated and compared to that in wild-type fish receiving normal zinc diet (feed A). Gene expression was calculated with the formula described in section 2.2.7.2, and data expressed as fold change or as a $\log_2$ fold change.

Gene	qPCR primer/probe sequences (5'-3')	Tm	Probe#	Amplicon size (bp)	Accession No
znt1 (*slc30a1*)	F: gttaatgcggagcggaag R: atatggagcactgccattaatct P: cagcctgg	59 59	64	78	NM_200879.1
znt2 (*slc30a2*)	F: atctgttcacatagccatcgac R: gttgtgctgtagaagccgaat P: ctcctcca	59 59	25	87	NM_001045020.1
znt4 (*slc30a4*)	F: tcagagacaccggcatcat R: tctgctctgatgaccgacac P: tgctggag	60 59	67	70	NM_200643.1
znt5 (*slc30a5*)	F: gctgtctgcaaccactgaga R: tgatcatggcaaatggaaag P: ctggtctc	60 59	54	68	NM_001002322.1
mt2	F: ccagtgtactacctgcaagaagag R: gccagaggcacacttgct P: gctgcca	59 60	44	70	ENSDARG00000041623.2
zip3 (*slc39a3*)	F: tcttctgctccgccagac R: cagaccctccacagcacag P:	60 60	152	107	NM_001080619.1
zip4 (*slc39a4*)	F: ccgtctccacagattcagc R: acatgaatcagcgtaggaagc P: gcagtgga	59 59	86	103	NM_001130777.1
zip7 (*slc39a7*)	F: ctcattcctcatgcactgga R: actggccatgggactcct P: cagccaca	59 60	5	70	NM_130931.2
zip10 (*slc39a10*)	F: gctgttactgctggcatgttt R: cactgtcaccgtgaagcatt P: tgttgcca	60 59	145	73	NM_200671.1
18s	F: aaactgtttcccatcaacgag R: gggacttaatcaacgcaagc P: ttcccagt	59 59	48	67	FJ915075.1

Table 4.2: Zebra fish zinc transporter and metallothionine genes with qPCR primer sequences, accession number, UPL probe number and product lengths. F, R and P denote forward primer, reverse primer and probe sequences.

Expression of the master circadian or clock genes was studied in the brain tissue homogenates of only the wild-type and homozygote fish at both zinc provisions (i.e. normal and high zinc diets) as described above. A 1:2 dilution of cDNA synthesized from 0.2µg of total RNA of each fish was used for the qPCR assay. The primer and probe sequences for each gene studied are shown in Table 4.3 below. The number or proportion of animals per group expressing the mRNA transcript in fish per group for each clock gene at both dietary zinc statuses was determined.

NB: The time of sample collection for all groups was during the photoperiod between 13:00–20:00hrs because it is reported that clock gene expression is daylength-dependent (Davie *et al.*, 2009) and it is assumed that the effect of *znt1* mutation and/or zinc level in zebrafish may affect this expression pattern during the photoperiods.

Gene	qPCR primer/probe sequences (5'-3')	Tm	Probe#	Amplicon size (bp)	Accession No
Clock	F: ctgagatctccgcagacaagt R: tcgctctagggcctcct P: ctccagct	59 60	78	83	NM_130957.1
Bmal1	F: gcattcttgtcggatgatga R: gttgtgctgtagaagccgaat P: ggctgctg	59 59	66	75	AF144689.1
Cry2a	F: aaaagcaatgtctcgcatga R: ccctcttccctgtcacactt P: ggcagcag	59 59	74	73	NM_131791.1
Per2	F: gcttcaccacaccatacagg R: gtctgacggggacgagtct P: cctggagc	59 60	1	68	NM_182857.1

Table 4.3: Zebrafish circadian genes with qPCR primer sequences, accession number, UPL probe number and product lengths. F, R and P denote forward primer, reverse primer and probe sequences.

4.3.5.3 Data and statistical analysis

Data from all different genotype groups per diet or feed groups were analysed by 2-way ANOVA to detect the effect and/or interaction between the 2 variables (Diet and Genotype). One-way ANOVA followed by Dunnett's post-hoc test was used for multiple comparisons within the groups to determine which group means were different to others. Data (ΔCT values) are expressed as means ± SEM of 7 observations per group. Statistical analysis was carried out using GraphPad Prism 5 (San Diego, CA, USA) and significance was indicated when $p \leq 0.05$.

4.3.6 Metal analysis from different genotypes

Caudal (tail) tissues obtained from different fish genotypes that received different zinc diets were digested in 65% HNO_3 as described in section 2.2.5 and metal concentrations measured by ICP-MS (Perkin Elmer, model ELAN 6100DRC) at the mass spectrometry unit, King's College London. Portions of these samples were also analysed by ICP-MS at NIFES.

Data from all genotypes per diet group were analysed by 2-way ANOVA to detect the effect and/or interaction between the 2 variables (Diet and Genotype). One-way ANOVA followed by Dunnett's post-hoc test was used for multiple comparisons within the groups to determine which group means were different to others. Data are expressed as means ± SEM of 7 observations per group. Statistical analysis was carried out using GraphPad Prism 5 (San Diego, CA, USA) and significance was indicated when $p \leq 0.05$.

4.3.7 Extracellular signal-regulated kinase (ERK) activity in different genotypes

A caudal transverse section of body tissue was collected from each genotype for both zinc treatments and assayed for protein abundance as described in section 2.2.7 for phosphorylated ERK 1/2 (p-P42/44) and total ERK 1/2 (P42/44), which was used for normalization. p-P42/44 antibodies (#4370) were used at 1: 2000 while P42/44 (#9102) was used at 1:1000 and secondary antibodies were used at 1:5000 for both. For phosphorylated protein detection, 5% BSA was used as blocking buffer in TBST and 3% and 1% of the blocking buffer was used for primary and secondary antibody dilutions respectively. Milk or PBST was not used because of possible non-specific reaction of the phosphorylated antibody with phospho-proteins in the milk or phosphate buffer.

4.4 Results

4.4.1 Elemental composition of experimental feeds

Analysed concentrations of zinc in the experimental feeds were close to the intended levels, with 23 mg/kg in feed A representing the dietary requirement and 220 mg/kg in feed B targeting the upper permissible limit for zinc inclusion in commercial feeds (250 mg/kg for pets; 200 mg/kg for farmed fish; EC, 2003) (Table 4.4). The iron contents of the two feeds were similar (43.3 and 40.3mg/kg respectively) and are within the range of requirements reported for cyprinids especially the channel catfish, although lower than for the common carp (30–150 mg/kg). Both feeds had high selenium contents, presumably because the protein source originated from marine fish (Feed A: 3.25 mg/kg, Feed B: 10.8 mg/kg), but these levels were below those causing selenium

toxicity to adult fish (above 10µg/g in egg) and thus did not pose a concern in the present study (Lemly, 2002). The concern can only be in fish intended for human consumption. The concentrations of copper and manganese were very similar between the feeds and close to the intended levels. Mercury, cadmium and lead levels were very low and hence did not pose a concern.

Feeds	Zn mg/kg	Cu mg/kg	Cd mg/kg	Fe mg/kg	Hg mg/kg	Mn mg/kg	Pb mg/kg	Se mg/kg
Feed A	23	25.7	<0.005	43.3	0.011	36.6	0.01	3.25
Feed B	220	21.5	<0.005	40.3	0.027	35.5	<0.03	10.8

Table 4.4: Composition of trace elements in different feeds as analysed by NIFES

4.4.2 Metal accumulation in tissue of different genotypes

A caudal section of the body (at the level of the anal fin) was analysed for deposition of metals both at KCL and NIFES (Norway). The results of tissue metal analysis from the two facilities were very similar and therefore only results from KCL are presented. There was a tendency for wild-type fish to accumulate more zinc than either of the heterozygote and homozygote mutants, but this was not statistically different (Fig. 4.2). The two diets did, however, differ in their effect on tissue zinc levels as the 220 mg Zn/kg feed resulted in a two-fold higher tissue zinc content compared with the 23 mg Zn/kg feed (Fig. 4.2). Thus, the total tissue zinc content responded to the feed inclusion level of zinc, but there was no genotype difference. The selenium concentration of the tissue was significantly higher in homozygote mutants fed the high zinc diet (220 mg Zn/kg) compared with the homozygotes fed the normal zinc diet (23 mg/kg; Fig. 4.2.1). This may be due to the higher selenium content of the high zinc diet. However, this effect was not statistically significant in wild-type fish (Fig. 4.2.1). On the other hand,

the elemental content of feaces for zinc was not significantly different between wild-type and homozygote irrespective of the diet (Fig. 4.2.3A) but feacal selenium level was significantly higher in the homozygote on both diets (at equal level) and in wild-type in high zinc diet when all were compared with wild-type on normal zinc diet, indicating that the homozygote lost less selenium in the feaces on the high zinc diet resulting in high tissue selenium accumulation as mentioned above (Fig. 4.2.3B). Specifically, about 0.1 & 5.7 µg/g feaces of selenim was lost on the normal and high zinc diet in wild-type fish and about 3.52 and 3.56 µg/g in homozygotes for normal and high Zn diet respectively. All other elements analysed in the tissue, including Cu, Cd, Fe, Mn and Pb, showed no statistically significant differences between genotypes or diets (Fig. 4.2.2A-D).

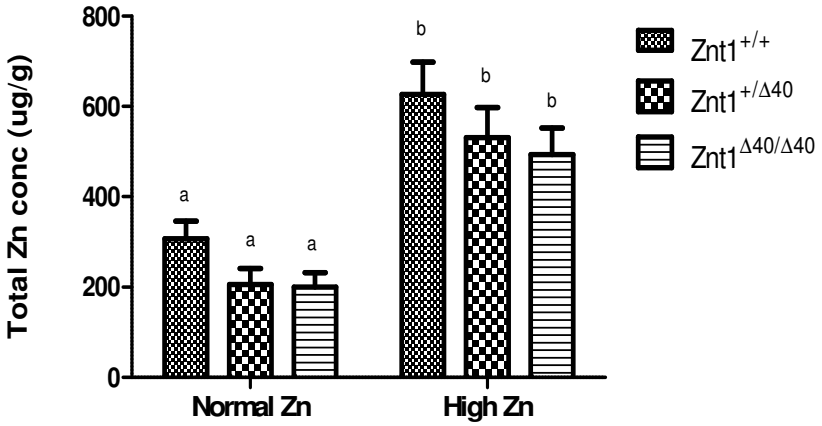

Fig 4.2: Effect of Zn diets on total Zn level in the body of different fish genotypes. ICP-MS measurement for Zn in the body tissues following four weeks of feeding of low and high Zn diets in wild-type, heterozygote and homozygote fish. Data are presented as the mean ± SEM (n =10) where $p \leq 0.05$ is considered significant following 1-way ANOVA with each other or following 2-way ANOVA to detect effect/interaction for zinc diet and/or genotype. **Key**: Groups with the same letter showed no significant difference while groups with different letters differ at $p \leq 0.001$. $Znt1^{+/+}$, $Znt1^{+/\Delta 40}$ and $Znt1^{\Delta 40/\Delta 40}$ denote wild-type, heterozygote and homozygote respectively.

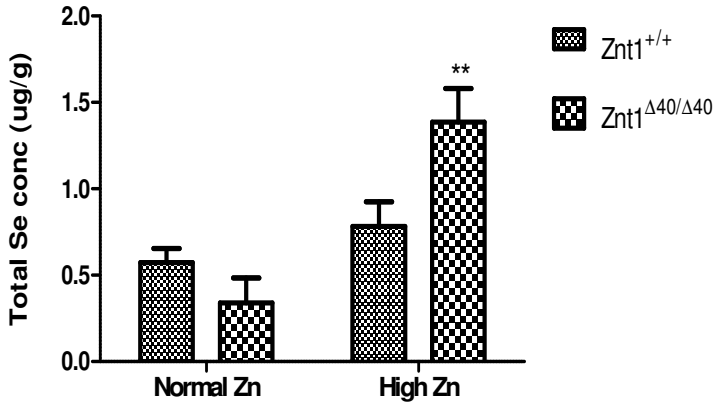

Fig 4.2.1: Effect of Zn diets on total Se level in the body of WT and mutant fish. ICP-MS measurement for Se in the body tissues following four weeks of feeding of normal and high Zn diets in wild-type and homozygote fish. Data are presented as the mean ± SEM (n =10) where $p \leq 0.05$ is considered significant (relative to WT on normal-Zn) following 1-way ANOVA with each other or following 2-way ANOVA to detect effect/interaction for zinc diet and/or genotype. **Key**: (**); very significant at $p \leq 0.01$. $Znt1^{+/+}$ and $Znt1^{\Delta 40/\Delta 40}$ denote wild-type and homozygote respectively.

.

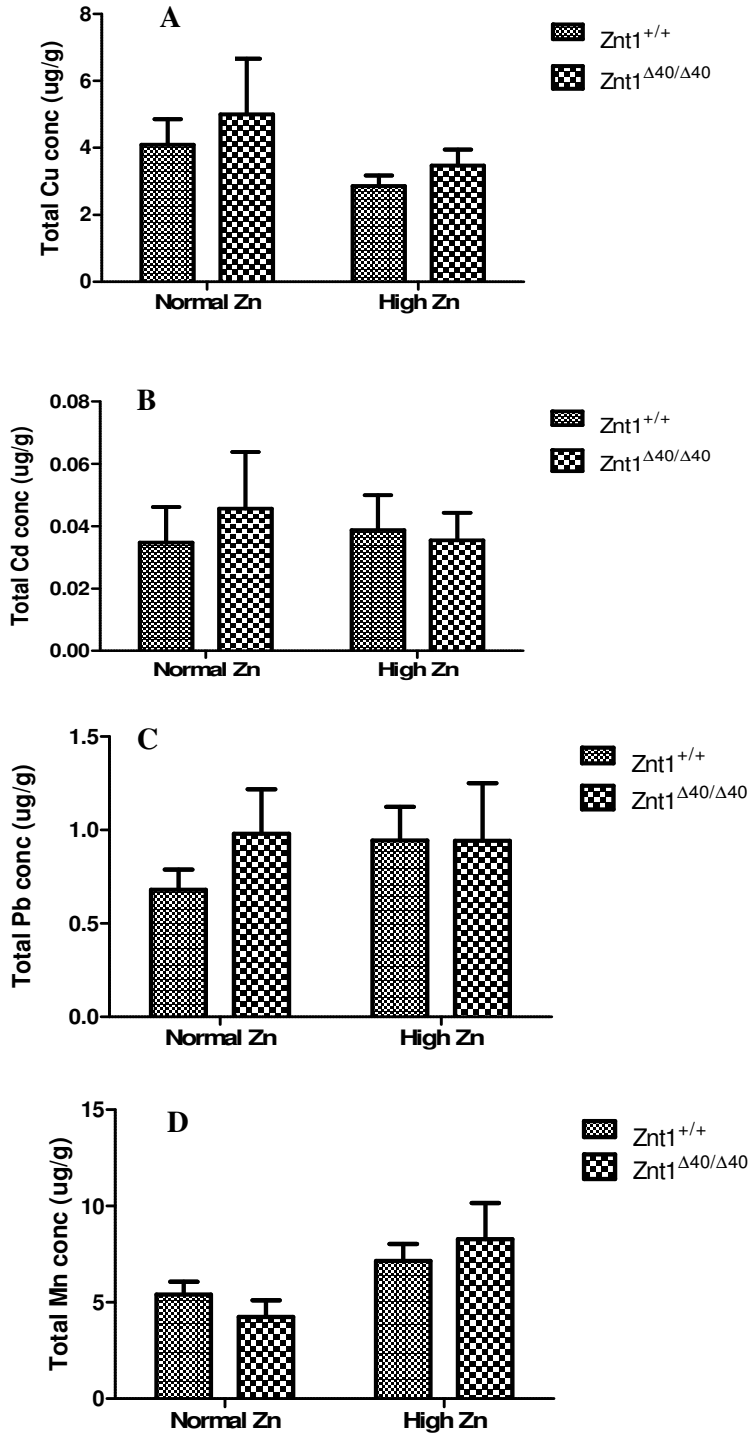

Fig 4.2.2: Effect of Zn diets on total Cu, Cd, Pb and Mn level in the body of WT and mutant fish. ICP-MS measurement for Cu, Cd, Pb and Mn in the body tissues following four weeks of feeding of low and high Zn diets in wild-type and homozygote fish. Data are presented as the mean ± SEM (n =10) where $p \leq 0.05$ is considered significant following 1-way ANOVA with each other. $Znt1^{+/+}$ and $Znt1^{\Delta 40/\Delta 40}$ denote wild-type and homozygote respectively.

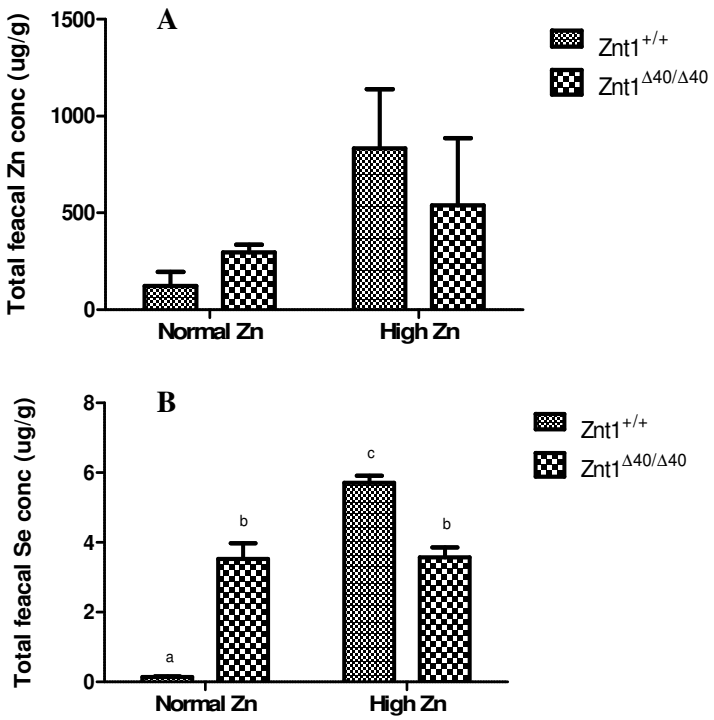

Fig 4.2.3: Effect of Zn diets on total feacal Zn loss in WT and mutant fish. ICP-MS measurement for Zn in the body tissues following four weeks of feeding of low and high Zn diets in wild-type, heterozygote and homozygote fish. Data are presented as the mean ± SEM (n =10) where $p \leq 0.05$ is considered significant following 1-way ANOVA with each other or following 2-way ANOVA to detect effect/interaction for zinc diet and/or genotype. **Key**: Groups with the same letter showed no significant difference while groups with different letters differ at $p \leq 0.01$. $Znt1^{+/+}$ and $Znt1^{\Delta 40/\Delta 40}$ denote wild-type and homozygote respectively.

4.4.3 Effect of zinc diets on expression of zinc transporters and MT in different genotypes

There was differential expression of genes for some of the analysed intestinal zinc transporters and for metallothionein following varying zinc diets in different genotypes as shown in Figure 4.3 and 4.4. Expression levels (1/**Δ**CT) and qPCR amplification curves for each gene are shown in Appendix 9.13a & b). The *znt1* mutation changes the expression patterns of some of these zinc regulatory genes especially *znt1*, *znt4*, *znt5* and *zip7* in fish fed either normal or supplemented zinc diets which suggests genotype effects. Metallothionein showed increased expression in response to the high zinc diet in all the genotypes and this effect was more pronounced in the homozygote mutant (~92-

FC) than in the heterozygote (~40-FC) or wild-type (~19-FC) relative to control wild-type on the normal zinc diet, thus signifying both diet and genotype effect. The increased expression of MT2 on the high zinc diet (Feed B) in all genotypes further confirmed the difference in biological effect of the two diets. Znt1 on the other hand showed an increased expression in heterozygotes and homozygotes on the high zinc diet relative to control wild-type with normal zinc diet but there was no statistical difference in expression in wild-type fish on the high zinc diet, thus indicating both genotype and diet effects. Znt4 showed a highly significant diet and genotype effect in which case there was significant up-regulation in homozygotes on the normal zinc diet and the high zinc diet compared to control wild-type with the normal zinc diet. Heterozygotes also showed statistically increased expression on the high zinc diet but no statistical difference in expression of Znt4 in wild-type fish on both diets. A similar pattern of expression was observed in Znt5 except that heterozygotes on the high zinc diet did not differ statistically from the control wild-type on the normal zinc diet giving overall significant diet and genotype effects. ZIP expression patterns were somewhat different from ZnTs. No statistically significant differences in expression on either diet was observed for any of the genotypes in Zip3 and Zip10 signifying no diet or genotype effects. For Zip7 there was an increased expression only in homozygotes on the high zinc diet, indicating mild diet and genotype effects. Zip4 showed a highly statistically significant difference of negative expression (down-regulation) to the high zinc diet in all the genotypes showing only a diet effect but no genotype effect. The Zip2 transcript was not detected in the intestinal tissue of any of the fish groups.

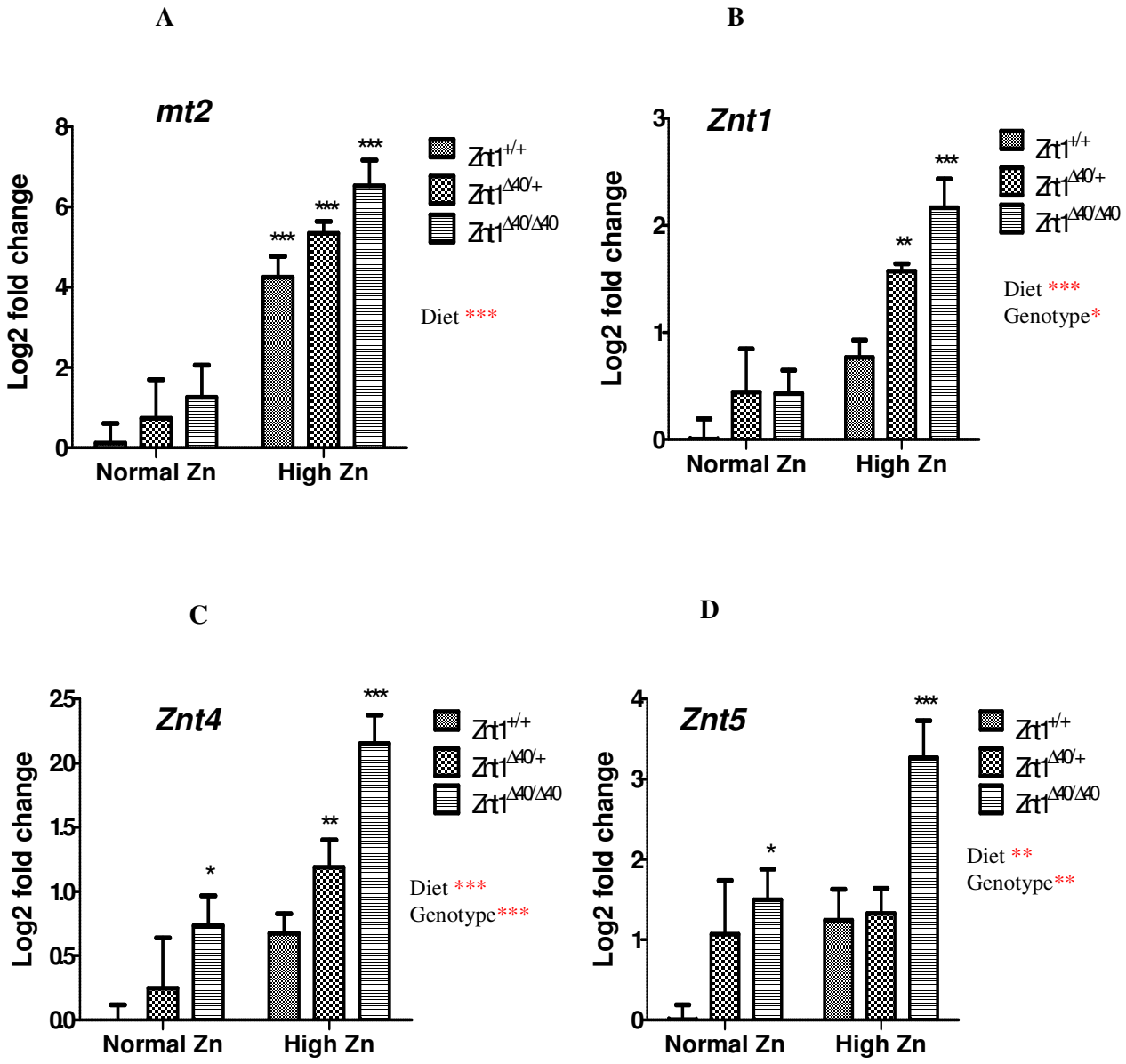

Fig 4.3: Effects of znt1 mutation on expression of zinc transporters of the Znt family and metallothionein. Intestinal gene expression of Znt transporters and metallothionein in response to zinc diets in different fish genotypes were measured by qPCR after four weeks of feeding. Data are presented as the mean ± SEM (n =7) where $p \leq 0.05$ is considered significant following 1-way ANOVA (black asterics) or following 2-way ANOVA (red asterics) to detect effect/interaction for zinc diet and/or genotype. **Key:** (*); p<0.05, (**); p <0.01, (***); p<0.001. $Znt1^{+/+}$, $Znt1^{+/\Delta 40}$ and $Znt1^{\Delta 40/\Delta 40}$ denote wild-type, heterozygote and homozygote respectively, mt2; metallothionein, znt 1,4 and 5; zinc transporters.

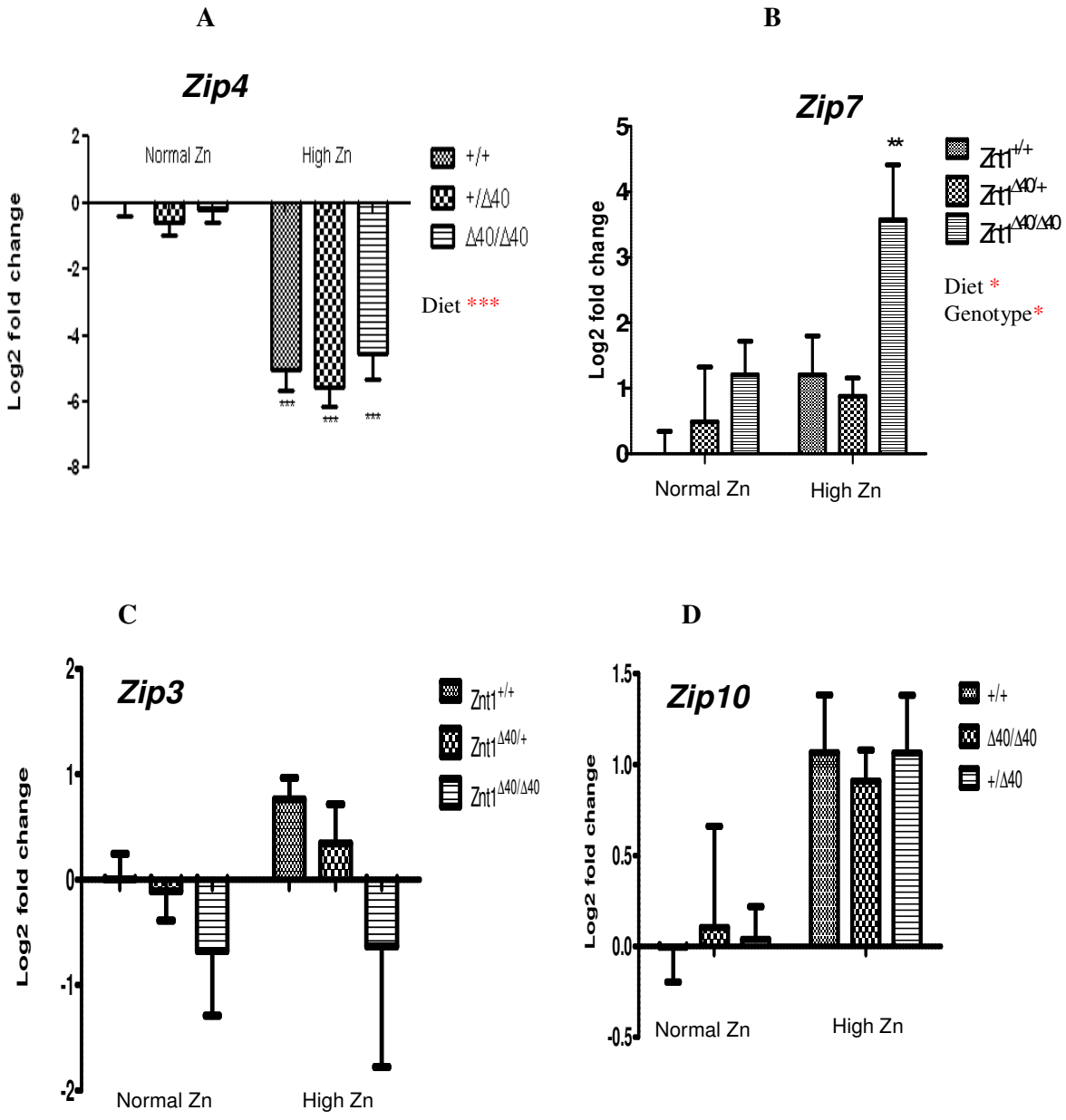

Fig 4.4: Effects of znt1 mutation on expression of zinc transporters/channels of the Zip family. Intestinal gene expression of Zip transporters or channels in response to zinc diets in different fish genotypes were measured by qPCR after four weeks of feeding. Data are presented as the mean ± SEM (n =7). $p \leq 0.05$ is considered significant following 1-way ANOVA (black asterics) or following 2-way ANOVA (red asterics) to detect effect/interaction for zinc diet and/or genotype. **Key:** (*); P<0.05, (**); p <0.01, (***); p<0.001. $Znt1^{+/+}$, $Znt1^{+/\Delta 40}$ and $Znt1^{\Delta 40/\Delta 40}$ denote wild-type, heterozygote and homozygote respectively, zip2, 3, 4, 7 and 10; zinc channels.

4.4.4 Circadian or clock gene expression

All clock genes measured in brain showed increased expression with zinc supplementation. *Clock* and *bmal1(arnt1)* genes showed also differential regulation in homozygotes compared with wild-type with or without zinc supplementation suggesting a genotype effect as shown in Figure 4.5 Expression data (1/**Δ**CT) and qPCR amplification curves for each gene are shown in Appendix 9.14a & b). The abundance of mRNA for the four clock genes on the normal and zinc supplemented diet was in the following order; *Bmal1*>*Per2*≥*Cry2a*>*Clock* and *Bmal1*≥*Per2*>*Cry2a*≥*Clock*. That is, the mRNA transcript level was highest for *Bmal1* and lowest for *clock* for both conditions of zinc status. The *per2* gene transcript was only detected or expressed in some of the fish samples irrespective of the genotype or zinc status, but the incidence of detection of expression was higher in wild-type (80%) for both normal and high zinc diets than in homozygotes (20%) for normal diet, but zinc supplementation (high zinc diet) increased the frequency of expression in homozygotes (60%). For other genes, transcripts were detected or expressed in all of the fish brain samples irrespective of genotype or zinc status at 100% (Fig. 4.5.1).

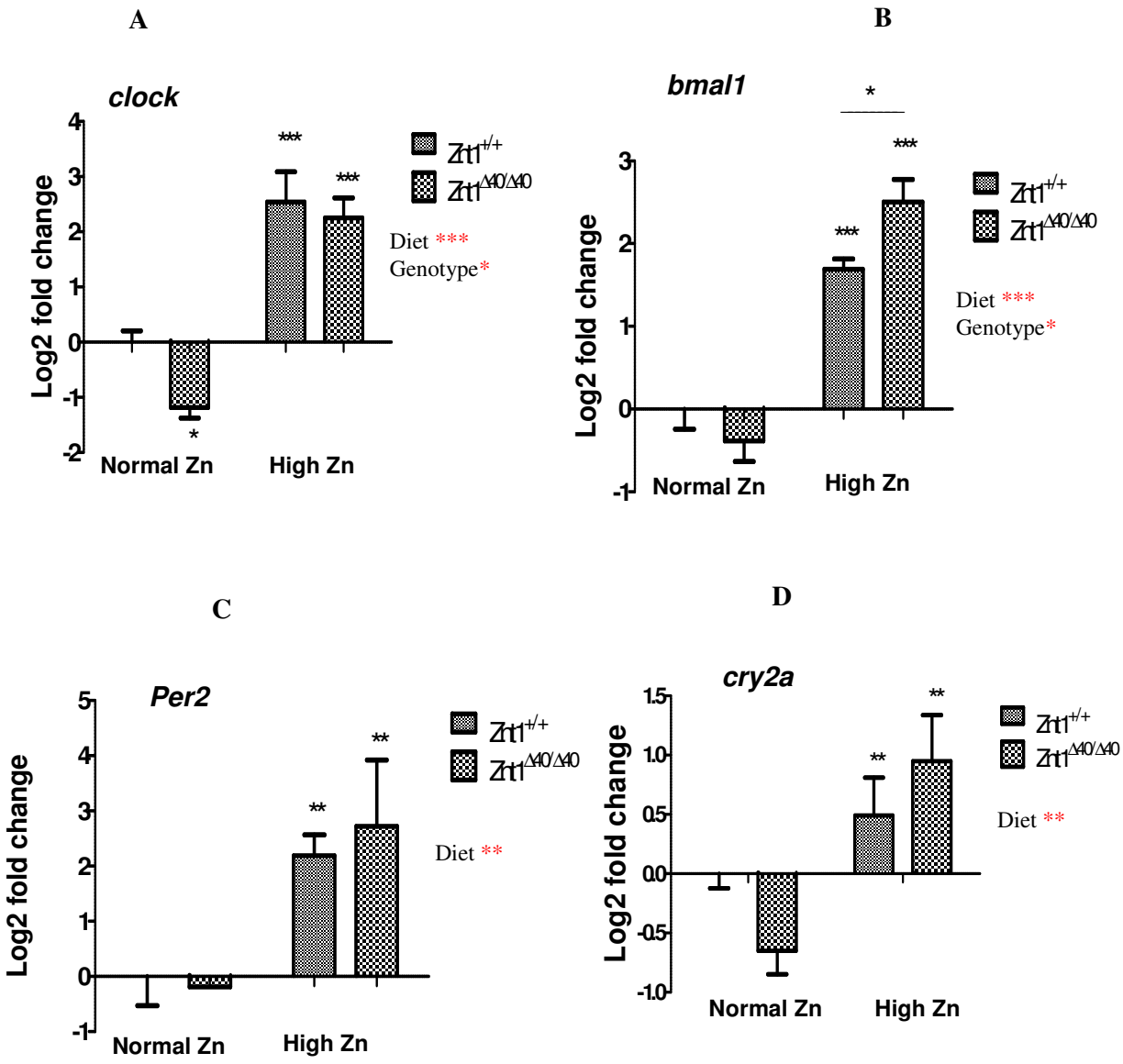

Fig 4.5: Effects of znt1 mutation on expression of brain core circadian genes. Expression of master circadian (clock) genes in response to zinc diets were measured by qPCR in the brain of wild-type and homozygote mutants after four weeks of feeding. Data are presented as the mean ± SEM (n =5). $p \leq 0.05$ is considered significant following 1-way ANOVA (black asterics) or following 2-way ANOVA (red asterics) to detect effect/interaction for zinc diet and/or genotype. **Key**: (*); P<0.05, (**); p <0.01, (***); p<0.001. $Znt1^{+/+}$ and $Znt1^{\Delta 40/\Delta 40}$ denote wild-type and homozygote respectively, *clock*, *Bmal1, per2* and *cry2a*; clock genes.

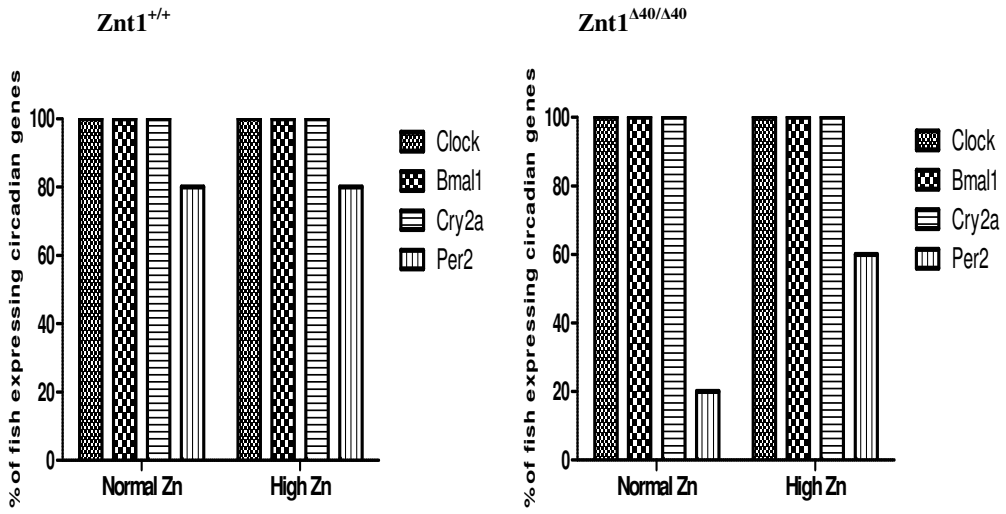

Fig 4.5.1: Effect of znt1 mutation on detection of expression of brain core circadian transcripts. Percentage of fish showing transcript detection of master circadian genes in response to zinc diets was measured by qPCR in the brain of groups of wild-types and homozygote mutants after four weeks of feeding. $Znt1^{+/+}$; wild-type, $Znt1^{\Delta 40/\Delta 40}$; homozygote, clock genes; *clock*, *Bmal1, per2* and *cry2a.*

4.4.5 Effect of zinc diet and/or *znt1* mutation on Ras-ERK signalling in adult fish

There was a reduced level of phosphorylated Erk in homozygous mutants compared with the wild-type for both diets. Although pErk protein was below detection level in all fish genotypes fed the low zinc diet, interestingly, adequate or high zinc diet enhanced Erk expression or phosphorylation in heterozygotes and wild-type fish (Fig. 4.6).

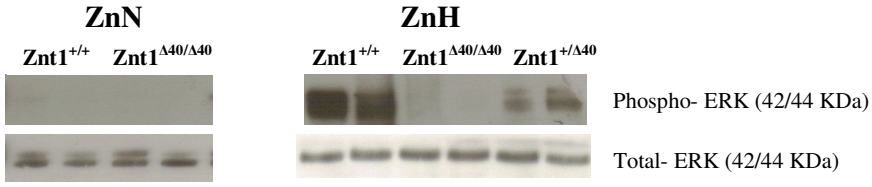

Fig 4.6: Effect of *znt1* mutation on phospho-ERK signalling in adult fish. Phosphorylated ERK protein was measured by Western blotting in different genotypes after four weeks of feeding with 'low' (feed A) and 'adequate' (feed B) zinc diet. p-Erk was barely detected in all genotypes in zinc 'low' condition (ZnN) but detection was greatly enhanced in zinc 'adequate' condition (ZnH). Mutants show reduced phosphorylation. Total-Erk serves as loading control or house-keeping (reference) protein (N=3).

4.5 Discussion

4.5.1 Metallothionein and zinc transporter expression

Accumulation of zinc in the body along with the increased gene expression of metallothionein in the intestine of all the genotypes that received high dietary zinc confirmed the efficacy of the treatment feed supplemented with high zinc. There was increased MT2 expression in response to zinc supplementation as previously reported in fish (Zheng *et al.,* 2008), rat (McMahon and Cousins, 1998) and human (Cragg *et al.,* 2005). The results of the present study also indicated that expression of MT2 in the intestine was higher in homozygotes (5.7 FC) and heterozygotes (2.0 FC) relative to wild-type on the high zinc diet suggesting that more Zn^{2+} might be accumulated or trapped in the intestine of mutants than wild-type, however zinc measurements in the body tissue (not including the intestine and major organs) was not statistically different between genotypes on the high zinc diet. When the effect of the high zinc diet in all genotypes was compared to wild-type on the normal zinc diet, intestinal MT2 expression was up-regulated more in the homozygote than the heterozygote, which in turn showed greater up-regulation than wild-type (92.4, 40.5 and 19-fold change respectively), indicating that mutants required more buffering capacity by MT2 to control intracellular zinc. This effect is in agreement with the effect of *znt1* mutation in the *Drosophila* model, which showed less zinc accumulation in the whole body (minus gut) indicating that fly metallothionein B (MtB) buffered or trapped more zinc in the gut and made it not readily available for distribution to the whole body because of defective function of the Znt1 transporter (Wang *et al.*, 2009). But because the function of MT2 (through the activity of the zinc sensing transcription factor MTF-1) is to act as the first line of defense to bind and buffer excess free zinc ions, which may be toxic to the cells,

any un-buffered Zn^{2+} after MT2 saturation needs to be taken care of by other defense mechanisms such as ZnTs, especially ZnT1 which is under the same MTF-1 regulation as MT2 to remove excess cytosolic Zn^{2+} (Palmiter, 2004). When incoming zinc is beyond the binding capacity of MT2 and with concomitant MTF-1 activation, ZnT1 may be induced through MTF-1 to efficiently lower the total intracellular zinc by zinc efflux, suggesting that both MT2 and ZnT1 work in concert to provide maximum protection when cells are exposed to high zinc levels, with MT2 being more sensitive as a result of more putative MRE sites (7) in the promoters than Znt1 (3) (Zheng *et al.*, 2008). It is assumed that a complete loss-of-function mutation of ZnT1 would result in an inability to transport the metal ion from the basolateral membrane of the intestinal cells to the systemic circulation, which would result in less zinc in various tissues of the body and high accumulation in the intestine with lack of expression of the *znt1* gene because of complete gene knockout, as reported in the fly and worm models (Wang *et al.*, 2009 and Davis *et al.*, 2009). But in the present study, it is assumed that the ZnT1 mutation is not a complete loss-of-function mutation but instead has altered-function because only part of the cytosolic C-terminus was truncated, hence there was *znt1* gene expression in homozygous mutants which was statistically significantly higher than in the wild-type following high zinc diet (~3-fold increase). The increased intestinal Znt1 expression of the mutant fish compared to wild-type fish might explain why there was no statistically significant difference in zinc level in the body between genotypes (as opposed that observed in fly Znt1 mutant). This might be because of the compensatory regulation in the mutant fish to prevent toxicity, thereby pumping adequate zinc to the systemic circulation in order to maintain homeostasis when fed the high zinc diet. In the intestine of fish fed the normal zinc diet, the *znt1* genes of all genotypes were equally expressed for the homeostatic control of the metal ion indicating that the zinc level is

well tolerated by the mutants as in the wild-type. Interestingly, wild-type fish did not show a statistical difference in Znt1 expression between the normal zinc and high zinc diets contrasting with the effect observed on MT2 expression, indicating that the level of zinc in the high zinc diet was under the normal buffering or binding capacity of MT2 without ZnT1 induction in wild-type fish unlike the heterozygote and homozygote mutants where *znt1* genes were induced by about 2.4 and 4.0-fold respectively relative to the wild-type control fed the normal zinc diet, and by about 2.0 fold in homozygotes relative to wild-type on the high zinc diet. The lack of statistical difference in expression of Znt1 of wild-type fish fed high zinc diet relative to those on the normal zinc diet may also be due to the fact that MT2 is more zinc responsive than Znt1. This observation is consistent with a previous study in which intestinal Znt1 expression did not change significantly in response to high zinc in normal wild-type fish (Feeney *et al.*, 2005). Although in that study a semi-quantitative assay was used and number of fish per experiment were three. A contrasting effect was observed in rat and human where ZnT1 was up and down regulated, respectively, following zinc supplementation, indicating that a fundamentally different regulatory response to increased zinc levels may exist between those species (Cragg *et al.,* 2005). Our findings suggest that in mutant fish the high zinc diet leads to more MTF-1 activity in order to lower the concentration of zinc in the cytosol as compared to wild-type, and this leads to induction of Znt1 (through the activation of MTF-1 following initial induction of MT2 expression) to work in concert with MT2 in the mutant fish for homeostatic control (Zheng *et al.*, 2008). Therefore, the zebrafish *znt1* mutation model showed an altered regulation in the homeostatic control of intestinal zinc uptake and distribution following a high zinc diet in adult fish.

The compensatory pathways of other zinc transporters to the effect of the mutation was observed in the case of Znt4, which showed a drastic change in expression to the effect

of *znt1* mutation in fish suggesting it might be an alternative pathway of maintaining zinc homeostasis in mutant fish. There was a statistically significant increase expression of *znt4* in homozygotes compared with wild-type on both of the zinc diets suggesting that Znt4 regulation is affected by the zinc level in the diets as well as the *znt1* mutation (i.e. genotype). This might possibly be supported by observations in worm and mouse models by Davis *et al.*, (2009) and Murgia *et al.*, (2006) respectively, who suggested that *znt4* is a close relative of *znt2* (a gene that is not normally expressed in the intestine of zebrafish) and resides in endosomes (vesicles) for compartmentalization of excess zinc in order to reduce toxicity (Fukada and Kambe, 2011, Cousin *et al.*, 2006). Using a *C. elegans* model, *znt1* knockdown caused an increased intestinal cytosolic zinc level with concomitant up-regulation of vesicular *znt2* (Davis *et al.*, 2009). It is therefore possible that intestinal Znt4 in the present study takes the function of Znt2, which was not expressed in the intestine of zebrafish as observed in a previous study (Feeney *et al.*, 2005) and also confirmed in our present study for both dietary zinc conditions where the transcript was not expressed. Similarly, Murgia *et al.,* (2006) showed in a mouse model of *ZnT4* mutation (lethal milk syndrome) high accumulation of zinc in the enterocytes with concomitant compensatory increased expression of ZnT2, MT I & II and ZnT1. This is as a result of the defect in zinc compartmentalization into the vesicles or zinc transportion to the systemic circulation, thus inducing another zinc effluxing protein, ZnT1, in order to keep the intracellular zinc concentration below threshold level. Moreso, it was shown that a fraction of the vesicular ZnT4 translocates from the trans-Golgi region to the basolateral surface of the plasma membrane upon zinc addition or when the intracellular zinc level is high or when the transporter is over-expressed in fully differentiated, polarized epithelia cells (Huang *et al.*, 2002; Henshall, *et al.*, 2003; Murgia, *et al.*, 2006). This phenomenon helps to flux zinc into the systemic circulation

probably as a compensatory measure when the expression of ZnT1 cannot cope with the cyosolic zinc load for systemic extrusion. The plasma membrane translocation of ZnT4 could possibly be as a result of vesicular fusion with the plasma membrane thereby mediating zinc secretion into the bloodstream (Murgia, *et al.*, 2006).

In previous studies, intestinal Znt4 did not show differential expression in response to high zinc in wild-type zebrafish (Feeney *et al.*, 2005) and in human (Cragg *et al.,* 2005) and this was consistent with the present study with wild-type fish. However, both homozygote and heterozygote mutants showed a statistically significant increased expression in response to the high zinc diet indicating that *znt1* mutation affects Znt4 expression in zebrafish, in a similar pattern as ZnT4 mutation also affects ZnT1 expression in mouse (Murgia, *et al.*, 2006). It is therefore possible that intestinal Znt4 in mutant fish was up-regulated to reduce intracellular zinc by either taking the function of Znt2 for vesicular compartmentalization or by vesicular fusion and translocation to the plasma membrane as a compensatory mechanism for defective Znt1 for zinc extrusion into the bloodstream (Huang *et al.*, 2002; Henshall, *et al.*, 2003; Murgia, *et al.*, 2006).

The expression of Znt5 was also shown to be highly induced only in homozygote mutants following the high zinc diet, suggesting another alternative mechanism (as observed in Znt4 expression) for controlling high cytosolic zinc caused by the *znt1* mutation. Interestingly, both wild-type and heterozygote mutants did not show such a highly induced expression following high zinc diet as seen in the homozygote. Two variants of ZnT5 exist; variant A, which resides on Golgi-enriched vesicles responsible for zinc efflux from the cytosol, and variant B, which is found throughout the cell including the plasma membrane (and endoplasmic reticulum) for dietary zinc uptake into the cytosol with opposing function to ZnT1 (Kambe *et al.*, 2002, Cragg *et al.*, 2002, Cragg *et al.*, 2005; Valentine *et al.,* 2007; Jackson *et al.,* 2007; Thornton *et al.,* 2011).

This is as a result of of the difference in their C-terminal region, which determines their subcellular localization (Thornton *et al.,* 2011). In a previous study it was shown that there was increased intestinal expression of Znt5 in response to high dietary zinc in zebrafish (Feeney *et al.*, 2005) and conversely there was decreased expression in fish gills (Zheng *et al.*, 2008) as well as human intestinal tissues (Cragg *et al.,* 2005). Therefore, the expression of Znt5 in the present study, which like Znt1 serves to reduce the level of zinc in the cytosol, suggests that variant A might be involved in vesicular compartmentalization of excess cytosolic zinc in the homozygotes to maintain homeostasis following high zinc diet as shown by its increased expression. It is suggested that the expression level of variant B is very low and can only be detected after stimulation in specific cell-type (Thornton *et al.,* 2011). Therefore, lack of detection in this and other previous studies of fish enterocytes could be as a result of the fact that variant B cDNA is difficult to generate by RT-PCR (Thornton *et al.,* 2011). Recently, ZnT5 was shown to be transcriptionally regulated as well as regulated through mRNA stability in response to zinc (Coneyworth *et al.,* 2012). In addition, contrary to the existence of the consensus metal response element (MRE) in the promoter region of most metal regulatory genes, there is presence of zinc transcriptional regulatory element (ZTRE) in *ZnT5* gene playing a role in cellular zinc homeostasis (Coneyworth *et al.,* 2012).

Regulation of members of the ZIP family by zinc is complex and may involve control at transcriptional, posttranscriptional, translational and posttranslational levels (Dufner-Beattie *et al.*, 2003, Dufner-Beattie *et al.*, 2003b; Mao *et al.*, 2007; Weaver *et al.*, 2007). ZIP4, among other ZIP transporters, localizes on the apical membrane of enterocytes for dietary zinc uptake and a mutation of *ZIP4* in human results in a genetic disease of mal-absorption syndrome known as acrodermatitis enteropathica (Wang *et al.*, 2002; Kury *et*

al., 2002; Nakano *et al.*, 2009), which was also confirmed in studies with a mouse model (Dufner-Beattie *et al.*, 2007; Geiser *et al.*, 2012). In mammals, this gene is not known to be transcriptionally regulated in response to zinc levels but is regulated through accumulation and increased stability of mRNA transcripts following low zinc and also through endocytosis and subsequent degradation following high zinc (Weaver *et al.*, 2007). Contrary to this view, Liuzzi *et al.*, (2009) suggested an adaptive transcriptional regulation of *Zip4* in the intestine of mouse by a zinc finger kruppel-like transcription factor 4 (klf4) following zinc depletion. This was in cells with extremely low basal expression of Zip4. How *zip4* is regulated in the intestine of fish in response to zinc status has not been demonstrated. However, previous studies have indicated decreased expression of this gene in fish enterocytes following high zinc with increased expression in low zinc and vice-versa but lack of expression in fish gills with high zinc (Feeney *et al.*, 2005). In the present study, *zip4* mRNAwas down-regulated in response to the high zinc diet as expected and showed no differential expression in the mutants compared to the wild-type, i.e. the opposite effect as observed for MT2 expression. This observation did not confirm but may suggest that intestinal *zip4* in zebrafish is transcriptionally regulated through zinc-sensing MTF-1 to oppose MT2 for zinc, as reported for Zip10 in fish gills (Zheng *et al.*, 2008). However, the existence of MREs in *zip4* to confirm regulation through MTF-1 activation in fish is not known. It is possible that intestinal Zip4 in zebrafish is the first line of zinc absorption as it is more highly responsive to dietary zinc than Zip10, which was previously reported to show little or no change in intestine in response to different dietary zinc conditions (Feeney *et al.*, 2005), and was only affected in the gills (Zheng *et al.*, 2008). Hence, we can speculate that zebrafish Zip10 is located at the basolateral membrane of enterocytes like Zip5 or might also be expressed in submucosal tissues. It may function as a second line of

protection and work in concert with Zip4 to raise cytosolic zinc during zinc deficiency just like Znt1 works in close concert as a second line of protection with MT2 to reduce cytosolic zinc under zinc excess conditions. The result of the present study suggests that intestinal zinc absorption mediated by Zip4 may be the same for all the genotypes but the problem of zinc dysregulation in mutants may be the inability of zinc efflux protein(s) to traffic zinc out of the cytosol, and that is why there was no difference in the expression patterns of each of the ZIP protein that participates in zinc uptake (i.e. Zip4, Zip10 or Zip3) in mutants or wild-type (especially when the zinc is under the buffering capacity of MT2 in wild-type fish). This contrasts with the effect seen in zinc transporters that participate in zinc extrusion (i.e. Znt1, Znt4 and Znt5), which showed differential expressions between the wild-type and mutants, because these transporters help to reduce excess intracellular zinc that is normally absorbed by ZIP proteins but could not be adequately buffered by MT2 in Znt1 mutants. Similarly, Zip3 expression did not show differential expression between the genotypes on normal and high zinc diets as also observed for Zip10. This was also in agreement with a previous study where Zip3 expression in the intestine or gills did not change at high zinc status in normal fish (Feeney *et al.*, 2005), although an increased expression was reported in gill following zinc deficiency but the reverse was not the case under conditions of excess zinc (Zheng *et al.*, 2008).

Zip7 mRNA was another transcript that showed a differential regulation between the wild-type and homozygous mutant following the high zinc diet. The up-regulation of Zip7 in the mutant only on the high zinc diet compared to the wild-type control at the basal zinc level is intriguing because Zip7 is a zinc channel that releases zinc into the cytosol from the ER where it resides, assuming similar localization and function for fish as in mammals. In a previous study, intestinal Zip7 either did not change or it showed a

down regulation in response to high dietary zinc, but there was no difference in Zip7 expression in gills between normal and high zinc diets (Feeney *et al.*, 2005). This is similar to the observations in the present study where there was no change between normal and high zinc diets for any of the genotypes except the homozygote on the high zinc diet when compared with wild-type on the control diet. It is possible that intestinal Zip7 is highly expressed in mutants to return labile Zn^{2+} into the cytosol after initial entry for diverse cellular processes. Interestingly, in zinc-exposed cells where ZIP7 was silenced by siRNA, there was no labile Zn^{2+} in the cytosol, no growth factor receptor activation, and no effect on growth or invasiveness. The conclusion must be that before zinc has effects on proteins in the cytosol it has to emerge from the ER and it must get there very quickly and efficiently following zinc treatment of the cells (Hogstrand *et al.*, 2009; Taylor *et al.*, 2008). Thus, according to the latest understanding, zinc that enters the cell is muffled, perhaps by MT in combination with glutathione, and then immediately moved into organelles, such as the ER, before it can re-enter the cytosol. What controls this re-entry, if it is at all controlled, is currently unknown. It is also interesting to note that ZnT1 has recently been speculated to also flux zinc into the ER (Fukada and Kambe, 2011), therefore an excess of ZnT expression in the mutant, including Znt1 (and other Znts e.g Znt5) on the ER may also contribute to increased movement of Zn^{2+} out of cytosol in the mutant fish, in addition to the action of the ‘‘muffler’’ thereby causing higher induction of Zip7 expression on the ER in mutants than wild-type for Zn^{2+} re-entry into the cytosol (Fig. 4.7). Another alternative explanation could be that a variant of Zip7 might be available in zebrafish, performing zinc efflux activity, which was more highly regulated in the mutants than in the wild-type.

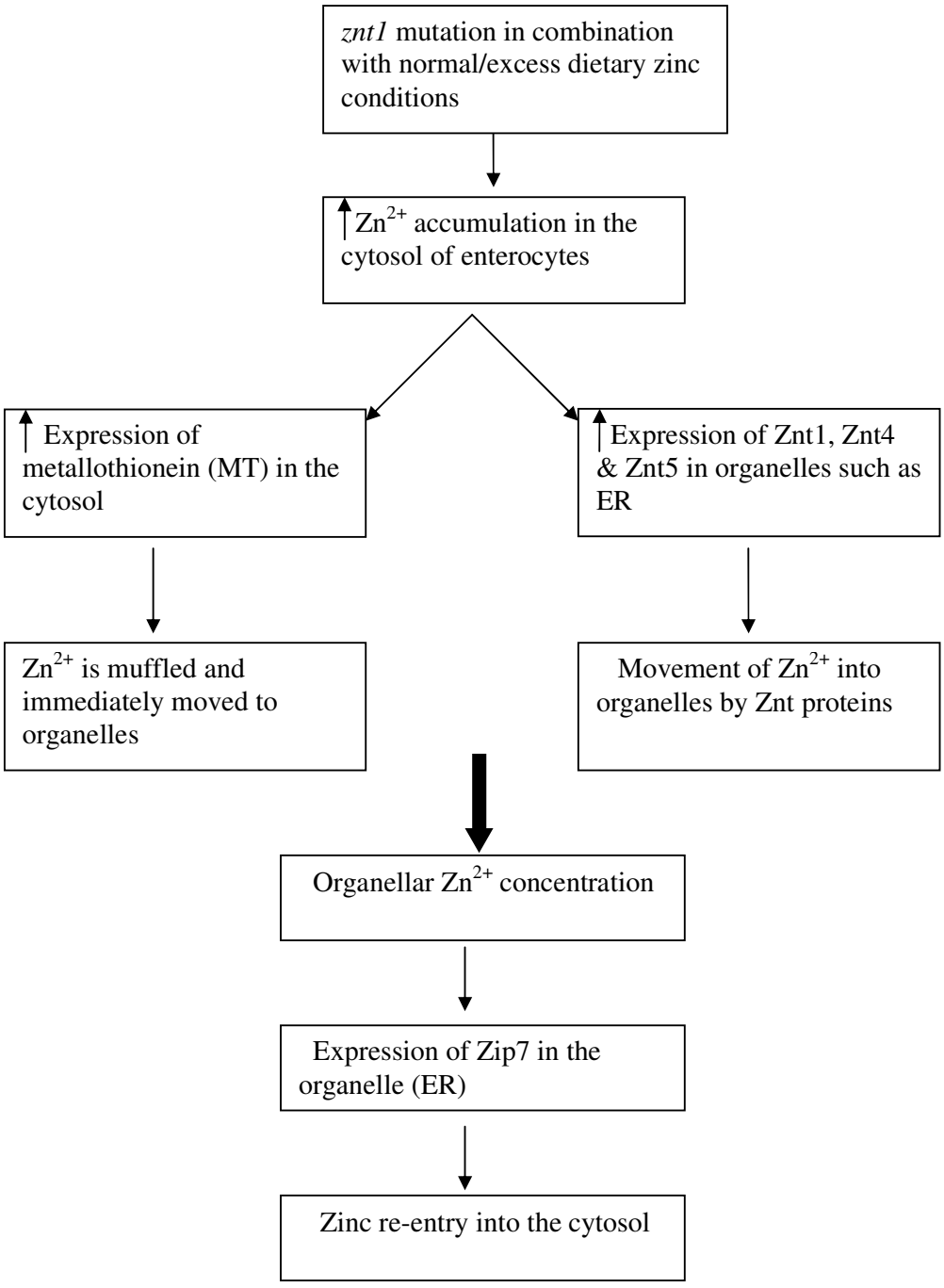

Fig 4.7: Schematic illustrating the proposed interactions between different zinc efflux proteins in Znt1 mutants following normal or excess dietary zinc. The mutation caused increased Zn^{2+} accumulation in the enterocytes leading to increased expression of MT in the cytosol and Znt1, Znt4 & Znt5 in the ER resulting in increased movement of zinc into the organelles, which may cause increased expression of Zip7 in the ER, thus enhancing Zn^{2+} re-entry into the cytosol.

4.5.2 Metal compositions

It is a known fact that high dietary zinc concentrations inhibit copper (Cu) uptake as well calcium (Ca), and Cu deficiency as well as hypocalceamia are signs of toxic effect of excess water-borne zinc (Hogstrand *et al.*, 1995, 1998). On the other hand, Cu level does not always change when zinc intake is within the permissible limit (20-220 mgZn/kg) that does not pose a threat to the organism, as also observed in the present study with the experimental feeds A and B. Cu level can only fall when the level of zinc is excess of the permissible limit (i.e. ≥2000). Similarly, excess Cu or cadmium (Cd) can inhibit or antagonize zinc absorption. Excess zinc also antagonizes Ca absorption and vice versa thereby making the calcium ion a principal factor in reducing water-borne zinc toxicity (Hogstrand *et al.*, 1995; Santore *et al.*, 2002, De Schamphelaere *et al.*, 2005 and Todd *et al.*, 2009). This effect was noticed in the course of the present project, where embryos incubated in zinc-supplemented water, also containing Ca ion supplementation, showed less mortality compared to those without Ca supplement. In organisms, mechanisms exist to regulate the uptake of zinc in case of excess either by reducing uptake or increasing excretion. This also occurs in the regulation of other metals such as Cu or manganese (Mn) due to overlapping specificity. In *C. elegans* with high zinc supplementation there was a 2-fold decrease in Cu and Mn levels in normal wild-type worms compared with the *cdf-1* mutant worms suggesting higher metal (Cu & Mn) accumulation in mutant worm (Davis *et al.*, 2009). Similarly it was reported in human that excess dietary zinc can cause Cu deficiency (Davis *et al.*, 2009). Recently, high accumulation of Mn level was reported in human patients with a genetic mutation in ZnT10 (which is a close relative of ZnT1) suggesting that ZnT10 may also be involved in co-transportation of manganese ions as well as zinc (Quadri *et al.*, 2012). It is therefore possible that Znt1 may take the function of Znt10 (which from the previous

study is absent or not detected) in zebrafish (Feeny *et al.*, 2005). But recently, with the presence or detection of zebrafish Znt10 from Ensembl data (Zv9), it is also possible that both transporters (Znt1 and Znt10) may interact together (for metal transport) due to their close relatedness, thus explaining the high Mn level with mutation of human *ZnT10* and worm *cdf-1* (*znt1*) genes. Recently, the efflux activity and cellular localization of ZnT10 in response to zinc level was shown in human adult (Bosomworth *et al.,* 2012). The protein resides on Golgi apparatus in normal zinc but translocates to the plasma membrane at high extracellualar zinc. Expression was detected at highest level in the intestine, brain and liver tissue suggesting similar efflux function to Znt1 in the enterocytes in response to high zinc. In the present study, the metal analysis in adult tissue which showed no difference in the level of metal deposition in the body of Znt1 mutants and wild-type fish irrespective of the zinc diets, may be as a result of homeostatic control in mutant fish whereby the truncated Znt1 (located in the basolateral enterocytes) and possibly the Znt4 (located in the same region) were both up-regulated to flux out enough or required zinc to the systemic circulation from the zinc trapped in the intestinal tissue. This may explain why there were no obvious physiological ‘‘abnormalities’’ in adult homozygote fish. The difference in the level of accumulated tissue zinc between normal and high zinc diets (irrespective of genotype) confirmed the efficacy of the zinc supplementation as was also confirmed by increased intestinal MT2 expression. In the present study, there were also no genotype differences in the tissue concentrations of Cu, Cd, Mn, Fe and Pb, but only Se. The reason could also be that the compensatory mechanisms of some of the zinc transporters in the mutant also assisted in maintaining these metal ions at normal or required levels because the mutation is likely not a loss-of-function one. It could also be because of the levels of zinc in the two diets (23 and 230mg/kg) were actually within the normal range

that can be well tolerated by the animal (EC, 2003) and so could not affect the metabolism of other metal ions except Se, which has varying concentrations in both feeds unlike others (although this does not explain differences in Se accumulation between genotypes in fish embryos observed in Chapter 3). Another interesting aspect in the compensatory mechanism to maintain adequate tissue level of some of these metal ions (Zn and Se) is the excretory process through the feacal loss. Because of the essentiality of zinc to support life and maintain homeostasis, fish regulate and assimilate zinc irrespective of diet to an optimal level that is not too low or too high for normal biological processes. For instance, on feed A (i.e. ZnN) with low level of zinc of 23mg/kg, zinc was regulated or assimilated in the body to maintain close to optimal level of about 390µg/g and 360µg/g in the tissues of homozygote mutants and wild-type respectively, whereas on feed B (i.e. ZnH), with adequate zinc of 230mg/kg, zinc was regulated to about twice the tissue achieved with feed A, i.e. about 722µg/g and 784µg/g for homozygote and wild-type respectively. This indicates that the difference in tissue zinc accumulation between the two diets (irrespective of genotypes) was only about 2 folds compared to about 10 folds difference in zinc content between the two feeds. Thus, fish, through the help of zinc transporters was able to regulate zinc (whether high or low) close to optimal level. Both genotypes were able to achieve an equal level of zinc on each diet probably by differential expression of zinc transporters between the genotypes or by other regulatory mechanisms, but the feacal loss did not show a statistically significant difference. Interestingly, it was observed that homozygotes produced a total feacal volume twice that of wild type on each diet over a period of two weeks of feeding and feacal collection, thus suggesting a sign of diarrhoea in the homozygotes.

On the other hand, because of the fact that selenium is also essential for life but in a minute quantity, especially for enzyme activity, fish rapidly eliminate this metal in the feaces to achieve an optimal level (Table 4.1). Selenium is known to be important in thyroid gland functions, immunity, antioxidant and anticancer properties. The absorption, assimilation and excretion of selenium involve multiple transport mechanism but the identity of the transporter protein responsible for dietary selenium still remains uncertain (Fairweather-Tait et al., 2011). It was reported that the SLC26 multifunctional anion exchanger family is a good candidate of intestinal selenium transport (Wolfframet al., 1985; Shennan, 1988). It appears from the present study that Znt1 also affects selenium deposition in zebrafish.

On the normal zinc diet (feed A) with a relatively low level of zinc (23mgZn/kg), which contained selenium at about 3.25mg Se/kg feed, homozygote mutants lost more selenium (3.52µg/g feaces) compared to wild-type fish (0.14µg/g feaces). However, there was no significant difference in tissue accumulation (i.e. 0.34 and 0.57 µg/g tissue for the homozygote mutant and wild-type respectively). On the other hand, in fish fed the high zinc diet (feed B) with an adequate zinc level (220mg Zn/kg), which also contained a relatively high selenium level of 10.8mg/kg feed, wild-type first lost more selenium (5.4 µg/g feaces) than homozygote mutants (3.56µg/g feaces). This difference in fecal selenium loss resulted in a significantly higher tissue selenium accumulation in homozygote mutants (1.39µg/g tissue) than wild-type (0.78µg/g tissue). These data suggested that the homozygote mutant cannot regulate selenium when it's high in the diet unlike the wild-type as observed whereby homozygote mutants lost almost equal amounts in feaces for both low and high selenium diets (i.e. 3.52µg/g and 3.56µg/g respectively). It is possible that increased expression of various zinc transporters to maintain homeostasis in mutants might have an effect on the regulation of selenium

concentration by affecting its trafficking, accumulation and excretion. It is equally possible that the regulation of other essential elements might also be affected if their levels are high in the diet as seen for selenium.

For embryo metal analysis (see Chapter 3), in contrast, it was observed that in the 24hpf embryo there was high accumulation of Cu and Se in whole body in the Znt1 mutant embryo similar to what was reported for the *C. elegans* with defective *cdf-1,* which showed a higher Cu level than the wild-type counterpart. There was no difference in total zinc concentration between Znt1 mutant/morphant and wild-type. There was also no difference between Znt1 mutant and wild-type embryos in Fe accumulation, which corresponds to earlier findings in *C. elegans.* The increased accumulation of Cu and Se in Znt1 mutant embryos may possibly be because Znt1 interacts with the proteins responsible for the metabolism of these metal ions which is then affected as a result of the defective *znt1* gene or its altered function. It may also be as a result of Znt1 inability to control or regulate intracellular Zn^{2+} ions in mutant which then affects copper and probably selenium absorption and elimination. The influence of the Znt1 mutation on selenium deposition in zebrafish is unclear and therefore deserves further attention.

4.5.3 *Znt1* mutation and Ras-ERK signalling

The reduction in phosphorylated ERK in mutants suggested that the MAPK signalling pathway is affected either because of the inappropriate binding of the N-terminal regulatory portion of Raf-1 to the C-terminal end of truncated ZnT1, which is responsible for pathway activation, or because of the inability of truncated ZnT1 of the mutant to regulate intracellular Zn^{2+} which is a suppressor of the pathways (Bruinsma *et*

al., 2002; Jirakulaporn and Muslin, 2004; Beharier *et al.*, 2012) or both. As previously demonstrated in embryos (see Chapter 3), this pathways was also affected in Znt1 mutant and morphant embryos and as suggested it may be responsible for the growth retardation observed because suppression or inactivation of this pathway has been reported in various vertebrate models as being responsible for their impaired growth and development or delayed oocyte maturation (Jirakulaporn and Muslin, 2004; Lazarczyk *et al.*, 2008; Bruinsma *et al.*, 2002). Similarly, knockdown of *erk2* produced a very similar effect of impaired growth in zebrafish (Krens *et al.*, 2008) as that observed in Znt1 mutant or morphant zebrafish in the present study. The effect of *erk2* deficiency was also observed in mouse embryos (Saba-El-Leil *et al.*, 2003) lending support to the interaction between ZnT1 and MAPK pathway activation being necessary for diverse cellular process including cell growth, proliferation, differentiation, survival and vertebrate development (Ballif and Blenis, 2001). Based on the observations that addition of a supraphysiological concentration (250 μM) of zinc to the culture medium reduced Ras signaling-dependent events in *C. elegans* and that increasing the total concentration of zinc in *Xenopus laevis* oocytes from 1 to 2.5 mM through injection of $ZnSO_4$ also inhibited Ras signalling, it was proposed that CDF-1 (ZnT1) activates Ras signalling by lowering the intracellular Zn^{2+} concentrations (Bruinsma *et al.*, 2002). However, the same group later showed that binding of Raf-1 to *C. elegans* CDF-1 or human ZnT1 was required for its activation and ERK phosphorylation (Jirakulaporn and Muslin, 2004). In the present study, there was no difference in tissue zinc concentrations between genotypes, irrespective of the level of dietary zinc intake, but ERK phosphorylation was lower in the Znt1 mutant as compared to the control. These results support the idea that Raf-1 activation is dependent on the C-terminus of Znt1 and not on the tissue zinc concentration.

Our results are not entirely conclusive because although there was no difference in total zinc levels between the genotypes, there could be a difference in zinc distribution within the tissue or the cell thus affecting the signalling cascades in the cyotosol. Interestingly, we found that zinc supplementation increased deposition of zinc in the body of wild-type and mutant fish as well as enhanced phospho-ERK abundance in wild-type fish, but not in the mutant. This contradicts the earlier suggestion that Zn^{2+} inhibits Ras signalling (Bruinsma *et al.,* 2002) and futher indicates that the C-terminus of Znt1, in addition to increased cellular zinc, stimulates the MAPK signalling cascade. Since expression of Znt1 is induced by cellular zinc, as confirmed in the present study, it is possible that the observed increased in phospho-ERK is secondary to an increased expression of Znt1. In addition, Zn^{2+} may promote phosphorylation of ERK1/2 by inhibiting dual specific phosphatases (DUSP) (Ho *et al.,* 2008, Sato *et al.,* 1995), which would act cooperatively to enhance the intensity of ERK activation (see schematic; Fig. 7.1). In several models, in which ZnT1 is lacking the C-terminal domain or is completely absent, Ras-ERK signalling was reduced or inhibited with or without addition of zinc to the medium (Beharier *et al.,* 2012, Jirakulaporn and Muslin, 2004; Bruinsma *et al.,* 2002). Conversely, in cells expressing wild-type ZnT1, supplementation of zinc increases ERK phosphorylation (Beharier *et al.,* 2012), suggesting that the C-terminal of ZnT1 is required for zinc-mediated activation of Raf1. It is therefore concluded that Znt1 protein interaction is responsible for MAPK signalling, although zinc supplementation may also enhance the phosphorylation state of ERK and other kinase, through the inhibition of DUSP activity.

4.5.4 Circadian clock gene expression

In vertebrates, the circadian system is responsible for maintaining a tight correlation between environmental light cycles and the regulation of biochemical and physiological events that control complex behavioural patterns so that the organism is best suited to thrive in its natural surroundings (Pettendrigh, 1993). Previous studies have suggested that melatonin secretion from the pineal gland may regulate the circadian clock located in the supraschiasmatic nucleus (SCN) of the hypothalamus and this is responsible for circadian rhythm sleep disorders and some form of insomnia (Turek and Gillette, 2004). The pineal gland is also known to contain high zinc (Demmel *et al.,* 1982) and metallothionein isoforms (Ebadi, 1991). Melatonin secretion is under the control of zinc turnover (Mocchegiani *et al.,* 1998) and this is reduced in old age probably due to low zinc status (Fairweather-Tait *et al;* 2008). Studies using an *in vitro* assay have linked zinc or selenium or zinc-dependent signalling cascades (such as MAPK pathways) in the modulation of circadian rhythm (Munoz *et al.*, 2006; Hu *et al.*, 2011; Cermakian *et al.*, 2002). Therefore the erratic spawning observed in homozygote mutants might be as a result of the *znt1* mutation affecting the rhythm of core circadian genes. In zebrafish, both *Clock* and *Bmal1* normally display rhythmic oscillations in gene expression and on average peak early during the night phase (Whitmore *et al.*, 1998, Cermakian *et al.*, 2000, Pando *et al.*, 2001, Zhuang *et al.*, 2000). This was similar to what was reported in the brain homogenate of the Atlantic salmon (*Salmo salar*) which displays rhythmic expression under short day photoperiods but arrhythmic expression under long day photoperiods (Davie *et al.,* 2009; Pando and Sassone-Corsi, 2002). In the present study where fish were raised under almost equal light and dark phases and with the samples taken during light phase, there was differential expression of the clock genes in the brain homogenate between the Znt1 mutant and wild-type with the mutant showing

down regulation of *clock* (-2.3-fold change) compared to the wild-type on a 23 mg Zn/kg diet, but on the zinc supplemented diet (220 mg Zn/kg) both genotypes displayed equal expression of *clock* suggesting genotype effect which was corrected by zinc supplementation. *Bmal1* on the other hand showed equal expression in both genotypes at the 23 mg Zn/kg diet but treatment with the 220 mg Zn/kg feed increased its expression in both genotypes but with a bigger effect in mutant than wild-type (~5.7 and 3.2-fold change respectively) when compared with control wild-type on the normal zinc diet, suggesting genotype effect only when zinc is supplemented. The expression of *Per2* was similar in both genotypes. That is, there was no difference in expression in either genotype whether at 23 mg Zn/kg or at 220 mg Zn/kg diets, although an effect of zinc to increase expression of this gene was observed in both genotypes at equal levels indicating that the *znt1* mutation does not affect the expression of *Per2* gene. From the results, it is seen that an increased zinc supply enhanced, the expression of all the core clock genes, even those that are not normally expressed during the light phase such as *Bmal1*, *clock* and *cry2a* (Pando and Sassone-Corsi, 2002). *Cry2a* is known to be bi-phasic in regulation. To the best of our knowledge, this is the first *in vivo* experiment demonstrating the influence of zinc in modulating or regulating circadian rhythm genes in a vertebrate. Previous studies only demonstrated in an *in vitro* assay the influence of zinc in modulating the interaction or the binding of the *Bmal1/Clock* transcription factors with E-box element, which is a key event in the regulation of clock-controlled gene expression (Munoz *et al.*, 2006). The *znt1* mutation also affects the regulation of these night or dark-phase oscillating genes but while zinc supplementation helps to correct or modulate the regulation of the *clock* in the mutant to the same level as wild-type, it enhanced the expression of *Bmal1* to a greater extent in mutant than in wild-type fish, whereas there was no change in expression on the normal zinc diet. This showed

that the modulation of clock genes is a direct effect of zinc and/or zinc tranporters. Interestingly the *Drosophila Catsup* mutant, which displays a sleep behavioural disorder, was found to have a disorder in the gene that encodes a protein similar to Zip7 (Harbison *et al.*, 2009).

Another interesting feature worth mentioning in Bmal1 (Arnt1) regulation is the possibility that the high selenium accumulation in the tissue of homozygotes with the high zinc (and high selenium) diet may contribute to the increased modulation of *Bmal1,* resulting in a higher expression level than wild-type receiving same diet, because it was recently shown that selenium is a positive regulator of Bmal1 at the transcriptional level and that this accounts for its protective effect against toxicity induced by anticancer chemotherapy (Hu *et al.*, 2011). The effect seen in the present study indicates that *znt1* mutation could possibly affect Bmal1 expression through selenium dysregulation on the high zinc (and high selenium) diet suggesting that zinc may or may not have a direct effect. The observed changes in regulation of most of the core clock genes may be as a result of light-induced gene expression by blue light photoreceptors in the retina (presumably the cryptochromes or melanopsins) which is enhanced by zinc availability (Cermakian *et al.*, 2002). The zinc could be made available through either from the effect of the *znt1* mutation and/or zinc supplementation which influences the MAPK signalling pathways. This effect may explain the erratic reproduction or spawning pattern and other phenotypic features observed in the mutant adult fish such as shorter life span with delay of puberty/early ceasation of breeding and arched spine/kinked tail as observed and reported in Chapter 3. Previous reports have shown that, in addition to defects in the clock, Bmal1 null-mice also have reproductive problems (Boden *et al.,* 2006), are small in stature, age quickly (Kondratov, 2007), and have progressive arthropathy (Bunger, 2005) that results in

them having less overall locomotor activity than wild type mice. The observed effect of the zebrafish *znt1* mutation of the same or similar functions could arguably be as a result of the altered (decreased or delayed) rhythms of *clock* gene (due to disturbance in MAPK signalling) in mutants on normal diet compared to the wild-type counterpart, which normally oscillate or peak at night (Whitmore *et al.*, 1998, Cermakian *et al.*, 2000, Pando *et al.*, 2001, Zhuang *et al.*, 2000). It's possible the genes oscillate or peak normally in wild-type during the night phase but display erratic oscillation in the mutant (as observed in the present study), thus causing sleeping disorder or making the mutant unable to immediately respond to light after the dark phase. It is hypothesized that since Znt1 and zinc concentration affects MAPK signalling as well as modulation of the *Clock:Bmal1* interaction, Znt1 mutants may have problems in regulation of basal zinc level (for *Clock* gene expression) or supplemental zinc and/or selenium (for *Bmal1* gene expression) which may affect the expression or rhythmicity of clock and clock-controlled genes in fish exposed to light-dark photoperiods through the light-induced MAPK and PKA signalling pathways as illustrated in Figure 4.0 (Fu and Lee, 2003). These pathways are important in stimulating or coordinating the behaviour of animals such as sleep and wakefulness, mating, spawning and reproductive behaviours (Fu and Lee, 2003). In mice, *clock* is the gene that encodes a core clock component and a dominant mutation in this gene (or a mutation that affects its regulation) has been shown to result in various metabolic syndromes in the animal (Turek *et al.*, 2005). Recent phenotype data suggests that both *clock* gene and its partner *Bmal1* play a role in regulation of glucose homeostasis and metabolism which can lead to hypoinsulinaemia, or diabetes, when disrupted. In regards to other functions, another study shows that the CLOCK/BMAL1 complex upregulates human LDLR promoter activity, suggesting that they also play a role in cholesterol homeostasis (Marcheva *et al.,* 2013; Turek *et al.*,

2005; Rudic *et al.,* 2004). *Per2* was unaffected during the day in both genotypes and this was in agreement with previous report about this gene which rhythms during the light-phase, in contrast to its other isoforms (*Per1* and *Per3*), which oscillate at night, suggesting that *Per2* expression is strictly light-dependent in the zebrafish system as also reported in *Xenopus laevis* retina but not in the mammalian system (Zylka *et al.*, 1998, Pando *et al.*, 2001, Zhuang *et al.*, 2000). It was observed that the *Per2* gene transcript, unlike other circadian genes, was absent in some fish that were sampled towards the end of the light-phase. This effect which was more pronounced in homozygote mutants than wild-type, may be due to some individual biological variations. Interestingly it was also observed that the proportion of transcript detection was higher in fish on the high zinc diet than normal zinc diet in those that were sampled towards the end of light-phase. This result indicates that zinc and/or selenium (especially for Bmal1) may affect the circadian rhythm through the activity of ZnT1 because a defect in this protein affects both zinc and selenium metabolism as well as well zinc-dependent MAPK signalling pathways, all of which might have affected the expression of master circadian genes which probably caused the abnormal spawning behavior sometimes observed in homozygote mutant fish. The effects observed on *clock* gene regulation further proved that only zinc (and not the change in selenium level) in the diets accounts for the effect produced in the mutant fish because the effect of selenium was only noticed in Bmal1 expression of mutant, which has high tissue selenium (and not zinc) accumulation which is known to be a positive regulator of Bmal1 transcription (Hu *et al.,* 2011). Therefore, selenium supplementation was accountable for Bmal1 dysregulation in mutants because of their inability to regulate selenium metabolism. It is thus reasonable to conclude that in a normal zinc diet, only the *clock* gene (among other circadian genes) is affected by zinc dysregulation in mutant

and this may be solely responsible for the observed behavioural defect noticed in Chapter 3. Meanwhile, the effect of dietary supplementation of zinc or selenium or combination of both metals in the differential regulation of Bmal1 expression in mutant compared to wild-type fish should be further clarified in a controlled experiment, because in the present study, the higher selenium level in the high zinc diet was never a plan but an accidental inclusion.

4.6 Summary

The defect in the *znt1* gene caused increased mRNA expression of Znt1 and other zinc efflux transporters (specifically Znt4 and Znt5) and a zinc importer (Zip7) in mutants compared with their wild-type counterparts following the high zinc diet, probably as a compensatory response by the efflux proteins to reduce cytosolic free Zn^{2+} ion in the enterocytes of the mutants. The increased free Zn^{2+} ion accumulation was indicated by higher expression of MT2 in homozygote mutants on the high zinc diet than wild-type on the same diet when both were compared to wild-type with normal diet. This defect did not affect the concentration of zinc in body tissue (minus gut and other organs) and feaces but selenium level was affected following high zinc/selenium diets suggesting that mutants may have impaired regulation of selenium metabolism. The maintained control of total zinc accumulation in the body tissue can probably be explained by the compensatory responses by some of the zinc transporters, which probably do not contribute to selenium regulation. The concentrations of other trace elements did not change in mutants and wild-type on the high zinc diet when compared with wild-type on the normal zinc diet probably because their concentrations were similar in both normal and high diets. The defect in the *znt1* gene also affected the expression of brain core circadian genes (especially the *clock* gene) probably due to defective Znt1 in regulation

of zinc metabolism or as a result of its inability to activate ERK1/2 in homozygote mutants compared to wild-type and this might be related to the erratic behaviour in spawning of adult homozygotes.

4.7 Future studies

As stated in the previous chapter, further work is needed to consolidate the data generated from this study especially on downstream activation of MAPK and on clock gene regulation. These include experiments to demonstrate:

i. The interaction of Znt1 with Raf1 in adult mutant and wild-type fish with or without zinc supplementation.

ii. The effect of dietary supplementation of zinc or selenium or combination of both in mutants and wild-types to clarify which one was responsible for the differential regulation of Bmal1 expression.

iv. The involvement and/or mechanism of ZnT1 in selenium metabolism and/or transport.

CHAPTER FIVE

THE ROLE OF ZINC AND ZINC TRANSPORTERS (ZIP10 & ZNT1) IN HATCHING OF ZEBRAFISH EMBRYOS

5 The role of zinc and zinc transporters (Zip10 & Znt1) in hatching of zebrafish embryos

5.1 Introduction

It has been known for over 60 years that zinc is an essential microelement for plants and animals (Prasad, 1995) required in minute quantities for enzyme activity (Vallee, 1959). An estimated 10% of all vertebrate proteins contain zinc with approximately 3,000 zinc protein in the human genome (Passerini *et al.*, 2007). But with the discoveries of new coordination binding environments, this number is likely to rise (Maret, 2009; Andreini and Bertini, 2011). In many proteins, including those with zinc finger and RING finger domains, zinc is used to generate tertiary structure. However, there are likely in excess of 1,000 metalloenzymes belonging to all major functional classes (Vallee and Auld, 1990; Maret, 2009; Andreini and Bertini, 2011). More recently, it has been recognised that the Zn^{2+} ion is involved in cell signalling through physiological inhibition of some enzymes, occurring at picomolar concentrations of free Zn^{2+} (Hase and Maret, 2003; Wilson *et al.*, 2012).

Vertebrate hatching is one of the processes that involves enzymatic activity and in zebrafish hatching occurs between 48-72hpf (Kimmel *et al*., 1995). Zinc has been shown to influence hatching of fish embryos because waterborne zinc exposure caused delayed hatching, probably through zinc binding to the vitelline envelope (aka chorion or egg shell) (Somasundaram *et al.*, 1984; Dave *et al.*, 1986). However, the hatching enzyme (HE) is a zinc-dependent protease contained in the hatching liquid that is activated by zinc (~10^{-5}M) under alkaline pH (Luberda *et al.*, 1993). The enzyme is secreted by hatching gland cells (HGCs) which are located in different areas of the embryo according to the species, but they all have in common the ultrastructural

features of secreting holocrine cells (Schoots *et al.*, 1983) or more appropriately, merocrine cells (Rhodin, 1974). Because the HE is a zinc-dependent protease, there may be a need to supply high quantities of zinc into the HGC. This supply might be regulated by the activity of zinc transporters like ZIPs and ZnTs trafficking Zn^{2+} in and out of the cells and their organelles. Zebrafish Zip10, which is an orthologue of human SLC39A10 (Zheng *et al.*, 2008), is highly expressed in zebrafish hatching gland cells (Thisse *et al.*, 2004). Tissue-specific expression of *zip10* is notable at pre-polster mesendoderm, polster and hatching gland and persists there until 48hpf before it disappears (Thisse *et al.*, 2004). This pattern suggests that this gene is an early marker of mesendoderm, playing a role in early embryonic development and possibly may be involved in hatching of the zebrafish embryo. It was noticed in Chapter 3 that *znt1* is also expressed in the HGC of developing embryos in addition to the presence of free Zn^{2+} ions in the gland cells, suggesting that this may have a role to play in hatching process. Differentiation of HGC is controlled by specific gene regulation, a process programmed early in embryogenesis (Inohaya *et al.*, 1995 & 1999). There are several other genes that are expressed in the anterior-most cells of the head processs (pre-polster), which are important in hatching gland formation and the best characterised among them include *cathepsin L1b (catL1b), hatching enzyme 1a (he1a), kruppel-like factor 4 (klf4), cyclase associated protein-1 (cap1), bone morphogenic protein 4 (bmp4), tetraspanin (cd63), xbp1, goosecoid (gsc), forkhead (foxe3)* and *T-box family of transcription factor (tbx16)*, among others (Vogel and Gerster, 1997; Thisse *et al.*, 1994; Gardiner, 2005; Trikic *et al.*, 2011; Sano *et al.*, 2008; Swindell *et al.*, 2008). It is reasonable then to presume that these genes are members of the same synexpression group and therefore may be involved in the same signalling pathways (Thiese and

Thiese 2008). Most of these genes are nodally regulated and are involved in nodal signalling pathways (Trikic *et al.*, 2011).

In the present study, expression of five HGC markers, namely *zip10*, *znt1*, *catL1b, he1a* and *klf4*, was measured to follow hatching gland development and its dependency upon zinc and zinc transporters; Zip10 and Znt1.

5.1.1 Cathepsin L

Cathepsin L (later known as cathepsin L1b) is a member of the papain superfamily of lysosomal cysteine proteolytic hatching enzymes abundantly produced by the hatching gland cells (Vogel and Gerster, 1997; Gardiner, 2005 and Trikic *et al.*, 2011). The enzyme is a product of the gene known as *CatL* (or *hgg1* or *cstl*). Although, several research articles have demonstrated the inhibitory effect of Zn^{2+} ions on lysosomal cysteine proteases such as cathepsins B, S & L (Inayat *et al.*, 2012; Tully *et al.*, 2006 and Kusunoki *et al.*, 2001), it is not known whether or not there is involvement of Zn^{2+} ion in the regulation of the activity of cathepsin L in the hatching of zebrafish embryo, but it is interesting that HGC simultaneously expresses very high levels of HE, which requires zinc for its activity. If zebrafish cathepsin L1b in the hatching gland is regulated by zinc inhibition, it might serve as a suitable model for studying the pathogenesis of cathepsin L-related diseases in man such as prostate diseases, cancer, Alzeimer's disease, reproductive and bone disorder (Gelb *et al.*, 1996). Phylogenetic and gene structure analysis have shown that zebrafish *catL1a* and *1b* genes show a high degree of structural conservation with human *cathepsin L* but zebrafish *cathepsin L1c* present different exon organisation (Tingaud-Sequeira, 2007). Cathepsins have also been shown to participate in apoptosis, although the mechanisms are not clearly understood (Turk *et al.*, 2000).

5.1.2 Hatching enzyme

Zebrafish hatching enzyme (zHE1) is an astacin family of zinc metalloproteases that digest the egg envelope at the time of hatching (Kawaguchi *et al.*, 2008; Kawaguchi *et al.*, 2006; Kawaguchi *et al.*, 2005; Kawaguchi *et al.*, 2010). Orthologus genes to *zHE1* are found in all vertebrate genomes (refer to section 1.8.2 for more details). Hatching enzyme is activated by zinc (Fan *et al.*, 2010) which suggests zinc might have an opposing function on zHE1 and CatL1b. The crystal structure of zHE1 has been elucidated and solved at 1.10Å resolution (Okada *et al.*, 2010). Astacins are found throughout the animal kingdom as well as in bacteria and several of these enzymes are crucial in embryonic development, tissue differentiation, and extracellular matrix assembly and many are therapeutic targets. It is suggested that ovastacin, which is the closest human homologue to zHE1, could play a physiological function similar to that performed by hatching proteases in evolutionary distant species like arthropods, birds, amphibians and fish (Quesada *et al.*, 2004). This function was also seen in cathepsin L involvement in the hatching of the mammalian blastocysts known as zonal escape or zonal lysis (Seshagiri *et al.*, 2009).

5.1.3 KLF4

Klf4 belongs to the Kruppel-like factor family of zinc finger family of transcription factors characterized by a highly conserved DNA-binding domain at the C-terminus, consisting of three C_2H_2 zinc fingers which bind GC-rich or CACC box elements in the promoters of many genes involved in polster and hatching gland formation required for hatching (Swindell, 2008). It is the only known transcription factor reported in

zebrafish in the control of polster formation which is required for further specification of the polster into hatching gland (Gardiner, 2005). Interestingly, knockdown of *klf4* in zebrafish by morpholino oligonucleotide resulted in apparently normal embryonic development until 24hpf, but the embryos fail to hatch at 3dpf due to lack of expression of the hatching enzyme gene *cathepsin L* and other polster markers (such as *cap1*, *bmp4* and *foxe3*) in the polster and the hatching gland (Gardiner, 2005; Swindell, 2008). Incidentally, Klf4 has been reported to drive expression of Zip4 in response to zinc depletion in cells derived from mouse small intestine (Liuzzi *et al.*, 2009).

5.1.4 Zip10 and apoptosis of the HGC

The release of HE from the HGC is accompanied by degeneration of the cells by apoptosis contrary to the function of true holocrine cells (Schoots *et al.*, 1983) but suggestive of merocrine cell function (Rhodin, 1974). During screening for anti-apoptotic drugs, apoptosis of the HGC was observed in wild-type zebrafish embryos as early as 24hpf even before the HE formation or release (Parng *et al.*, 2004) suggestive of developmental apoptosis rather than cell degeneration accompanied by HE release. This developmental apoptosis was inhibited by a caspase 3 enzyme inhibitor (Parng *et al.*, 2004). Therefore, it is possible there is a difference between developmental apoptosis (with no HE release) and hatching-induced apoptosis (following HE release) in the HGC of zebrafish regulated by different pathways for different function or expression. It is possible that both apoptotic processes might be induced or inhibited by Zn^{2+} ions through the activity of Zip10.

5.2 Study Objectives

Because of the hatching effect observed in Chapter 3 in embryos of mixed genotypes incubated in zinc excess or zinc chelation, we aimed to find out in controlled experiment using wild-type embryos, whether zinc has a role to play in hatching processes. In addition, it was indicated that among various zinc transporters in zebrafish embryos, *zip10* is the only gene that is expressed in the HGC (Thiese *et al.*, 2004). From our incidental findings in Chapter 3, there was detection of *znt1* mRNA as well as presence of free Zn^{2+} ions in the HGC of developing embryos, thus, making us to assume that zinc may have a role in the process of hatching probably through the activity of zinc transporter/channel (s), which then led us to the second objective of finding out the effect of zinc transporters (Zip10 and Znt1) in the process of hatching and their effects on the developmental apoptosis of the HGC.

5.3 Materials & Methods

5.3.1 Water-borne zinc exposure and zinc depletion in wild-type embryos

Embryos from wild-type fish were collected and incubated in excess zinc or in zinc depletion (by TPEN) for 5dpf as described in Chapter 3 (section 3.3.2.2). The control embryos were incubated in standard fish tank water (see composition in appendix 9.1). The time and number of hatching were observed and recorded for different treatments.

5.3.2 Expression of hatching gland markers on HGC of zinc excess and zinc depleted wild-type embryos

ISH probes for four hatching glands marker genes in zebrafish (viz; *CatL 1b, He1a, klf4* and *zip10*) were produced as previously described in Chapter 2 (section 2.2.7.1.1-2.2.7.1.1.8.8). The primer sequences, annealing temperatures, amplicon size, restriction enzymes (for orientation) and RNA polymerases used for different genes are also described in these sections.

The ISH expression of each of the four markers was carried out (as described in Chapter 2; Thiese *et al.*, 2004) on wild-type embryos (dechorionated) incubated in 100µM zinc or 5µM TPEN at 24hpf of development while the expression at 48hpf was performed with two of the markers (*CatL 1b* and *He1a*) at each treatment condition and compared with the expression in wild-type control incubated in normal standard fish tank water at the same developmental stages. The ISH expression of *CatL 1b* was also performed on chorionated embryos at 48hpf in both treatment conditions.

5.3.3 Generation of Zip10 (Slc39a10) and Znt1 (Slc30a1) morphants

Anti-sense morpholino modified oligonucleotides for *zip10* and *znt1* were designed and procured from GeneTools LLC (Philomath, USA) and zebrafish embryos were injected for each gene knockdown as described in chapter 2 and 3. The sequences for each MO types (translational blocker or splice blocker) for *zip10* and *znt1* were shown in Table 2.2.2. Wild-type embryos were injected with 2-4 ng of either *znt1* or *zip10* MO as previously described (Chapters 2 & 3) and the time to hatch was observed and recorded. Un-injected embryos from Znt1$^{\Delta 40/\Delta 40}$ homozygote mutants were also observed for hatching and all were compared with control wild-type embryos.

5.3.4 Expression of *zip10* and *znt1* on hatching gland of Zip10^{MO}, Znt1^{MO} and Znt1$^{\Delta 40/\Delta 40}$

ISH probes for *zip10* and *znt1* were prepared as mentioned in section 5.3.2. The expression of *znt1* and *zip10* genes in HGC of 24-48hpf control wild-type embryos was compared with Zip10^{MO}, Znt1^{MO} and Znt1$^{\Delta 40/\Delta 40}$ at the same developmental stage, using the whole mount ISH method described in section 2.2.7.1.2 (Thiese *et al.*, 2004).

5.3.5 Expression of hatching gland markers on Zip10^{MO}, Znt1^{MO} and Znt1$^{\Delta 40/\Delta 40}$

The ISH expression of each of the four markers (*catL 1b, he1a, klf4* and *zip10*) was carried out on Zip10^{MO} at various developmental stages (10, 24, 33, 48, 55 and 72hpf) and compared with wild-type embryos at similar stages of development. Similarly the expression of two of the markers (*catL 1b* and *he1a*) was performed on Znt1^{MO} and Znt1$^{\Delta 40/\Delta 40}$ at 24 and 48hpf of development and compared with wild-type un-injected control.

5.3.6 Fluorometric imaging of free zinc ion (Zn^{2+}) in the hatching glands

The synthetic ZTRS zinc probe was incubated (as detailed in Chapter 3) with Znt1$^{\Delta 40/\Delta 40}$ homozygote, Znt1^{MO}, Zip10^{MO}, and wild-type embryos with or without zinc or TPEN added to the incubation medium. The hatching gland from each embryo was imaged with epi-fluorescence microscope and photograph taken in both chorionated and dechorionated embryos.

5.3.7 Fluorometric imaging of apoptotic cells of hatching glands

Acridine orange dissolved in water was first measured spectrophotometrically for its sensitivity to Zn^{2+} supplementation and depletion. Thereafter wild-type, $Znt1^{\Delta 40/\Delta 40}$ homozygote, $Znt1^{MO}$ and $Zip10^{MO}$ embryos with or without zinc or TPEN addition to the incubation medium were incubated in 5-10µg/ml of acridine orange for 10 minutes at 28.5 ^{o}C. The embryos were washed 2-3 times in standard fish tank water and then mounted for imaging of apoptotic cells in the hatching gland. $p53^{MO}$ injected embryo as well as embryos treated with the caspase III enzyme inhibitor, fluoromethylketone (Z-DVD-FMK; $C_{30}H_{41}FN_4O_{12}$) which were incubated in 500µM solution at 12hpf for 24 hrs were also imaged for observation of apoptosis of HGC.

5.4 Results

5.4.1 Effects of zinc and TPEN exposure on hatching of wild-type embryos

Excess zinc in the incubation medium delayed the time of hatching and reduced the number of hatched embryos whereas zinc depletion by TPEN exposure accelerated hatching (Fig. 5.1). At 48hpf, zinc depletion by TPEN hatched about 75% of embryo and by 51hpf almost all the zinc-depleted embryos had hatched. For control embryos only 13% hatched at 48hpf and 27% at 51hpf. On the other hand, zinc addition significantly reduced the number of hatched embryos to none by 48hpf and 6% by 51hpf which slightly increased to 13% by 72hpf, when all other groups showed 100% hatching. Embryos co-incubated in zinc and TPEN did not differ much from the control embryos indicating that the effect of zinc or TPEN on hatching of embryo is zinc specific. Survival of embryos was >90% for all groups after normal hatching at 72hpf (3dpf) until 168hpf (7dpf) except in the zinc treated group where only about 40% of the

hatched embryos survived. The impressions of HGC were visible in embryos in all treatment groups at 30 and 48hpf indicating that zinc exposure or depletion does not influence the presence of HGC (Fig. 5.1.1).

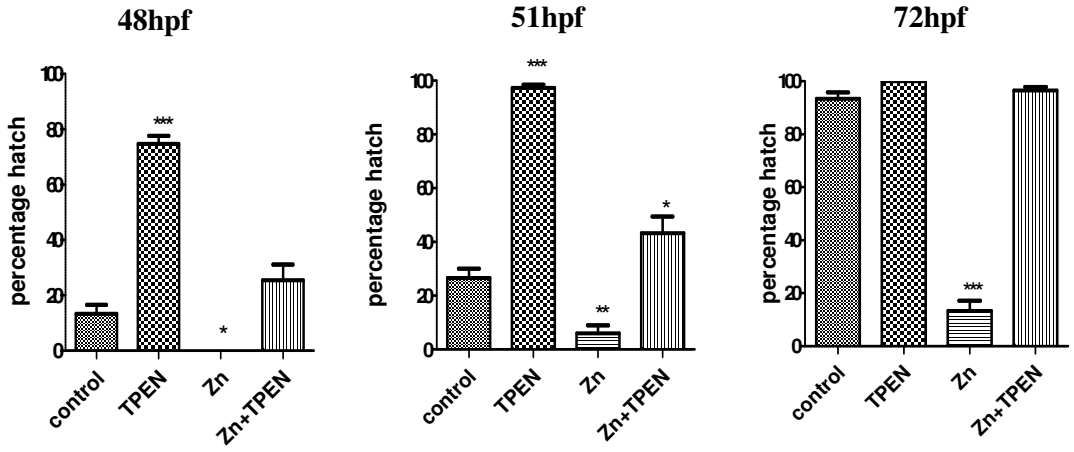

Fig 5.1: **Effects of zinc and TPEN treatment on hatching in wild-type embryos at 48, 51 & 72hpf**. Zinc exposure at 100µM retards hatching whereas zinc chelation by TPEN at 5µM speeds up hatching. Data are expressed as percentage of hatched embryos and presented as the mean ± SEM with significance accepted at $p \leq 0.05$ using 1-way ANOVA followed by Dunnett's post-hoc test for multiple comparison within each group. n=15 with 10 embryos per n in each group. **Key;** *: significant at $p \leq 0.05$, **: significant at $p \leq 0.01$, ***: significant at $p \leq 0.001$.

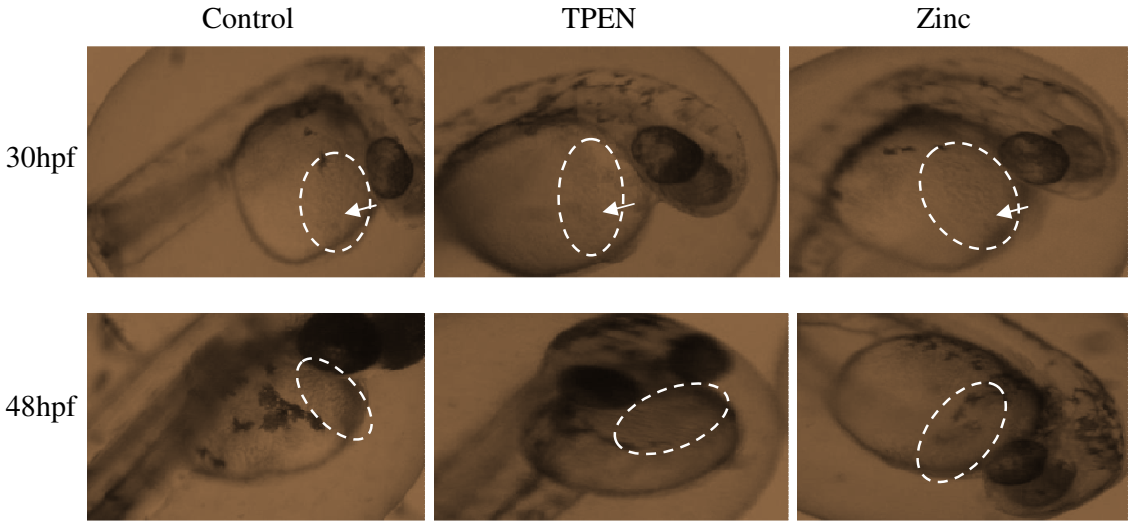

Fig 5.1.1: Presence of HGC impression is visible in all treatment groups at 30hpf & 48hpf prior to hatching (white highlight). Embryos showed no obvious morphological differences in stages of development between treatments.

5.4.2 Effect of zinc excess or depletion on ISH expression of hatching gland markers in wild-type embryos

The results of gel electrophoresis for generating the DIG-labelled antisense RNA probes (hatching gland markers) used in section 5.3.2-5.3.5 are shown in Appendix 9.16 (Fig. 9.2).

Zinc exposure or depletion did not affect the presence of HGC and the expression of hatching gland markers at 24 and 48hpf in dechorionated embryos (Fig. 5.2 & 5.2.1) but incidentally, it was noticed that the expression of the HGC marker *catL1b* was blocked in chorionated embryos in the zinc exposed group (Fig. 5.2.3).

A. 24hpf (dechorionated)

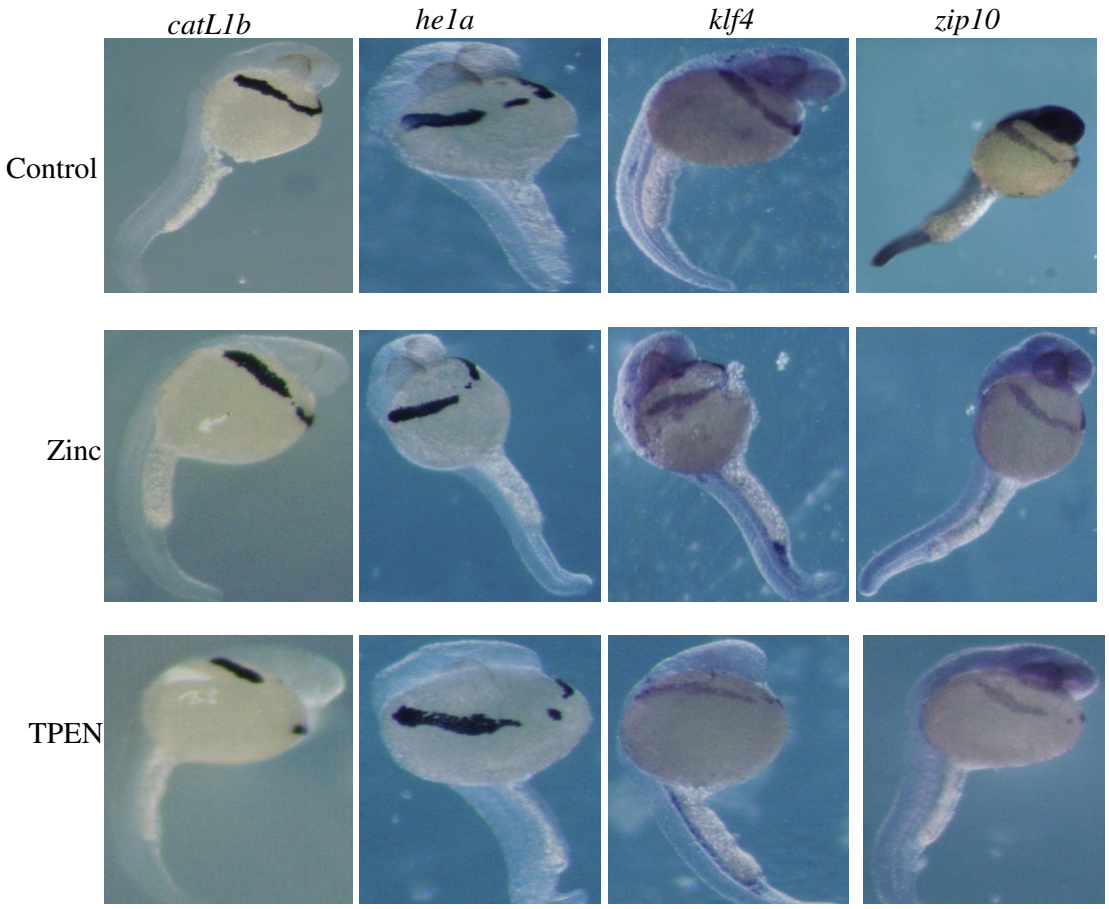

Fig 5.2: Effect of zinc exposure or depletion on the expression of hatching gland markers in wild-type embryo. Expression of the four hatching gland markers in HGC of 24hpf wild-type embryos incubated in 100µM zinc or 5µM TPEN from 10hpf. The ISH technique was performed on the embryos after chorion removal at 24hpf. All markers were present under all three conditions (n=10 embryos where N=3 experiments per treatment).

B. 48hpf (dechorionated)

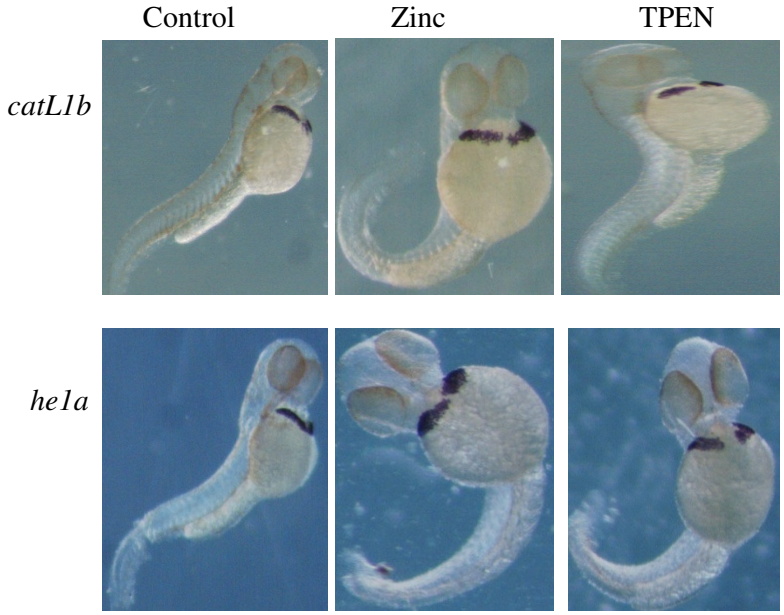

Fig 5.2.1: Effect of zinc exposure or depletion on the expression of hatching gland markers in wild-type embryos. Expression of *catL1b* and *he1a* markers in HGC of 48hpf wild-type embryos incubated in 100µM zinc or 5µM TPEN from 10hpf of development. The ISH technique was performed on the embryos after chorion removal at 48hpf. Both markers were expressed under all three conditions (n=10 embryos where N=3 experiments per treatment).

C. 48hpf (chorionated)

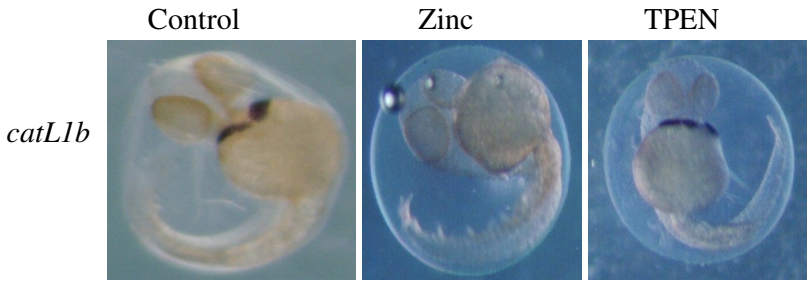

Fig 5.2.2: Effect of zinc exposure or depletion on the expression of hatching gland markers in chorionated wild-type embryo. Expression of the *catL1b* marker in HGC of 48hpf wild-type embryos incubated in 100µM zinc or 5µM TPEN from 10hpf of development. The ISH technique was performed on intact embryos at 48hpf. The probe (marker) was able to penetrate the chorion and marked the hatching gland cells in normal and TPEN treated embryos but apparently not in zinc treated embryos (n=10 embryos where N=3 experiments per treatment).

5.4.3 Effects of zinc transporter deficiencies on hatching of embryos

Knockdown of *zip10* (Zip10^{MO}) drastically delayed hatching and reduced the percentage of hatched embryos at 72hpf (Fig. 5.3) with no delay in development. Deficiencies in Znt1, either through morpholino knockdown (Znt1^{MO}) or lack of the last 40 amino acids of the protein (Znt1$^{\Delta 40/\Delta 40}$), hastened hatching with increased numbers of hatched embryos at 51hpf (even with delay in the stages of development) compared to the wild type control. Scrambled or mis-matched control MO injected embryos did not show a difference from the un-injected wild-type control (Fig. 5.3). At 51hpf, a high proportion of embryos injected with the *znt1* MO or carrying the *znt1*$^{\Delta 40/\Delta 40}$ mutation hatched compared to wild-type whereas a significantly lower number of Zip10^{MO} hatched. Specifically, 82% of Znt1^{MO} and 71% of Znt1$^{\Delta 40/\Delta 40}$ embryos compared to 40% of wild-type embryos control hatched by 51 hpf. On the other hand the frequency of hatching of Zip10^{MO} embryos was significantly reduced to 5% at 51hpf which slightly increased to 12% at 72hpf when all other groups had 100% hatching. Survival of embryos was >90% for all groups after normal hatching at 72hpf (3dpf) until about 168hpf (7dpf) in Zip10^{MO} where only about 38% of the hatched embryos survived.

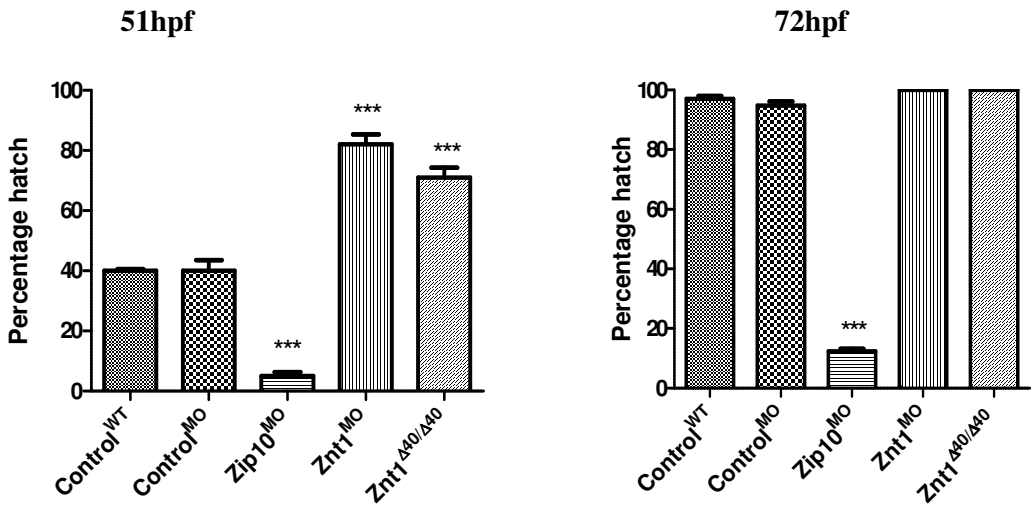

Fig 5.3: Effect of zinc transporter deficiencies on percentage of hatching. Wild-type embryos were injected with mis-matched control MO or zip10 MO or znt1 MO and hatching was compared to wild-type uninjected control at 51 and 72hpf. Hatching of $Znt1^{\Delta 40/\Delta 40}$ mutant was also compared. Zip10 deficiency delayed hatching while znt1 deficiency shortened hatching time. Data are expressed as percentage of hatched embryos and presented as the mean ± SEM with significance accepted at $p \leq 0.05$ using 1-way ANOVA followed by Dunnett's post-hoc test for multiple comparison within each group. n=15 with 10 embryos per n in each group. **Key;** *: significant at $p \leq 0.05$, **: significant at $p \leq 0.01$, ***: significant at $p \leq 0.001$.

5.4.4 Effects of zinc transporter deficiencies on hatching gland expression and development

Whole mount ISH showed distinct expression of *zip10* and *znt1* in HGCs of 24hpf wild-type embryos (whether or not injected with control/scrambled MO), and the expression disappeared in embryos treated with the respective MO to *zip10* and *znt1* demonstrating the efficacy and specificity of each MO. The Znt1 homozygote mutants also had less or no expression of *znt1* in the HGCs (Fig. 5.4). The expression of *znt1* in the HGC was shown for this first time in this study.

All the four selected hatching gland markers (*catL1b, he1a, klf4* and *zip10*) were expressed in wild-type embryos at 10hpf & 24hpf (Fig. 5.4.1 & 5.4.2) but the expression of *klf4* and *zip10* began to disappear at 33hpf (Fig. 5.4.3) and had completely gone by 48hpf (Fig. 5.4.4) whereas *catL1b* and h*e1a* began to disappear at 55hpf (Fig.

5.4.5) with complete disappearance at 72hpf (Fig. 5.4.6). It was observed that both *catL1b* and *he1a* were highly expressed genes with signal detection by ISH within 30 min whereas *klf4* and *zip10* showed weak expression with detectable staining between 3-4hrs (NB: *znt1*also showed weak expression with staining detected around this time as well). On the other hand, the Zip10 morphant did not show expression of *zip10* throughout the developmental stages but there was expression of *catL1b* & *he1a* up to 33hpf before the stained cells or the gland tissues began to dislodge and started peeling off (red arrows) (Fig. 5.4.3) leading to complete loss of staining at 48hpf (Fig. 5.4.4), but the expression of *klf4* was completely lost by 33hpf (Fig. 5.4.3). Wild-type embryos still showed slight expression of *catL1b* and *he1a* around the pericardial membrane at 55hpf but this completely disappeared at 72hpf and without any sign of peeling or sloughing off (Fig 5.4.5 & Fig 5.4.6). The Znt1 morphant and mutant showed similar but abundant expression of *catL1b* and *he1a* similar to the wild-type but no expression of the *znt1* marker was present throughout the period of observation at 24 and 48hpf (Fig. 5.5 & 5.5.1).

5.4.4.1 Expression of *zip10* & *znt1* in HGC in Zip10^{MO}, Znt1^{MO} and Znt1$^{\Delta 40/\Delta 40}$ embryos at 24hpf

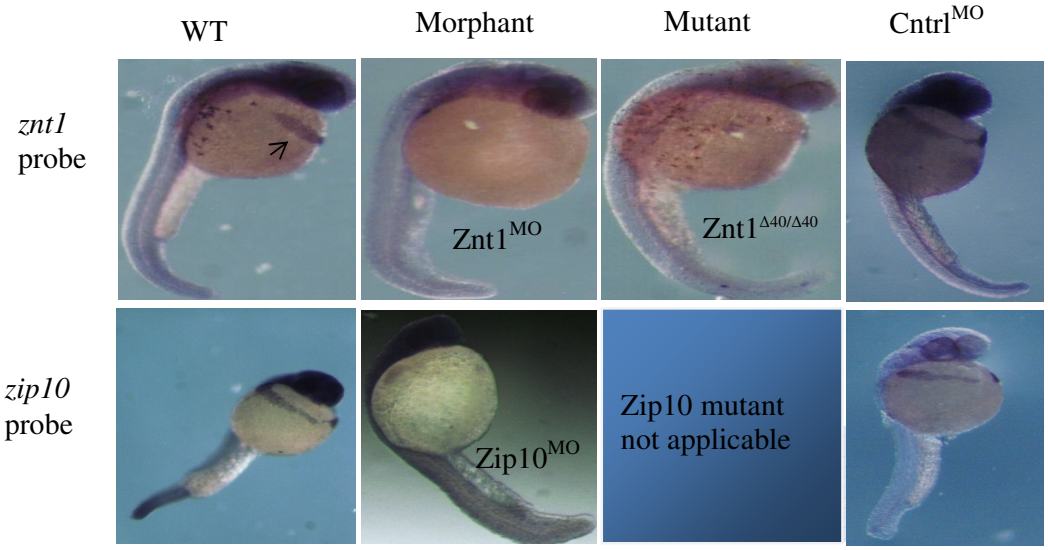

Gene expression	WT	Control morphant	Zip10 morphant	Znt1 morphant	Znt1 mutant
znt1	97%	93%	-	*3%	*10%
zip10	100%	97%	*0%	-	-

Fig 5.4: Effect of Znt1 or Zip10 deficiency on the expression of the respective gene marker. mRNA expression of *znt1* and *zip10* gene markers on the hatching glands of 24hpf embryos of wild-type, morphants (Znt1, Zip10 & control) and Znt1 homozygote mutant. Note the absence of expression in the respective morphant (except embryo injected with control or scramble MO) and Znt1 homozygote mutant. Table showed the percentage of embryos of different types showing expression of the respective gene. NB: *znt1* expression was demonstrated for the first time in the HGC of wild-type embryos (arrow). N=3 experiments per treatment where n=10 embryos.

5.4.4.2 Effect of *zip10* knockdown on expression of hatching gland markers

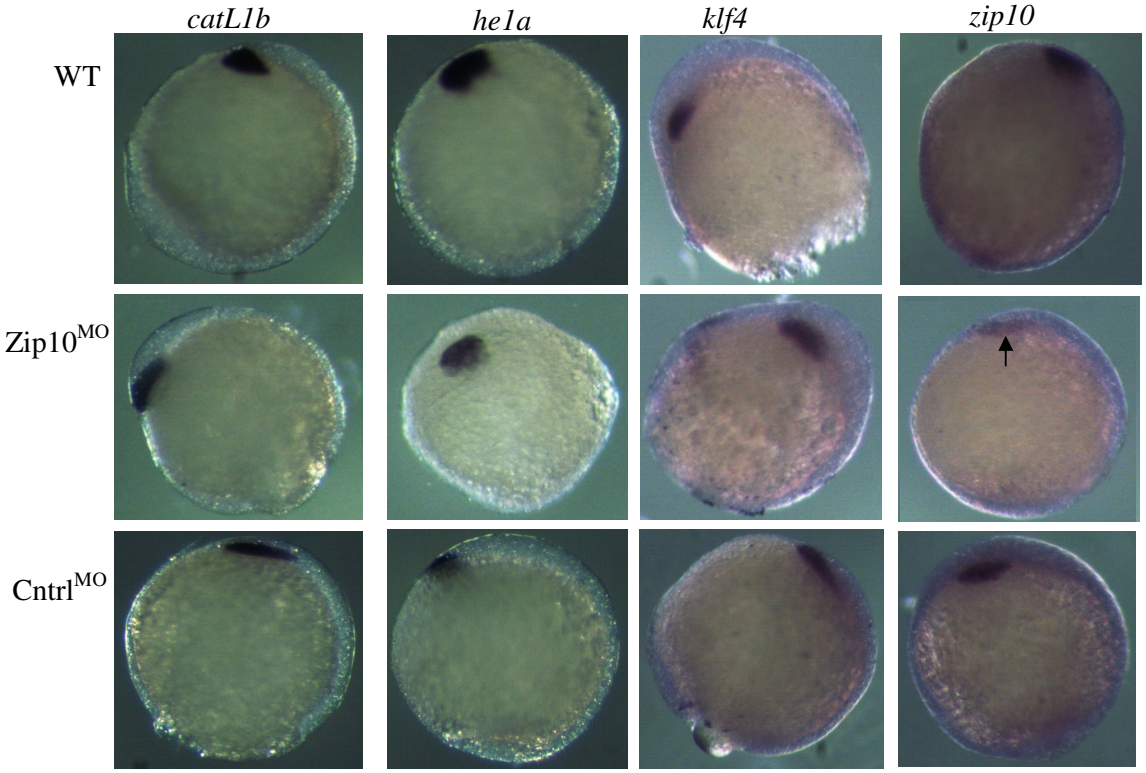

Embryo types	*catL1b*	*he1a*	*klf4*	*zip10*
WT	100%	100%	100%	100%
Cntrl morphant	100%	100%	100%	100%
Zip10 morphant	100%	100%	100%	*3%

Fig 5.4.1: Effect of *zip10* knockdown on expression of hatching gland markers in 10hpf embryo. mRNA expression of the four hatching gland markers at the polster region of 10hpf wild-type embryos, Zip10 and control morphants. Expression of the *zip10* marker was reduced or completely lost in Zip10 morphant (arrow). Table indicated the percentage of embryos showing expression of respective hatching gland gene marker (N=3 experiments per treatment where n=10 embryos).

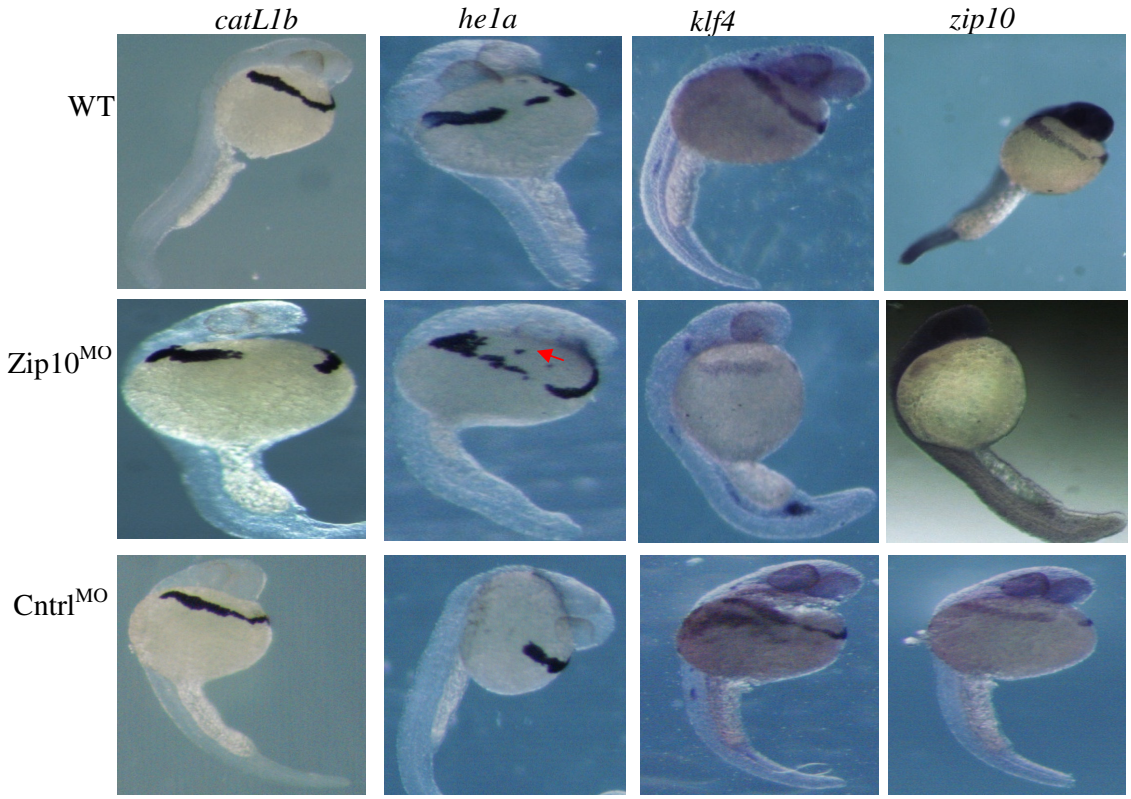

Embryo types	*catL1b*	*he1a*	*klf4*	*zip10*
WT	100%	100%	100%	100%
Cntrl morphant	100%	100%	100%	100%
Zip10 morphant	100%	100%	100%	*0%

Fig 5.4.2: Effect of *zip10* knockdown on expression of hatching gland markers in 24hpf embryo. mRNA expression of the four hatching gland markers on the HGC of 24hpf wild-type embryos, Zip10 and control morphants. Expression of the *zip10* marker was completely abolished in the morphant. Arrow showed the position of the mislocalized cells in the morphant. Table indicated the percentage of embryos showing expression of respective hatching gland gene marker (N=3 experiments per treatment where n=10 embryos).

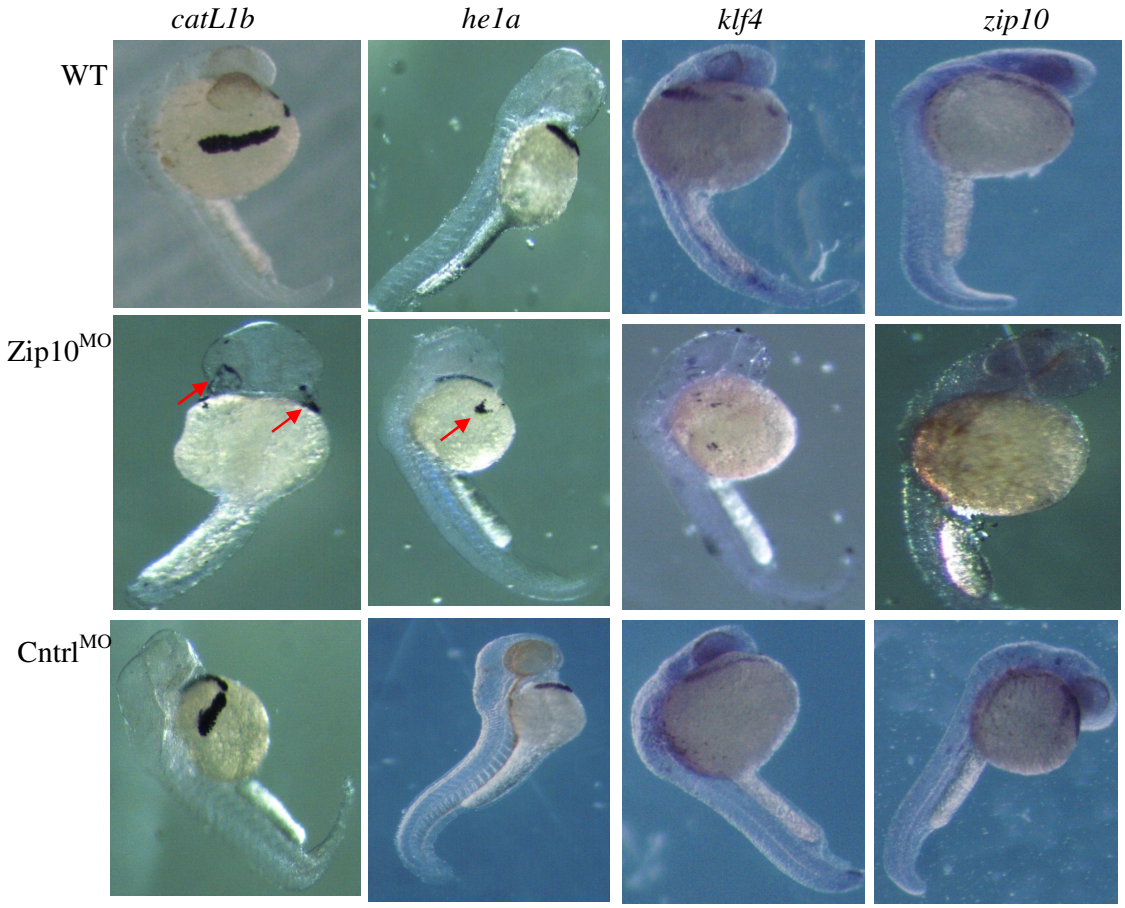

Embryo types	*catL1b*	*he1a*	*klf4*	*zip10*
WT	0%	0%	0%	0%
Cntrl morphant	0%	0%	0%	0%
Zip10 morphant	*97%	*97%	*100%	*100%

Fig 5.4.3: Effect of *zip10* knockdown on expression of hatching gland markers in 33hpf embryo. mRNA expression of the four hatching gland markers on the hatching gland cells at 33hpf in wild-type embryos, Zip10 and control morphants. There is evidence of gland tissues in Zip10 morphants, gradually sloughing off or detaching from the normal position on the yolk and becoming scattered over the body (red arrows) as observed for all markers except the *zip10* marker which was never expressed. Table indicated the percentage of embryos showing complete lack of expression or sloughing of gland tissue to each gene marker (N=3 experiments per treatment where n=10 embryos).

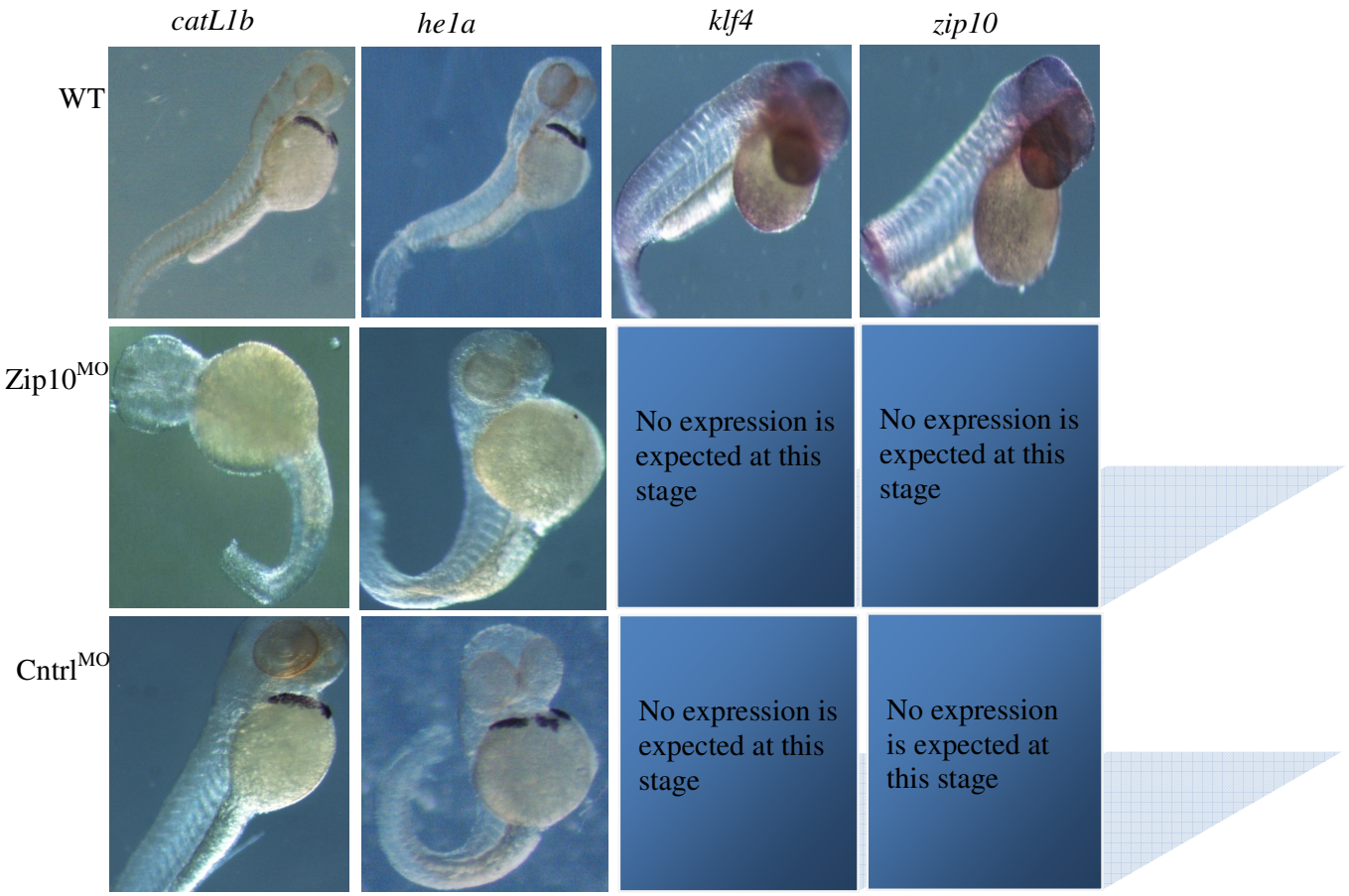

Embryo types	*catL1b*	*he1a*	*klf4*	*zip10*
WT	0%	0%	100%	100%
Cntrl morphant	0%	0%	100%	100%
Zip10 morphant	*100%	*97%	100%	100%

Fig 5.4.4: Effect of *zip10* MO on expression of hatching gland markers in 48hpf embryo. mRNA expression of the four hatching gland markers on the hatching gland cells at 48hpf in wild-type embryos, Zip10 and control morphants. Expressions of *klf4* and *zip10* markers normally disappeared in wild-type at 48hpf while those of *catL1b* and *he1a* still persisted in control wild-type embryos but were completely absent in the zip10 morphant. Table indicated the percentage of embryos showing complete lack of expression to each gene marker (N=3 experiments per treatment where n=10 embryos).

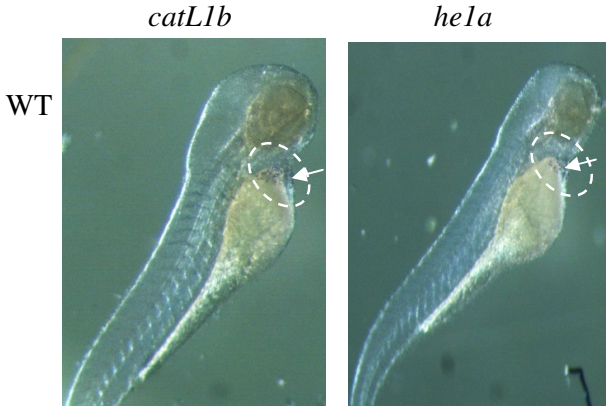

Fig 5.4.5: ISH expression of *catL1b* and *he1a* in the hatching gland cells at 55hpf in wild-type embryos (pre-hatched). The expression still persists on the pericardial membrane but was gradually regressing and absorbing into the body (white highlight). No sign of sloughing off was observed (n=10 embryos where N=3 experiments per treatment).

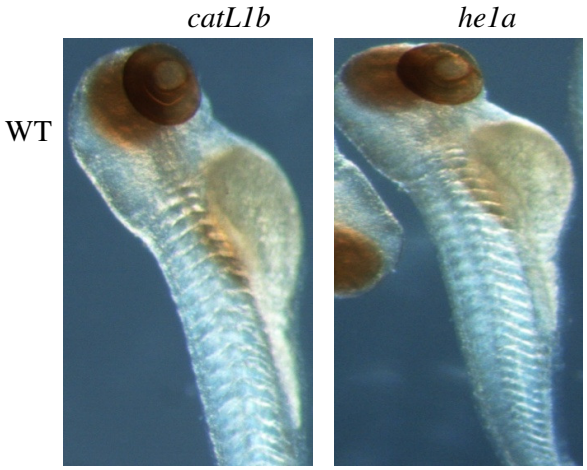

Fig 5.4.6: ISH expression of *catL1b* and *he1a* on the hatching gland cells at 72hpf in wild-type embryos. The expression normally disappeared or absorbed into the body with no indication of sloughing off (n=10 embryos where N=3 experiments per treatment).

5.4.4.3 Effect of *znt1* knockdown or mutation on expression of hatching gland markers

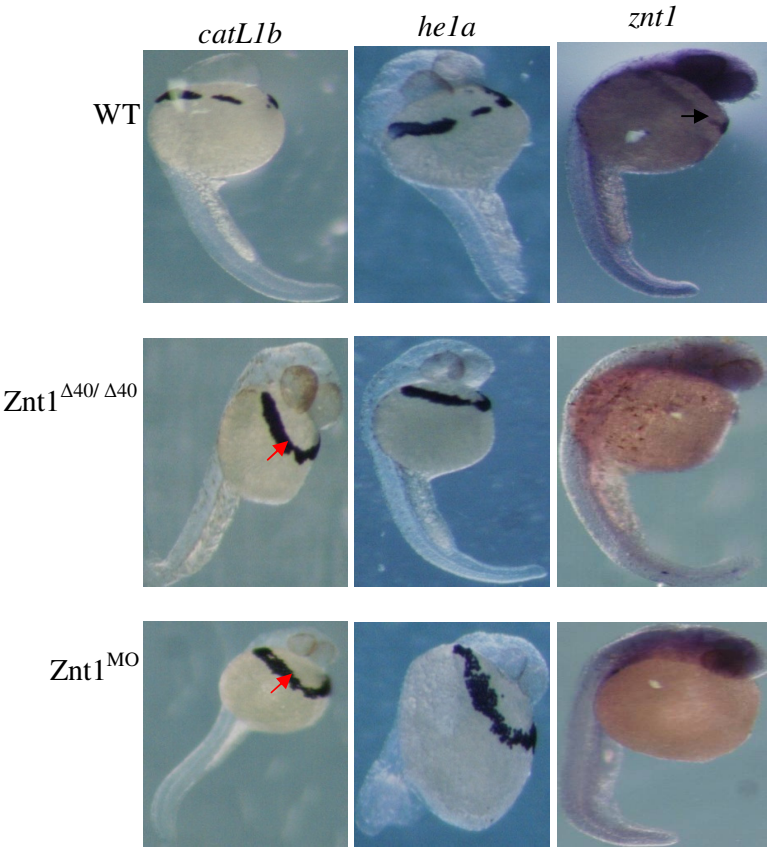

Fig 5.5: Effect of Znt1 deficiency on the expression of HGC markers. ISH expression of *catL1b, he1a* and *znt1* in the hatching gland cells at 24hpf in wild-type, Znt1 mutant and Znt1 morphant embryos. Expression of *znt1* was present in the HGC of wild-type (black arrow) but was abolished in the HGC of Znt1morphant and Znt1 homozygote mutant. There's possible abundant expression of *catL1b* and *he1a* in the mutant and morphant (red arrows). N=3 experiments per treatment where n=10 embryos.

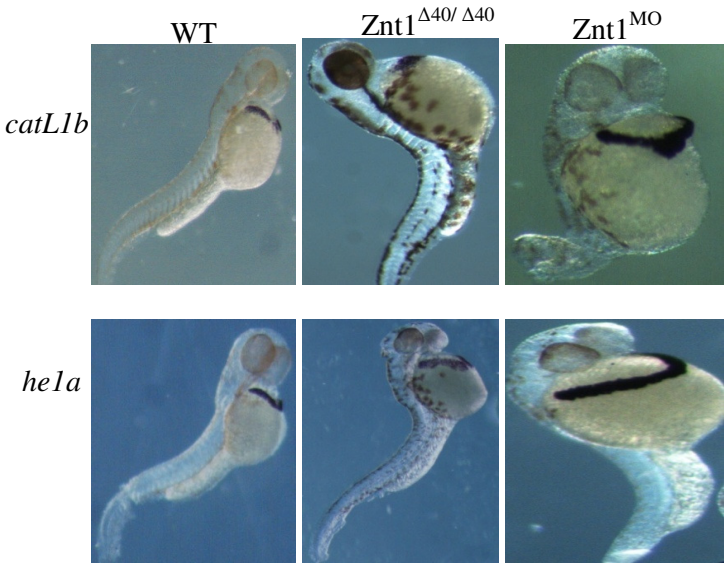

Fig 5.5.1: Effect of Znt1 deficiency on the expression of HGC markers in 48hpf embryo. ISH expression of *catL1b* and *he1a* in the hatching gland cells at 48hpf in wild-type and Znt1 mutant and Znt1 morphant embryos. Expression of *catL1b* and *he1a* was still present and abundant in morphant and mutant. NB: The Znt1 mutant and morphant embryos were not properly de-pigmented which account for the diffused brownish pigmented cells over their bodies (n=10 embryos where N=3 experiments per treatment).

5.4.5 Fluorometric imaging of free zinc ions (Zn^{2+}) in the hatching glands

Intense fluorescence from the 'ZTRS' zinc probe was observed in the HGC of wild-type embryos at 24hpf (Fig. 5.6) indicating high levels of free Zn^{2+} ions, which began to diminish by 48hpf (Fig. 5.6.1). There was similar fluorescence in the Znt1 morphant and mutant as in wild-type but no fluorescence in the Zip10 morphant at 24hpf (Fig. 5.6), only at 48hpf (Fig. 5.6.1) after which began to diminish. At 72hpf, the signal from free Zn^{2+} ions was almost gone in the HGCs of wild-type and Znt1 deficient embryos but still persisted in the Zip10 morphant at a reduced level (Fig 5.6.2). Exposure of the wild-type embryos at 24hpf to 100µM of zinc did not block or abolish the fluorescence (Fig. 5.7), but at 200µM there was no fluorescence from free Zn^{2+} ions (in both dechorionated and intact embryo) presumably because ZTRS was saturarated with zinc

and was not taken up by the HGCs in the embryos (Fig. 5.7.1). However, 100µM of zinc abolished the fluorescence signal in Znt1 morphant and Znt1 mutant embryos (Fig. 5.7). Interestingly, the fluorescence of free Zn^{2+} ions was restored when the exposed wild-type embryos (200µM) or Znt1 deficient embryos (100µM) were first incubated in standard fish tank water for 2 hr before treatment with 10µM of ZTRS, or alternatively when the concentration of ZTRS was increased to 100µM (with no pre-incubation in fish water) indicating free Zn^{2+} ions in the HGC (Fig 5.7.1). Intriguingly, zinc chelation increased the fluorescence intensity of free Zn^{2+} ions in the HGC of 24hpf wild-type embryos but abolished the intensity at 52hpf when compared to the untreated control wild-type (Fig. 5.7.2). The Zip10 morphant on the other hand when exposed to 100µM zinc showed free Zn^{2+} fluorescence at 33hpf (Fig. 5.7).

5.4.5.1 Effect of Znt1 and Zip10 deficiencies on the fluorescence of free Zn^{2+} ions in HGC

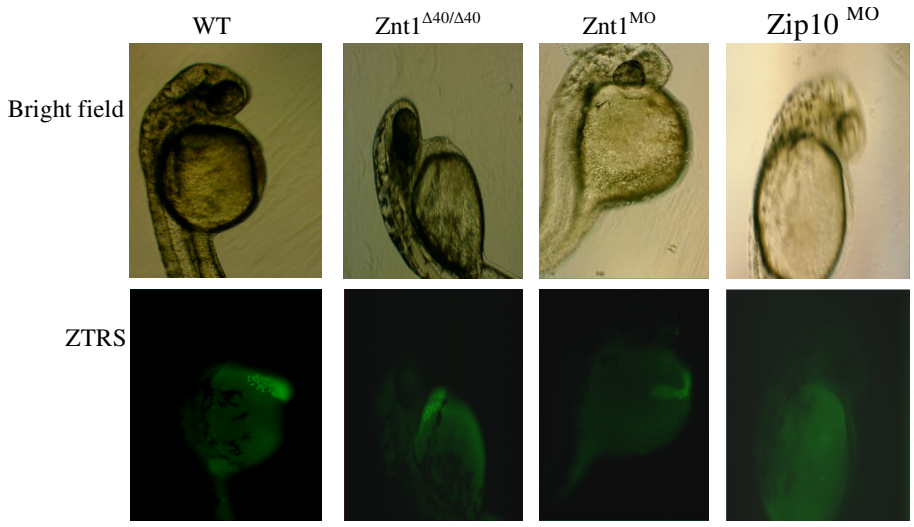

Fig 5.6: ZTRS fluorescence was intense in the hatching glands of 24hpf dechorionated WT, Znt1 homozygote and Znt1 morphant but was absent in the Zip10 morphant. Experiment repeated 4-5 times (n=5) with consistent observation (i.e. 90-100% of embryo observed for each phenotype).

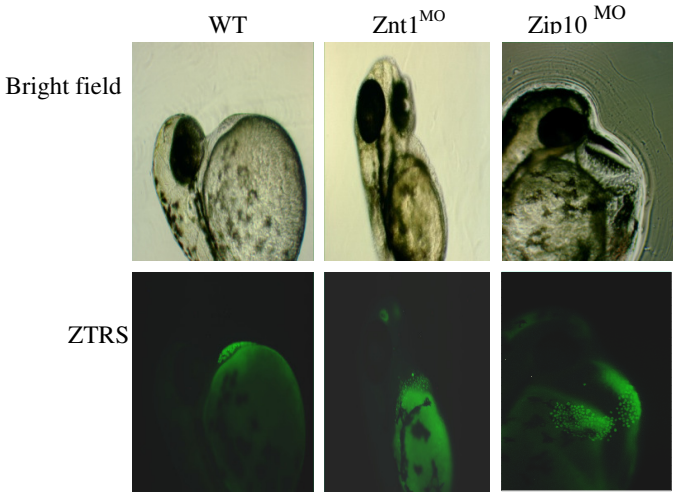

Fig 5.6.1: ZTRS fluorescence for free Zn^{2+} starts to appear with high intensity in the hatching glands of 48hpf dechorionated Zip10 morphants but gradually diminishes in wild-type and Znt1 morphant embryos. Experiment repeated 4-5 times (n=5) with consistent observation (i.e. 90-100% of embryo observed for each phenotype).

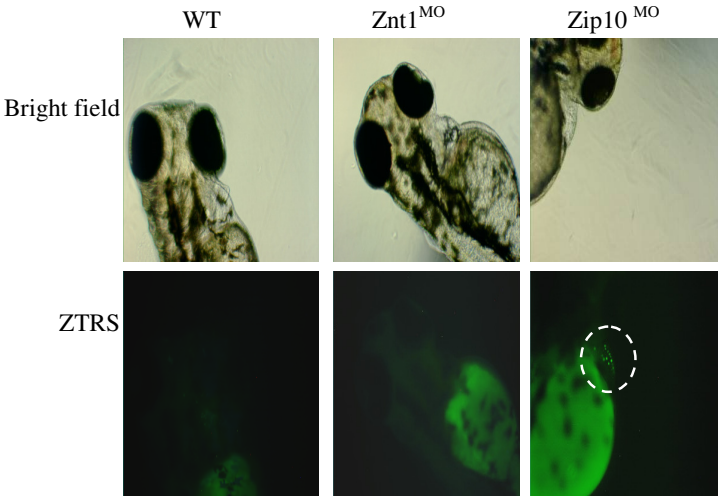

Fig 5.6.2: ZTRS fluorescence for free Zn^{2+} had almost disappeared in the hatching glands of 72hpf dechorionated wild-type and Znt1 morphant embryos but was still present at lower intensity in Zip10 morphants. Experiment repeated 4-5 times (n=5) with consistent observation (i.e. 90-100% of embryo observed for each phenotype).

5.4.5.2 Effect of Znt1 and Zip10 deficiencies on the fluorescence of free Zn^{2+} ions in HGCs of zinc exposed embryos

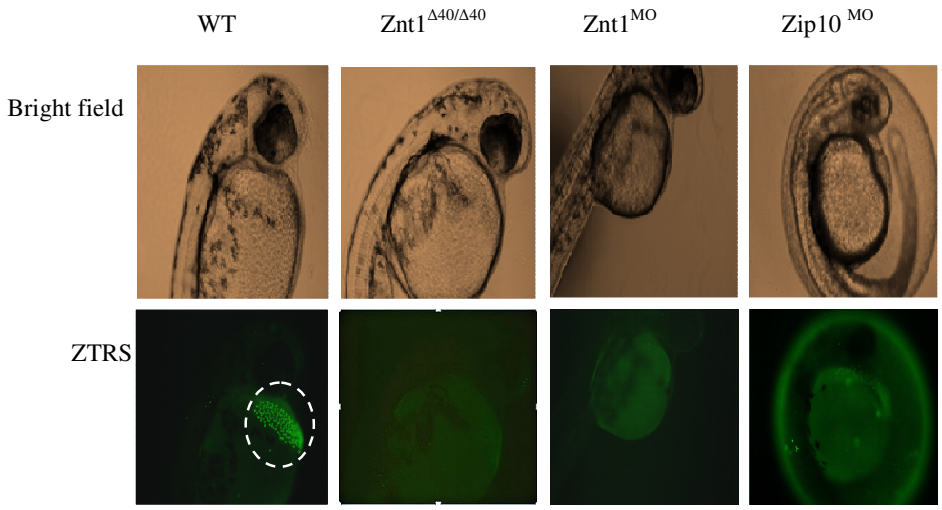

Fig 5.7: Zinc exposure at 100µM reduced ZTRS fluorescence in the HGC of 24hpf wild-type embryo with complete loss of fluorescence in znt1 deficient embryos. Meanwhile fluorescence began to appear in the HGC of zip10 morphants at 33hpf. Experiment repeated 4-5 times (n=5) with consistent observation (i.e. 90-100% of embryo observed for each phenotype).

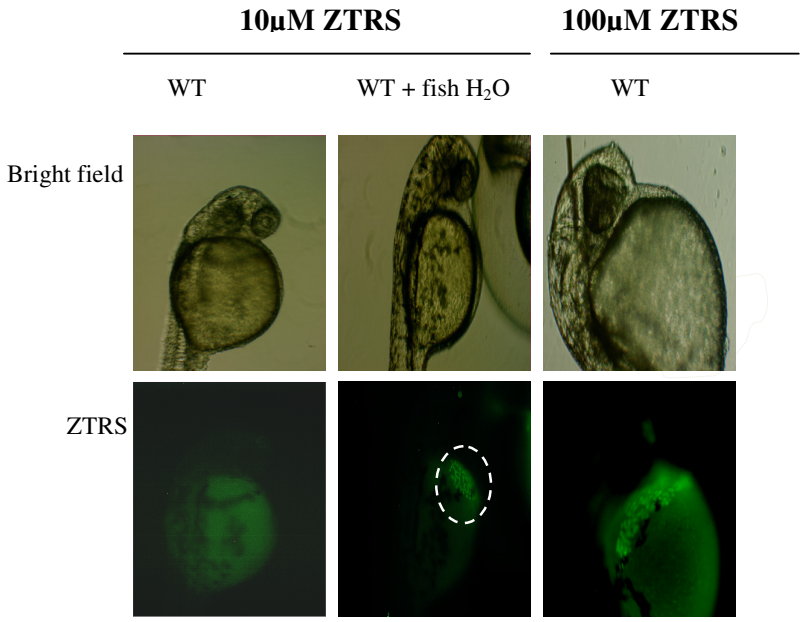

Fig 5.7.1: Zinc exposure of 24hpf wild-type embryos at 200µM abolished the fluorescence of Zn^{2+} in HGC of embryos treated with 10µM ZTRS but prior incubation of exposed embryos in fish H_2O for 2 h before treatment lead to the return of fluorescence in the HGC but with low intensity. Interestingly fluorescence was not abolished when ZTRS was used on exposed embryos at 100µM. Experiment repeated 4-5 times (n=5) with consistent observation (i.e. 90-100% of embryo observed for each phenotype).

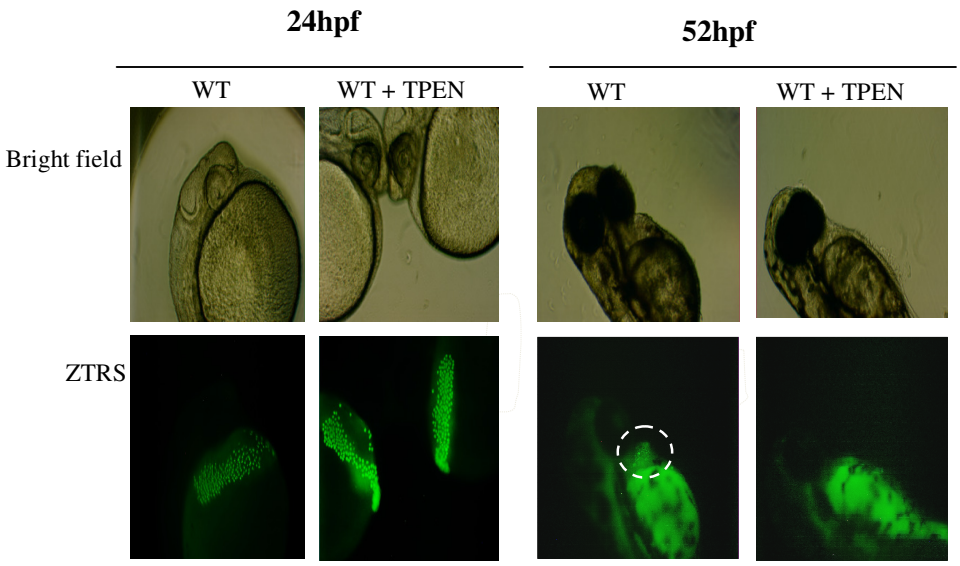

Fig 5.7.2: Zinc chelation in wild-type embryos increased the fluorescence intensity of the HGC at 24hpf but abolished the signal at 52hpf. Experiment repeated 4-5 times (n=5) with consistent observation (i.e. 90-100% of embryo observed for each phenotype).

5.4.6 Fluorescence imaging of apoptotic cells in hatching glands

Apoptosis of the HGC as indicated by acridine orange staining was observed in a similar pattern as that shown by ZTRS staining for free Zn^{2+} ions in the hatching gland, although the staining of HGC by acridine orange was not as prominent as that observed by ZTRS. Spectrophotometrically, acridine orange did not show sensitivity or changes to Zn^{2+} supplemented or depleted dH_2O unlike ZTRS confirming that the acridine orange does not measure free Zn^{2+} ion (as does by ZTRS) but detects DNA breaks as a marker of apoptotic or dead cells of the hatching gland. Thus, acridine orange responding to zinc did not account for the similar staining pattern of HGCs. There was stainining in the HGCs of Znt1 morphants and mutants as well as wild-type at 24hpf, which began to diminish by 48hpf (Fig. 5.8 & 5.8.1). However, Zip10 morphants showed no staining of the HGCs at 24hpf, but staining was present at 48hpf and began to diminish therafter (Fig. 5.8 & 5.8.1). The wild-type embryos showed staining

(apoptosis) in HGCs under conditions of both zinc exposure and zinc depletion (Fig. 5.8.2). This was in contrast to the result from Zn^{2+} imaging in which fluorescence from ZTRS could not be seen in zinc exposed embryos, thus, further confirming that acridine orange does not measure or respond to Zn^{2+}. Apoptosis appeared to occur also in *p53* knockdown embryos (although slightly reduced in intensity) but not in embryos treated with fluoromethylketone (caspase 3 inhibitor). However, the ZTRS signal was not affected by either treatment (Fig. 5.8.3 & 5.8.4).

It should be noted that strong acridine orange fluorescence intensity was observed on the yolk body, head and the olfactory bulb in all the treatment groups but the apoptosis of the HGCs, revealed by weaker staining (and hardly visible in print), is specific to each treatment group and is our concern in this study as it relates to hatching.

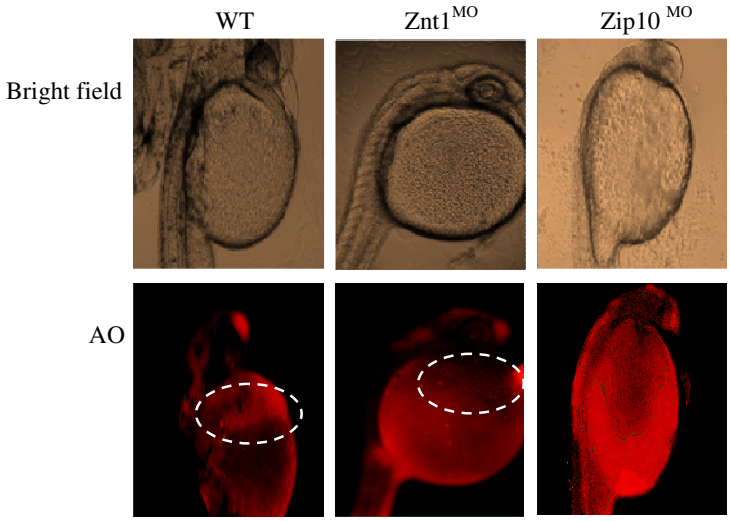

Fig 5.8: Effect of zinc transporter deficiencies on apoptosis of HGC at 24hpf. There was specific acridine orange fluorescence in HGCs of wild-type and Znt1 morphant embryos, this was but absent in Zip10 morphants. Experiment repeated 4-5 times (n=5) with consistent observation (i.e. 90-100% of embryo observed for each phenotype).

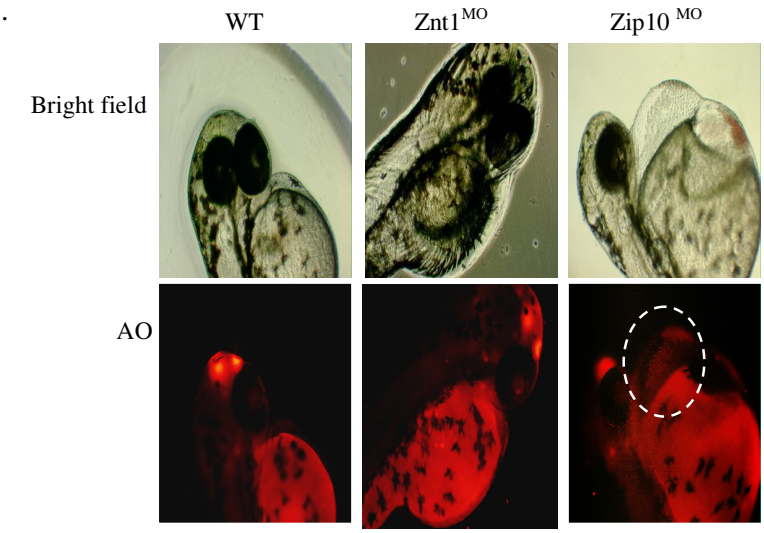

Fig 5.8.1: Effect of zinc transporter deficiencies on apoptosis of HGCs at 48hpf. The staining began to appear in Zip10 morphants at 48hpf but began to fade or disappear in wild-type and Znt1 embryos. Note the generalised apoptosis of the olfactory bulb in all the groups. Experiment repeated 4-5 times (n=5) with consistent observation (i.e. 90-100% of embryo observed for each phenotype).

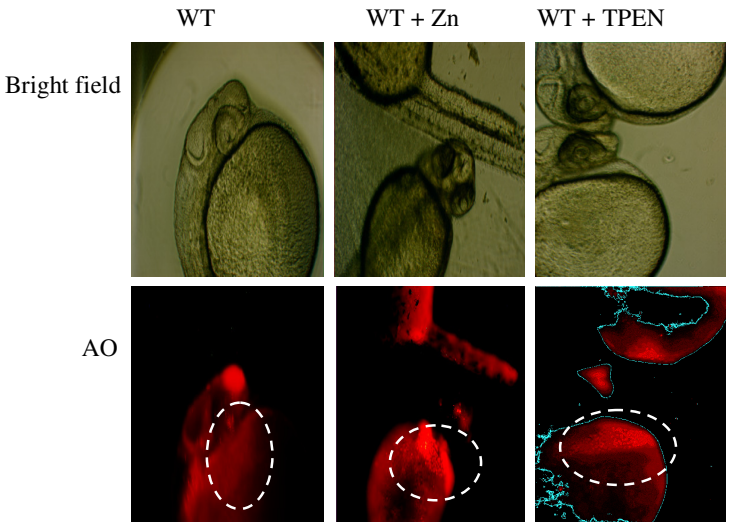

Fig 5.8.2: Effect of zinc exposure and depletion on HGC fluorescence of ZTRS and acridine orange in 24hpf wild-type embryo. Zinc supplementation (200µM) and zinc depletion of wild-type embryos did not affect the apoptotic cell staining of the HGCs. Experiment repeated 4-5 times (n=5) with consistent observation (i.e. 90-100% of embryo observed for each phenotype).

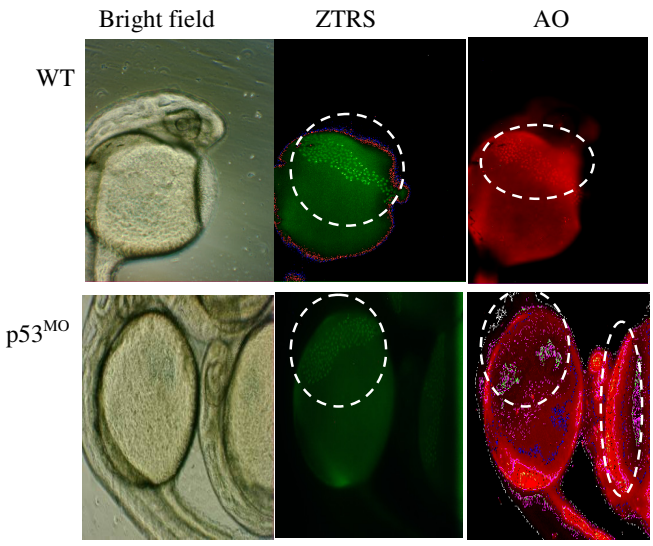

Fig 5.8.3: Effect of *p53* knockdown on HGC fluorescence of ZTRS and acridine orange in 24hpf wild-type embryo. *p53* knockdown in wild-type embryos did not affect the fluorescence of ZTRS (10µM) and acridine orange staining of HGC for free Zn^{2+} ions and apoptotic cells of the gland respectively as observed in untreated wild-type control. Experiment repeated 4-5 times (n=5) with consistent observation (i.e. 90-100% of embryo observed for each phenotype).

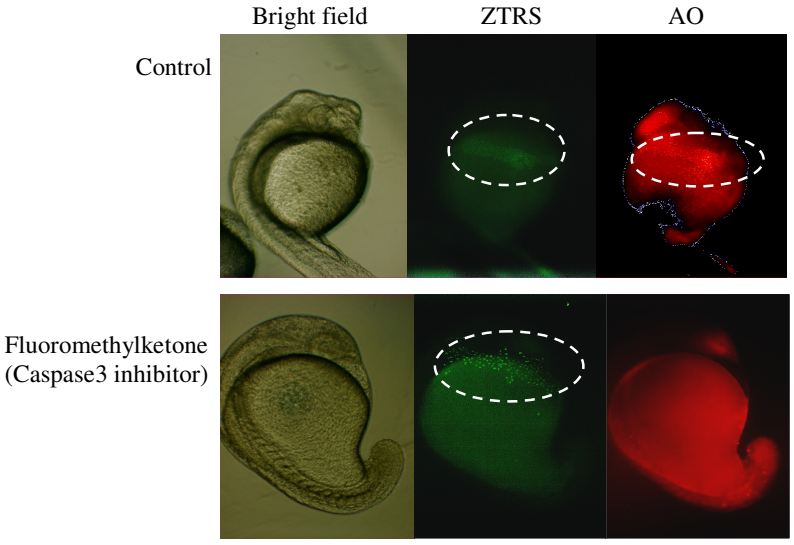

Fig 5.8.4: Effect of caspase III enzyme inhibitor on the fluorescence of ZTRS and acridine orange in 24hpf wild-type embryos. Caspase 3 enzyme inhibition abolished the fluorescence indicating apoptotic HGCs but did not abolish the fluorescence of ZTRS staining of the HGCs. Experiment repeated 4-5 times (n=5) with consistent observation (i.e. 90-100% of embryo observed for each phenotype).

5.5 Discussion

5.5.1 Hatching of wild-type embryos

Our results confirmed the effect from a previous study of excess zinc in delaying the time of hatching and reducing the number of hatched embryos (Dave *et al.*, 1986). In addition, we demonstrated that zinc depletion reduces the time to hatch in zebrafish. The effect of zinc and TPEN mimicked that observed in Zip10 morphant and Znt1 morphant/mutant respectively suggesting that possibly *zip10* knockdown reduces zinc mobilization and accumulation in the HGCs whereas *znt1* knockdown reduces zinc mobilization out of HGCs but enhances its zinc accumulation, thus leading to increased and decreased levels of zinc in the yolk/perivitalline environment respectively. The amount of zinc in all the conditions investigated in zebrafish embryo in this study that influences hatching may or may not affect the level of 'free' Zn^{2+} of the hatching gland cells that produce the hatching enzymes responsible for hatching of zebrafish embryos. It is possible that zinc at a particular level is needed for hatching at normal the time of 72hpf and that anything that disturbs this set zinc level will affect hatching either by retardation or accelaration (Kimmel et al 1995, Somasundaram,1984; Dave *et al.*, 1986 and Luberda, 1993). Because Znt1 mediates zinc efflux while Zip10 mediates zinc influx, it is possible that Znt1 might be involved in exporting excess zinc out of the HGC whereas Zip10 may mediate import into the cells, both contributing to maintaining the homeostatic set point of zinc in HGC. Knockdown or mutation of *znt1* would increase zinc accumulation of the HGC because of reduced efflux whereas *zip10* knockdown would result in decreased zinc influx. Thus, these effects of zinc transporters and exporters in HGC on the time to hatching indicates that a high zinc content of the HGC speeds up the function and/or release of hatching enzymes from the HGC.

5.5.2 Expression of hatching gland markers

The lack of expression (at 48hpf) or sloughing off (at 33hpf) of hatching gland markers such as *catL1b* and *he1a* in Zip10 morphants may explain the lack of or delayed hatching in these embryos. This might be due to an insufficient amount of zinc in the HGCs causing transient expression of hatching gland markers until 33hpf when the HGCs began to lose the signal, probably because the cells are no longer able to synthesize and accumulate mRNA transcripts. It could also be due to the inactivation of the hatching enzyme (He1a), which is a zinc metalloprotease enzyme or premature activation of the zinc inhibitable cysteine protease hatching enzyme (CatL1b) or both mechanisms leading to destruction of hatching gland tissues and inappropriate production and secretion of chorionase needed for hatching. On the other hand, there was abundant expression of these enzymes in Znt1 morphant and mutant embryos even until 48hpf and beyond, which possibly explained the reduced hatching time observed. This phenomenon may be explained by the opposing effect of both transporters where Znt1 and Zip10 export and import zinc respectively into the HGC, so knockdown of each has opposing effect on HGC Zn^{2+} content. Knockdown of *znt1* may decrease zinc efflux from HGCs and therefore increase their zinc content. Conversely, knockdown of *zip10* reduced free Zn^{2+} in HGC presumably because of decreased uptake. We therefore propose a model for the activities of Zip10 and Znt1 transporters in the homeostatic control of zinc inside the HGC of zebrafish as shown in Figure 5.9. The effects of zinc exposure or depletion on hatching of wild-type embryos may have nothing to do with the hatching gland, but rather may be as a result of physicochemical effects of excess zinc or TPEN in the chorion/perivitalline fluid, especially zinc, which was previously reported to cause delay hatching (Dave *et al.*, 1986).

Because zinc is an inhibitor of CatL and similar proteases, it is possible that the proteolytic destruction or the sloughing off of the hatching gland tissues in Zip10 morphant at 33hpf (arrows in Fig. 5.4.3) may be as a result of improper or premature activation of CatL or its pre-pro-enzyme due to insufficient or lack of zinc to inhibit the enzyme activity after its proteolytic cleavage processing to a mature form in the HGC (lysosomes), which protects the tissue before its release, thus resulting in the enzyme exerting its proteolytic activity on the hatching gland tissue and subsequent tearing or sloughing off. If this is the case, then the assumption indicates the usefulness of this model to study the inappropriate activation of this enzyme in various pathological condition such as in prostate (or seminal vesicle) disease or cancer, Alzeimer's disease and reproductive disorders in both male and female (Seshagiri *et al.*, 2009; Wang *et al.*, 2001, Ronquist *et al.*, 2011). Furthermore, the Alzeimer's disease model suggests that while Zn^{2+} inhibits β-secretase cysteine protease, it activates α-secretase zinc metalloprotease of the metizicin superfamily (which cleaves the APP in a non-amyloidogenic pathways) to prevent the formation of β-amyloid plaque in the neurones (Tougu *et al.*, 2011). A similar cathepsin acts as β-secretase cleaving APP. This event had resemblance to what was observed in the expression of HGC markers (*catL1b* or *he1a*) in zebrafish embryo where lack of zinc supply by *zip10* knockdown may have lifted the inhibition of the cysteine protease CatL and inactivate zinc metalloprotease He1a resulting in gland destruction at 33hpf and subsequent failure to hatch. Another alternative explanation of the effect of sloughing off or mislocalization of CatL1b (or hatching enzyme) positive cells in hatching gland tissue of 48hpf Zip10 morphant (arrow in Fig. 5.5.2) could be as a result of the role of CatL1b and/or Zip10 in migratory behaviour of cells whereby inhibition of either of Zip10 or CatL1b reduces the migration and tumorigenicity of malignant cells probably through inducing the

epithelial-mesenchymal transition; EMT (Kirschke *et al.*, 2000 and Kagara *et al.*, 2007). This was similar to abnormal positioning or mis-localization and morphology of hatching gland cells observed in E-cadherin mutant or morphant zebrafish caused by defect in migratory activity of the cells (Shimizu *et al.*, 2005; Babb and Marrs, 2004). Therefore, it's possible that Zip10 by itself or through the provision of Zn^{2+} for CatL1b in the HGC is responsible for regulation of cell movement from the polster to the hatching gland region and to the pericardial membrane where the HGC are subsequently absorbed or phagocytosed (Wyllie *et al.*, 1980). Interestingly, in the present study, knockdown of *zip10* abolished or caused impaired movement and mislocalization of hatching gland cells (arrow in Fig. 5.4.2) by affecting *catL1b* expression through EMT down regulation which is similar to what was observed in another recent study with knockdown of tetraspanin (*cd63*) in zebrafish embryo, which also resulted in delayed hatching (Trikic *et al.*, 2011).

5.5.3 Zinc ion acumulation and apoptotic processes of hatching gland cells

It is generally known that zinc can inhibit apoptosis but high amount of zinc can as well induce apoptosis (Schrantz *et al.*, 2001). The zinc in the HGC may have a role in inducing developmental apoptosis as early as 18-24hpf and this early apoptosis may not be connected to the subsequent cell death (or sloughing off) occuring at 33hpf in Zip10 morphant that possibly might be caused by inability of the cells to further synthesize and accumulate mRNA transcripts or by premature production/activation and release of protease (chorionase). The pattern of detection of zinc by ZTRS and early developmental apoptosis by acridine orange in the HGC was similar in both wild-type and Znt1 morphant/mutant embryos but different in Zip10 morphant. There was fluorescence of free Zn^{2+} ions and apoptotic cells of HGC in Znt1 morphant/mutant and

wild-type at 24hpf which start diminishing by 48hpf but the signal for both staining was not seen in Zip10 morphant at 24hpf except at 48hpf which start diminishing therafter (i.e there was delayed in the fluorescence of zinc and apoptotic cell of the HGC and probably may be responsible for the delay in the process of hatching). Although, Znt1 morphant and mutant showed lack of free Zn^{2+} ions detection in the HGC of zinc-exposed embryos at 100µM similar to zinc-exposed wild-type embryos at 200µM (either chorionated or dechorionated embryos), there was acridine orange signal in their HGC confirming that acridine orange was not responsive to zinc supplementation. The lack of free Zn^{2+} ions detection by ZTRS in HGC of zinc-exposed embryos was because the probe (used only at 10µM) was presumably saturated with zinc and was not taken up by the HGCs in the embryos indicating that zinc was present but can not be detected because of the low concentation of ZTRS, which results in little or no ZTRS to bind the zinc in the HGC that is probably high in concentration; about 1mM. To support this argument, there was presence of intense ZTRS fluorescence when the probe was used at a ten times higher concentration (i.e. 100µM) which made it available to the zinc in the HGC or when the zinc-exposed embryos were first incubated in standard fish tank water for about 2 h prior to fluorescence staining with 10µM ZTRS zinc probe. In contrast, Zip10 morphant showed neither free Zn^{2+} ions nor apoptosis of HGC even when first rinsed or incubated in standard fish water (although they showed presence of free Zn^{2+} ions when exposed to zinc which could be the effect of zinc exposure or because of the stage of the development (i.e. 33hpf) when the signal is close to the detection period (i.e. 48hpf). In other word, the presence of apoptosis as indicated by acridine orange staining is induced by the presence of zinc as indicated by ZTRS staining (i.e. without zinc presence, apoptosis cannot be induced). This test further supports our argument in chapter 3 that Znt1 mutant or morphant embryos accumulate more zinc than the wild-

type counterparts because Znt1 homozygotes or morphants only required lower zinc concentration (~100 µM) than wild-type (~200 µM) to add to the endogenous zinc (which is assumed to be higher in mutant/morphant than wild-type embryos) causing over saturation of the 10µM ZTRS probe and making it unavailable to bind the free Zn^{2+} ion in the HGC. On the other hand zinc depletion by TPEN showed intense fluorescence of free Zn^{2+} ion of the HGC (and apoptosis) than observed in zinc exposure which further supports the notion that the ZTRS probe was over saturated by high level of zinc in the incubation water and was not available to bind zinc in the HGC, hence little or no fluorescence. The *p53* knockdown could not inhibit the apoptosis of HGC, but the caspase III enzyme inhibitor (fluoromethylketone) prevented apoptosis of HGC. Interestingly, there was presence of free Zn^{2+} ions in HGC of *p53* knockdown embryos and in caspase III enzyme inhibited embryos, suggesting that the developmental apoptosis of the HGC is not through the mitochondria p53-dependant pathway but probably through other pathway(s) that all converged on caspase III which is the executioner of apoptosis. This apoptosis was inhibited by caspase III inhibitor (Parng *et al.*, 2002) as observed in our present study. *p53* knockdown embryos were previously reported to have normal development and were also shown not to suppress the developmental apoptosis, especially the tail-specific apoptosis induced by loss-of-function of *chordin*, suggesting that this type of apoptosis was not through p53-related pathways. Thus, *p53* is probably not required for normal development (Donehower *et al.*, 1992; Berghmans *et al.*, 2005). In another study, where co-injection of *p53* MO was used to prevent possible neural apoptosis induced by some morpholinos, it was observed that knockdown by *p53* MO does not prevent the developmental apoptosis of the HGC (Robu *et al.*, 2007; Kwan *et al.*, 2006). The study by Robu and his colleagues also showed that *p53* is not transcriptionally regulated.

In summary, it is possible that the presence of both zinc and early developmental apoptosis of the HGC work in concert or synchronize together to regulate early cellular events which may or may not be connected with activation and release of hatching enzymes for hatching. Although, from the result it was shown that the blockage of apoptosis of HGC does not block zinc accumulation in the HGC, it is possible that the absence of zinc accumulation or its reduction may block apoptosis i.e. apoptosis may depend on the presence of zinc accumulation but zinc accumulation does not depend on apoptosis. To cast more light into this process, there is need to use a non-toxic agent (if available) that can remove all the zinc in the HGC without affecting the survivability of embryos unlike the TPEN used in the present study which cannot chelate the HGC zinc at lower concentrations compatible with embryo survival.

Because ZnT-2 (among others) is also expressed in the vesicle of small intestine and other tissue such as kidney, mammary gland, seminal vesicle, testis, and prostate and also localized on the membrane of secondary lysosomes/lysosome-related organelles of the endosomal compartment, there is possibility that ZnT-2 or its invertebrate homologue CDF-2 functions to provide zinc for endosomal enzymes (e.g. lysosomes) within the vesicle of these tissues (Palmiter *et al.,* 1996) including hatching gland tissue. So therefore, it is possible that Zip10 supplies zinc to the HGC which is transported by Znt2 (assuming this is expressed in the HGC) into the vesicle to supply the endosomal proteases (He1a and/or CatL1b) with zinc for either activation or inactivation. Because *cdf-2* mutant worm model showed less zinc content or storage (about 2/3) in the intestinal vesicle than the wild-type counterpart (Dave *et al.*, 2009), it is suggested that zinc storage in the vesicle of zebrafish HGC is reduced or absent in Zip10 morphant due to inability of Zip10 to supply enough cytosolic zinc for Znt2 to enrich the vesicle for enzyme activation thus causing delay hatching whereas the opposite effect is observed

in Znt1 morphant. To understand the potential role of zinc in modulating the activities of He1a and CatL1b in HGC, and the feasibility of ligand exchange between these two enzymes, it would be helpful to know their respective affinities for zinc. A general concept is that a zinc-requiring enzyme (such as He1a) has high affinity for zinc whereas a zinc-inhibited enzyme (such as CatL1b) has low affinity, but the variation of affinities is presently unknown (Maret, 2011).

Another alternative model as described by Chwieralski *et al.,* (2006), is proposed in Figure 5.9, which shows the mechanism by which cathepsin may participate in apoptotic pathway(s) and subsequent hatching in Zip10 morphant model. This is slightly different from the previous assumption of premature activation of cathepsins in Zip10 morphant due to lack of zinc (resulting in gland tissue destruction) or cathepsin roles in migratory behaviour of cells. In this model (Fig. 5.9), it's possible that the two proteases (CatL1b and He1a) are contained in different endosomal compactments, with CatL1b found in the lysosome. The cathepsin (a cysteine protease of papain family) is released or leaked into the cytosol to bring about initiation of apoptosis of endosomes (through activation of caspases; also cysteine proteases of caspase family) leading to the release and activation of choriolysin into the cytosol causing choriolysis and subsequent hatching of embryo.

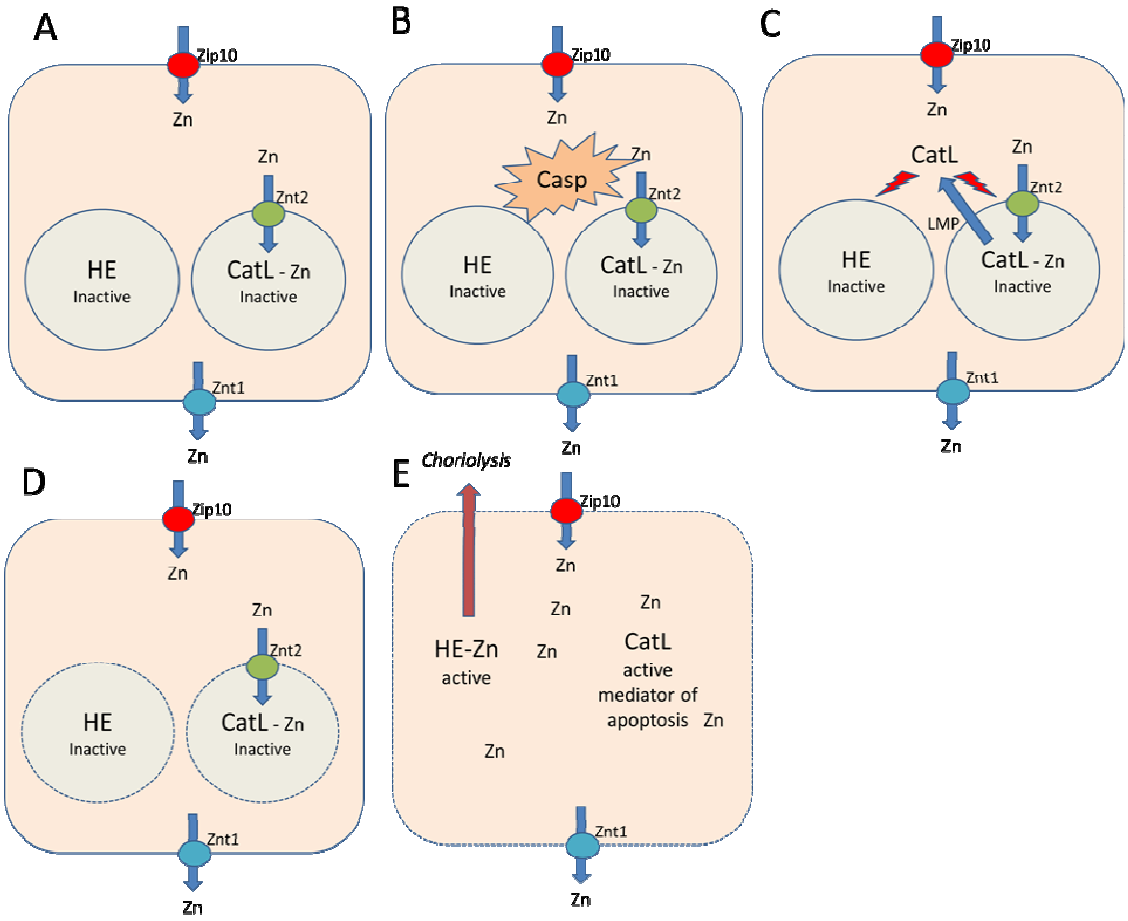

Fig 5.9: A model of how zinc transporters in the HGC control zinc homeostasis in hatching. (A) Zip10 is assumed to mobilize zinc into the cytosol of the HGC whereas Znt1 functions to flux out excess cytosolic zinc. Znt2 is localised on endosome (lysosomal compactment) for zinc compartmentalization forming a CatL-Zn complex which renders the mature enzyme inside the lysosome inactive. On the other hand, hatching enzyme (He1a), a zinc-active enzyme contained in a different endosomal compartment, is also rendered inactive due to lack of zinc supply. **(B) & (C)** Lysosomal cathepsin (a known initiator of apoptosis) leaks out of the lysosome as a result of lysosomal membrane permeabilization (LMP) causing activation of caspase (casp) enzymes and/or the release of proapoptotic factors due to mitochondria damage, thus triggering the apoptotic signalling cascade. **(D) & (E)** Rupturing of both endosomal compartments by the action of caspase causes release of both proteases and the zinc ions into the cytosol. The zinc then forms a complex with hatching enzyme (He1a) in the cytosol for enzyme activation capable of lysing the chorion (choriolysis) and subsequent hatching. In the knockdown model of *zip10* or *znt1*, zinc uptake or extrusion is affected leading to decreased or increased zinc accumulation in the cytosol of the HGC respectively needed for activation of choriolysin. The effects of *zip10* knockdown lead to decreased mRNA expression of markers of HGC, destruction of hatching gland tissue and subsequent delayed hatching whereas opposite effects are observed with *znt1* knockdown.

5.5.4 Summary

Zinc exposure prolonged the time to hatching whereas zinc chelation accelerated the hatching time. This effect was not related to the expression of Zip10 and Znt1, which are the two zinc transporters expressed in the plasma membrane of HGC that work in opposite ways to maintain zinc homeostasis. Defect in Zip10 delayed hatching time, coincident with lack of expression of markers of hatching enzymes (CatL1b or He1a) at the time of hatching, which is caused probably by low Zn^{2+} ions in the HGC. Conversely, a defect in Znt1 speeds up hatching time, coincident with overexpression of markers of hatching enzymes in the HGC caused probably by adequate or increased Zn^{2+} ion in the HGC. Intriguingly, knockdown of *zip10* blocked the early developmental apoptosis of the HGC that is usually seen at the early stage of development around 18-24hpf which normally disappears at the time of hatching. It is not known whether this is related to delayed hatching of Zip10 morphants or not, but it is possible that the zinc level in the HGC of Zip10 morphants is reduced to a level that can inhibit this apoptotic process, thus making the *zip10* gene an essential marker for early developmental apoptosis.

5.5.5 Future studies

This should include the following experiments:

i. A double knockdown of both *zip10* and *znt1* genes in wild-type embryos to further test and confirm the hypothesis that these transporters play a key roles in zinc homeostasis during hatching. In this condition hatching is expected not to be affected.

ii. A knockdown of *catL1b* with and without *zip10* knockdown in wild-type embryos and study of the mRNA expression patterns of *he1a* & *catL1b* and subsequent hatching will give a better understanding and also confirm the hypothesis that zinc interacts with proteases in hatching, thus modelling certain disease conditions in human such as Alzeimer's and prostate.

iii. Immunostaining of He1a and CatL1b in HGC to investigate if they are co-localized or are in separate endosomes. Ultrastructural localization of Zn^{2+} in HGC will also give a better insight.

iv. A better understanding of role of *zip10* gene as essential marker of early developmental apoptosis in zebrafish embryos.

CHAPTER SIX

ROLE OF ZIP10 IN EMBRYONIC DEVELOPMENT AND CELL MIGRATION

6 Role of Zip10 in embryonic development and cell migration

6.1 Introduction

Although zinc is essential trace element for life, too much of it if not tightly regulated is toxic to cells (Cummings and Kovacic, 2009). More than half a century ago, it was shown that higher cellular zinc content was strongly associated with tumor tissue in mice compared to normal tissue in the same animal (Tupper *et al.*, 1955). In recent years, several research articles have demonstrated a role of zinc in the activation of kinases primarily through the inhibition of protein phosphatases that are involved in dephosphorylation and inactivation of protein receptors such as EGFR, HER2, IGF1-R, Src and tyrosine kinase receptors (Haase and Maret, 2003 & 2005, Hogstrand, 2009), which are proliferative signalling molecules often responsible for agressiveness of cancer (Knowlden *et al*., 2005). Other recent reports have also associated zinc dysregulation with increased risk of cancer progression (Prasad and Kucuk, 2002) and in some instances the involvement of some zinc transporters have also been implicated (Taylor, *et al.,* 2007, Kagara *et al.*, 2007). Among the zinc transporters involved in cancer cell migration is the LIV-1 subfamily of ZIP transporters (Manning *et al.*, 1988; Taylor *et al.,* 2003b) including ZIP6 and ZIP10, which are closely related paralogues in the subfamily. These proteins have long N-terminal domains which have sequences and predicted structure very similar to those of prion proteins (Ehsani *et al.*, 2011) and it has been proposed that LIV-1 proteins are evolutionarily related to prion proteins (Malaga-Trillo *et al.*, 2009, Ehsani *et al.*, 2011). However, reports have implicated some other ZIP proteins in carcinogenesis and progression such as ZIP4 (also a LIV-1 subfamily member) in pancreatic and hepatocellular carcinoma (Zhang *et al.*, 2010; Weaver *et al*., 2010) as well as ZIP7 (which is also a member of LIV-1 subfamily) in metastasis of

breast and cervical cancer (Hogstrand *et al.,* 2009). ZIP6 (SLC39A6), originally named LIV-1, was the first ZIP protein to be associated with breast cancer progression and was found to be over-expressed in oestrogen-receptor breast cancers that spread to the lymph nodes (Manning *et al.,* 1993 & 1994). This transporter has been shown in the zebrafish model to be a down stream target of signal transducer and activator of transcription (STAT3) to regulate the formation of epithelial-mesenchymal transition (EMT) during gastrulation, by causing Snail (a zinc-finger transcription factor) nuclearization and subsequent down regulation of intercellular adhesion molecules (E-cadherin) which ultimately affects the movement of gastrula organizer cells (Yamashita *et al.,* 2004). EMT is one of the central events that occurs during gastrulation for normal embryonic development, organ and tissue regeneration and cancer metastasis (Thiery, 2002 and Savanger, 2001). During EMT, typical cell-cell adhesive interactions are altered such that connections between cells and with their local environment become weaker; the cells also acquire a more mesenchymal, spindle-shaped morphology as a result of cytoskeletal rearrangements (Creighton *et al.*, 2010). STATs are also important in EMT during gastrulation, organogenesis, wound healing and cancer progression (Sano *et al.,* 1999; Yamashita and Hirano, 2003) and STAT3 was shown to promote expression of ZIP6 in zebrafish and this was important for anterior migration of axial mesendoderm, but not for dorsal convergence and not for lateral migration (Yamashita *et al.*, 2004). An alternative model was also proposed by Yamashita and colleagues (2004) whereby the mitogen-activated protein kinase (MAPK) was thought to directly induce the expression of Snail that is required for EMT formation but later in 2007, Zhao and co-workers demonstrated the involvement of ZIP6 in this model whereby over expression of ZIP6 mRNA in human cervical cancer/invasion was found to be through the MAPK-mediated Snail or Slug expression pathways. The expression of Snail was shown to be positively

correlated with that of Zip6 (LIV-1), and *zip6* knockdown significantly reduced both Snail abundance and the proliferation, invasiveness, and migratory behaviour of HeLa cells providing evidence that this zinc transporter plays a role in EMT by regulating the activity of Snail (Zhao *et al.,* 2007).

ZIP10 was also found to be over-expressed in aggressive breast cancer cells that metastasised to the lymphnodes. Knockdown of *ZIP10* in these cancer cell lines or treatment of the cells with zinc chelator suppressed the invasiveness and metastasis suggesting that only free zinc transported via ZIP10 and not ZIP6 (as previously suggested by Manning, *et al.*, 1994) was responsible for invasive behaviour of the cancer cells (Kagara *et al.*, 2007). This indicates that not only the free zinc ions but specifically the free zinc ions transported by ZIP10 stimulate the increased migratory activity of these particular breast cancer cells. The close relationship of ZIP10 and ZIP6 in the ZIP family of zinc transporters indicates that they may have similar functions in regulating cell migration (Kagara *et al.,* 2007). This was especially shown in zebrafish gastrulation where ZIP6 was responsible for EMT formation through the repression of E-cadherin which also occured in cancer cell lines with ZIP6 as well as ZIP10. It was shown that *zip6* knockdown in zebrafish results in shorter and broader anterior-posterior axis with abnormal head position (Yamashita *et al.,* 2004). Therefore epithelial-mesenchymal transition (EMT) is an important developmental process in which the molecular mechanisms resemble those that underlie tumor cell metastasis as well as organ regeneration. These processes require increased cell motility which is regulated by ZIP6 and/or its closest relative ZIP10 through the repression of E-cadherin causing increased EMT formation. It can be speculated that in mammals ZIP10 protein might performs the same function as Zip6 proteins in teleosts, or an interaction between these proteins might be required in a certain signalling pathway. It is not known whether these

closely related proteins can assume each other's functions, or if there is interaction such as heterodimerization between the two proteins or if the dorsal convergent extension movement that does not require ZIP6 activity can be performed by a closely related ZIP10.

6.2 Study objective

While studying the effect of *zip10* knockdown on hatching in the previous chapter (Chapter 5), it was incidentally noticed that at 24hpf of development, the Zip10 morphant presented a similar phenotype as described for the Zip6 morphant by Yamashita and colleagues (2004) (Fig. 9.8). Because of this observation, and the close relatedness of the two zinc transporters, and the documented role of ZIP10 in migration and invasiveness of human breast cancer cells, it was hypothesized that zebrafish Zip10 might be involved in cell migration during early zebrafish embryonic development. Therefore, the objectives of the present study were to investigate the role of Zip10 in development and also if Zip10 is involved in EMT during zebrafish embryonic development as previously shown for ZIP6. The objectives were addressed through observation of effect of *zip10* knockdown by MOs on zebrafish embryo development, epiboly progression and on other proteins or genes previously implicated in Zip6-mediated EMT, such as E-cadherin and Stat3.

6.3 Materials and methods

6.3.1 Generation of Zip10 (Slc39a10) morphants

Anti-sense morpholino modified oligonucleotide for zebrafish *zip10* were designed by and procured from GENE TOOLS. The sequences for each MO types (i.e. the translational blocker and splice blocker which were described in section 2.2.1.2) for *zip10* were shown in Table 2.2.2. Wild-type embryos were injected with 2-4 ng of each MO as previously described in chapter 2, 3 and 5 and the development of embryos were monitored pre- and post- hatching.

6.3.2 Detailed study of Zip10 morphants

6.3.2.1 Developmental study

Wild-type embryos were collected and injected with approximately 1-2 nl of 1:10 dilution of 20 ng/nl stock (2-4ng) of either of the 2 types of Zip10 morpholinos (translational blocker and splice blocker) at 2-4 cell developmental stage. The morphants were collected in embryo or fish water and incubated at 28.5^{o}C and the stages of development monitored compared to the un-injected control and injected morpholino control (i.e. mismatch or scramble sequences) (Table 2.2.2). In some experiments, a *p53* translational blocking MO was co-injected with either of the 2 types of MOs in a ratio of 1.5 : 1.0 and the effect on embryonic development was compared to that resulting from injection of either morpholino against *zip10* without *p53* knockdown.

6.3.3 Gastrulation cell movement and expression of molecules associated with EMT

Injected embryos were observed for epiboly and gastrulation cell movement at 10hpf which is the tail bud stage signifying the end of gastrulation stage. Embryos were collected at 10hpf, RNA extracted, cDNA synthesized and assayed by RT-qPCR as previously described in chapter 2. Genes that were assayed in relation to un-injected control were *cdh1* (E-cadherin), *Zip10, Zip6*, *stat3* (signal transduction and activator of transcription 3) and *snail* (zinc-finger transcription repressor). The primer and probe sequences for these genes are shown below (Table 6.0). The expression of E-cadherin in morphant and control embryos was also confirmed by ISH technique for mRNA abundance and by Western blotting and immunohistochemistry techniques for protein abundance as previously described in chapter 2 (section 2.2.7.1.2 and 2.2.8). ISH anti-sense probe to *cdh1* was produced by the alternative simple method as described in section 2.2.7.1.1.9. Primary antibody against E-cadherin (rabbit polyclonal; Abcam®) was used at 1:1000 and secondary antibody conjugated to HRP (goat anti-rabbit IgG) was used at 1:7500 for western blotting technique. After detection the antibodies were stripped off the membrane using the stripping buffer and then re-probed with a primary antibody to β-actin (rabbit monoclonal; Sigma®) which was used for normalisation (i.e. house keeping protein) at 1:000 using the same secondary antibody (goat anti-rabbit) at 1:2000. Alternatively, since the two proteins (E-cadherin and β-actin) have different molecular weights apart (i.e. 97KDa and 42KDa respectively), the membrane was cut horizontally into two at around molecular weight of 70KDa immediately after the transferring procedure and each separate membrane was incubated in their respective primary antibodies before they were incubated in the same secondary antibodies. This has advantage over stripping procedure in that it saves time and reduces some loss of

proteins from the membrane after stripping which sometimes make the band very faint or undetectable.

For, immuno-staining technique, the primary antibody to cdh1 (rabbit polyclonal; Abcam®) was used at 1:100 and the secondary antibody (goat anti-rabbit conjugated to Alexa Fluor 488; Abcam®) was used at 1:300. Nuclear staining by Hoechst (DAPI) or propium iodide was used as normalisation as described previously. Expression and cellular location of E-cadherin (Cdh1) protein in stained embryos were observed under normal laser scanning confocal microscope (Leical, DMIRE2), 2-photon laser scanning confocal microscope (Nikon; Eclipse Ni-EFN Upright/ A1R Si MP Confocal) and epi-fluorescence microscope (Nikon eclipse 400).

Gene	qPCR primer/probe sequences (5'-3')	Tm	Probe#	Amplicon size (bp)	Accession No
cdh1	F: tgtcagagttgagcgtgtcc R: ggaataatccaacctctctttactctt P: ttcctctg	60 59	6	93	NM_131820.1
stat3	F: gtgtgtattgacaaggagtcaggt R: ggatgttgaacttgcgtgaa P: gcagccat	59 59	46	64	NP_571554
zip6	F: gaacgcgcttactttcgagt R: acagcagtgccagtgacatc P: tggtggcc	59 59	49	94	NM_001001591.1
zip10	F: gctgttactgctggcatgttt R: cactgtcaccgtgaagcatt P: tgttgcca	60 59	145	73	NM_200671.1
18s	F: aaactgtttcccatcaacgag R: gggacttaatcaacgcaagc P: ttcccagt	59 59	48	67	FJ915075.1
Snai 3	F: gtgcaagctttgtggaaagg R: gcacgtgaatggtttctcac P: tctccagg	60 59	80	88	NM_001077385.1

Table 6.1: Zinc transporter genes and genes of other molecules associated with EMT with their qPCR primer sequences, UPL probe number, product lengths and accession number. F, R and P denote forward primer, reverse primer and probe sequences.

6.4 Results

6.4.1 Effect of Zip10 knockdown on general embryonic development

Zip10 morpholino (MO) showed a dose-dependent response relationship in developmental abnormality and mortality with high abnormality/mortality at doses above 2ng per embryo. At concentration below 2ng, similar effects were observed for the translation blocking MO or splice blocking MO, whether injected alone or co-injected with p53 MO. Some of the developmental abnormalities observed in morphants injected with the translational blocking MO include delayed epipoly and EMT movement, abnormally small head with abnormal eye development, general underdevelopment with shorter anterior-posterior axis (i.e. stumpy embryo), oedema of the pericardial sac with abnormal string-heart, coiled or twisted tail, delayed hatching and generalised oedema or ballooning of the embryo post hatching (Fig. 6.2).

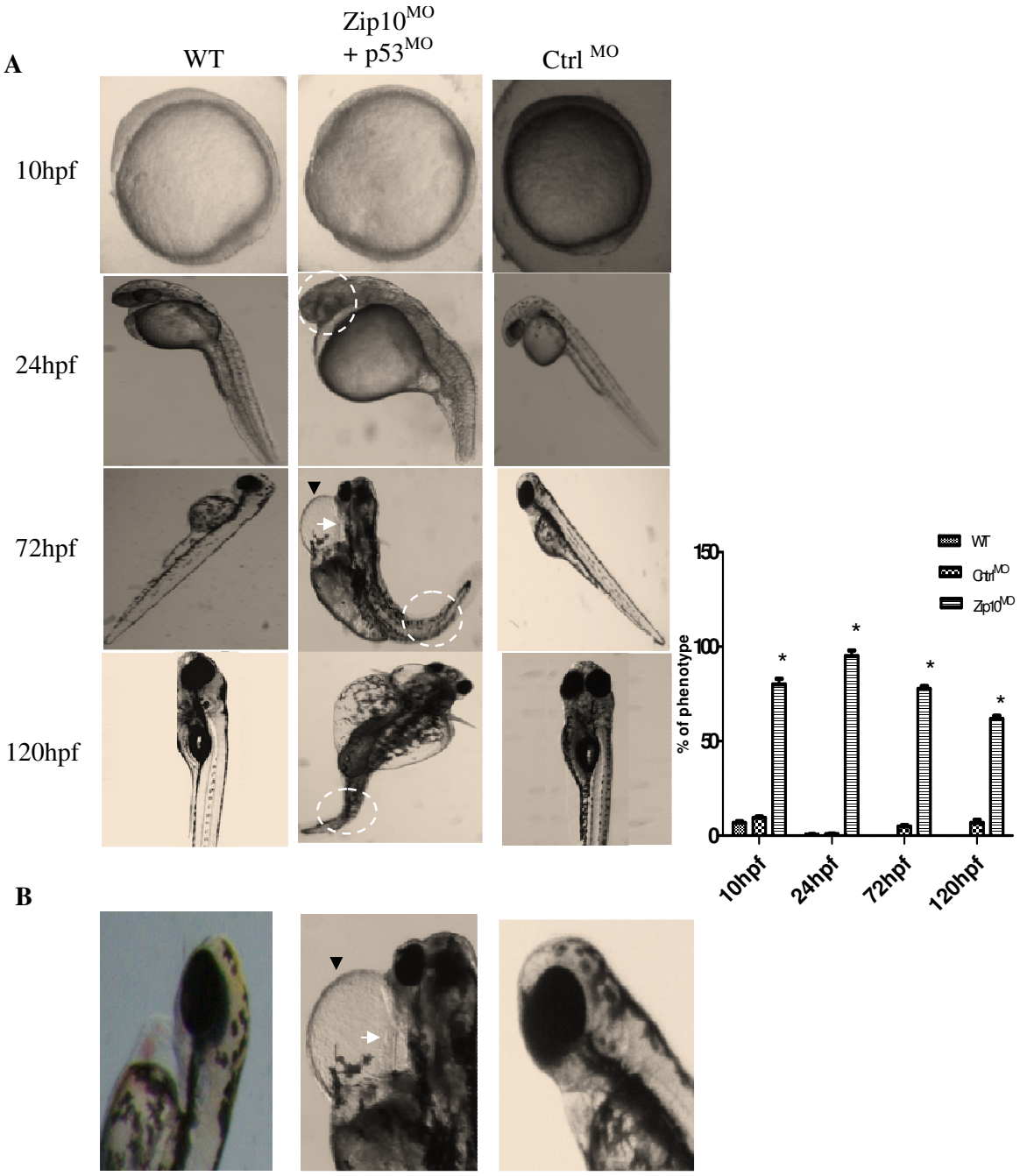

Fig 6.2: Developmental stages of embryos in wild-type embryo, Zip10 morphant and control morphant (N=5 experiments where n= 50 per group). Note the Zip10 morphant embryo at 24hpf with shorter anterio-posterior axis which looks like Zip6 morphant (Fig 9.5) with abnormal head and eye formation (highlighted with white broken circle). Also note the oedema of the pericardial sac (black arrow-head) and the string-heart feature (white arrow) in 72hpf Zip10 morphant that failed to hatch but manually dechorionated (higher magnification in panel B). There was generalized oedema (ballooning) of the body post hatching (black arrow) at 120hpf. Note also the curled or twisted tail at 72 & 120hpf (white broken circles). Graph on the right hand side showed the percentage of embryos displaying abnormalities (phenotypes) at different development stages.

6.4.2 Effect of *zip10* knockdown on epipoly and EMT migration

There was delayed epipoly movement and/or EMT migration at 6hpf and 10hpf in embryos injected with *zip10* MO

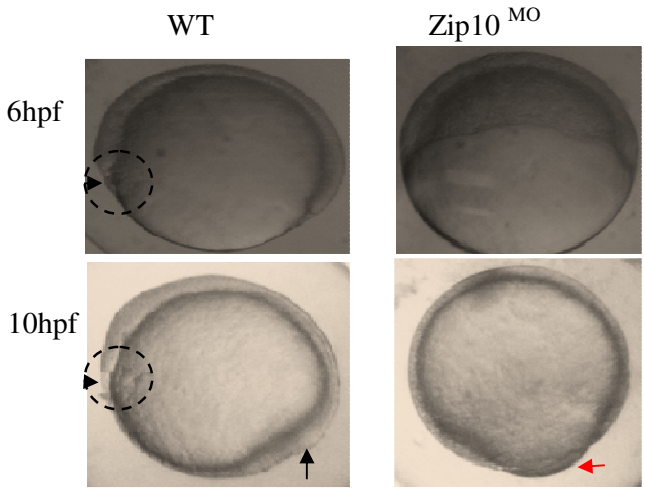

Fig 6.3: Epiboly and/or EMT migration in Zip10 morphant and wild-type embryo (N=5 experiments where n= 20 per group). Note the extension of epipoly migration with EMT which was more advanced in WT than morphant (broken black circles with arrow-heads) at 6hpf and 10hpf with resultant delay in the time of tail bud formation in morphant at 10hpf compared to wild-type. Morphant was yet to complete epiboly (85% complete) at 10hpf (red arrow) when tail bud has already formed in wild-type (black arrow).

6.4.3 Effect of *zip10* knockdown on E-cadherin (*cdh1*) mRNA and protein expression

The results of gel electrophoresis for generating the DIG-labelled antisense RNA probe for cdh1 used in section 6.3.3 was shown in Appendix 9.17 (Fig. 9.3).

Zip10 MO caused increased expression (compared to wild-type) of *cdh1* mRNA by both qPCR (~2.4 fold change) (Figure 6.4.0) and ISH (6.4.1) techniques. Interestingly, there was increased expression of E-cadherin (Cdh 1) at protein level as analysed by Western blotting technique showing about 2.3 fold increase by densitometry analysis (Fig. 6.5.0 A & B) and as also analysed by immunohistochemistry technique (Fig. 6.5.1).

Intriguinly, the expected molecular weight of 97 KDa for E-cadherin was not detected but instead a 150KDa which was distinct and consistent for all the samples analysed by Western blotting.

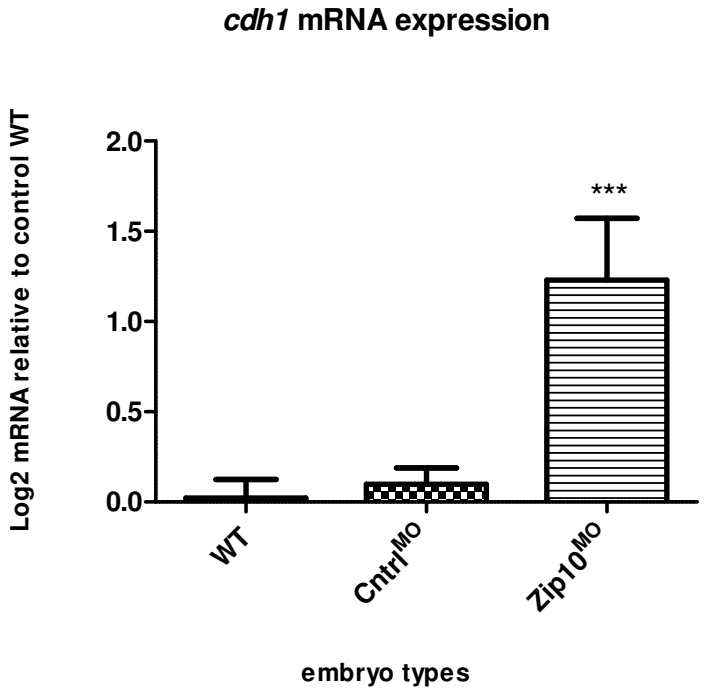

Fig 6.4.0: mRNA expression of *cdh1* in wild-type embryo, control and zip10 morphants by RT-qPCR. Data are presented as the mean ± SEM (N=2 experiments where *n*=6 per group). Zip10 morphant was significantly up-regulated following Livak or REST software analysis method for fold change expression relative to control WT. Data were also analyzed statistically using log2 of ΔΔct values relative to control WT. Key: (***) indicates a statistically significant difference from WT embryos and control morphants at $p \leq 0.001$ (1-way ANOVA)

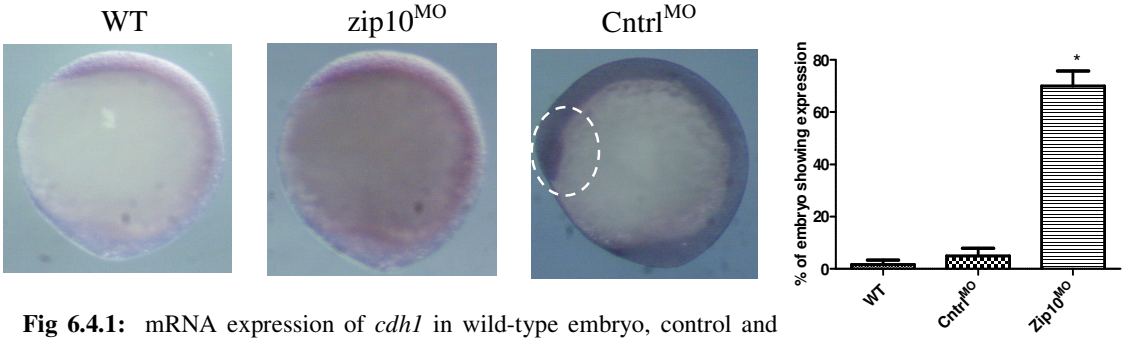

Fig 6.4.1: mRNA expression of *cdh1* in wild-type embryo, control and Zip10 morphants by ISH (N=2 experiments where n= 10 per group). Expression was abundant in morphant than WT (broken white circle). Graph indicated percentage of each embryo showing gene expression.

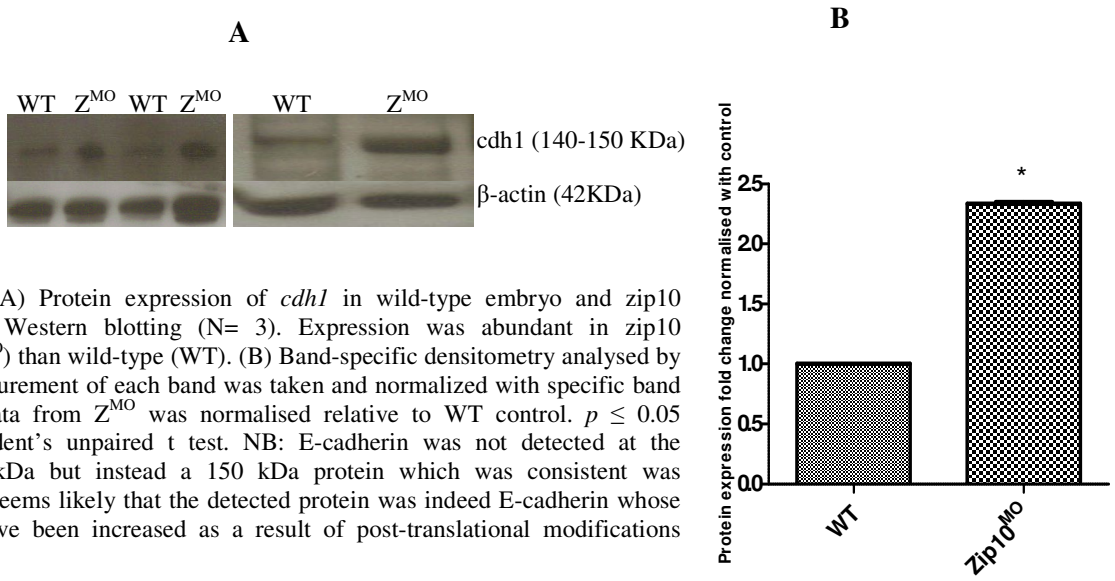

Fig 6.5.0: (A) Protein expression of *cdh1* in wild-type embryo and zip10 morphant by Western blotting (N= 3). Expression was abundant in zip10 morphant (Z^{MO}) than wild-type (WT). (B) Band-specific densitometry analysed by image J. Measurement of each band was taken and normalized with specific band of β-actin. Data from Z^{MO} was normalised relative to WT control. $p \leq 0.05$ following student's unpaired t test. NB: E-cadherin was not detected at the expected 97 kDa but instead a 150 kDa protein which was consistent was visualized. It seems likely that the detected protein was indeed E-cadherin whose size might have been increased as a result of post-translational modifications (PTM)

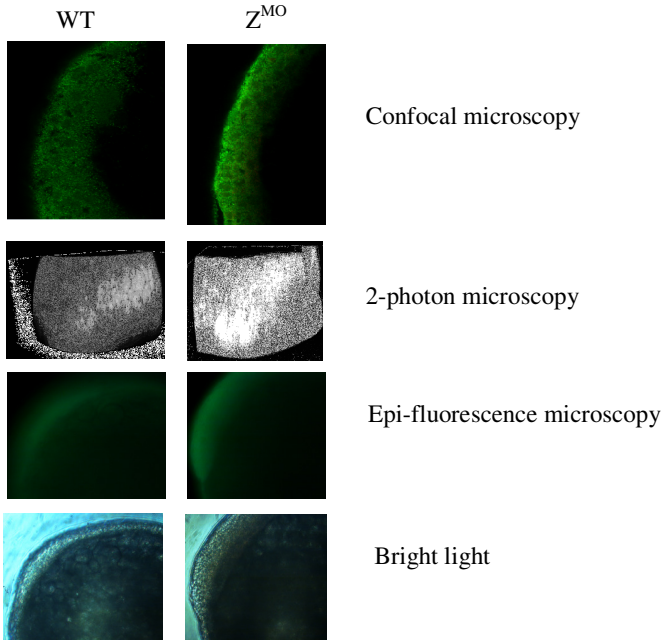

Fig 6.5.1: Protein expression of *cdh1* of the ebipoly in wild-type embryo and zip10 morphant by immunohistochemistry (n= 3). Expression was more intense in zip10 morphant (Z^{MO}) than wild-type (WT).

6.4.4 Effect of *zip10* knockdown on mRNA expression of other molecules associated with cell migration

There was up-regulation of the mRNA expression of *stat3* and *zip6* in Zip10 morphants but mild significant change in *zip10* expression relative to the control (i.e. 2.5, 1.96 and 1.35 FC for *stat3*, *zip6* and *zip10* respectively; Fig 6.6 A, B & C). Zebrafish snail homologue 3 (*snai3)* was assayed but transcripts were not detected in either the morphant or control wild-type.

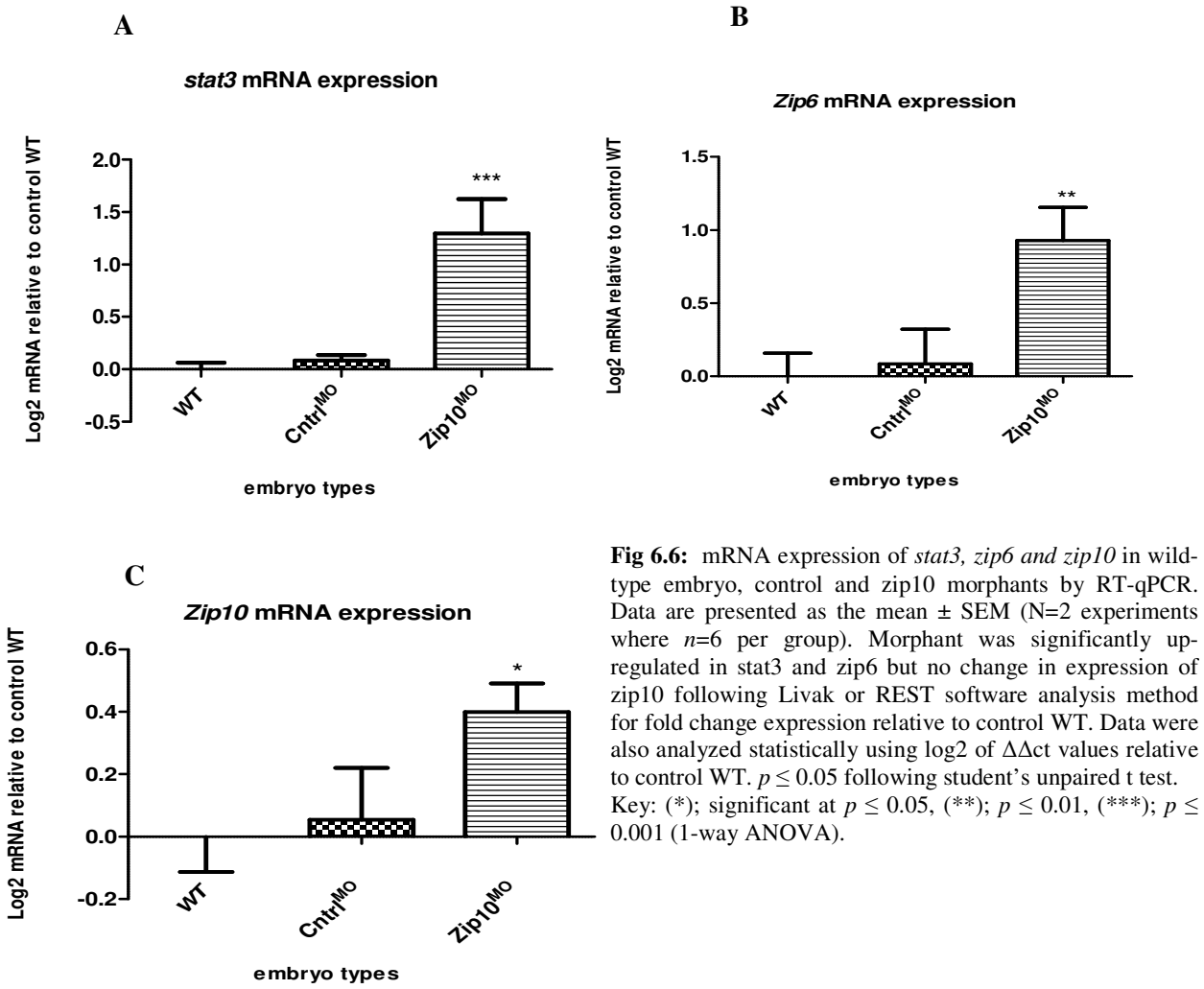

Fig 6.6: mRNA expression of *stat3, zip6 and zip10* in wild-type embryo, control and zip10 morphants by RT-qPCR. Data are presented as the mean ± SEM (N=2 experiments where *n*=6 per group). Morphant was significantly up-regulated in stat3 and zip6 but no change in expression of zip10 following Livak or REST software analysis method for fold change expression relative to control WT. Data were also analyzed statistically using log2 of ΔΔct values relative to control WT. $p \leq 0.05$ following student's unpaired t test. Key: (*); significant at $p \leq 0.05$, (**); $p \leq 0.01$, (***); $p \leq 0.001$ (1-way ANOVA).

6.5 Discussion

The results show that *zip10* is required for normal zebrafish development because knockdown of this gene produced a distinct phenotype (among others) with shorter anterio-posterior axis at 24hpf of development. The embryo at 24hpf looked stumpy and underdeveloped and resembles that of *zip6* knockdown in zebrafish described by Yamashita *et al.,* (2004) (Fig. 9.8). This observation supports the important role of Zip10 in embryonic development, consistent with detection of the *zip10* gene very early in life in the zebrafish embryo (Ho *et al.*, 2012). Central nervous system abnormalities, like a severely dysmorphic head and missing eyes, were observed in most affected embryos with shorter and thickened anterio-posterior hypoblast which was similar to the ones obtained by z*ip6*, s*tat3* and *snail1* knockdown as demonstrated by Yamashita *et al.*, (2004). Thus, Zip10 is required for cell migration responsible for anterior-posterior axis formation because of the effect of Zip10 on EMT formation. It might also be involved in the development and function of some organs such as the heart.

It has been shown that E-cadherin is required for epiboly, as well as convergence and extension cell movements (Shimizu *et al.*, 2005; Babb and Marrs, 2004), where it was shown to be connecting deep cell and enveloping cell layers. Epiboly is a process during which a multilayered sheet of ectodermal cells spreads over and encloses deeper cell layers, becoming thinner as a result and in zebrafish it takes place between 4-10hpf (Lepage and Bruce, 2010). It was interesting to note that a subset of E-cadherin mutants looked similar to Zip10 morphants in our study i.e. delayed epiboly, short stature and no tail (Shimizu *et al.*, 2005). Considering the numerous signalling pathways involved in gastrulation, like Stat3, Wnt and prostaglandin signalling, disrupting any of these pathways results in a similar shortened anterior-posterior and broadened mediolateral body axes, so that these similar phenotypes can be the result of quite distinct

mechanisms (Solnica-Krezel, 2006). E-cadherin has a predicted size of 97 kDa, but has frequently been reported to produce bands of around 120 or even 140 kDa, including specifically in zebrafish (Babb and Marrs, 2004). It contains 8 potential phosphorylation sites and 4 potential *N*-glycosylation sites, and can also be regulated by *O*-glycosylation (Pinho *et al.,* 2011; Zhao *et al.,* 2008). So, it is possible that the 150 kDa band consistently detected in our experiment was indeed E-cadherin whose molecular weight had been increased due to post-translational modifications (PTM). Moreso, some authors have also reported on abcam review website (http://www.abcam.com/E-Cadherin-antibody-ab53033/reviews/16938), the detection of specific bands of approximately 140-150 KDa in zebrafish using Abcam anti-E-cadherin antibody (which was also used in the present study) thus further supporting the evidence that the detected protein was indeed E-cadherin.

It was previously shown that ZIP6 is essential for the nuclear translocation of Snail (a zinc-finger protein) thereby affecting its transcriptional activity required for EMT by repressing E-cadherin expression through AKT- GSK3β pathways (Taylor *et al.,* 2006). It is thought that zinc transported by ZIP6 inhibits GSK3β either directly or indirectly through increase phosphorylation of Akt thus inhibiting phosphorylation of Snail, which allows Snail to remain in the nucleus where it acts as a repressor on cdh1 (An *et al.*, 2005; Ilous *et al.*, 2002). It is proposed that Zip10 may have a similar function and participate in the process either redundantly or as a heterodimer with Zip6 (Fig. 6.8). Up-regulation or over-expression of E-cadherin at mRNA and protein levels in Zip10 MO injected embryos (Fig. 6.4.0, 6.4.1 & 6.5.0), suggest that Zip10 might also acts on Snail but intriguingly, zebrafish snail homolog 3 (*snai3*) mRNA transcripts which was measured could not be detected in either morphant or wild-type control. This could possibly mean that snail or *snai3* is not transcriptionally regulated in zebrafish because

previous study in zebrafish embryo has only looked at nuclear translocation and not expression of Snail (Yamashita *et al.*, 2004). It is also possible that the lack of transcript detection could be due to failure of the qPCR primers-probe sets. Our qPCR assay was not validated and we did not include positive control to verify whether or not Snail is transcriptionally regulated. This needs to be considered along with trying different primer sets or using other zebrafish snail paralogs before a conclusion can be arrived at. Considering the heartstring phenotype and/or a phenotype with pericardial oedema observed in Zip10 morphants, it is possible that Zip10 affects another zinc finger transcription factor, Tbx5, which was shown to affect heart development (Camarata *et al.*, 2010; Lu *et al.*, 2011). It was shown that Pdlim7/Tbx5 interaction is required for healthy heart and pectoral fin formation in zebrafish. Perhaps, it can be speculated that Zip10 protein regulates Pdlim7/Tbx5 interaction through, for example, providing zinc for Pdlim7 to regulate its binding to Tbx5 or vice versa (Jalen *et al.*, 2003) and thus dysregulation or zinc deficiency by Zip10 MO caused abnormal heart formation with subsequent pericardial or generalized oedema. It was also shown in rats that zinc deficiency in the dam result in fetuses with heart anomalies because of the alterations in the expression and distribution of certain heart proteins such as HNK-1, Cx43, SMA, GATA-4 and FOG-2 (Lopez *et al.*, 2008). Interestingly, knockdown of either of Pdlim7 or Tbx5 in zebrafish produce a similar heartstring phenotype or a phenotype with pericardial oedema like Zip10 morphant observed in our present study (Camarata *et al.*, 2010; Lu *et al.*, 2011). Tbx5 also affects transcription of a number of genes of which natriuretic peptide family protein (nppa) is one of them (Plageman and Yutzey, 2006). Nppa is regulating extra-cellular fluid volume and electrolyte homeostasis. This supports the observed oedematous condition in cases of cardiac anomalies or malfunctions. Observing that the Zip10 morphants have oedematous pericardial sac

could be a piece of evidence that Zip10 could affect this particular transcription factor, thus affecting cardiac formation and/or function with direct effect on fluid or electrolyte homeostasis (oedema). However it remains uncertain if defects in heart development are a result of EMT disruption by *zip10* knockdown, or disrupted interaction with specific transcription factors regulating normal heart formation.

The effects of a particular zinc channel or transporter on a particular signalling pathway can be as a result of transporting zinc or other cations, as well as its ability to interact with other proteins. For instance, the ZIP family of zinc transporters especially the ZIP6/10 subgroup have been shown to be closely related to prion proteins and it is likely these proteins have stemmed from the ZIP family (Malaga-Trillo *et al.*, 2009, Ehsani *et al.*, 2011). This prion-like motif in the N-terminal of ZIP10 or ZIP6 could mean that they can dimerise or otherwise form complexes with the prion protein. It has been shown in a number of studies that prion proteins play a role in Ca^{2+}-independent and Ca^{2+}-dependent cell adhesion by regulating E-cadherin delivery to the cell membrane, which seems to be particularly important in autonomous cell movement (Malaga-Trillo *et al.*, 2009, Muras *et al.*, 2009). This somewhat supports the findings that ZIP6 is important for cell autonomous anterior mesendodermal cell movement (Yamashita *et al.*, 2004). Prion proteins was shown to be involved in maintenance of adherens junctions (Malaga-Trillo *et al.*, 2009) and removal of cell of prion proteins promoted cancer cell metastases (Muras *et al.*, 2009). It has been suggested that prion proteins specifically interact with their closest relation in the ZIP family, i.e. ZIP10, ZIP6 and ZIP5 (Malaga-Trillo *et al.*, 2009, Ehsani *et al.*, 2011).

There are a lot of questions that remain open about ZIP10 signalling mechanisms. These mechanisms might be specific interaction with chaperone proteins that deliver zinc to specific intracellular targets to influence cell behaviour (Kagara *et al.*, 2007), or there

are specialist intracellular protein networks that exist which require and condition a specific zinc transporter interaction with specific target molecules, including other zinc transporters.

Overall, our findings indicate a fundamental role of Zip10 in development, particularly in anterio-posterior body axis formation, heart and central nervous system development. The results also suggest possible interaction of Zip10 with Zip6 signalling and it is possible that the defect in Zip10 morphant results in a compensatory response by increased expresion of a close relative *Zip6* mRNA which is under the regulation of *Stat3*, which was also highly up-regulated at mRNA level (Figure 6.6A & B). The mild significant difference in Zip10 mRNA expression of morphants could also be due to a feedback mechanism by the gene trying to cope with the defective protein synthesis or it is just a difference between the data sets because the value of 1.35 FC expression was not statistically significant. It is possible this type of compensatory mechanism can also be found in the Zip6 morphant. It is apparent from the morphological observations that cell movement is affected, and E-cadherin up-regulations appears to be a marker of *zip10* knockdown but whether this is acting through snail pathways was not known.

6.5.1 Summary

Zip10 knockdown in zebrafish embryo affects the EMT and epipoly progression due to overexpression of E-cadherin that resulted in an embryo with a shorter antero-posterior axis as previously observed in *zip6* knockdown embryo. Because of the close relationship of ZIP10 and ZIP6, it is possible they perform similar function to control EMT in embryonic development.

6.5.2 Future studies

This should include experiments on:

i. Snail expression at protein level in Zip10 morphant to determine whether the expression of E-cadherin during gastrulation movement is under the regulation of snail or slug pathway.

ii. MAPK signalling to investigate whether this pathway is connected to EMT formation during the gastrular cell movement in Zip10 morphants.

v. *Zip6* knockdown in embryo to evaluate possible compensatory response of a close relative Zip10 during the gastrulation movement.

vi. Phenotype rescue using human ZIP10 to confirm specificity of *zip10* knockdown in embryos.

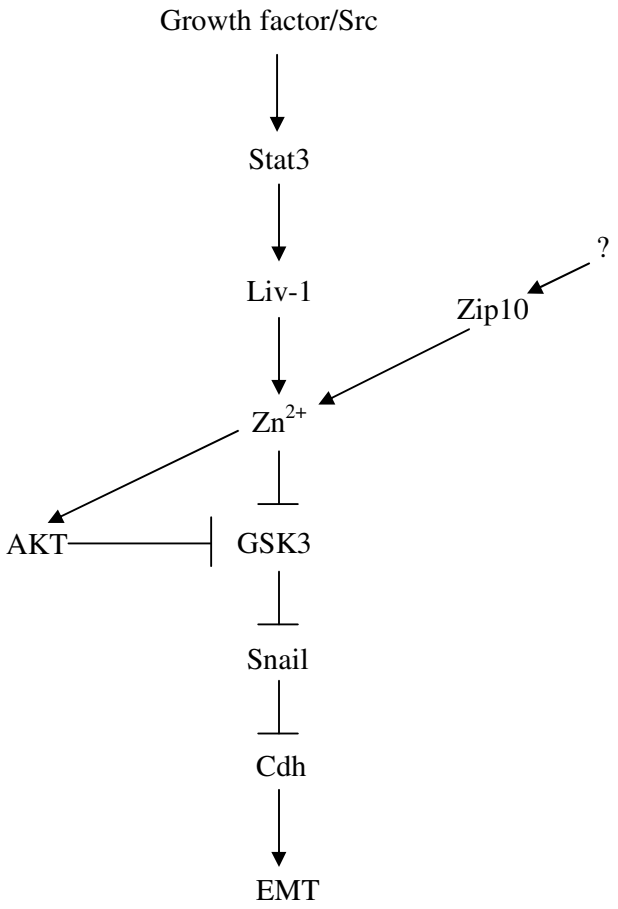

Fig 6.7. Schematic model of Zip 10 and Liv-1 (Zip6) in cell migration. Zip6 and/or Zip10 is required for zinc acquisition necessary for direct inhibition of GSK3 or indirectly through AKT phosphorylation. This leads to nuclearization of Snail, which is a transcriptional repressor of E-cadherin (*cdh*1), thus influencing cell migration. While Liv-1 (Zip6) is activated by Stat3 through activation by the growth factor, what regulates Zip10 is unknown.

CHAPTER SEVEN

GENERAL DISCUSSION AND CONCLUSION/RECOMMENDATION

7 General Discussion

7.1 Zinc transporters and zinc homeostasis

7.1.1 Fish embryo

Maintenance of zinc homeostasis in organisms is a complex biological process requiring cellular proteins that participate in its uptake, sequestration and efflux at both cellular and organismal level. Disturbances in any of these processes can thus influence the strict regulation of this metal ion leading to myriads of zinc-imbalance related diseases in man. ZnT1 is the zinc efflux protein and the first zinc transporter to be cloned (Palmiter and Findley 1995). Disturbances in the regulation of this protein have previously been reported in some animal models to affect some cellular processes such as MAPK signalling resulting in impairment of growth and development among other anomalies (Bruinsma *et al.*, 2002; Lazarczyk *et al.*, 2008). Similarly, we have shown in the present study the importance of Znt1 in some cellular events in the zebrafish model. Our results clearly demonstrated that mutation of the *znt1* gene caused impairment of functions at cellular and organismal level. We have shown that deletion of the last 40 amino acids from the C-terminus of Znt1 in zebrafish or temporary *znt1* gene knockdown resulted in impairment of Zn^{2+} regulation causing abnormal Zn^{2+} accumulation and/or altered distribution of labile Zn^{2+} as well as deregulation of copper and selenium in embryos. The slower embryogenesis observed in zebrafish with Znt1 deficiency also supported the findings of previous workers implicating ZnT1 or CDF-1 in growth and development (Andrew *et al.*, 2004; Bruinsma *et al.*, 2002).

In the study of hatching of zebrafish embryos, we have shown for the first time the importance of Znt1 in the hatching process. Znt1 mRNA was found to be expressed in the HGC of embryos and deficiency of this gene either through mutation or gene knockdown blocked this expression but intriguinely it resulted in embryos that hatched

earlier. In a related study, we similarly showed for the first time the involvement of another zinc transporter or channel, Zip10, in the hatching process. The expression of this gene in HGC was shown by previous workers but there had been no investigation of its functional significance in hatching. We showed here for the first time that knocking down this gene blocked its expression in the HGC resulting in embryos that hatched late. This process of hatching caused by expression of *znt1* or *zip10* in the HGC clearly demonstrated the function of their proteins in maintaining zinc homeostasis of the HGC. This was shown with *zip10* knockdown whereby there was probably lack of Zn^{2+} uptake by Zip10 in the HGC and, conversely, with *znt1* knockdown there was a defective Zn^{2+} extrusion from the cell by Znt1. These two events may have changed the expression of Znt2, which is involved in the movement of Zn^{2+} ions into the endosomal compartment (lysosome) for activation and/or expression of hatching enzymes. Znt2 expression was possibly enhanced in *znt1* knockdown forcing more Zn^{2+} ions inside the lysosomal compartment leading to an increased activation and/or expression of hatching enzyme, and the reverse might be the case with *zip10* knockdown in which the activation or expression of hatching enzyme was reduced or even completely abolished (see the models in Figure 5.9). These effects might explain early and late hatching observed in *znt1* and *zip10* knockdown respectively. The relevance of this study, apart from understanding zinc homeostasis in hatching, is that it reveals how the zebrafish may be a suitable model to study some apoptotic pathways or the pathogenesis of some zinc-protease related diseases in man such as Alzeimer's or prostate diseases whereby lack of Zn^{2+} ions is associated with premature activation of cathepsin or related enzymes (Tougu *et al.*, 2011; Liang *et al.*, 1999). This effect was shown here with *zip10* knockdown where lack or insufficient Zn^{2+} caused premature activation of cathepsin L1b which then exerted its destructive or proteolytic effect on hatching gland tissue

resulting in tearing or sloughing off. The importance of Zip10 in early development of embryos was also shown in our study, where it controlled gastrulation movement as was previously demonstrated for its close relative Zip6 (Liv-1) in zebrafish embryo (Yamashita *et al.*, 2004). A similar mechanism has been reported for cancer progression and metastasis in breast cancer cell lines for both ZIP proteins (Kagara *et al.*, 2007; Taylor *et al.*, 2007). Therefore, the zebrafish Zip10 model (as well as Zip6) could serve as another suitable model for studying disease condition as well as normal development in man, specifically tumorigenesis and embryogenesis (see Figure 6.7). We could not fully demonstrate the efficacy of protein expression knockdown by respective zinc transporter MO in embryos due to lack of availability of antibodies cross-reacting with zebrafish Znt1 or Zip10, and preliminary Western blot experiments using antibodies to the respective mammalian orthologs failed. However, the lack of observable mRNA expression of each zinc transporter in the HGC of embryos injected with the respective MO strongly indicated that the knockdown was efficacious. In addition, the use of two different MO types (translation or splice blocker) for each transporter with and without p53 MO co-injection that resulted in similar phenotypes also indicated the efficacy of MO knockdown in our study.

7.1.2 Adult Fish

The importance of the zinc transporter ZnT1 and zinc homeostasis in the regulation of various biological processes were both demonstrated in adult fish. Absence of the last 40 amino acids of Znt1 in zebrafish was shown to affect uptake and distribution of dietary zinc. High dietary zinc affected the expression of Znt1, Znt4, Znt5, Zip7 and MT2 differentially in mutants than in normal fish, which could be a compensatory mechanism in the mutants to cope with the zinc load so as to achieve homeostatic balance. We showed up-regulation or over-expression of the genes coding for these proteins in the intestine following high dietary zinc in mutants. The expression of MT2 indicates high zinc accumulation in the enterocytes supporting previous reports based on other models where ZnT1 or CDF-1 was shown to be important in the basolateral transfer of the Zn^{2+} ions from the eneterocyte into the systemic circulation (Wang *et al.*, 2009; Davis *et al.*, 2009). ZnT1 is known to be important in controlling or regulating other cellular events apart from homeostatic regulation of the Zn^{2+} ions in adults as well as in embryos. This was demonstrated in the present study whereby the data were consistent with a scheme in which the protein interacts with other cellular proteins to influence the activation of the Ras-ERK (MAPK) signalling cascade. Although, several reports have suggested that Zn^{2+} activation of the Ras-ERK (MAPK) signalling cascade is due to inhibition of dual specific protein phosphatases; DUSP (Sato *et al.*, 1995; Wu *et al.*, 1999; Ho *et al.*, 2008), other studies have equally shown that activation of this pathway is due to ZnT1 activation of Raf-1, and that Zn^{2+} in cells deficient in ZnT1 actually inhibits ERK (Jirakulaporn and Muslin 2004; Bruinsma, 2002; Beharier *et al.*, 2012). Our observations made in zebrafish with mutated Znt1 lacking its C-terminal 40 amino acids clearly support a direct role of Znt1 in Raf-1 activation and pin-point the region of Znt1 required for this process. An alternative model, which might consolidate

the apparently contradictory findings in different studies, could be that the activation of MAPK by Zn^{2+} is through two different signalling pathways or through a single pathway involving two steps whereby disturbances in either of the steps affects the downstream activation process as shown in the model presented in Figure 7.1. It is possible that physiologically increased concentration of cytosolic Zn^{2+} following zinc supplementation up-regulates full length ZnT1 thereby enhancing its interaction through its C-terminus with activated Raf1 kinase. This interaction alongside Zn^{2+} inhibition of DUSP cooperatively activates the MAPK pathway. Therefore with abnormal ZnT1, especially when lacking the full length protein or lacking the C-terminal part of the protein, the endogenous cytosolic Zn^{2+} would be higher relative to wild-type ZnT1 causing DUSP inhibition, but ZnT1 would be unable to interact with Raf1 even when zinc is supplemented thereby leading to reduction in the downstream activation of the pathway when compared with normal ZnT1 as observed in the present study. This model could be supported by the ability of truncated ZnT1 that contained its C-terminus to cause a 'relative' increase in endogenous cytosolic Zn^{2+} level as well as capable of activating the downstream MAPK signalling cascade but being unable to protect cells against Zn^{2+} toxicity following zinc exposure because of inability to flux Zn^{2+} (Beharier *et al.*, 2012). Disturbances in the signalling cascade as a result of a ZnT1 defect was previously shown to affect oocyte maturation (Jurakulaporn and Muslin, 2004), embryonic development (Bruinsma et al 2002; Andrew *et al.*, 2004) as well as to cause cardiovascular defects (Beharier *et al.,* 2012; Ren *et al.*, 2010). We showed here also that the impairment of this signalling event in Znt1 mutant fish might contribute to delayed embryonic development and erratic breeding behaviour/abnormal development that were observed more frequently in mutants in the present study, including broken pigmentation, kinked tail, arched back, unfitness (Appendix 9.19; Figure 9.5),

occasional disturbances in breeding and spawning with delayed maturation and early ceasation of breeding in adults. The defect in breeding and spawning behaviour could be attributed to the effect of Znt1 in regulation of circadian-controlled genes through the MAPK signalling processes (Fig. 4.0). We showed that this defect also caused a defect in *clock* gene regulation and we equally showed for the first time that zinc supplementation in zebrafish modulates the circadian rhythm.

In conclusion, the present study utilized the reverse genetic approach in a zebrafish model to investigate the functional role of zinc and zinc transporters in the control and regulation of many biological processes at molecular, cellular and organismal levels. The findings have undoubtedly further opened areas of research opportunities that could be explored to unravel the mechanism of the development of some metabolic diseases in man and animals. The findings in this study would be relevance in the field of medicine, agriculture/aquaculture and in general, in the advancement of scientific knowledge.

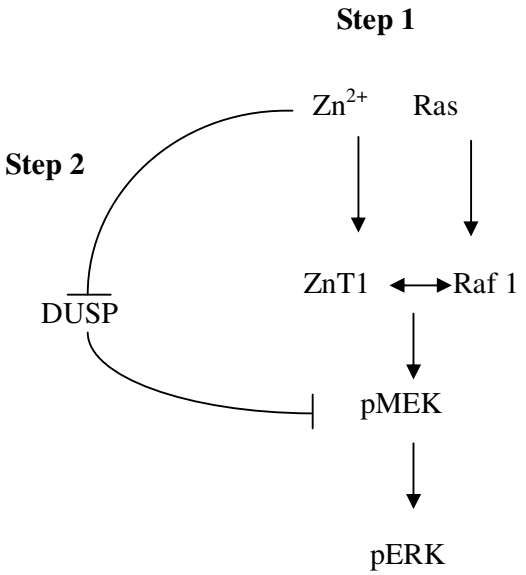

Fig 7.1. Schematic model showing the relationship of zinc and ZnT1 in MAPK signalling pathway. Extracellular zinc supplementation is assumed to cause over-expression of full-length ZnT1 and at the same time inhibition of DUSP which altogether enhances ZnT1-Raf1 interaction leading to downstream activation of MAPK pathway. On the other hand, a C-terminally truncated ZnT1 is unable to interact perfectly with Raf-1 causing a 'relative' increase in cytosolic zinc which could not inhibit DUSP activity thus, affecting downstream signalling of MAPK. Zinc supplementation in this condition may improve the activation but at a lesser degree compared to the full-length ZnT1.

7.2 General recommendation/future perspective

The data and experience obtained from the present work no doubt provide valuable information for the planning of future studies that aim to further assess the biological and functional relevance of *znt1* and *zip10* genes in zebrafish model. The limitations as well as the strengths of the study design employed have been highlighted and more targeted studies have been elaborated for future research. It is recommended that further works are done in this area of research to give better understanding on the role of zinc and zinc transporters in health and disease. In recent years, polymorphisms of several zinc transporters have been associated with a number of conditions in humans (Sladek *et al.,* 2007; Nakano *et al.,* 2009; Quadri *et al.,* 2012) and animals (Simonehauser and Baumgartner, 2005; Yuzbasiyan-Gurkan and Bartlett, 2006; Siebert *et al;* 2013). Although it has not been well studied, a significant correlation ($p < 1 \times 10^{-6}$) exists between a Singe Nucleotide Polymorphism, rs1614866, in *ZnT1*, and hypertention in African Americans (Lettre et al, 2011). Further studies should be geared towards identification of such associations with *ZnT1* in other population. The importance of truncated region of Znt1 in protein-protein interaction with signalling peptides or molecules relevance in regulating or modulating crucial biological processes in the body should be investigated using suitable model systems for *in vitro* or *in vivo* assay. This line of research should be intensified to address the area that involves the relationship of Znt1 protein with vertebrate development and breeding behaviour. Moreover, the work should be extended further so as to fully understand the role of Znt1 and Zip10 in regulation of zinc and other proteins such as proteases involvement in hatching of teleost. This will be of relevance in commercial fish production whereby the time to hatch of embryo can be induced or accelerated, thus enhancing productivity. It will also be of benefit in the area of biomedical research to study the involvement of

proteases viz-a-viz zinc and zinc transporter(s) in the pathogenesis of diseases such as Alzeimer's and prostate which currently are receiving serious attention globally. More importantly, the involvement of Zip10 in early embryonic development should be extended further to fully understand the mechanism of cellular migration which is of importance in understanding cancer metastasis and invasiveness, a condition that's also receiving very serious concern and attracting huge research funding. This research can also be of importance if further investigated to unravel the effect of Zip10 in cardiac formation and function which is also getting utmost attention at present. Thus, in future studies, if these areas of research are thoroughly looked into, there are lots of benefit to be derived which will be a veritable arsenal for solving some problems bedevilling human society.

CHAPTER EIGHT

REFERENCES

8 REFERENCES

Aggett PJ, Comerford JG (1995). Zinc and human health. *Nutr Rev* 53:S16-22.

Akashi M, Nishida E (2000). Involvement of the MAP kinase cascade in resetting of the mammalian circadian clock. *Genes Dev*. 14: 645-649.

An WL, *et al.* (2005). Mechanism of zinc-induced phosphorylation of p70 S6 kinase and glycogen synthase 3beta in SH-SY5Y neuroblastoma cells. *Journal ofneurochemistry,* 92 (5): 1104-15.

Andreini C, Banci L, Bertini I, Rosato A (2006). Counting the zinc-proteins encoded in the human genome. *J Proteome Res.*;5:196-201.

Andreini, C, Bertini, I (2011). A bioinformatics view of zinc enzymes. *J Inorg Biochem*, 10.1016/j.jinorgbio.2011.11.020.

Andrew JM, Daut J, Schwappach B (2011). Membrane proteins as 14-3-3 clients in functional regulation and intracellular transport. *PHYSIOLOGY* 26:181-191.

Andrews GK (2008). Regulation and function of Zip4, the acrodermatitis enteropathica gene. *Biochem. Soc. Trans.* 36:1242-1246.

Andrews GK (2001). Cellular zinc sensors: MTF-1 regulation of gene expression. *Biometals* 14: 223-237.

Andrews GK, Wang H, Dey SK, Palmiter RD (2004). Mouse zinc transporter 1 gene provides an essential function during early embryonic development. *Genesis* 40: 74-81.

Babb SG and Marrs JA (2004). E-Cadherin Regulates Cell Movements and Tissue Formation in Early Zebrafish Embryos. *DEVELOPMENTAL DYNAMICS* 230:263-277.

Balesaria S (2004). Znt1 and zinc regulation in teleost fish. PhD thesis, King's College London.

Balesaria S, Hogstrand C (2006). Identification, cloning and characterization of a plasma membrane zinc efflux transporter, TrZnT-1, from fugu pufferfish (Takifuglu ruhripes). *Biochemical Journal* **394**, 485-493.

Ballif BA, and Blenis J (2001). Molecular mechanisms mediating mammalian mitogenactivated protein kinase (MAPK) kinase (MEK)-MAPK cell survival signals. *Cell Growth Diff*., 12:397-408.

Barman RP (1991). A taxonomic revision of the Indo-Burmese species of Danio rerio. Record of the Zoological Survey of India Occasional Papers 137, 1-91.

Barrett AJ, Rawlings ND, Woessner JF Jr. (Eds.), (1998). *Handbook of Proteolytic Enzymes.* Academic Press, London.

Beharier O, Dror S, Levy S, Kahn J, Mor M, Etzion S, Gitler D, Katz A, Muslin AJ, Moran A, Etzion Y (2011). ZnT-1 protects HL-1 cells from simulated ischemia-reperfusion through activation of Ras-ERK signaling. *J Mol Med (Berl).* doi:10.1007/s00109-011-0845-0

Berghmans S, Murphey RD, Wienholds E, Neuberg D, Kutok JL, *et al.* (2005). tp53 mutant zebrafish develop malignant peripheral nerve sheath tumors. *Proc Natl Acad Sci* U S A 102: 407-412.

Besecker B, Bao S, Bohacova B, Papp A, Sadee W, Knoell DL (2008). The human zinc transporter SLC39A8 (Zip8) is critical in zinc-mediated cytoprotection in lung epithelia. *Am. J. Physiol. Lung Cell. Mol. Physiol*. 294: L1127-L1136 .

Bettger WJ, O'Dell BL (1993). Physiological roles of zinc in the plasma membrane of mammalian cells. *J Nutr Biochem* 4:194-207.

Beyersmann D. and Haase H. (2001). Functions of zinc in signaling, proliferation and differentiation of mammalian cells. *Biometals* 14: 331-341

Bodar CW, Pronk ME, Sijm DT (2005). The European Union risk assessment on zinc and zinc compounds: the process and the facts. *Integr. Environ. Assess Manag.* 1: 301-319.

Boden MJ, Kennaway DJ (2006). "Circadian rhythms and reproduction". *Reproduction* 132 (3): 379-92. doi:10.1530/rep.1.00614. PMID 16940279.

Bosomworth HJ, Thornton JK, Coneyworth LJ, Ford D, Valentine RA (2012). Efflux function, tissue-specific expression and intracellular trafficking of the zinc transporter ZnT10 indicate roles in adult zinc homeostasis. *Metallomics* 4:771-779.DOI: 10.1039/c2mt20088k.

Bunger MK, Walisser JA, Sullivan R, Manley PA, Moran SM, Kalscheur VL, Colman RJ, Bradfield CA (2005). Progressive arthropathy in mice with a targeted disruption of the Mop3/Bmal-1 locus. *Genesis* 41 (3): 122-32. doi:10.1002/gene.20102. PMID 15739187.

Bruinsma JJ, Jirakulaporn T, Muslin AJ, Kornfeld K (2002). Zinc ions and cation diffusion facilitator proteins regulate Ras-mediated signaling. *Dev. Cell.* 2: 567-578.

Camarata T, Krcmery J, Snyder D, Park S, Topczewski J, Simon HG (2010). Pdlim7 (LMP4) regulation of Tbx5 specifies zebrafish heart atrio-ventricular boundary and valve formation. *Dev Biol* 337: 233-45, 10.1016/j.ydbio.2009.10.039.

Carlsson L, Ronquist G, Ronquist G, Eliasson R, Egberg N, Larsson A (2011). Association of cystatin C with prostasomes in human seminal plasma. *Int J Androl* 34:363-368.

Cermakian N, Pando MP, Thompson CL, Pinchak AB, Selby CP et al (2002). Light induction of a vertebrate clock gene involves signaling through blue-light receptors and MAP Kinases. *Current Biology* 12:844-848.

Cermakian N, Whitmore D, Foulkes NS, Sassone-Corsi P (2000). Asynchronous oscillations of two zebrafish CLOCK partners reveal differential clock control and function. *Proc Natl Acad Sci* USA; 7:4339-4344.

Chan DW, Yager TD (1998). Preparation and imaging of nuclear spreads from cells of the zebrafish embryo. Evidence for large degradation intermediates in apoptosis. *Chromosoma*;107:39-60.

Chang HB, Lin CW, Huang HJ (2005). Zinc-induced cell death in rice (*Oryza sativa* L.) roots. *Plant Growth Regul* 46:261-266.

Chen JN, Fishman MC (1996). Zebrafish tinman homolog demarcates the heart field and initiates myocardial differentiation. *Development* 123:293-302.

Chimienti F, Aouffen M, Favier A, Seve M. (2003). Zinc homeostasis-regulating proteins: new drug targets for triggering cell fate. *Curr Drug Targets* 4: 323-338.

Chwieralski CE, Welte T, Bühling F (2006). Cathepsin-regulated apoptosis. *Apoptosis* 11: 143-149.

Cho YH, Lee SJ, Lee JY, Kim SW, Lee CB, Lee WY, Yoon MS (2002). Antibacterial effect of intraprostatic zinc injection in a rat model of chronic bacterial prostatitis. *Int. J. Antimicrob. Agents* 19:576-582.

Chowanadisai W, Lönnerdal B, Kelleher SL (2006). Identification of a mutation in SLC30A2 (ZnT-2) in women with low milk zinc concentration that results in transient neonatal zinc deficiency. *J. Biol. Chem.* 281: 39699-39707.

Cole LK, Ross LS (2001). Apoptosis in the developing zebrafish embryo. *Dev Biol*, 240:123-142.

Coleman JE (1998). Zinc enzymes. *Curr Opin Chem Biol.,* 2:222-234.

Colvin RA, Fontaine CP, Laskowski M, Thomas D (2003). Zn^{2+} transporters and Zn^{2+} homeostasis in neurons. *Eur. J. Pharmacol.* 479:171-185.

Colvin RA, Bush AI, Volitakis I., Fontaine CP, Thomas D, Kikuchi K, Holmes WR (2008). Insights into Zn2+ homeostasis in neurons from experimental and modeling studies. *American Journal of Physiology-Cell Physiology,* 294: C726-C742.

Colvin RA., Holmes WR, Fontaine CP Maret W (2010). Cytosolic zinc buffering and muffling: Their role in intracellular zinc homeostasis. *Metallomics* 2: 306-317.

Coneyworth LJ, Jackson KA, Tyson J, Bosomworth HJ, van der Hagen E, Hann GM, Ogo OA, Swann DC, John C. Mathers JC, Valentine RA, Ford D (2012). Identification of the Human Zinc Transcriptional Regulatory Element (ZTRE): A palindromic protein-

binding DNA sequence responsible for zinc-induced transcriptional repression. *J Biol Chem* 28 (43): 36567-36581. doi 10.1074/jbc.M112.397000.

Cousins RJ, Liuzzi JP, Lichten LA (2006). Mammalian zinc transport, trafficking, and signals. *J Biol Chem* 281: 24085-24089.

Cousins RJ, Blanchard RK, Popp MP, Liu L, Cao J, et al (2003). A global view of the selectivity of zinc deprivation and excess on genes expressed in human THP-1 mononuclear cells. *Proc. Natl. Acad. Sci.* USA 100:6952-57.

Cousins RJ, McMahon RJ (2000). Integrative aspects of zinc transporters. *Journal of Nutrition* 130: 1385S-1387S.

Cragg R A, Christie GR., Phillips SR, Russi RM, Kury S, Mathers, JC, Taylor PM, Ford D (2002). *J Biol Chem* 277(25): 22789-22797

Cragg RA, Phillips SR, Piper JM, Varma JS, Campbell FC, Mathers JC, Ford D (2005). Homeostatic regulation of zinc transporters in the human small intestine by dietary zinc supplementation. *Gut* 54(4): 469-478.

Creighton, C. J.; Chang, J. C.; Rosen, J. M (2010). Epithelial-Mesenchymal Transition (EMT) in Tumor-Initiating Cells and Its Clinical Implications in Breast Cancer. *Mammary*
Gland Biol Neoplasia 15:253–260.

Crespo S, Sala R (1986). Ultrastructural alterations of the dogfish (Scyliorhin us canicula) gill filament related to experimental aquatic zinc pollution. *Dis. aquat. Org* 1:91-104.

Cummings JE and Kovacic JP (2009). The ubiquitous role of zinc in health and disease, *Journal of veterinary emergency and critical care,* 19:215-240.

Czerkies P, Brzuzan P, Kordalski K, Luczynski M (2001).Critical partial pressures of oxygen causing precocious hatching in *Coregonus lavaretus* and *C. albula* embryos. *Aquaculture* 196:151-158.

Dahl SW, Halkier T, Lauritzen C, Dolenc I, Pedersen J, Turk V, Turk B (2001) Human recombinant pro-dipeptidyl peptidase I (cathepsin C) can be activated by cathepsins L and S but not by autocatalytic processing. *Biochemistry*, 40:1671-1678.

Dave G, Damgaard B, Grade M, Martelin JE, Rosander B, Viktor T (1987). Ring test of an embryo-larva toxicity test with zebrafish (Brachydanio rerio) using chromium and zinc as toxicants. *Environmental toxicology and chemistry*, 6:61-71.

Davie A, Minghetti M, Migaud H (2009). Seasonal variations in clock-gene expression in Atlantic salmon (*Salmo salar*). *Chronobiology International*, 26(3): 379-395.

Davis DE, Roh HC, Deshmukh K, Bruinsma JJ, Schneider DL, Guthrie J, Robertson JD, Kornfeld K (2009). The Cation Diffusion Facilitator Gene *cdf-2* Mediates Zinc Metabolism in Caenorhabditis elegans. *Genetics,* 182: 1015-1033.

De Schamphelaere KAC, Lofts S, Janssen CR (2005). Bioavailability models for predicting acute and chronic toxicity of zinc to algae, daphnids, and fish in natural surface waters. *Environmental Toxicology and Chemistry,* 24: 1190-1197.

Demmel U, Hock A, Kasperek K, Feinendegen LE (1982). *Sci. Total Environ*. 24: 135-146.

Donehower LA, Harvey M, Slagle BL, McArthur MJ, Montgomery CA Jr, *et al.* (1992). Mice deficient for p53 are developmentally normal but susceptible to spontaneous tumours. *Nature* 356: 215-221.

Draper BW, Morcos PA, Kimmel CB (2001). Inhibition of zebrafish fgf8 pre-mRNA splicing with morpholino oligos: a quantifiable method for gene knockdown. *Genesis*. 30:154-156.

Dufner-Beattie J, Langmade SJ, Wang F, Eide D, Andrews GK (2003b). Structure, function, and regulation of a subfamily of mouse zinc transporter genes. *J Biol Chem* 278: 50142-50150.

Dufner-Beattie J, Wang F, Kuo YM, Gitschier J, Eide D, Andrews GK (2003) The acrodermatitis enteropathica gene ZIP4 encodes a tissue-specific, zinc-regulated zinc transporter in mice. *J. Biol. Chem.* 278: 33474-33481.

Dufner-Beattie J, Huang ZL, Geiser J, Xu W, Andrews GK (2006). Mouse ZIP1 and ZIP3 genes together are essential for adaptation to dietary zinc deficiency during pregnancy. *Genesis* 44(5):239-251.

Dufner-Beattie J, Weaver BP, Geiser J, Bilgen M., Larson M, Xu WH, Andrews GK (2007). The mouse acrodermatitis enteropathica gene Slc39a4 (Zip4) is essential for early development and heterozygosity causes hypersensitivity to zinc deficiency. *Human Molecular Genetics,* 16: 1391-1399.

EC (2003). Opinion of the Scientific Committee for Animal Nutrition on the use of zinc in feedingstuffs., vol. 2010: European Commission.

Ebadi M (1991). *Methods Enzymol.* 205: 263-387.

Ehsani S, Huo H, Salehzadeh A, Pocanschi CL, Watts JC, Wille H *et al.* (2011). Family reunion-the ZIP/prion gene family. *Prog Neurobiol* 93: 405-20.

Eid AE, Ghonim SI (1994). Dietary zinc requirement of fingerling *Oreochromis niloticus*. *Aquaculture* 119: 259-264.

Eide DJ (2011). The oxidative stress of zinc deficiency. *Metallomics* 3:1124-1129.

Eide DJ (2004). The SLC39 family of metal ion transporters. *Pflugers Arch.* 447:796-800.

Ekker SC, Larson JD (2001). Morphant technology in model developmental systems. *Genesis* 30: 89-93.

Ekker SC (2008). Zinc finger-based knockout punches for zebrafish genes. *Zebrafish* 5 (2): 1121-3. doi:10.1089/zeb.2008.9988.PMC 2849655. PMID 18554175

Ellis CD, Macdiarmid CW, Eide CW (2005). Heteromeric protein complexes mediate zinc transport into the secretory pathway of eukaryotic cells. *J. Biol. Chem*. 280: 28811-28818.

Eng BH, Guerinot ML, Eide D, Saie MH Jr (1998). Sequence analyses and phylogenetic characterization of the ZIP family of metal ion transport proteins. *J. Membr. Biol.* 166:1-7.

Falchuk KH, Montorzi M, and Vallee BL (1995). Zinc uptake and distribution in Xenopus laevis oocytes and embryos. *Biochemistry* 34: 16524-16531.

Fairweather-Tait SJ, Harvey LJ, Ford D (2008). Does ageing affect zinc homeostatsis and dietary requirement? *Experimental Gerontology* 43: 382-388.

Fairweather-Tait SJ, Bao Y, Broadley MR, Collings R, Ford D, Hesketh JE, Hurst R (2011). Selenium in human health and disease (A comprehensive invited review). *Antioxid Redox Signal* 14, 1337-1383.

Fan T, Wang J, Yuan W, Zhong Q, Shi Y, Cong R (2010). Purification and characterization of hatching enzyme from brine shrimp Artemia salina. *Acta Biochim Biophys* 42(2):165-71

Fang F (2001). *Phylogeny and species diversity of the South and Southeast Asian cyprinid genus Danio Hamilton (Teleostei, Cyprinidae)*. Thesis (PhD). Stockholm University, Stockholm, Sweden.

Feeney GP, Zheng D, Kille P, Hogstrand C (2005). The phylogeny of teleost ZIP and ZnT zinc transporters and their tissue specific expression and response to zinc in zebrafish. *Biochim Biophys Acta* 1732: 88-95.

Foote and Delves (1984). Albumin bound and alpha 2-macroglobulin bound zinc concentrations in the sera of healthy adults. *J Clin Pathol*. 1984 Sep;37(9):1050-4.

Fosmire GJ (1990). Zinc toxicity. *Am J Clin Nutr* 51: 225–227.

Frederickson, C. J. and Bush, A. I. (2001). Synaptically released zinc: physiological functions and pathological effects. *Biometals* 14: 353-366

Fu D (2010). Zinc transporter YiiP from Escherichia coli. Handbook of metalloproteins. 1-11.

Fu L and Lee CC (2003). The circadian clock: pacemaker and tumour suppressor. Nature review. *Cancer.* 3:350-361.

Fukada T, Civic N, Furuichi T, Shimoda S, Mishima K, *et al.* (2008). The zinc transporter SLC39A13/ZIP13 is required for connective tissue development: its involvement in BMP/TGF-beta signaling pathways. *PLoS ONE* 3(11):e3642

Fukada T, Kambe T (2011). Molecular and genetic features of zinc transporters in physiology and pathogenesis. *Metallomics* 3: 662-674.

Fung EB, Ritchie LD, Woodhouse LR, Roehl R, King JC (1997). Zinc absorption in women during pregnancy and lactation: a longitudinal study. *Am. J. Clin. Nutr.*66:80–88

Gaither LA and Eide DJ (2001). Eukaryotic zinc transporters and their regulation. *Biometals* 14:251–270.

Gardiner MR, Daggett DF, Zon LI, Perkins AC (2005). Zebrafish *KLF4* is essential for anterior mesendoderma/pre-poster differentiation and hatching. *Developmental Dynamics*, 234:992-996.

Gatlin DM, Wilson RP (1983). Dietary zinc requirement of fingerling channel catfish. *Journal of Nutrition* 113: 630-635.

Geiser J, Venken KJT, De Lisle RC, Andrews GK (2012) A Mouse Model of Acrodermatitis Enteropathica: Loss of Intestine Zinc Transporter ZIP4 (Slc39a4) Disrupts the Stem Cell Niche and Intestine Integrity. *PLoS Genet* 8(6): e1002766. doi:10.1371/journal.pgen.1002766.

Gelb BD, Shi GP, Chapman HA, Desnick RJ (1996) Pycnodysostosis, a lysosomal disease caused by cathepsin K deficiency: *Science* 273:1236-1238

Glover CN, Bury NR, Hogstrand C (2003). Zinc uptake across the apical membrane of freshwater rainbow trout intestine is mediated by high affinity, low affinity, and histidine-facilitated pathways, *Biochim. Biophys. Acta* 1614, pp. 211–219.

Golovine K, Makhov P, Uzzo RG, Shaw T, Kunkle D, Kolenko VM (2008). Overexpression of the zinc uptake transporter hZIP1 inhibits nuclear factor kappaB and reduces the malignant potential of prostate cancer cells in vitro and in vivo. *Clin.Cancer Res.* 14, 5376-5384.

Granato M, Nusslein-Volhard C (1996). Fishing for genes controlling development. *Curr Opin Gene Dev* 6:461-468

Groff JL, Gropper SS (2000). *Advanced Nutrition and Human Metabolism*' Belmont: Wadsworth/Thompson Learning, pp 419-430.

Guerinot ML (2000) The ZIP family of metal transporters. *Biochim Biophys*. Acta 1465: 190-198.

Guevara T, Yiallouros I, Kappelhoff R, Bissdorf S, Sto¨ cker W, Gomis-Ru¨th FX (2010). Proenzyme Structure and Activation of Astacin Metallopeptidase. *J Biol Chem* 285 (18): 13958-13965

Gutman HR, Fruton JS (1948). On the proteolytic enzymes of animal tissues VIII. An intracellular enzyme related to chymotrypsin. *J. Biol. Chem.* 174: 851-858.

Haase H and Maret W (2003). Intracellular zinc fluctuations modulate protein tyrosine phosphatase activity in insulin/insulin-like growth factor-1 signaling. *Experimental Cell Research*, 291: 289-298.

Haase H, Maret W (2004b). Protein tyrosine phosphatases as targets of the combined insulinomimetic effects of zinc and oxidants. In *4th International Biometals Symposium (BIOMETALS 2004)*, pp. 333-338. Garmisch Partenkirchen, GERMANY.

Haase H, and Maret W (2005). Protein tyrosine phosphatases as targets of the combined insulinomimetic effects of zinc and oxidants, *Biometals : an international journal on the role of metal ions in biology, biochemistry, and medicine* 18: 333-338.

Hansson A (1996). Extracellular zinc ions induce mitogen-activated protein kinase activity and tyrosine phosphorylation in bombesin-sensitive swiss 3T3 fibroblasts. *Arch. Biochem. Biophys* 328: 233-238.

Hambidge M. (2000). Human zinc deficiency. *J. Nutr.* 130: 1344S-1349S

Harbison ST, Carbone MA, Ayroles JF, Stone EA, Lyman RF, Mackay TFC (2009). Co-Regulated Transcriptional Networks Contribute to Natural Genetic Variation in *Drosophila* Sleep. *Nat Genet*. 41(3): 371-375. doi:10.1038/ng.330.

Hardy RW, Sullivan CV, Koziol AM (1987). Absorption, body distribution, and excretion of dietary zinc by rainbow trout (*Salmo gairdneri*), *Fish Physiol. Biochem.* 3 (3):133-143.

Henshall SM, Afar DE, Rasiah KK, Horvath LG, Gish K, Caras I, amakrishnan V, Wong M, Jeffry U *et al.* (2003) Expression of the zinc transporter ZnT4 is decreased in the progression from early prostate disease to invasive prostate cancer. *Oncogene* 22: 6005-12.

Hirano T, Murakami M., Fukada T, Nishida K, Yamasaki S, Suzuki T (2008). Roles of zinc and zinc signaling in immunity: Zinc as an intracellular signaling molecule. *Adv. Immunol.* 97: 149-176.

Ho E, Dukovcic S, Hobson B, Wong CP, Miller G, Hardin K, *et al.* (2012). Zinc transporter expression in zebrafish (Danio rerio) during development. *Comp Biochem Physiol C Toxicol Pharmacol* 155: 26-32, 10.1016/j.cbpc.2011.05.002.

Ho Y, Samarasinghe R, Knoch ME, Lewis M, Aizenman E, DeFranco DB (2008). Selective Inhibition of Mitogen-Activated Protein Kinase Phosphatases by Zinc Accounts for Extracellular Signal-Regulated Kinase 1/2-Dependent Oxidative Neuronal Cell Death.
Mol pharmacol, 74:1141-1151.

Hogstrand C, Kille P, Nicholson RI, Taylor KM (2009). Zinc transporters and cancer: A potential role for ZIP7 as a hub for tyrosine kinase activation. *Trends Mol. Med*. 15,101-111.

Hogstrand C and Haux C (1996). Naturally high levels of zinc and metallothionein in liver of several species of the squirrelfish family from Queensland, Australia. *Marine Biology* 125: 23-31.

Hogstrand C and Wood CM (1996). *The physiology and toxicology of zinc in fish*. In Aquatic Toxicology, (ed. E. W. Taylor), pp. 61-84. Cambridge, U.K. Cambridge University Press.

Hogstrand C, Reid SD, Wood CM (1995). Ca^{2+} versus Zn^{2+} transport in the gills of freshwater rainbow trout and the cost of adaptation to waterborne Zn^{2+}. *J. Exp. Biol.*198, pp. 337–348.

Hogstrand C, Gassman NJ, Popova B,. Wood CM, Walsh PJ (1996). The physiology of massive zinc accumulation in the liver of female squirrelfish and its relationship to reproduction, *J. Exp. Biol.* 199, pp. 2543-2554.

Hogstrand C, Webb N, Wood CM (1998). Covariation in regulation of affinity for branchial zinc and calcium uptake in freshwater rainbow trout. *J. Exp. Biol.* 201: 1809-1815.

Hogstrand C (2011). *Zinc*: In homeostasis and toxicology of essential metals. (Ed. Chris M. Wood, Anthony Peter Farell, Colin J. Brauner), *Science,* vol 1. Academic press. 497p.

Hsu K, Sheikh H, Bruce AEE (2009). Expression pattern of the family 30 (zinc transporter), member 7, slc30a7 (www.zfin.org).

Hu Y, Spengler ML, Kuropatwinski KK, Comas M, Jackson M, Chernov MV, Gleiberman AS, Fedtsova N, Rustum YM, Gudkov AV, Antoch MP (2011). Selenium is a modulator of circadian clock that protects mice from the toxicity of a chemotherapeutic drug via upregulation of the core clock protein, BMAL1. *Oncotarget* 2: 1279-1290.

Huang L, Kirschke CP, Gitschier J (2002). Functional characterization of a novel mammalian zinc transporter, ZnT6. *Journal of Biological Chemistry* 277, 26389-95.

Huang L, Yu YY, Kirschke CP, Gertz ER, Lloyd KK (2007). Znt7 (Slc30a7)-deficient mice display reduced body zinc status and body fat accumulation. *J Biol Chem* 282:37053-37063.

Hunt CD, Johnson PE, Herbel J, Mullen LK (1992). Effects of dietary zinc depletion on seminal volume and zinc loss, serum testosterone concentrations, and sperm morphology in young men. *Am J Clin Nutr* 56(1): 148-157.

Ilouz R., *et al.* (2002) Inhibition of glycogen synthase kinase-3beta by bivalent zinc ions: insight into the insulin-mimetic action of zinc', *Biochemical and biophysical research communications, 95(1), 102-6*

Inayat S, Larsson A, Ronquist GK, Ronquist G, Egberg N, Eliasson R, Carlsson L (2012). High levels of cathepsins B, L and S in human seminal plasma and their association with prostasomes. *Andrologia* 2012, XX, 1-5. doi:10.1111/j.1439-0272.2012.01299.x

Inohaya K, Yasumasu S, Araki K, Naruse K, Yamazaki K, Yasumasu I, Iuchi I, Yamagami K (1997). Species-dependent migration of fish hatching gland cells that express astacin-like proteases in common. *Dev Growth Differ* 39:191-197.

Inohaya K, Yasumasu S, Ishimaru M, Ohyama A, Iuchi I, Yamagami K (1995). Temporal and spatial patterns of gene expression for the hatching enzyme in the teleost embryo, *Oryzias latipes*. *Dev Biol* 171: 374-385.

Inohaya K, Yasumasu S, Yasumasu I, Iuchi I, Yamagami K (1999). Analysis of the origin and development of hatching gland cells by transplantation of the embryonic shield in the fish, *Oryzias latipes*. *Dev Growth Diffe*r 41: 557-566.

Inoue K, Matsuda K, Itoh M, Kawaguchi H, Tomoike H, Aoyagi T, Nagai R, Hori M, Nakamura Y, Tanaka T (2002). Osteopenia and male-specific sudden cardiac death in mice lacking a zinc transporter gene, Znt5. *Hum.Mol.Genet.* 11: 1775-1784.

Ishiguro NB, Miya M, Nishida M (2003). Basal euteleostean relationships: a mitogenomic perspective on the phylogenetic reality of the “Protacanthopterygii”. *Mol Phylogenet Evol* 27:476-488.

Jackson KA, Helston RM, McKay JA, O'Neill ED, Mathers JC, Ford D (2007). Splice variants of the human zinc transporter ZnT5 (SLC30A5) are differentially localized and regulated by zinc through transcription and mRNA stability. *Journal of Biological Chemistry* 282, 10423-10431.

Jalen F, Oleksy A, Smietana K, Otlewski J (2003) PDZ domain-common players in the cell signalling. *Acta Biochem* vol 50 (4): 985-1017. doi: 035004985.

Jiang LJ, Maret W, Vallee BL (1998). The glutathione redox couple modulates zinc transfer from metallothionein to zinc-depleted sorbitol dehydrogenase. *Proc.Natl.Acad.Sci.U.S.A.* 95, 3483-3488.

Jirakulaporn T, and Muslin AJ (2004). Cation diffusion facilitator proteins modulate Raf-1 activity. *J Biol Chem* 279: 27807-27815.

Kagara N, Tanaka N, Noguchi S, Hirano T (2007). Zinc and its transporter ZIP10 are involved in invasive behavior of breast cancer cells. *Cancer Sci* 98: 692-7, 10.1111/j.1349-7006.2007.00446x.

Kambe T, Narita H., Yamaguchi-Iwai Y, Hirose J, Amano T, Sugiura N, Sasaki R, Mori K, Iwanaga T, Nagao M (2002) Cloning and characterization of a novel mammalian zinc transporter, zinc transporter 5, abundantly expressed in pancreatic beta cells. *Journal of Biological Chemistry* 277, 19049-55.

Kambe T, Suzuki T, Nagao M, Yamaguchi-Iwa Y (2006). Sequence similarity and functional relationship among eukaryotic ZIP and CDF transporters. *Geno. Prot. Bioinfo*., 4(1): 1-9.

Kambe T, Yamaguchi-Iwai Y, Sasaki R, Nagao M (2004). Overview of mammalian zinc transporters. *Cell. Mol. Life Sci*. 61: 49-68.

Kavanagh JP, Darby C, Costello CB, Chowdhury SD (1983). Zinc in post prostatic massage (VB3) urine samples: a marker of prostatic secretory function and indicator of bacterial infection. *Urol Res* 11(4):167-70.

Kawaguchi M, Hiroi J, Miya M,, Nishida M, Iuchi I, Yasumasu S (2010). Intron-loss evolution of hatching enzyme genes in Teleostei. *BMC Evolutionary Biology* 10:260. http://www.biomedcentral.com/1471-2148/10/260

Kawaguchi M, Yasumasu S, Hiroi J, Naruse K, Suzuki T, Iuchi I (2007). Analysis of the exon-intron structures of fish, amphibian, bird and mammalian hatching enzyme genes, with special reference to the intron loss evolution of hatching enzyme genes in Teleostei. *Gene 3*92:77-88.

Kawaguchi M, Nakagawa M, Noda T, Yoshizaki N, Hiroi J, Nishida M. *et al.* (2008). Hatching enzyme of the ovoviviparous black rockfish Sebastes schlegelii-environmental adaptation of the hatching enzyme and evolutionary aspects of formation of the pseudo-ene. *FEBS J.* 275, 2884-2898.

Kawaguchi M, Yasumasu S, Hiroi J, Naruse K, Inoue M, Iuchi I (2006). Evolution of teleostean hatching enzyme genes and their paralogous genes. *Dev. Genes Evol.* 216, 769-784.

Kawaguchi M, Yasumasu S, Shimizu A, Hiroi J, Yoshizaki N, Nagata K. *et al.* (2005). Purification and gene cloning of Fundulus heteroclitus hatching enzyme. A hatching enzyme system composed of high choriolytic enzyme and low choriolytic enzyme is con-served between two different teleosts, Fundulus heteroclitus and medaka Oryzias latipes. *FEBS J.* 272,4315-4326.

Keen CL and Hurley LS (1989): In: Mills, CF (Ed.), *Zinc in Biology*. Springer-Verlag, UK, pp. 183-220;

Kimmel CB, Ballard WW, Kimmel SR, Ullmann B, Schilling TF (1995) Stages of embryonic development of the zebrafish. *Dev Dyn* 203*:* 253-310.

King, J. C., Shames, D. M., and Woodhouse, L. R. (2000) Zinc homeostasis in humans. *J. Nutr.* 130, 1360S-1366S.

King DP, et al. (1997). Positional cloning of the mouse circadian clock gene. *Cell* 89: 641-653

Kirschke H, Eerola R, Hopsu-Havu VK, Bromme D, Vuorio E (2000). Antisense RNA inhibition of cathepsin L expression reduces tumorigenicity of malignant cells. *European Journal of Cancer* 36: 787-795.

Knowlden JM, Hutcheson IR, Barrow D, Gee JM, Nicholson RI (2005). Insulin-like growth factor-I receptor signaling in tamoxifen-resistant breast cancer: a supporting role to the epidermal growth factor receptor, *Endocrinology* 146, 4609-4618.

Ko GYP, Ko ML, Dryer SE (2001). Circadian regulation of cGMP-gated cationic channels of chick retinal cones: Erk MAP kinase and Ca^{2+}/calmodulin-dependent protein kinase II. *Neuron* 29, 255-266.

Kondratov RV (2007). A role of the circadian system and circadian proteins in aging. *Ageing Res. Rev.* 6 (1): 12-27. doi:10.1016/j.arr.2007.02.003. PMID 17369106.

Krebs NE and Hambidge KM (2001). Zinc metabolism and homeostasis: the application of tracer techniques to human zinc physiology, *Biometals* 14 (3-4), pp. 397-412.

Krens SFG, He S, Lamers GEM, Meijer AH, Bakkers J Schmidt T Spaink HP, Snaar-Jagalska BE (2008). Distinct functions for ERK1 and ERK2 in cell migration processes during zebrafish gastrulation. *Developmental Biology* 319: 370-383.

Krezel A and Maret W (2007). Dual nanomolar and picomolar Zn(II) binding properties of metallothionein. *Journal Of The American Chemical Society* 129, 10911-10921.

Kury S, Dreno B, Bezieau S, Giraudet S, Kharfi M, Kamoun R, Moisan JP (2002) Identification of SLC39A4, a gene involved in acrodermatitis enteropathica. *Nat. Genet.* 31, 239-240

Kusunoki T, Nishida S, Murata K, Kobashi K, Nakatani H, Hiwasa T, Tomura T (2001). Cathepsin L activity and its inhibitor in human otitis media. *J Otolaryngol.* 30(3):157-61.

Kwan TT, Liang R, Verfaillie CM, Ekker SC, Chan LC, Lin S, Leung AYH (2006). Regulation of primitive hematopoeisis in zebrafish embryos by the death receptor gene. *Experimental Hematology* 34:27-34.

Kwun IS, Cho YE, Lomeda RA, Shin HI, Choi JY, Kang YH, Beattie JH (2010). Zinc deficiency suppresses matrix mineralization and retards osteogenesis transiently with catch-up possibly through Runx 2 modulation. *Bone* 46: 732-41.

Lavoué S, Miya M, Inoue JG, Saitoh K, Ishiguro NB, Nishida M (2005). Molecular systematics of the gonorynchiform fishes (Teleostei) based on whole mitogenome

sequences: implications for higher-level relationships within the Otocephala. *Mol Phylogenet Evol* 37:165-177.

Lazarczyk M, Pons C, Mendoza JA, Cassonnet P, Jacob Y, Favre M (2008) Regulation of cellular zinc balance as a potential mechanism of EVER-mediated protection against pathogenesis by cutaneous oncogenic human papillomaviruses. *J Exp Med* 205:35-42. doi:10.1084/jem.20071311.

Lee KS, Yasumasu S, Nomura K, Iuchi I (1994). HCE, a constituent of the hatching enzyme of Oryzias latipes embryos, releases unique proline-rich polypeptides from its natural substrate, the hardened chorion. *FEBS* Lett 39, 281-289.

Leitzmann MF, Stampfer MJ, Wu K, Colditz GA, Willett WC, Giovannucci EL. Zinc supplement use and risk of prostate cancer. *J NatlCancer Inst* 2003;95:1004-7.

Lekven AC, Helge K.A, Thorpe CJ, Rooke R, Moon RT (2000). Reverse genetics in zebrafish. *Physiol Genomics*, 2:37-48.

Lemaire K, Ravier MA, Schraenen A et al (2009). Insulin christalization depends on zinc transporter ZnT8 expression, but is not required for normal glucose homeostasis in mice. *Proc Natl Acad Sci* USA 106:14872-14877.

Lemly AD (2002). Symptoms and implications of selenium toxicity in fish: the Belews Lake case example. *Aquatic toxicology* 57: 39-49.

Lepage SE, Bruce AEE (2010). Zebrafish epiboly: mechanics and mechanisms. *Int. J. Dev. Biol.* 54: 1213-1228

Levy S, Beharier O, Etzion Y, Mor M et al (2009*). J Biol Chem* 284(47):32434-32443.

Liang JY, Liu YY, Zou J, Franklin RB, Costello LC, Feng P (1999). Inhibitory effect of zinc on human prostatic carcinoma cell growth. *Prostate*. 40:200-207.

Lichten LA, Cousins RJ (2009). Mammalian zinc transporters: Nutritional and physiologic regulation. *Annu. Rev. Nutr*, 29:153-176.

Lichten, L.A., Cousins, R.J. (2009). Mammalian zinc transporters: Nutritional and physiologic regulation. *Annu. Rev. Nutr*, 29:153-176.

Lin L, Horng J, Kunkel JG, Hwang P (2006). Proton pump-rich cell secretes acid in skin of zebrafish larvae. *Am J Physiol Cell Physiol* 290: C371–C378. doi:10.1152/ajpcell.00281.2005

Lettre G, Palmer CD, Young T, Ejebe KG, Allayee H, et al. (2011) Genome-Wide Association Study of Coronary Heart Disease and Its Risk Factors in 8,090 African Americans: The NHLBI CARe Project. PLoS Genet 7(2): e1001300. doi:10.1371/journal.pgen.1001300

Liuzzi JP, Bobo JA, Cui L, McMahon RJ, Cousins RJ (2003). Zinc transporters 1, 2 and 4 are differentially expressed and localized in rats during pregnancy and lactation. *J. Nutr.* 133(2):342-51

Liuzzi JP, Cousins RJ (2004). Mammalian zinc transporters. *Annu Rev Nutr*. 24:151-172.

Liuzzi JP, Guo L, Chang S-M, Cousins RJ (2009). Kru¨ppel-like factor 4 regulates adaptive expression of the zinc transporter *Zip4* in mouse small intestine. *Am J Physiol Gastrointest Liver Physiol* 296: G517-G523.

Livak KJ, Schmittgen TD (2001) Analysis of relative gene expression data using real-time quantitative PCR and the 2(-Delta Delta C(T)) Method. *Methods* 25: 402-408.

Lopez V, Keen CL, Lanoue L (2008). Parental zinc deficiency: Influence on heart morphology and distribution of key heart proteins in a rat model. *Biol Trace Elem Res*, 122: 238-255.

Lopez V, Kelleher SL (2010). Zip6-attenuation promotes epithelial-to-mesenchymal transition in ductal breast tumor (T47D) cells. *Exp. Cell Res*.316, 366-375.

Lu M, Fu D (2007). *Science* 31795845):1746-1748.

Lu J, Tsai T, Choo S, Yeh S, Tang R, Yang A, Lee H, Lu J (2011). Induction of apoptosis and inhibition of cell growth by tbx5 knockdown contribute to dysmorphogenesis in Zebrafish embryos. *Journal of Biomedical Science* 18:73. http://www.jbiomedsci.com/content/18/1/73

Luberda S, Strzezek J, Luczynski M (1993). Some proteolytic properties of hatching liquid in the sea trout, *Salmo trutta* m. *trutta* L. *Fish Physiology and Biochemistry* 12, 75-80.

MacDiarmid CW, Gaither LA, Eide DJ (2000). Zinc transporters that regulate vacuolar zinc storage in Saccharomyces cerevisiae. *EMBO J*. 19: 2845-2855.

Madsen EC, Gitlin JD (2008). Zebrafish mutants calamity and catastrophe define critical pathways of gene-nutrient interactions in developmental copper metabolism. *PLoS Genet,* 4(11): e1000261. doi: 10.1371/journal.pgen.1000261.

Makhov P, Golovine K, Uzzo G, Wuestefeld T, Scoll BJ, Kolenko VM (2009). Transcriptional regulation of the major zinc uptake protein hZip1 in prostate cancer cells. *Gene* 431, 39-46.

Malaga-Trillo E, Solis GP, Schrock Y, Geiss C, Luncz L, Thomanetz V*, et al.* (2009). Regulation of embryonic cell adhesion by the prion protein. *PLoS Biol* 7: e55, 10.1371/journal.pbio.1000055.

Manning DL, McClelland RA, Gee JM, Chan CM, Green CD, Blamey RW, Nicholson RI (1993). The role of four oestrogen-responsive genes, pLIV1, pS2, pSYD3 and

pSYD8, in predicting responsiveness to endocrine therapy in primary breast cancer, *European journal of cancer* 29A, 1462-1468.

Manning DL, Robertson JF, Ellis IO, Elston CW, McClelland RA, Gee JM, Jones RJ, Green CD, Cannon P, Blamey RW and *et al.* (1994). Oestrogen-regulated genes in breast cancer: association of pLIV1 with lymph node involvement, *European journal of cancer* 30A, 675-678.

Manning DL, Daly RJ, Lord PG, Kelly KF, Green CD (1988). Effects of oestrogen on the expression of a 4.4 kb mRNA in the ZR-75-1 human breast cancer cell line. *Mol Cell Endocrinol* 59: 205-12.

Mao X, Kim BE, Wang F, Eide DJ, Petris MJ (2007). A histidine-rich cluster mediates the ubiquitination and degradation of the human zinc transporter, hZIP4, and protects against zinc cytotoxicity. *J Biol Chem* 282: 6992–7000.

Marcheva B, et al. (2013). Disruption of the clock components CLOCK and BMAL1 leads to hypoinsulinaemia and diabetes. Nature 466: 627–631. doi:10.1038/nature09253. Retrieved 13 April 2013.

Maret W, and Li Y (2009). Coordination dynamics of zinc in proteins. *Chem. Rev.* 109:4682-4707.

Maret W (2009). Molecular aspects of human cellular zinc homeostasis: redox control of zinc potentials and zinc signals. *Biometals* 22: 149-57, 10.1007/s10534-008-9186-z.

Maret W (2011). Redox biochemistry of mammalian metallothioneins. *J Biol Inorg Chem* 16:1079–1086.

Mathews WR, Daniel O, Allison B, Milutinovich B, Doren MV (2006). Zinc transport activity of fear of intimacy is essential for proper gonad morphogenesis and DE-cadherin expression. *Development* 113:1143-1153.

McCallum CM, Comai L, Greene EA. Henikoff S. (2000). Targeted screening for induced mutations. *Nature Biotechnology*, 18: 455-457.

McMahon RJ and Cousins RJ (1998). Regulation of the zinc transporter ZnT-1 by dietary zinc. *Proc. Natl. Acad. Sci. U. S. A.*95, 4841-4846.

Mishra A, Seshagiri PB (2000). Evidence for the involvement of species-specific embryonic protease in zona dissolution of hamster blastocysts. *Mol. Hum. Reprod.* 6, 1005-1012.

Miya M, Takeshima H, Endo H, Ishiguro NB, Inoue JG, Mukai T, Satoh TP, Yamaguchi M, Kawaguchi A, Mabuchi K, Shirai SM, Nishida M (2003). Major patterns of higher teleostean phylogenies: a new perspective based on 100 complete mitochondrial DNA sequences. *Mol Phylogenet* Evol 26:121-138.

Mocchegiani E, Santarelli L, Tibaldi A, Muzzioli M, Bulian D, Cipriano C, Olivieri F, Fabris N (1998). *J. Nueroimmunol*. 86: 111-122.

Mocchegiani E. *et al.* (2008) Zinc signalling and subcellular distribution: emerging targets in type 2 diabetes. *Trends Mol. Med.* 14, 419-428

Moens CB, Donn TM, Wolf-saxon ER, Ma TP (2008). Reverse genetics in zebrafish by TILLING. Briefings in functional genomics and proteomics. 7 (6): 454-459.
Mol Pharmacol 74:1141–1151.

Montanini B, Blaudez D, Jeandroz S, Sanders D, Chalot M (2007). Phylogenetic and functional analysis of the cation diffusion facilitator (CDF) family:improved signature and prediction of substrate specificity. *BMC Genomics* 8:107.

Mor M, Beharier O, Levy S, Kahn J, Dror S, Blumenthal D, Gheber LA, Peretz A, Katz A, Moran A, Etzion Y (2012). ZnT-1 Enhances the activity and surface expression of T-type calcium channels through activation of Ras-ERK signalling. *Am J Physiol Cell Physiol.* doi:10.1152/ajpcell.00427.

Morcos PA (2007). Achieving targeted and quantifiable alteration of mRNA splicing with Morpholino oligos. *Biochem Biophys Res Commun*. 358:521-527.

Mu˜noz E, Brewer M, Baler R (2006). Modulation of BMAL/CLOCK/E-Box complex activity by a CT-rich *cis*-acting element. *Molecular and Cellular Endocrinology* 252:74-81.

Muras, AG, Hajj, GN, Ribeiro, KB, Nomizo, R, Nonogaki, S, Chammas, R, *et al.* (2009). Prion protein ablation increases cellular aggregation and embolization contributing to mechanisms of metastasis. *Int J Cancer* 125: 1523-31, 10.1002/ijc.24425.

Murgia C, Vespignani I, Rami R, Perozzi G (2006). The Znt4 mutation in lethal milk mice affects intestinal zinc homeostasis through the expression of other Zn transporters. *Genes Nutr.* 1:61-70.

Musil DI et al. (1991). The refined 2.15 A X-ray crystal structure of human liver cathepsin B: the structural basis for its specifcity. *EMBO J.*, 10, 2321-2330.

Muylle FAR., Adriaensen D, De Coen W, Timmermans JP, Blust R (2006). Tracing of labile zinc in live fish hepatocytes using FluoZin-3. *Biometals* 19, 437-450.

Nakano H, Nakamura Y, Kawamura T, Shibagaki N, Matsue H, Aizu T, Rokunohe D, *et al.* (2009). Novel and recurrent nonsense mutation of the SLC39A4 gene in Japanese patients with acrodermatitis enteropathica. *Br J Dermatol* 161, 184-6.

Nasevicius A and Ekker SC (2000). Effective targeted gene “knockdown” in zebrafish. *Nat Genet.* 26:216-220

Nelson JS (1994). *Fishes of the world.* 3rd edn. Wiley, New York.

Nicolson TJ, Bellomo EA, Wijesekara N, Loder MK, Baldwin JM, Gyulkhandanyan AV, Koshkin V et al (2009). Insulin storage and glucose homeostasis in mice null for

the granule zinc transporter ZnT8 and studies of the type 2 diabetes-associated variants. *Diabetes* 58, 2070-2083.

Nishi Y (1996). Zinc and Growth. *J. Am Coll Nutr.* 15:340-344.

Norton W and Bally-Cuif L (2010). Adult zebrafish as a model organism for behavioural genetics. *BMC Neuroscience* 11:90.

NRC (1993). *Nutrient requirements of fish*. National Academy of Sciences. Washington D.C., USA. 114p.

Okada A, Sano K, Nagata K, Yasumasu S, Ohtsuka J, Yamamura A, Kubota K, Iuchi I, Tanokura M (2010). Crystal Structure of Zebrafish Hatching Enzyme 1 from the Zebrafish *Danio rerio*. *J. Mol.Biol.* (2010), doi:10.1016/j.jmb.2010.08.023

Overbeck S, Rink L, Hasse H (2008). Modulating the immune response by oral zinc supplementation: A single approach for multiple diseases. *Arch Immunol Ther Exp* 56:15-30.

Palmiter RD (2004). Protection against zinc toxicity by metallothionein and zinc transporter 1. *Proc Natl Acad Sci USA* 101: 4918-4923.

Palmiter RD, Huang L (2004;). Efflux and compartmentalization of zinc by members of the SLC30 family of solute carriers. *Pflugers Arch*. 447:744-751.

Palmiter RD and Findley SD (1995) *Embo J* 14(4), 639-649

Palmiter RD, Cole TB and Findley SD (1996). ZnT-2, a mammalian protein that confers resistance to zinc by facilitating vesicular sequestration. *EMBO J.* 15: 1784-1791.

Pando MP, Pinchak AB, Cermakian N, Sassone-Corsi P (2001). A cell-based system that recapitulates the dynamic light-dependent regulation of the vertebrate clock. *Proc Natl Acad Sci* USA 98:10178–10183.

Pando, MP and Sassone-Corsi, P (2002). Unraveling the mechanisms of the vertebrate circadian clock: zebrafish may light the way. *BioEssays* 24:419-426.

Parichy DM (2006a). Evolution of danio pigment pattern development. *Heredity* 97, 200-210.

Parichy DM (2006b). Homology and the evolution of novelty during Danio adult pigment pattern development. *Journal of Experimental Zoology* 306B, 1-13.

Parng C, Seng WL, Semino C, McGrath P (2002). Zebrafish: A Preclinical Model for Drug Screening. *Assay and Drug Development Technologies* Volume 1, Number 1-1.

Passerini A, Andreini C, Menchetti S, Rosato A, Frasconi P (2007). Predicting zinc binding at the proteome level. *Bmc Bioinformatics* 8, 39.

Pfaffl M W, Horgan GW *et al.* (2002). "Relative expression software tool (REST (c)) for group-wise comparison and statistical analysis of relative expression results in real-time PCR." *Nucleic Acids Research* 30(9).

Pickart MA, Klee EW, Nielson AL, Sivasubbu S, Mendenhall EM, *et al.* (2006). Genome-wide reverse genetics framework to identify novel functions of the vertebrate secretome. *PLoS One* 1: e104. doi:10.1371/journal.pone.0000104.

Pinho SS, Seruca R, Gartner F, Yamaguchi Y, Gu J, Taniguchi N, Reis CA (2011). Modulation of E-cadherin function and dysfunction by N-glycosylation. *Cell. Mol. Life Sci.* 68:1011-1020.

Pittendrigh CS (1993). Temporal organization: reflections of a Darwinian clockwatcher. *Ann Rev Physiol* 55:16-54.

Plageman TF,Jr, Yutzey KE (2006). Microarray analysis of Tbx5-induced genes expressed in the developing heart. *Dev Dyn* 235: 2868-80, 10.1002/dvdy.20923.

Prasad AS (1995): Zinc: an overview. Nutrition 11:93-99.

Prasad AS (2001). Recognition of zinc-deficiency syndrome. *Nutrition* 17: 67–69.

Prasad AS (2004). Zinc deficiency: its characterization and treatment. *Metal ions in biological systems* 41, 103-137.

Prasad AS (2008). Zinc in human health: Effect of zinc on immune cells. *Mol. Med.* 14, 353-357.

Prasad AS, Kucuk O (2002). Zinc in cancer prevention. Cancer metastasis Rev. 21; 291-295.

Prasad AS (2009). Impact of the Discovery of Human Zinc Deficiency on Health. *Journal of the American College of Nutrition* 28, 257-265.

Prasad AS, Halsted JA Nadimi M (1961). Syndrome of iron deficiency anemia, hepatosplenomegaly, hypogonadism, dwarfsm and geophagia. *American Journal of Medicine* 31, 532-&.

Quadri M, Federico A, Zhao T, Breedveld GJ, Battisti C, Delnooz C, Severijnen L, Mammarella LD, Mignarri A, Monti L Sanna A, Lu P, Punzo F, Cossu G, Willemsen R, Rasi F, Oostra BA, Warrenburg BP, BonifatiV (2012). Mutations in SLC30A10 Cause Parkinsonism and Dystonia with Hypermanganesemia, Polycythemia, and Chronic Liver Disease. *The American Journal of Human Genetics* 90, 467-477.

Quesada V, Sanchez LM, Alvarez J, López-Otın S (2004). Identification and Characterization of Human and Mouse Ovastacin. A novel metalloproteinase similar to hatching enzymes from arthropods, birds, amphibians, and fish. *The Journal of Biological Chemistry* vol. 279, No. 25, Issue of June 18, pp. 26627-26634.

Radtke F, Heuchel R, Georgiev O, *et al.*, (1993). Cloned transcription factor MTF-1 activates the mouse metallothionein -I promoter. The *EMBO Journal* 22:1355-1362.

Rappela A, Negrioli A, Melillo G, Pastorino S, Varesio L, Bosco MC (2002). Flavopiridol inhibits vascular endothelial growth factor production induced by hypoxia or picolinic acid in human neuroblastoma. *Int J Cancer* 99:658-664.

Redenti S, Chappell RL (2004). Localization of zinc transporter-3 (ZnT-3) in mouse retina. *Vision Res*.44:3317-3321.

Religa D *et al.* (2006) Elevated cortical zinc in Alzheimer disease. *Neurology* 67, 69–75

Ren B, Deng Y, Mukhopadhyay A, Lanahan AA, Zhuang ZW, et al (2010). ERK1/2-Akt1crosstalk regulates arteriogenesis in mice and zebrafish. *J.Clin Invest.* 120(4):1217-1228.

Rhodin JAG (1974). Histology. A text and atlas. Oxford University Press, New York London Toronto.

Robu ME, Larso JD, Nasevicius A, Beiraghi S, Brenner C, Farber SA, Ekker SC(2007). p53 activation by knockdown technologies. PLoS Genetics 3(5): e78.

Ronquist GK, Larsson A, Ronquist G, Isaksson A, Hreinsson J, Carlsson L, Stavreus-Evers A (2011). Prostasomal DNA characterization and transfer into human sperm. *Mol Reprod Dev* 78:467-476.

Rudic RD, McNamara P, Curtis AM, Boston RC, Panda S, Hogenesch JB, Fitzgerald GA
(2004). BMAL1 and CLOCK: Two essential components of the circadian clock, are involved in glucose homeostasis. *PLOS Biology* 2 (11): e377. doi:10.1371/journal.pbio.0020377. PMC 524471. PMID 15523558.

Saba-El-Leil MK., Vella FDJ, Vernay B, Voisin L, Chen L, Labrecque N, Ang SL, Meloche S (2003). An essential function of the mitogen-activated protein kinase Erk2 in mouse trophoblast development. *Embo Rep*. 4, 964-968.

Sano S. et al (1999). Keratinocyte-specific ablation of Stat3 exhibits impaired skin remodeling, but does not affect skin morphogenesis. *EMBO J*. 18, 4657-4668.

Sano K, Inohaya K, Kawaguchi M, Yoshizaki N,Iuchi I, Yasumasu S (2008). Purification and characterization of zebrafish hatching enzyme-an evolutionary aspect of the mechanism of egg envelope digestion. *FEBS J*. 275, 5934-5946.

Santore R C, Mathew R, Paquin PR, DiToro D (2002). Application of the biotic ligand model to predicting zinc toxicity to rainbow trout, fathead minnow, and Daphnia magna. *Comparative Biochemistry and Physiology Part C: Toxicology & Pharmacology* 133, 271-285.

Sato K *et al*. (1995). C-Src phosphorylates epidermal growth-factor receptor on Tyrosine-845. *Biochem. Biophys. Res. Commun.* 215: 1078-1087.

Savagner P (2001). Leaving the neighborhood: molecular mechanisms involved during epithelialmesenchymal transition. *Bioessays* 23, 912-923.

SCAN (2003). *Opinion of the Scientific Committee on Animal Nutrition on undesirable substances in feed,* Brussel.

Schoots AFM, Evertse PACM, and Denuce JM (1983). Ultrastructural changes in hatching-gland cells of pike embryos (Esox *lucius* L.) and evidence for their degeneration by apoptosis. Cell Tissue Res, 229:573-589.

Schoots AFM, Opstelten RJG, Denuc JM (1982). Hatching in the pike *Esox lucius* L.: Evidence for a single hatching enzyme and its immunocytochemical localization in specialized hatching gland cells. *Dev Biol* 89:48-55.

Schoots AFM, Janssen BJA, Denuce JM (1981). Antigenicity of highly purified hatching enzyme from the pike, *Esox lucius. Arch. Int. Physiol Biochim.*89:B75-B76.

Schrantz N, Auffredou MT, Bourgeade MF, Besnault L, Leca G, Vazquez A. Zinc-mediated regulation of caspases activity: dose-dependent inhibition or activation of caspase-3 in the human Burkitt lymphoma B cells (Ramos). *Cell Death Differ*. 2001;8:152-161.

Schmittgen TD, Livak KJ (2008). Analyzing real-time PCR data by the comparative C (T) method. *Nat Protoc* 3(6): 1101-1108.

Sekler I, Sensi SL, Hershfinkel M, Silverman WF (2007) Mechanism and regulation of cellular zinc transport. *Mol. Med.* 13, 337–343.

Seshagiri PB, Roy SS, Sireesha G, Rao RP (2009). Cellular and molecular regulation of mammalian blastocyst hatching. *Journal of Reproductive Immunology* 83: 79–84

Seve M, Chimienti F, Devergnas S, Favier A (2004). In silico identification and expression of SLC30 family genes: an expressed sequence tag data mining strategy for the characterization of zinc transporters' tissue expression. *BMC Genomics* 5: 32.

Sheline CT, Behrens M M, Choi DW (2000). *J. Neurosci*. 20, 3139-3146

Shennan BD (1988). Selenium (selenate) transport by human placenta brush border membrane vesicles. *Br J Nutr* 59: 13-19.

Shimizu T, Yabe T, Muraoka O, Yonemura S, Aramaki S, Hatta K*, et al.* (2005). E-cadherin is required for gastrulation cell movements in zebrafish. *Mech Dev* 122: 747-63, 10.1016/j.mod.2005.03.008.

Siebert F, Lu¨hken G, Pallauf J, Erhardt G (2013). Mutation in porcine Zip4-like zinc transporter is associated with pancreatic zinc concentration and apparent zinc absorption. *British Journal of Nutrition*, 109: 969-976.

Simonehauser, RK, Baumgartner, W (2005). Zinc-responsive dermatosis in goats suggestive of hereditary malabsorption: two field cases. *Veterinary Dermatology*, 16: 269-275.

Sladek R, Rocheleau G, Rung J, Dina C, Shen L, Serre D, Boutin P, Vincent D, Belisle A, *et al.* (2007). A genome-wide association study identifies novel risk loci for type 2 diabetes. *Nature* 445, 881-885.

Solnica-Krezel L (2006). Gastrulation in zebrafish: all just about adhesion? *Curr Opin Genet Dev* 16: 433-41, 10.1016/j.gde.2006.06.009.

Somasundaram P, King PE, Shackley S (1984). Theeffects of zinc on postfertilization development in eggs of *Clupea harengus* L. *Aquatic Toxicology*, 5 167-178.

Spry DJ and Wood CM (1985) Ion flux rates, acid-base status, and blood gases in rainbow trout, Salmo gairdneri, exposed to toxic zinc in natural soft water. *Can. J. Fish Aquat. Sci*. 42, 1332-1341

Stemple DL (2004). TILLING- a high-thoroughput harvest for functional genomics. Nature reviews (*Genetics*), 4:1-5.

Steven MR, David RW (2002). Coordination of circadian timing in mammals. *Nature* 418 (6901): 935-941. doi:10.1038/nature00965.

Sto¨cker W, Yiallouros I (2004) in *Handbook of Proteolytic Enzymes*, 2nd Ed. (Barrett, A. J., Rawlings, N. D., and Woessner, Jr., J. F., eds) pp. 595-598, Elsevier, London

Strauss O (2005). The retinal pigment epithelium in visual function. *Physiol Rev*.;85:845 881.

Stuart GW, Searle OF, Palmite RD (1985). Identification of multiple metal regulatory element in metallothionein-I promoter by assaying synthetic sequences. *Nature* 317:828-831.

Suh SW, Chen JW, Motamedi M, Bell B, Listiak K, Pons NF, Danscher G, Frederickson CJ. (2000). Evidence that synaptically-released zinc contributes to neuronal injury after traumatic brain injury. *Brain Res* 852: 268-273.

Summerton J (1999). Morpholino antisense oligomers: the case for an RNase H-independent structural type. *Biochim Biophys Acta.* 1489:141-158.

Suzuki T, Ymanaka H, Nakajima K, Kntamani K, Suzuki K, Kimura M, Nakasawa Y, Otaki N (1993). Induction of metallothionein by $CdCl_2$ administarion in rat prostate. *Prostate* 22: 163-170.

Swindell EC, Zilinski CA, Hashimoto R, Shah R, Lane ME, Jamrich M (2008). Regulation of function of *foxe3* during early zebrafish development. *Genesis* 46:177-183.

Takio K, Towatari T, Katunuma N, Teller DC, Titani K (1983). Homology of amino acid sequences of liver cathepsins B and H with that of papain. *Proc. Natl Acad. Sci.* USA, 80, 3660-3670.

Schmittgen TD, Livak KJ (2008). Analyzing real-time PCR data by the comparative C (T) method. *Nat Protoc* 3(6): 1101-1108.

Taylor KM, Hiscox S, Nicholson RI, Hogstrand C, Kille P (2012). Protein Kinase CK2 Triggers Cytosolic Zinc Signaling Pathways by Phosphorylation of Zinc Channel ZIP7 *Science Signaling* 5 (210), ra11. [DOI: 10.1126/scisignal.2002585.

Taylor KM, Morgan HE, Smart K, Zahari NM, Pumford S, Ellis IO, Robertson JF, Nicholson RI (2007). The emerging role of the LIV-1 subfamily of zinc transporters in breast cancer. *Mol. Med.* 13, 396-406.

Taylor KM, Vichova P, Jordan N, Hiscox S, Hendley R, Nicholson RI (2008). ZIP7-mediated intracellular zinc transport contributes to aberrant growth factor signaling in antihormone-resistant breast cancer cells. *Endocrinology* 149, 4912-4920.

Taylor KM. and Nicholson RI (2003 a). The LZT proteins; the LIV-1 subfamily of zinc transporters, *Biochim. Biophys. Acta* 1611 (1-2):16-30.

Taylor KM, Morgan HE, Johnson A, Hadley LJ, Nicholson RI (2003b). Structure-function analysis of LIV-1, the breast cancer-associated protein that belongs to a new subfamily of zinc transporters. *Biochem J.* 1; 375(Pt 1): 51-59. doi: 10.1042/BJ20030478. PMCID: PMC1223660.

Thiery JP (2002). Epithelial-mesenchymal transitions in tumour progression. Nature Rev. *Cancer* 2, 442-454.

Thisse C, Thisse B, Halpern ME, Postlethwait JH (1994). Goosecoid expression in neurectoderm and mesendoderm is disrupted in zebrafish cyclops gastrulas. Dev Biol 164:420-429.

Thiese C and Thiese B (2008). High-resolution *in-situ* hybridization to whole-mount zebrafish embryos. *Nature Protocol* 3 (1): 59-69.

Thiese B and Thisse C (2004) Fast Release Clones: A High Throughput Expression Analysis. ZFIN Direct Data Submission.

Thornton JK, Taylor KM, Ford D, Valentine RA (2011). Differential subcellular localization of the splice variants of the zinc transporter ZnT5 is dictated by the different C-terminal regions. *PLoS ONE* 6(8): e23878. doi:10.1371/journal.pone.0023878

Tingaud-Sequeira A, Cerdà J (2007). Phylogenetic relationships and gene expression pattern of three different cathepsin L (Ctsl) isoforms in zebrafish: Ctsla is the putative yolk processing enzyme. *Gene* 386: 98-106.

Todd AS, Brinkman S, Wolf RE, Lamothe PJ, Smith KS, Ranville JF (2009). An enriched stable-isotope approach to determine the gill-zinc binding properties of juvenile rainbow trout (<I>Oncorhynchus mykiss</I>) during acute zinc exposures in hard and soft waters. *Environmental Toxicology and Chemistry;* 28: 1233-1243.

Tougu V, Tiiman A, Palumaa P (2011). Interactions of Zn(II) and Cu(II) ions with Alzheimer's amyloid-beta peptide. Metal ion binding, contribution to fibrillization and toxicity. *Metallomics*, 3: 250-261

Trikic´ MZ, Monk P, Roehl H, Partridge LJ (2011) Regulation of Zebrafish Hatching by Tetraspanin cd63. *PLoS ONE* 6(5): e19683. doi:10.1371/journal.pone.0019683

Tully DC, Liu H, Chatterjee AK, Alper PB, Epple R, Williams JA, Roberts MJ, Woodmansee DH, Masick BT, Tumanut C *et al.,* (2006). Synthesis and SAR of arylaminoethyl amides as noncovalent inhibitors of cathepsin S: P3 cyclic ethers Bioorganic & Medicinal Chemistry Letters 16: 5112-5117.

Tupper R, Watts RW, Wormall A (1955). The incorporation of ^{65}Zn in mammary tumours and some other tissues of mice after injection of the isotope. *Biochem J* 59: 264-8.

Turek FW, Joshu C, Kohsaka A, Lin E, Ivanova G, McDearmon E, Laposky A, LoseeOlson S, Easton A, Jensen DR, Eckel RH, Takahashi JS, Bass J. (2005). Obesity and
metabolic syndrome in circadian Clock mutant mice. *Science* 308 (5724): 1043-5. doi:10.1126/science.1108750. PMID 15845877.

Turek FW, Gillette MU (2004). Melatonin, sleep, and circadian rhythms: rationale for development of specific melatonin agonists. *Sleep Med* 5: 523-532.

Turk B, Dolenc I, Turk V, Bieth JG (1993). *Biochemistry* 32:375-380.

Turk B, Turk D, Turk V (2000). Lysosomal cysteine proteases: more than scavengers. *Biochim. Biophys*. Acta 1477, 98-111.

Turk V, Turk B, Turk D (2001). Lysosomal cysteine proteases: facts and opportunities. *The EMBO Journal* , 20 (17): 4629-4633.

Valentine RA, Jackson AK, Christie GR, Mathers JC, Taylor PM, Ford, D (2007). ZnT5 variant b is a bidirectional zinc transporter and mediates zinc uptake in human intestinal caco-2 cells. *J Biol Chem* (http://www.jbc.org/cgi/doi/10.1074/jbc.M701752200).

Vallee BL. and Auld DS (1990) Zinc coordination, function and structure of zinc enzymes and other proteins. *Biochemistry* 29: 5647-5659.

Vallee BL. and Falchuk KH (1993). The biochemical basis of zinc physiology. Physiol. Rev. 73: 79-118.

Vallee BL (1959). Biochemistry, physilogy and pathology of zinc. *Physiol. Rev.* 39, 443-490.

Vallee B L (1986). A synopsis of zinc biology and pathology. In *Zinc Enzymes*, vol. 1 (ed. H. Gray), pp. 1-15. Basel: Birhäuser.

Venter J C, Adams MD, Myers EW, Li PW, Mural RJ, Sutton GG *et al.* (2001) The sequence of the human genome. *Science* 291: 1304-1351.

Vogel AM, Gerster T (1997). Expression of a zebrafish *Cathepsin L* gene in anterior mesendoderm and hatching gland. *Dev Genes Evol* 206*:* 477-479.

Wang J, Lundqvist M, Carlsson L, Nilsson O, Lundkvist O, Ronquist G (2001). Prostasome-like granules from the PC-3 prostate cancer cell line increase the motility of washed human spermatozoa and adhere to the sperm. *Eur J Obstet Gynecol Reprod Biol* 96:88-97.

Wang X, Wu Y, Zhou B (2009). Dietary zinc absorption is mediated by ZnT1 in *Drosophila melanogaster. FASEB Journal* 23: 2650-2661.

Wang ZY, Stoltenberg M, Jo SM, *et al.* (2004). Dynamic zinc pools in mouse choroid plexus. *Neuroreport* 15:1801-1804

Wang K, Zhou, B, Kuo Y M, Zemansky J, Gitschier J (2002) A novel member of a zinc transporter family is defective in acrodermatitis enteropathica. *Am. J. Hum. Genet.* 71, 66-73.

Weaver BP, Dufner-Beattie J, Kambe T, Andrews GK (2007). Novel zincresponsive post-transcriptional mechanisms reciprocally regulate expression of the mouse Slc39a4 and Slc39a5 zinc transporters (Zip4 and Zip5). *Biol Chem* 388: 1301-1312.

Weaver BP, Zhang Y, Hiscox S, Guo GL, Apte U, *et al.* (2010) Zip4 (Slc39a4) Expression is Activated in Hepatocellular Carcinomas and Functions to Repress Apoptosis, Enhance Cell Cycle and Increase Migration. *PLoS ONE* 5(10): e13158. doi:10.1371/journal.pone.0013158.

Westerfield M (1993). *The Zebrafish Book: A Guide for the Laboratory Use of Zebrafish.* The University of Oregon Press, Eugene, OR.

Whitmore D, Foulkes NS, Strahle U, Sassone-Corsi P (1998). Zebrafish Clock rhythmic expression reveals independent peripheral circadian oscillators. *Nature Neuroscience,* 1:701-707.

Williams JA, Su H, Bernards A, Field J, Sehgal A (2001). A circadian ouput mediated by NF1 and the Ras/MAPK pathway. *Science* 293, 2251-2256.

Willemse MTM, Denuce JM (1973). Hatching glands in the teleosts, *Brachydanio rerio, Danio malabaricus, Moenkhausia oligolepis* and *Barbus schuberti. Develop. Growth Differ* 15: 169-177.

Wilson M, Hogstrand C, Maret W (2012). Picomolar concentration of free Zn (II) ions regulate receptor tyrosine phosphatase beta activity. http://www.jbc.org/cgi/doi/10.1074/jbc.C111.320796.

Wilson JM, Laurent P (2002). Fish gill morphology: Inside out. *J. Exp. Zool.* 293:192-213.

Wijesekara N, Dai FF, Hardy AB, Giglou PR, Bhattacharjee A, Koshkin V, Chimienti F, Gaisano HY, Rutter GA, Wheeler MB (2010). *Diabetologia* 53: 1656-1668.

Wolffram S, Arduser F, Scharrer E (1985). Invitro intestinal absorption of selenate and selenite by rats. *J. Nutr* 115: 454-459.

Wong, VVT, Nissom PM, Sim SL, Yeo JHM, Chuah SH, Yap MGS (2006). Zinc as an insulin replacement in hybridoma cultures. *Biotechnology and Bioengineering* 93: 553-563.

Wyllie AH, Kerr JFR, Currie AR (1980). Cell death: the significance of apoptosis. In: Bourne GH, Danielli JF (eds) International Review of Cytology, vol 68, Academic Press, New York London, pp 251-306.

Wu W *et al.* (1999).Activation of the EGF receptor signalling pathway in human airway epithelial cells exposed to metals. *Am. J. Physiol.* 277: L924-L931.

Xu Z, Baek K, Kim H, Cui J, Qian X, Spring D, Shin I, Yoon J (2010). Zn^{2+}-Triggered Amide Tautomerization Produces a Highly Zn^{2+}-Selective, Cell-Permeable, and Ratiometric Fluorescent Sensor. *J. Am. Chem. Soc 132 (2)*: 601-610.

Yabu T, Kishi S, Okazaki T, Yamashita M (2001). Characterization of zebrafish caspase-3 and induction of apoptosis through ceramide generation in fish fathead minnow tailbud cells and zebrafish embryo. *Biochem J,* 360:39-47.

Yamamoto M, Iuchi I, Yamagami K (1979). Ultrastructural changes of the teleostean hatching gland cell during natural and electrically induced precocious secretion. *Dev Biol* 68:162-174.

Yamasaki S, Sakata-Sogawa K, Hasegawa A, Suzuki T, Kabu K, Sato E, Kurosaki T, Yamashita S, Tokunaga M, Nishida K *et al.* (2007). Zinc is a novel intracellular second messenger. *The Journal of Cell Biology* 177, 637-645.

Yamashita S and Hirano T (2003). in *Signal Transducers and Activators of Transcription (STATs)*: Activation and Biology (eds Sehgal, P. B., Levy, D. E. &Hirano, T.) 595-607 (Kluwer Academic, Dordrecht.

Yamashita S, Miyagi C, Fukada T, Kagara N, Che YS, Hirano T (2004). Zinc transporter LIVI controls epithelial-mesenchymal transition in zebrafish gastrula organizer. *Nature* 429: 298-302, 10.1038/nature02545.

Yan G, Zhang Y, Yu J, Yu Y, Zhang F, et al. (2012). Slc39a7/zip7 Plays a Critical Role in Development and Zinc Homeostasis in Zebrafish. *PLoS ONE* 7(8): e42939. doi:10.1371/journal.pone.0042939.

Yasumasu S, Iuchi I, Yamagami K (1989). Purification and partial characterization of high choriolytic enzyme (HCE), a component of the hatching enzyme of the teleost, Oryzias latipes. *J Biochem* 105:204-211.

Yasumasu S, Yamada K, Akasaka K, Mitsunaga K, Iuchi I, Shimada H, Yamagami K (1992). Isolation of cDNAs for LCE and HCE, two constituent proteases of the hatching enzyme of Oryzias latipes, and concurrent expression of their mRNAs during development. *Dev Biol* 153:250-258.

Yohizaki N and Katagiri C (1975). Cellular basis for the production and secretion of the hatching enzyme by frog embryos. *J Exp Zool* 192:203-212.

Yu YY, Kirschke C P, Huang L (2007). Immunohistochemical analysis of ZnT1, 4, 5, 6, and 7 in the mouse gastrointestinal tract. *J. Histochem. Cytochem.* 55, 223-234.

Yuzbasiyan-Gurkan V, Bartlett E (2006). Identification of a unique splice site variant in SLC39A4 in bovine hereditary zinc deficiency, lethal trait A46: An animal model of acrodermatitis enteropathica. *Genomics* 88: 521-526.

Zahedi RP, *et al.* (2008). *J Proteome Res* 7: 526-34.

Zhang Y, Bharadwaj U, Logsdon CD, Chen C, Yao Q, *et al.* (2010). ZIP4 regulates pancreatic cancer cell growth by activating IL-6/STAT3 pathway through zinc finger transcription factor CREB. *Clin Cancer Res* 16: 1423-1430.

Zhao L, Chen W, Taylor KM, Cai B, Li X (2007). LIV-1 suppression inhibits HeLa cell invasion by targeting ERK1/2-Snail/Slug pathway. *Biochemical and biophysical research communications,* 363 (1), 82-8.

Zhao H, Sun L, Wang L, Xu Z, Zhou F, Su J, Jin J, Yang Y, Hu Y, Zha X (2008). Nglycosylation at Asn residues 554 and 566 of E-cadherin affects cell cycle progression through extracellular signal-regulated protein kinase signaling pathway. Ecadherin N-glycosylation affects. *Acta Biochim Biophys Sin* 140, 1c4e8l.

Zheng D, Feeney GP, Kille P, Hogstrand C. (2008). Regulation of ZIP and ZnT zinc transporters in zebrafish gill: zinc repression of ZIP10 transcription by an intronic MRE cluster. *Physiol. Genomics* 34(2):205-14.

Zhuang M, Wang Y, Steenhard BM, Besharse JC (2000). Differential regulation of two period genes in the Xenopus eye. *Brain Research. Mol Brain Res*. 82:52-64.

Zylka MJ, Shearman LP, Weaver DR, Reppert SM (1998). Three period homologs in mammals: differential light responses in the suprachiasmatic circadian clock and oscillating transcripts outside of brain. *Neuron*. 20:1103-1110.

CHAPTER NINE

APPENDICES

9 Appendices

9.1. Composition of standard fish Tank water

Reagent	Concentration
Sea salt	60 mg/L of deionised water
$CaCl_2$ (VWR)	200µM

9.2. Composition of Lysis buffer-proteinase K mixture for DNA isolation

Reagent	Concentration
Tris-Hcl (pH 8.5)	100 mM
NaCl	200 Mm
EDTA	5 mM
SDS	0.5%
proteinase K	100 µg/ml

9.3. Composition of high-capacity reverse transcription reagents

Reagent	Volume per 2X reaction mix (µl)*
10X RT buffer	2.0
25X dNTP mix (100 mM)	0.8
10X random primers	2.0
MultiScribe™ reverse transcriptase	1.0
RNase inhibitor	1.0
Nuclease-free water	3.2

*2 µg of total RNA is added to the reaction and diluted with nuclease free water to make a final reaction volume of 20 µl. RT: reverse transcription; dNTP: deoxyribonucleotide triphosphate.

9.4. Composition of cell lysis buffer for zebrafish embryo protein isolation and quantification

Reagent	Concentration
PBS	50 mM
Protease inhibitor	1% (v/v)
SDS*	0.1% (w/v)

*SDS was excluded from cell lysis buffer when isolating membrane bound protein. PBS: phosphate buffered saline; SDS: sodium dodecyl sulphate.

9.5. Composition of 5X protein sample loading buffer

Reagent	Concentration
Bromophenol blue	0.1% (v/v)
Glycerol	25% (w/v)
SDS	2% (v/v)
B-mercaptoethanol	5% (v/v)

SDS: sodium dodecyl sulphate.

9.6. Composition of 10X SDS-PAGE running buffer

Reagent	Concentration (g/L)
Glycine	142.00
SDS	10.00
Tris-base	30.28

SDS: sodium dodecyl sulphate.

9.7. Composition of 10X SDS-PAGE-nitrocellulose semi-dry transfer buffer*

Reagent	Concentration (g/L)
Glycine	36.25
SDS	4.63
Tris-base	72.50

*10X transfer buffer in Table 2.13 was diluted into a 20% (v/v) methanol solution to make the 1X transfer buffer. SDS: sodium dodecyl sulphate.

9.8. Composition of 8, 10, 12% polyacrylamide gels for protein electrophoresis

Reagent	Volume per gel		
	8% (v/v) acrylamide	10% (v/v) acrylamide	12% (v/v) acrylamide
Distilled water	4.40 ml	3.75 ml	3.10 ml
Tris (pH 8.8)	2.15 ml	2.15 ml	2.15 ml
40% (w/v) acrylamide	1.65 ml	2.25 ml	2.85 ml
10% (w/v) APS	82.5 µl	82.5 µl	82.5 µl
10% (w/v) SDS	82.5 µl	82.5 µl	82.5 µl
TEMED	11.0 µl	11.0 µl	11.0 µl

APS: ammonium persulphate; SDS: sodium dodecyl sulphate; TEMED: tetramethylethylenediamine.

9.9. Composition of washing solution and antibody incubation solution.

Reagent	Concentration
Non-fat powdered milk	1% (w/v)
PBS	1X
Tween 20	0.1 % (v/v)

PBS: Phosphate buffered saline.

9.10. Composition of nitrocellulose membrane blocking solution.

Reagent	Concentration
Non-fat powdered milk	5% (w/v)
PBS	1X
Tween 20	0.1 % (v/v)

PBS: Phosphate buffered saline.

9.11. Composition of nitrocellulose membrane stripping buffer.

Reagent	Concentration (% v/v)
10% (w/v) SDS	20
Distilled water	69.22
Tris (pH 6.8)	10
B-mercaptoethanol	0.78

SDS: sodium dodecyl sulphate.

9.12. Composition of bloodworms

Components	Percentage
Crude protein (Min)	5.57%
Crude fat (Min)	0.93%
Crude fibre (Max)	0.2%
Moisture (Max)	92.05%
Ash (Max)	0.81%
Phosphorus (Min)	0.10%
Iron	0.35%

9.13a. Value of 1/ΔCT for different zinc transporters in different genotypes for both zinc diets

Normal zinc			**High** zinc		
$Znt1^{+/+}$	$Znt1^{\Delta 40/+}$	$Znt1^{\Delta 40/\Delta 40}$	$Znt1^{+/+}$	$Znt1^{\Delta 40/+}$	$Znt1^{\Delta 40/\Delta 40}$
		mt2			
0.150761	-9.80392	0.108849	0.348675	0.458085	7.518797
0.105119	0.139315	0.107296	0.78125	0.336022	3.125
0.120077	0.101112	0.131579	0.224467	0.4914	0.27248
0.115969	0.112931	0.250627	0.177936	0.66313	0.970874
0.126135	0.140449	0.166945	0.373134	0.325098	1.449275
0.171145	0.155207	0.196773	0.268097		
0.252525	0.150648	0.472813	0.286779		
0.12207	0.110436	0.130839			
0.122175	0.131372	0.143678			
0.1221					
0.108225					
		znt1			
0.087719	0.074627	0.085179	0.08547	0.093633	0.104822
0.084034	0.076982	0.080192	0.084175	0.094697	0.102564
0.077882	0.087184	0.086505	0.08285	0.093897	0.093721
0.078555	0.082169	0.092851	0.087642	0.091743	0.104167
0.087642	0.081367	0.08547	0.089928	0.095238	0.092937
0.0777	0.081766	0.090009	0.090498		
0.086207	0.090498	0.084104	0.090827		
0.07874	0.089206	0.07722			

0.079114	0.107643	0.083126			
0.086059					
0.089286					

znt4

0.098587	0.128403	0.093971	0.09733	0.105895	0.122499
0.092265	0.092997	0.092678	0.107066	0.101816	0.121758
0.091047	0.084602	0.097292	0.094832	0.099059	0.107933
0.090473	0.086919	0.101133	0.098457	0.112003	0.113938
0.08785	0.093633	0.107527	0.099206	0.099701	0.110072
0.094491	0.094491	0.107392	0.095785		
0.089405	0.092868	0.107875	0.096154		
0.089915	0.088028	0.090066			
0.090212	0.098312	0.095465			
0.097182					
0.093414					

znt5

0.074963	0.126263	0.072202	0.074738	0.08058	0.111732
0.072464	0.079051	0.079239	0.091827	0.074963	0.095147
0.072046	0.067522	0.088028	0.072727	0.082508	0.090992
0.072359	0.068823	0.083056	0.082508	0.087719	0.085763
0.071788	0.077942	0.083682	0.08726	0.079745	0.1
0.074184	0.081169	0.085837	0.07874		
0.07874	0.084962	0.098087	0.078064		
0.075415	0.073099	0.072622			
0.066578	0.076394	0.0815			
0.076104					
0.070522					

zip3

0.069832	0.068634	0.061958	0.074738	0.072833	0.067295
0.069348	0.068729	0.067705	0.075873	0.069109	0.070621
0.067114	0.066401	0.059524	0.078247	0.067204	0.070274
0.068966	0.067522	0.069686	0.073099	0.078555	0.08285
0.073964	0.073529	0.054377	0.07622	0.073206	0.052521
0.068493	0.076628	0.072727	0.072516		
0.069444	0.074074	0.078003	0.069396		
0.070522	0.069493	0.070323			
0.063857	0.06398	0.076982			
0.079239					
0.074239					

zip4

0.075415	0.077101	0.079177	0.055405	0.058962	0.069696
0.068259	0.070631	0.069541	0.059506	0.049172	0.054502
0.078555	0.07171	0.074683	0.052535	0.057422	0.055664
0.069348	0.07485	0.072632	0.057548	0.054324	0.053542
0.080775	0.078462	0.093327	0.068287	0.053456	0.057455
0.087889	0.079758	0.083773	0.053533		
0.071762	0.07776	0.074377	0.049871		
0.076295	0.062873	0.072108			
0.078462	0.083183	0.07758			
0.093985					
0.087873					

zip7

0.081182	0.152207	0.070922	0.075109	0.0815	0.141243
0.071429	0.076028	0.080354	0.111794	0.076336	0.114155
0.073368	0.067137	0.090009	0.078064	0.085763	0.091785
0.072516	0.067889	0.093371	0.080645	0.086806	0.085034
0.078927	0.081833	0.091659	0.09704	0.0815	0.113507
0.078753	0.082988	0.083612	0.08016		
0.094251	0.084388	0.108401	0.079428		
0.07722	0.070796	0.072622			
0.066291	0.074963	0.081566			
0.080128					
0.075758					

zip10

0.0668	0.087796	0.070872	0.073421	0.072254	0.081699
0.061805	0.06854	0.069493	0.08244	0.074906	0.084962
0.067295	0.064893	0.062933	0.066225	0.069784	0.074239
0.066711	0.066578	0.066711	0.07593	0.072727	0.079239
0.070274	0.071685	0.070077	0.074129	0.070472	0.075301
0.071174	0.06993	0.067204	0.071839		
0.068823	0.065104	0.069348	0.068446		
0.065963	0.056243	0.066269			
0.063939	0.069109	0.067476			
0.069013					
0.067751					
0.072516					

9.13b. qPCR amplification curves for different zinc transporters, metallothioneine and reference genes in all fish genotypes for both zinc diets

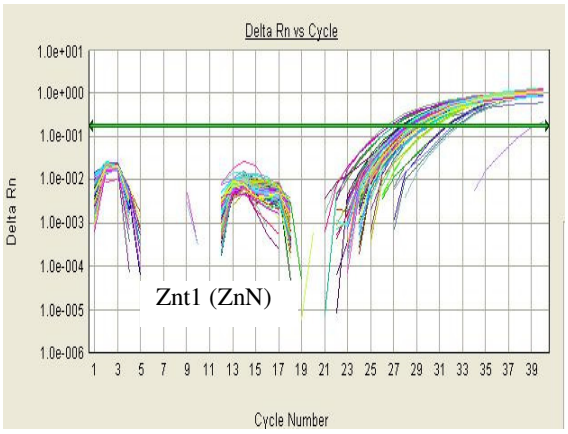

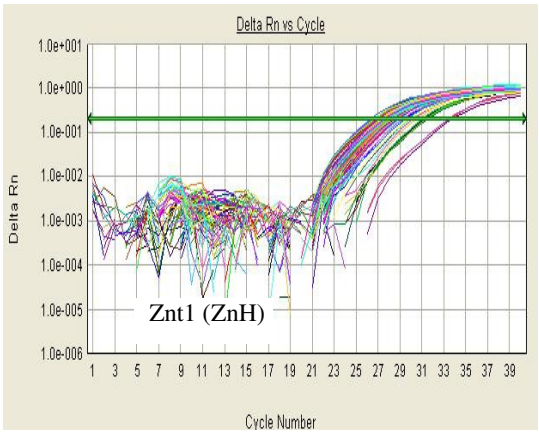

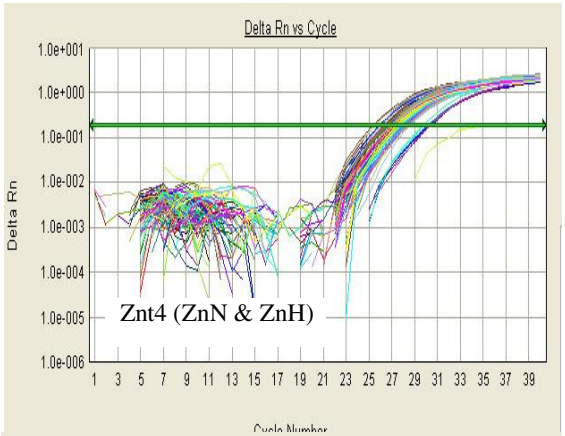

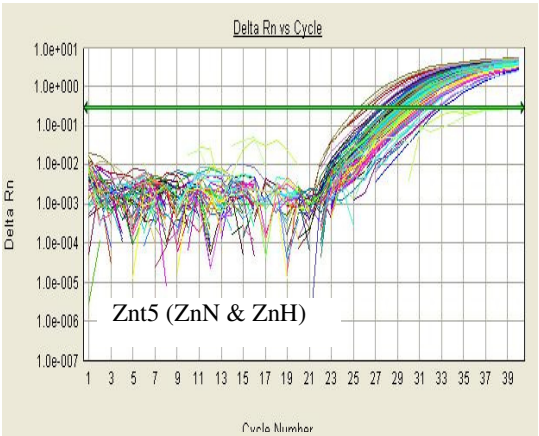

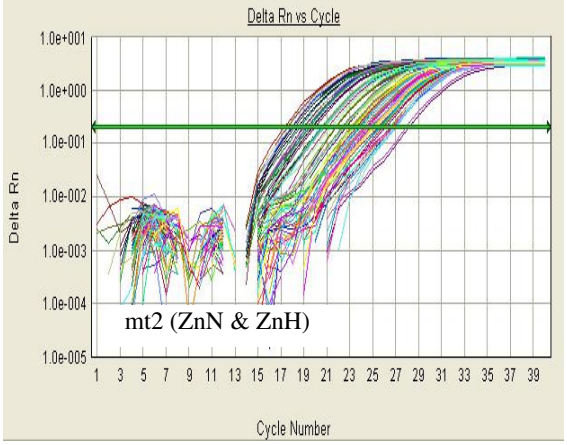

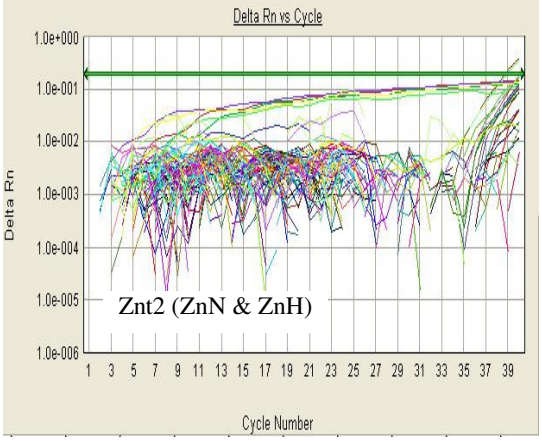

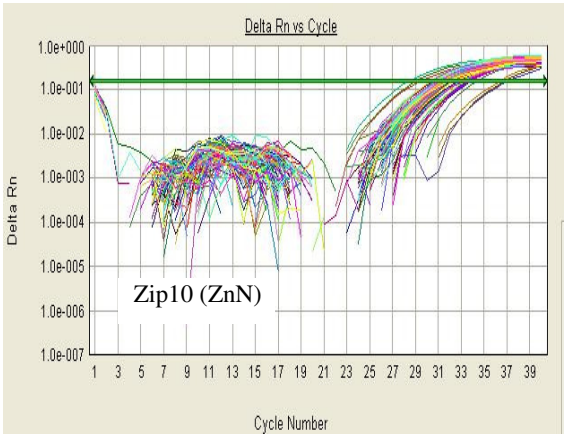
Delta Rn vs Cycle
Delta Rn
Cycle Number
Zip10 (ZnN)

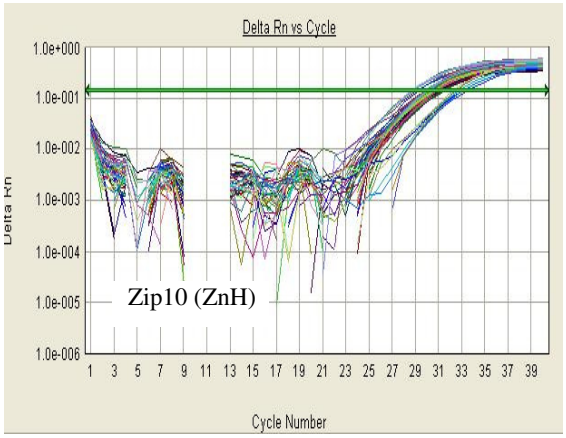
Delta Rn vs Cycle
Delta Rn
Cycle Number
Zip10 (ZnH)

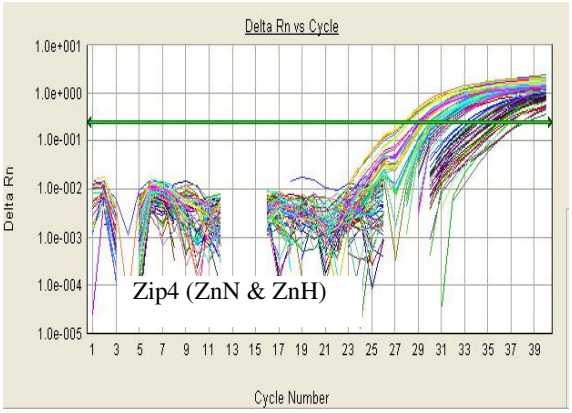
Delta Rn vs Cycle
Delta Rn
Cycle Number
Zip4 (ZnN & ZnH)

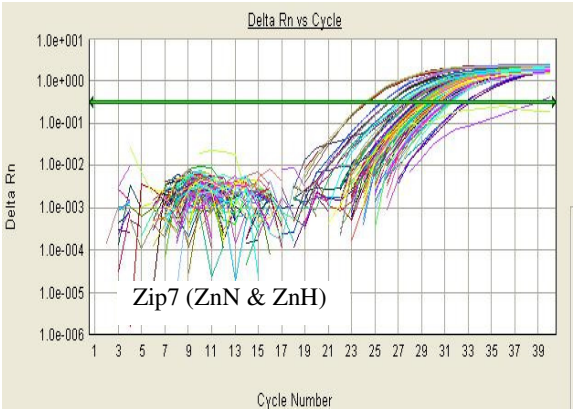
Delta Rn vs Cycle
Delta Rn
Cycle Number
Zip7 (ZnN & ZnH)

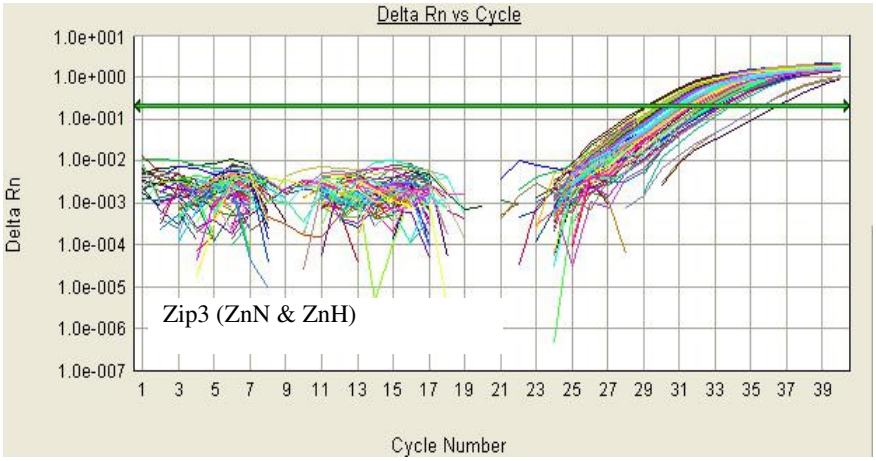
Delta Rn vs Cycle
Delta Rn
Cycle Number
Zip3 (ZnN & ZnH)

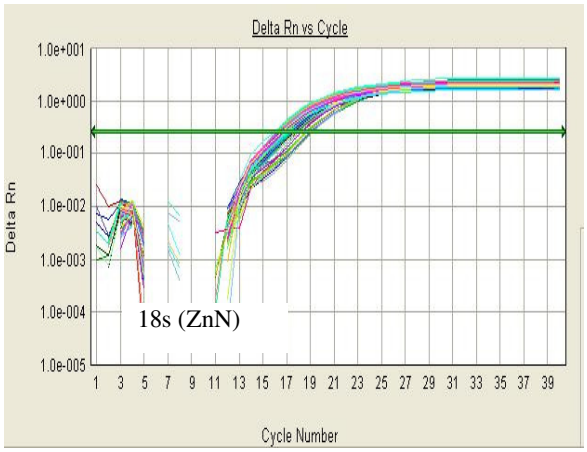

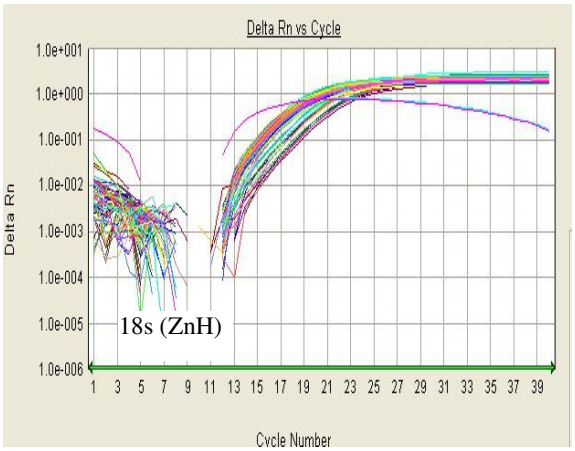

9.14a. Value of 1/ΔCT for master clock genes in mutant and wild-type for both zinc diets

Normal zinc		**High** zinc	
$Znt1^{+/+}$	$Znt1^{\Delta 40/\Delta 40}$	$Znt1^{+/+}$	$Znt1^{\Delta 40/\Delta 40}$
	Bmal1		
0.177369	0.16955	0.357011	0.402393
0.210069	0.204354	0.28108	0.640232
0.196765	0.209154	0.33125	0.356273
0.233843	0.173534	0.312191	0.335357
0.22408	0.207954	0.313913	0.535906
	Clock		
0.118704	0.099704	0.267891	0.157067
0.116806	0.105279	0.148137	0.175766
0.127944	0.110054	0.155072	0.145467
0.118101	0.111004	0.166791	0.169639
0.1332	0.110084	0.195114	0.212866
	Cry2a		
0.163306	0.149631	0.231879	0.214582
0.181178	0.16129	0.174555	0.203528
0.161055	0.165609	0.193688	0.157955
0.173432	0.139126	0.176953	0.202881
0.169798	0.150725	0.161178	0.254626
	Per2		
0.158071	0.132335	0.354045	1.155001
0.121533	0.164857	0.225933	0.273808
0.149235	0.126738	0.239265	0.224058
0.230201	0.122068	0.301501	0.201739
0.162653	0.116827	0.196213	0.200693

9.14b. qPCR amplification curves for different circadian genes and reference gene in wild-type and homozygote mutant for both zinc diets

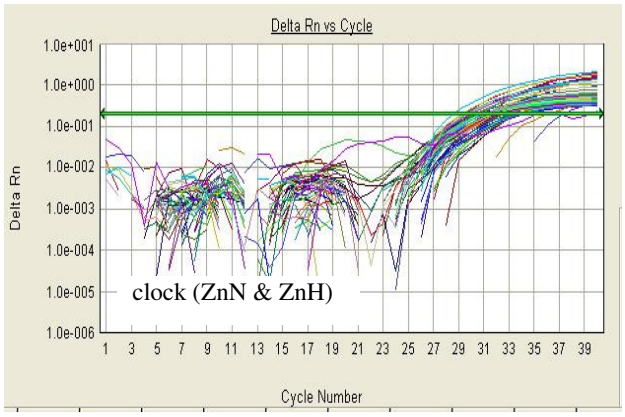

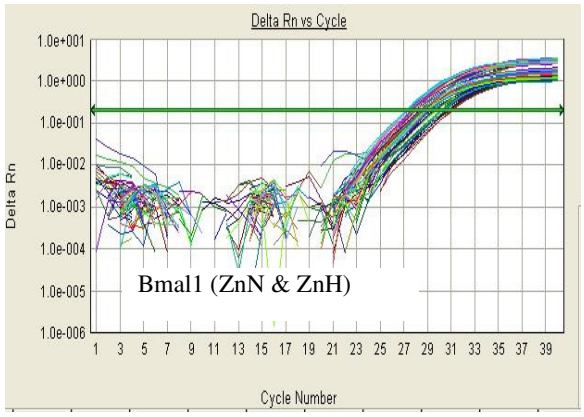

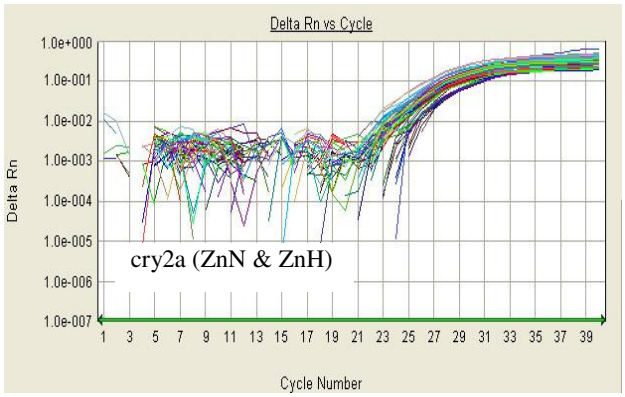

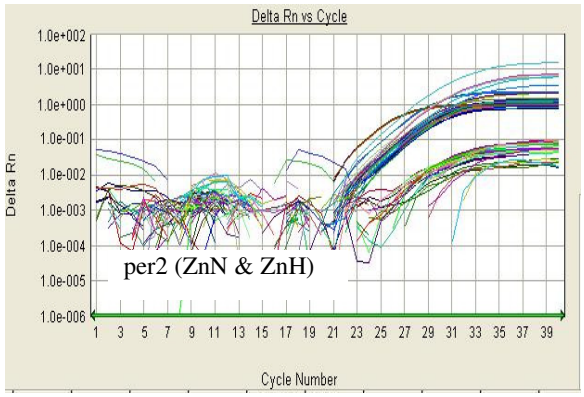

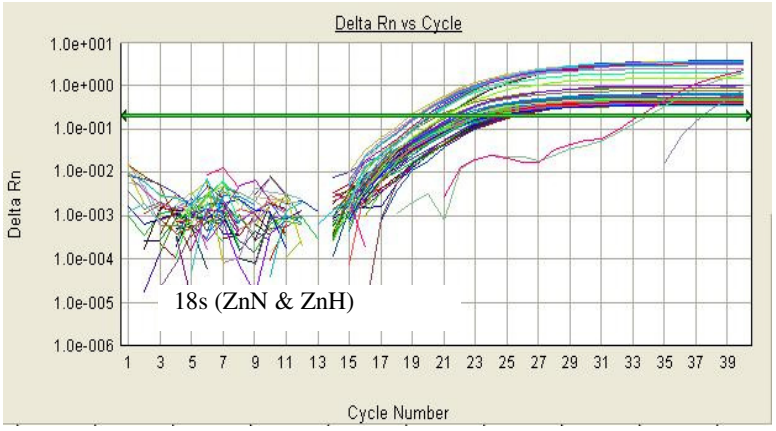

9.15. Gel electrophoresis for generating the znt1 antisense probe

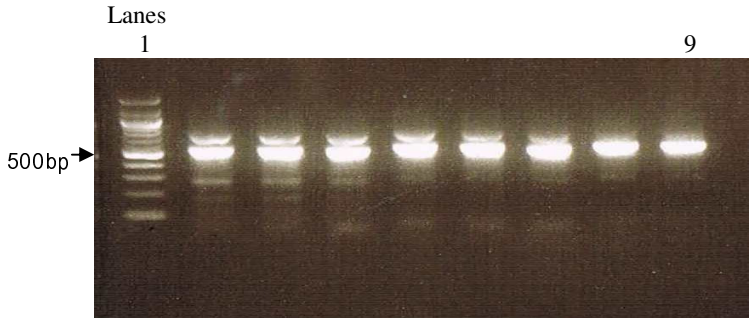

Fig. 9.1: Gel electrophoresis showing amplification and product length of znt1 fragmenet (538bp) at the best primer annealing temperatures of 64.8^{o}C in lane 9. Lane 1 represents 100bp ladder (Promega).

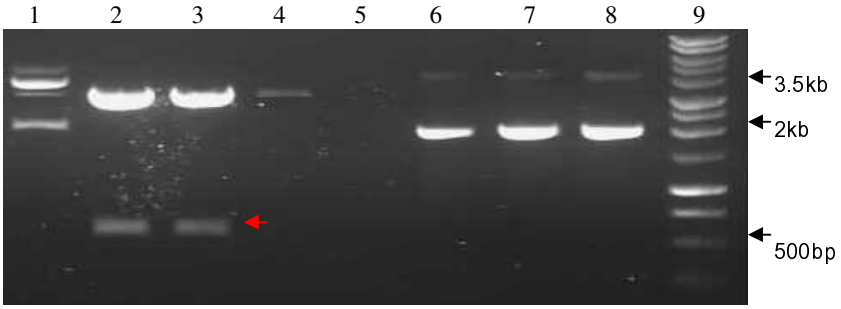

Fig. 9.1.1: Gel electrophoresis showing the presence or absence of the cDNA fragments (inserts) encoding Znt1 proteins in the plasmid vector (~3kb). Lane 1 shows improperly restricted (digested) plasmid by EcoR1 which contains no insert while lane 2 and 3 were properly restricted plasmids with presence of 538pb inserts in them (red arrow head). Lane 4 was properly digested but no insert whereas lane 6 to 8 are control plasmid constructs without EcoR1 digestion. Lane 9 represent 1kb ladder. Orientation of the insert in 2 and 3 were confirmed by sequencing.

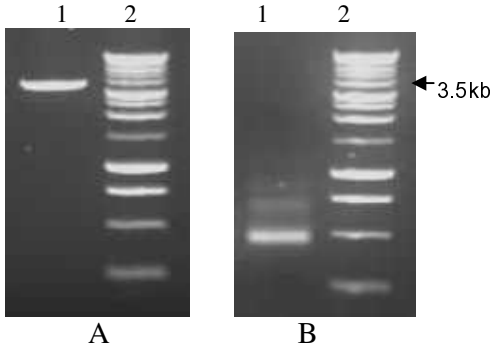

Fig. 9.1.2: (A). Gel electrophoresis of the linearized plasmid showing a single fragment of ~3.5kb in lane 1 while lane 2 was a 1kb ladder (Promega). B) Shows transcription of antisense RNA probe using T7 polymerase. Presence of antisense RNA bands (18s and 28s) in lane 1 with the degradation of plasmid DNA by DNase treatment confirmed proper transcription. Lane 2 represents a 1kb ladder.

9.16. Gel electrophoresis for generating antisense RNA probes for HGC markers

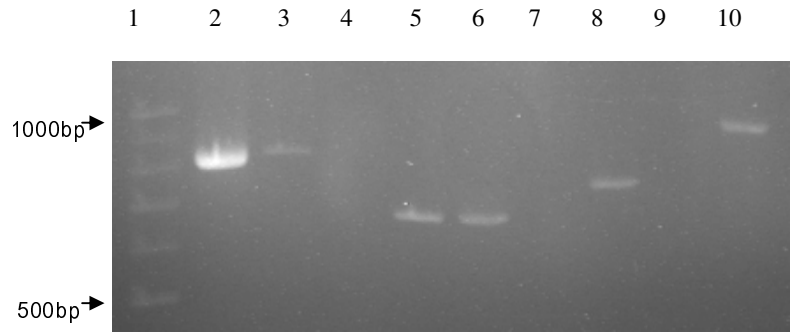

Fig. 9.2: Gel electrophoresis showing the product length of cDNA fragments of *zip10* (lane 2 & 3; 823bp), *he1a* (lane 5 & 6; 652bp), *klf4* (lane 8; 73 (lane 10, 935bp). Lane 1 is a 100bp ladder. The gel pictures at every stage of probe generation were not different from those of znt1 shown in appendix X above,, except for annealing temperatures and product sizes. Both *catL1b* and *klf4* perfectly annealed at all the gradient temperature between 55^{o}C and 66^{o}C whereas He1a and zip10 annealed better at 61.6^{o}C and 56.8^{o}C respectively.

9.17. Gel ectrophoresis for generating cdh1 antisense probe

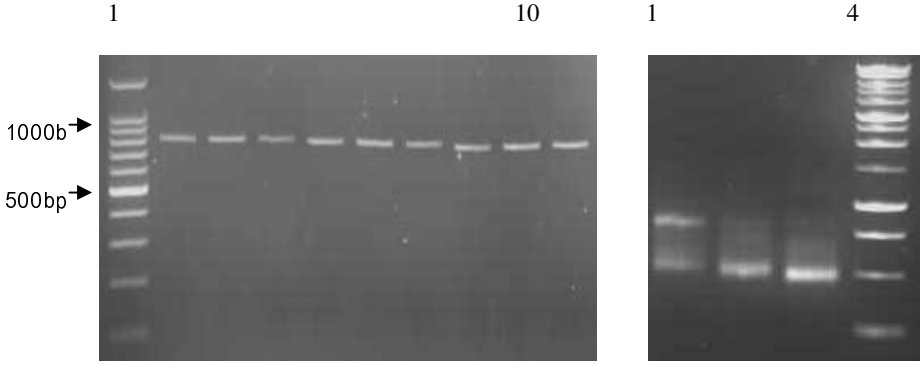

Fig. 9.3: (A). Gel electrophoresis of *cdh1* gene fragment showing annealing perfectly at all the gradient temperatures between 55^{o}C and 66^{o}C (lane 2-10) given a product length of 741bp. Lane 1 represents 100bp ladder. (B) Showed transcription of antisense RNA probe directly from the PCR products without cloning processes. T7 polymerase was used for transcription. Presence of RNA bands (18s and 28s) for samples in lane 1, 2 and 3 and degradation of plasmid DNA by DNase treatment confirmed proper transcription. Lane 4 represents a 1kb ladder.

9.18. Phenotypes of splice blocking MO and translational blocking + p53 MOs

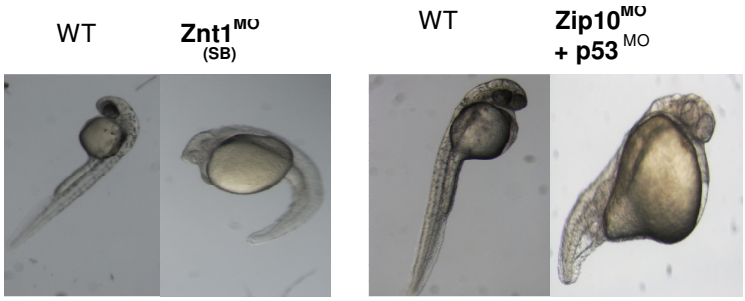

Fig 9.4: Phenotype of embryo following different MO injections compared to uninjected control (WT). SB; splice blocking MO.

9.19. Some phenotypic features frequently observed in mutant than wild-type adults

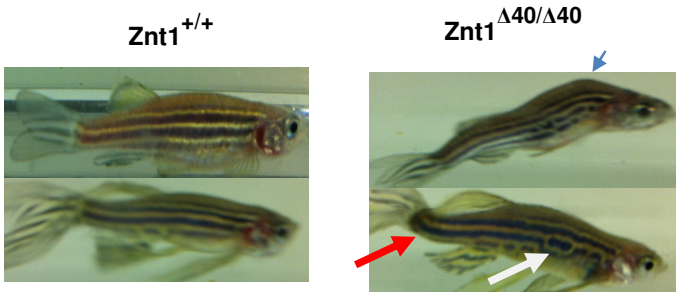

Fig 9.5: Phenotypic features commonly observed at high frequency in adult mutants. Note the split or broken pigmentation or stripes in mutant (white arrow), the kinked tail (red arrow) and the arched or curved back (blue arrow) which is a sign of unthriftness and waisting.

Fig 9.6: Stand-alone zebrafish tank system (Aquaneering Inc).

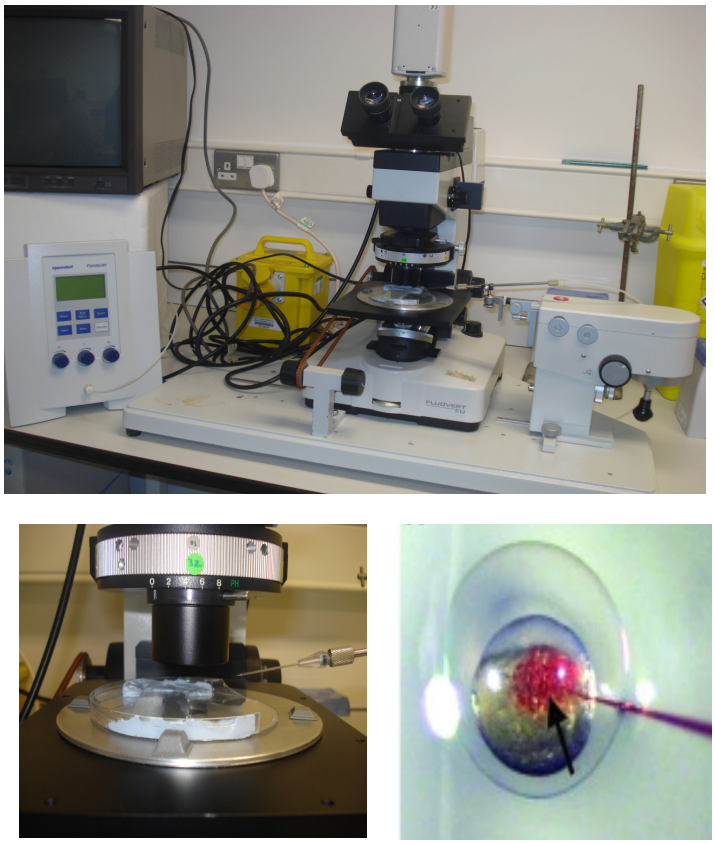

Fig. 9.7: Zebrafish microinjection facility. Arrow showed 1 cell stage embryo after MO injection.

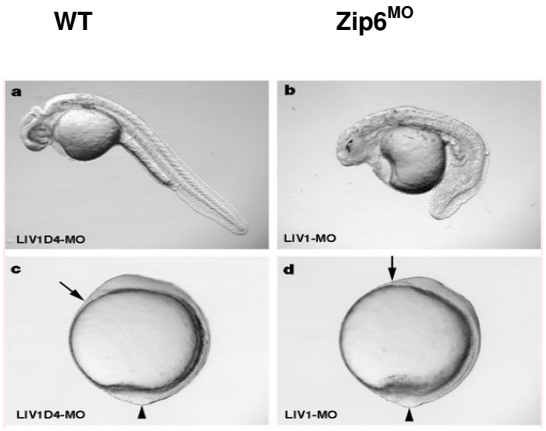

Fig. 9.8: Phenotypes of Zip6 (Liv-1) morphant (Yamashita *et al.,* 2004)

9.20. Results of ELM motif search after globular domain filtering, structural filtering and context filtering.

Elm Name	Instances (Matched Sequence)	Positions	View in Jmol	Elm Description	Cell Compartment	Pattern	PHI-Blast Instance Mapping	Structural Filter Info
LIG_14-3-3_3	KTPTLP	1-6	-	Consensus derived from reported natural interactors which do not match the Mode 1 and Mode 2 ligands.	nucleus, cytosol, internal side of plasma membrane	[RHK][STALV].[ST].[PESRDIF]	-	-
LIG_FHA_1	IITREVE	31-37	-	Phosphothreonine motif binding a subset of FHA domains that show a preference for a large aliphatic amino acid at the pT+3 position.	nucleus	..(T)..[ILV].	-	-
LIG_FHA_2	SVTSLEI	9-15	-	Phosphothreonine motif binding a subset of FHA domains that have a preference for an acidic amino acid at the pT+3 position.	nucleus, Replication fork	..(T)..[DE].	-	-
LIG_PDZ_1	ESSL	37-40	-	PDZ domains recognize short sequences at the carboxy terminus of target proteins	cytosol, plasma membrane, membrane	.[ST].[VIL]$	-	-
LIG_PDZ_3	LEII SESV PESV	13-16 17-20 26-29	- - -	Class III PDZ domains binding motif	cytosol, plasma membrane, membrane	.[DE].[IVL]	-	-
LIG_USP7_1	PSASV	6-10	-	The USP7 NTD domain binding motif variant based	nucleus	[PA][^P][^FYWIL]S[^P]	-	-

				on the MDM2 and P53 interactions.				
MOD_CK1_1	SVTSLEI	9-15	-	CK1 phosphorylation site	nucleus, cytosol	S..([ST])...	-	-
MOD_CK2_1	ASVTSLE EDTSRPE	8-14 21-27	- -	CK2 phosphorylation site	nucleus, cytosol, protein kinase CK2 complex	...([ST])..E	-	-
MOD_GlcNHglycan	PSAS	6-9	-	Glycosaminoglycan attachment site	extracellular, Golgi apparatus	[ED]{0,3}.(S)[GA].	-	-
MOD_GSK3_1	TLPSASVT ISESVEDT EDTSRPES	4-11 16-23 21-28	- - -	GSK3 phosphorylation recognition site	nucleus, cytosol	...([ST])...[ST]	-	-
MOD_PK_1	RPESVVI	25-31	-	Phosphorylase kinase phosphorlation site	cytosol	[RK]..(S)[VI]..	-	-